

CHIRAL BISAMIDINE CATALYSIS:  
ENANTIOSELECTIVE ALKYLATIONS AND HALOLACTONIZATIONS WITH  
APPLICATIONS TO SMALL MOLECULE THERAPEUTICS

By

Mark Christopher Dobish

Dissertation

Submitted to the Faculty of the  
Graduate School of Vanderbilt University

in partial fulfillment of the requirements

for the degree of

DOCTOR OF PHILOSOPHY

in

CHEMISTRY

May 2013

Nashville, Tennessee

Approved:

Professor Jeffrey N. Johnston (Chair)

Professor Timothy P. Hanusa

Professor Ned A. Porter

Professor Michael R. Waterman

Copyright © 2013 by Mark Christopher Dobish  
All Rights Reserved

To my beautiful wife Julia  
and my infinitely supportive family

## Acknowledgements

I am aware that this document is not the work of one person, but of the many people who have contributed to my success, not only in graduate school, but in all aspects of my life. Though some of these contributions may go unmentioned, I don't take them for granted and am incredibly grateful.

First and foremost, I would like to thank my loving parents, Dave and Cindy. They have always been my number one fans, whether in school, athletics, or life. Without their love and financial support, I would not have had the strength or means to complete my schooling. I love you both very much. I also want to thank four extraordinary people, my grandparents: Ted, Barbara, Pete, and Ann. So much of the man I am today can be attributed to my grandparents, who worked tirelessly to ensure we had everything we needed. I would like to recognize my talented sister Kristen and handsome brother Matthew for their continued love and encouragement and for not reminding me daily that it took me the longest to complete graduate school. I would also like to thank my in-laws, Ron and Michele, for welcoming me into their family and being so supportive these past five years. And to the rest of the family, immediate and extended, Dobish and Meyer, I thank you for being so encouraging and helpful throughout this process.

I would like to acknowledge the mentors from Allegheny College who helped set me on my current path: Prof. P. J. Persichini, for convincing me to not go to medical school, Prof. Nancy Lowmaster for introducing me to chemistry, and Angelo Panzetta for being an excellent coach and friend.

It is necessary that I thank my advisor Prof. Jeffrey Johnston for luring me to Nashville with the promise of better weather than Minnesota. His wealth of knowledge, demonstrated work ethic and problem solving ability have served as an inspiration. I would not be the scientist I am today if he had not invested so much of his time and resources in me, and for this I am grateful.

I would like to acknowledge the many members of the Johnston group that I have had the pleasure to work with and learn from over the years: Anand Singh and Tyler Davis for teaching me everything I know about catalysis, Ki Bum Hong for always demanding that I work harder, Priya Mathew and Dawn Makley, who were great classmates for communal commiseration, and Amanda Doody for her many hours of

proofreading. I have been fortunate to be surrounded not only by intelligent people in the Johnston Lab, but by some great entertainers and friends, who have made the long hours more fun.

I would like to thank my thesis committee for their guidance and help throughout this process: Prof. Timothy Hanusa, Prof. Ned Porter, and Prof. Michael Waterman. Additionally, my research could not have happened without support from an exceptional departmental staff. I would like to specifically thank Don Stec and Markus Voehler for ensuring we not only had working, but state of the art NMR facilities. This work was also possible because of fellowship support from the Vanderbilt Institute of Chemical Biology (VICB) and financial support from the NIH (GM084333).

We have been blessed to have made so many friends while living in Nashville. Specifically, our Sylvan Park family: Kyle, Jess, Christine, Amy, and Melinda. The many hours and meals we shared will forever be remembered. I am also thankful Melinda moved to Nashville and became a great friend before becoming an even better sister in law. I would like to acknowledge the time spent in Nashville with my childhood best friend, Marcus Smith, while he was stationed at Fort Campbell. There was never a dull moment when he would come to visit. I would also like to thank Ryan Castor and Dr. Chris Morgan for being great supportive friends from afar.

Finally, I would like to thank my wife Julia. She is an amazing, strong, and loving woman to whom I owe so much love and lost time for everything she has done for me. I am glad she said “yes” three years ago and couldn’t imagine my life without her. We have great chemistry.

## Table of Contents

|                         |      |
|-------------------------|------|
| DEDICATION PAGE .....   | III  |
| ACKNOWLEDGEMENTS .....  | IV   |
| TABLE OF CONTENTS ..... | VI   |
| LIST OF FIGURES .....   | IX   |
| LIST OF SCHEMES .....   | XI   |
| LIST OF TABLES .....    | XIII |
| LIST OF CHARTS .....    | XV   |

### CHAPTER

|   |    |
|---|----|
| I. CHIRAL BRØNSTED BASE-PROMOTED NITROALKANE<br>ALKYLATION: ENANTIOSELECTIVE SYNTHESIS OF <i>SEC</i> -ALKYL-3-<br>SUBSTITUTED INDOLES ..... | 1  |
| 1.1 Current Approaches Toward Indole Products Containing <i>sec</i> -Alkyl-3-<br>Substitutions .....  | 1  |
| Background and Relevance of Indoles .....   | 1  |
| Nucleophilic Indoles and C3-C3' Bond Formation.....   | 6  |
| Metal-Catalyzed Friedel-Crafts Reaction between Indole and<br>Nitrostyrene.....   | 7  |
| Organocatalyzed Friedel-Crafts Reaction between Indole and<br>Nitrostyrene.....   | 8  |
| Friedel-Crafts Reaction between Indole and $\alpha,\beta$ -Disubstituted<br>Nitrostyrenes .....   | 11 |
| Electrophilic Indole and C3'-C3'' Bond Formation .....  | 12 |
| Gramine as an Indolenine Precursor.....   | 13 |
| Arylsulfonyl Indoles as Indolenine Precursors.....  | 14 |
| Enantioselective Additions to Indolenines .....   | 19 |
| 1.2 Chiral Bisamidine-Promoted Nitroalkane Alkylations .....  | 24 |
| Previous Work in BAM Catalyzed Additions .....  | 24 |
| Preliminary Results from Bisamidine Catalyzed Additions.....  | 25 |
| Reaction Optimization.....  | 29 |
| Reaction Optimization: Catalyst Screen.....   | 32 |

|   |           |
|---|-----------|
| Reaction Scope: Electrophile Screen.....  | 38        |
| Reaction Scope: Nucleophile Screen.....   | 43        |
| Mechanistic Studies and the Development of New Reaction Protocol .....  | 45        |
| Influence of Water in the Reaction.....   | 46        |
| Performing the Indolenine Intermediate.....   | 49        |
| Application and Comparison of the Three Reaction Protocols .....  | 51        |
| Nitro Group Modification of the Indole Adducts.....   | 54        |
| Future Work.....  | 55        |
| <b>II. THE ENANTIOSELECTIVE SYNTHESIS OF VNI: A CURE FOR THE<br/>NEGLECTED TROPICAL CHAGAS DISEASE'</b> ..... | <b>57</b> |
| 2.1 Chagas Disease and the Limitations to Parasite Eradication .....  | 57        |
| Background of Chagas Disease .....  | 57        |
| Chagas Therapy and Sterol Biosynthesis .....  | 60        |
| Industrial Synthesis of Posaconazole .....  | 64        |
| VNI as a Treatment for Chagas Disease.....  | 66        |
| 2.2 The Short, Enantioselective Synthesis of VNI.....   | 70        |
| Background and Project Goals .....  | 70        |
| BAM Catalyzed aza-Henry .....   | 72        |
| Reduction of the aza-Henry Adduct.....  | 78        |
| Imidazole Formation .....   | 79        |
| Side Chain Synthesis and Completion of VNI.....   | 80        |
| VNI Analog Synthesis .....  | 84        |
| VNI Cures the Murine Model of Acute and Chronic Chagas Disease.....   | 88        |
| <b>III. BISAMIDINE CATALYZED ENANTIOSELECTIVE HALOGENATIONS'</b> .....  | <b>90</b> |
| 3.1 Enantioselective Halogenations and Asymmetric Organocatalysis.....  | 90        |
| History of Enantioselective Halocarboxylations .....  | 90        |
| Substoichiometric, catalytic halocyclizations .....   | 92        |
| Highly Enantioselective, Organocatalytic Halocyclizations .....   | 93        |
| Current limitations in enantioselective halocyclizations .....  | 100       |
| 3.2 Bisamidine Catalyzed Enantioselective Iodolactonization .....   | 103       |
| Preliminary Results .....   | 103       |
| Catalyst and Achiral Acid Screen.....   | 107       |
| StilbPBAM: A More Reactive and Selective Catalyst.....  | 120       |
| Substrate Scope for 1,1-Disubstituted Olefinic Acids.....   | 124       |
| Lower performing substrate optimization .....   | 128       |
| Mechanistic Observations .....  | 132       |
| Development of Reagent-Substrate Assembly Models for<br>Enantioselection .....                                | 138       |
| Application to endo-Iodolactonization.....  | 139       |
| Future Work.....  | 149       |

|   |     |
|---|-----|
| Tri- and Tetra-Substituted Olefinic Acids ..... | 149 |
| Cascade Reactions .....                         | 149 |
| Enantioselective capture of carbon dioxide..... | 151 |
| Additional modes of catalyst binding.....       | 153 |
| IV. EXPERIMENTALS .....                         | 155 |



## List of Figures

|  |     |
|--|-----|
| Figure 1. Representative Indole- and Pyrrole-Containing Pharmaceuticals in the Top 200 of Sales for the Year 2007 .....    | 2   |
| Figure 2. Indole Alkaloids with C3 <i>n</i> -Alkyl Substitution.....   | 3   |
| Figure 3. Representative Indole and Pyrrole Heterocycles Bearing Chiral C3 <i>sec</i> -Alkyl Substitution .....            | 4   |
| Figure 4. Different Disconnections for the Synthesis of Alkyl Indoles.....   | 6   |
| Figure 5. Chiral BOX-ligands for the Asymmetric Friedel-Crafts Reaction between Indole and Nitrostyrene .....              | 8   |
| Figure 6. Previously Reported BAM Reactivity and Desired Additions of Phenylnitromethane to Indolenine Intermediates ..... | 26  |
| Figure 7. Proposed Catalyst Binding Model.....   | 34  |
| Figure 8. Proposed Mechanism by Chiral and Achiral Routes.....   | 45  |
| Figure 9. Model for Further Catalyst Development.....  | 56  |
| Figure 10. Brazilian banknote recognizing Carlos Chagas and the life cycle of the deadly parasite.....                     | 58  |
| Figure 11. Benznidazole and Nifurtimox.....  | 59  |
| Figure 12. CYP51 reaction in sterol biosynthesis across the kingdoms (from ref. 74) .....                                  | 63  |
| Figure 13. Modeled docking of eburicol in <i>T. cruzi</i> CYP51 (from ref. 83).....  | 67  |
| Figure 14. Small Molecule Inhibitors of <i>T. cruzi</i> CYP51 (from ref. 73).....  | 68  |
| Figure 15. Overlay of Potential Inhibitors of <i>T. cruzi</i> CYP51 Crystal Structures (from ref. 81).....                 | 69  |
| Figure 16. Racemic synthesis of VNI and <i>epi</i> -VNI.....   | 71  |
| Figure 17. Achievable Points of Diversity in the Synthesis of VNI and other Analogs .....                                  | 84  |
| Figure 18. <i>Organic Syntheses</i> Preparation of PBAM. ....  | 86  |
| Figure 19. Prepared VNI analogs.....   | 87  |
| Figure 20. VNI Eradicates Parasite <i>in vivo</i> for Both Phases of Chagas Disease (ref. 62).....                         | 88  |
| Figure 21. Proposed Mode of Binding in Enantioselective Chlorolactonization. ....  | 95  |
| Figure 22. Proposed Transition State and Mechanism for Enantioselective Iodolactonization.....                             | 96  |
| Figure 23. First Catalytic and Highly Enantioselective Bromolactonizations.....  | 97  |
| Figure 24. Enantioselective Bromocyclization Work from the Yeung Laboratory.....   | 99  |
| Figure 25. Synthetically Useful Transformations of Products from Halocyclization Reactions.....                            | 100 |
| Figure 26. Proposal for Bisamidine and Electrophilic Halogen Complexation.....   | 103 |

|   |     |
|---|-----|
| Figure 27. Evidence by NMR of PBAM Iodination. ....   | 115 |
| Figure 28. Crystal structure of StilbPBAM dimer. ....   | 124 |
| Figure 29. The Problematic <i>para</i> -Methoxy Substrate. ....                                       | 128 |
| Figure 30. Proposed Reagent-Substrate Assemblies. ....  | 138 |
| Figure 31. Catalyst Modification Leading to Additional Chelation Control in<br>Diamine Backbone. .... | 154 |

## List of Schemes

|  |    |
|--|----|
| Scheme 1. First Reported Use of Nitrostyrenes as Michael Acceptors .....                                   | 7  |
| Scheme 2. Chiral Thiourea Catalyzed Addition of Indole to Nitrostyrene.....                                | 9  |
| Scheme 3. Chiral Stilbene Diamine Catalyzed Addition of Indole to Nitrostyrene .....                       | 9  |
| Scheme 4. Chiral Phosphoric Acid Catalyzed Addition of Indole to Nitroalkenes.....                         | 10 |
| Scheme 5. Protonated Thioureas as Highly Reactive and Selective Catalysts .....                            | 11 |
| Scheme 6. Enantioselective Friedel-Crafts Alkylation with $\alpha,\beta$ -Disubstituted Nitroalkenes ..... | 12 |
| Scheme 7. Nucleophilic Addition to Indolenines .....   | 13 |
| Scheme 8. Gramine as an Indolenine Precursor .....   | 13 |
| Scheme 9. Addition of Nitroalkanes to Gramine-derived Indolenine Intermediates.....                        | 14 |
| Scheme 10. Petrini's Synthesis of Arylsulfonyl Indoles .....   | 15 |
| Scheme 11. Modified Synthesis of Arylsulfonyl Indoles .....  | 15 |
| Scheme 12. Additions of Nitroalkanes and Malonates .....   | 17 |
| Scheme 13. Synthesis of Indole Starting Material for Further Functionalization .....                       | 18 |
| Scheme 14. Double Functionalization of <i>N</i> -Boc Protected Indoles .....                               | 18 |
| Scheme 15. Proline-Catalyzed Asymmetric Formal $\alpha$ -Alkylation of Aldehydes.....                      | 19 |
| Scheme 16. Imidazolidinone Catalyzed Addition of Aldehydes to Indolenine.....                              | 20 |
| Scheme 17. <i>N</i> -Heterocyclic Carbene Catalyzed Additions of Aldehydes to Indolenines .....            | 20 |
| Scheme 18. Enantioselective Alkylation Reaction of Enamides by Chiral Phosphoric Acid Catalysis .....      | 21 |
| Scheme 19. Chiral Brønsted-Base Catalyzed Addition of Malononitriles .....                                 | 22 |
| Scheme 20. Enantioselective aza-Henry Additions Using BAM Catalysis.....                                   | 24 |
| Scheme 21. Catalyst Screen: Thiourea Catalysts.....  | 36 |
| Scheme 22. Synthesis of UreaBAM Analogs .....  | 37 |
| Scheme 23. Catalyst Screen: UreaBAM Analogs.....   | 38 |
| Scheme 24. Synthesis of a Larger Variety of Electrophiles .....  | 39 |
| Scheme 25. One Pot Addition from 2-Me-Indole.....  | 48 |
| Scheme 26. Exposure of High dr Material to Reaction Conditions.....  | 55 |
| Scheme 27. Further Manipulation of Indole Adducts.....   | 56 |
| Scheme 28. Synthesis of Tricyclic Core of Posaconazole .....   | 65 |
| Scheme 29. Side Chain Synthesis and Completion of Posaconazole .....                                       | 66 |
| Scheme 30. Retrosynthetic Analysis of VNI .....  | 70 |
| Scheme 31. Synthesis of <i>N</i> -Boc-2,4-Dichlorobenzaldimine .....                                       | 73 |

|   |     |
|---|-----|
| Scheme 32. PBAM Catalyzed aza-Henry Reaction of Nitromethane: A Double Addition .....                                 | 73  |
| Scheme 33. Bromonitromethane aza-Henry Addition using an Unsymmetrical BAM Catalyst .....                             | 75  |
| Scheme 34. Synthesis of Imidazoles from Chiral Non-Racemic 1,2-Amino Alcohols .....                                   | 79  |
| Scheme 35. Scalable Imidazole Formation from Reduced aza-Henry Adduct .....   | 80  |
| Scheme 36. Synthesis of the Tri-Aryl Side Chain. ....   | 81  |
| Scheme 37. Endgame: The Synthesis of VNI.....   | 81  |
| Scheme 38. Large Scale Acylation to give VNI.....   | 83  |
| Scheme 39. Initial Reports of Enantioselective Halolactonizations using Chiral, Soichiometric Halogen Complexes.....  | 91  |
| Scheme 40. Cinchona Based Chiral Iodine Sources in Enantioselective Iodolactonization.....                            | 92  |
| Scheme 41. First Catalytic, Enantioselective Halolactonization with a Chiral Ammonium Derived from Cinchonidine. .... | 93  |
| Scheme 42 Enantioselective Chlorolactonization Reported by Borhan. ....   | 93  |
| Scheme 43. Effect of Halogen Source on Enantioselection and Yield.....  | 94  |
| Scheme 44. Urea/iodine Catalyzed Enantioselective Iodocyclization of $\delta$ -Unsaturated Acids. ....                | 95  |
| Scheme 45. Fujioka Bromolactonization of Tri- and Tetra-substituted Olefins.....                                      | 101 |
| Scheme 46. Tailored Cationic Halogenating Reagents in Halocyclization Reactions.....                                  | 102 |
| Scheme 47. Bromonitromethane Additions to Aliphatic Imines.....   | 119 |
| Scheme 48. Jacobsen's Modification of Conditions for Pentenoic Acid Derivatives. ....                                 | 130 |
| Scheme 49. Lewis Base Catalysis and Control of <i>endo</i> -/ <i>exo</i> -Selectivity in Halolactonizations.....      | 145 |
| Scheme 50. BAM Catalyzed <i>endo</i> -Bromolactonization.....   | 146 |
| Scheme 51. Initial Attempts to Study Tri-Substitued Olefinic Acids.....   | 149 |
| Scheme 52. Ishihara's Enantioselective Halocyclization of Polyprenoids. ....  | 150 |
| Scheme 53. Initial Attempts at a Cascade Reaction: Looking for Double Ring Closure. ....                              | 151 |
| Scheme 54. Carbon Dioxide Capture Using Alcohols and Amines. ....   | 152 |
| Scheme 55. Preliminary Results for the Enantioselective Iodocarboxylation of Homoallylic Alcohols. ....               | 153 |

## List of Tables

|   |     |
|---|-----|
| Table 1. Reaction Optimization from Petrini's Protocol .....  | 27  |
| Table 2. Further Reaction Optimization .....  | 28  |
| Table 3. Investigations into the Equivalents of Phenylnitromethane .....                                | 29  |
| Table 4. Phenylnitromethane Addition: Solvent Screen .....  | 30  |
| Table 5. Phenylnitromethane Addition: Exogenous Base Screen .....                                       | 31  |
| Table 6. Catalyst Screen: H,QuinBAM analogs .....   | 32  |
| Table 7. Catalyst Screen: Unsymmetrical PBAM Derivatives .....  | 33  |
| Table 8. Catalyst Screen: Steric Analogs of PBAM .....  | 35  |
| Table 9. Reaction Scope: Initial Electrophile Screen .....  | 40  |
| Table 10. Reaction Scope: Variations at the Indole 2-Position .....                                     | 41  |
| Table 11. Nucleophile Screen .....  | 43  |
| Table 12. Reaction Optimization with Water as a Cosolvent.....  | 47  |
| Table 13. Phenylnitromethane Addition to Isolated Indolenine Intermediate .....                         | 50  |
| Table 14. Comparison of BAM Catalysts in the Three Protocols .....                                      | 52  |
| Table 15. Substrate Screen Implementing all Three Methods.....  | 53  |
| Table 16. Reaction Optimization for the PBAM-Catalyzed Addition of<br>Nitromethane.....                 | 74  |
| Table 17. Optimization of Bromonitromethane Additions to <i>N</i> -Boc-2,4-<br>Dichloroaldimine.....    | 76  |
| Table 18. Large Scale Optimization of BAM Catalyzed aza-Henry .....                                     | 77  |
| Table 19. Large-Scale Optimization of One-pot Debromination/Nitro Reduction .....                       | 78  |
| Table 20. <i>T. cruzi</i> Detection by qPCR (ref. 62).....  | 89  |
| Table 21. Initial Catalyst Loading Studies with PBAM. ....  | 105 |
| Table 22. Role of Triflic Acid Equivalents.....   | 106 |
| Table 23. Catalyst Screen of BAM-Triflic Acid Salts.....  | 107 |
| Table 24. Optimization Studies and Reaction Parameter Limits for PBAM•HNTf.....                         | 112 |
| Table 25. Study of Operating Parameters for the Iodolactonization Reaction. ....                        | 114 |
| Table 26. Solvent Screen with PBAM•HNTf <sub>2</sub> as the Optimal Catalyst. ....                      | 117 |
| Table 27. Changing the Ratio of the Chiral, Brønsted Basic Catalyst to the Achiral<br>Acid.....         | 121 |
| Table 28. Final Reaction Optimization of the Most Selective Catalyst System.....                        | 122 |
| Table 29. Increasing Enantioselection for the Lactonization for the <i>para</i> -Methoxy<br>Acid.....   | 129 |
| Table 30. Attempts to Increase the Enantioselection of the $\gamma$ -Iodolactonization<br>Product. .... | 131 |

|  |     |
|--|-----|
| Table 31. Monitoring Enantiomeric Excess over Reaction Progress. ....        | 134 |
| Table 32. Catalyst Screen for <i>endo</i> -Iodolactonization.....            | 140 |
| Table 33. Reaction Optimization for the <i>endo</i> -Iodolactonization. .... | 141 |

## List of Charts

|  |     |
|--|-----|
| Chart 1. Reaction Optimization of <i>in situ</i> Indolenine Formation .....                            | 51  |
| Chart 2. Large Scale Bromonitromethane Additions to Imines Catalyzed by<br>PBAM. ....                  | 85  |
| Chart 3. Catalyst Screen of BAM-Protic Acid Salts.....   | 109 |
| Chart 4. The pK <sub>a</sub> Values of Achiral Acids used in BAM Catalyzed<br>Iodolactonizations. .... | 111 |
| Chart 5. Screen of Electronically and Sterically Diverse Pyrrolidine Bisamidine<br>Ligands. ....       | 118 |
| Chart 6. StilbPBAM and PBAM Comparison: Effect of Diamine Backbone on<br>Enantioselection .....        | 120 |
| Chart 7. Synthesis of Desired Olefinic Acids for Iodolactonization. ....                               | 125 |
| Chart 8. Substrate Scope in Enantioselective Iodolactonization of 1,1-<br>Disubstituted Acids. ....    | 126 |
| Chart 9. BAM Catalyzed Cyclizations of other Functional Groups. ....                                   | 132 |
| Chart 10. Role of the Product in Influencing Enantioselection. ....                                    | 137 |
| Chart 11. Substrate Scope for the <i>endo</i> -Iodolactonization. ....                                 | 143 |

## CHAPTER I

### I. CHIRAL BRØNSTED BASE-PROMOTED NITROALKANE ALKYLATION: ENANTIOSELECTIVE SYNTHESIS OF *SEC*-ALKYL-3-SUBSTITUTED INDOLES<sup>1</sup>

#### 1.1 Current Approaches Toward Indole Products Containing *sec*-Alkyl-3-Substitutions

##### *Background and Relevance of Indoles*

Indole and pyrrole containing alkaloids of natural and synthetic origin have garnered a significant amount of attention for their value as potential drugs. These alkaloids, produced by both terrestrial and marine organisms, are presumed to have evolved as defense mechanisms, explaining their high levels of potency and toxicity.<sup>2</sup> Over the years, the diversity and potency of these alkaloids have allowed a significant number to become viable drug leads.<sup>3</sup>

The significance of indoles and pyrroles in medicinal chemistry is validated by their recurring presence in top-grossing pharmaceuticals (Figure 1).<sup>4</sup>

---

<sup>1</sup> Dobish, M. C.; Johnston, J. N. *Org. Lett.* **2010**, *12*, 5744-5747.

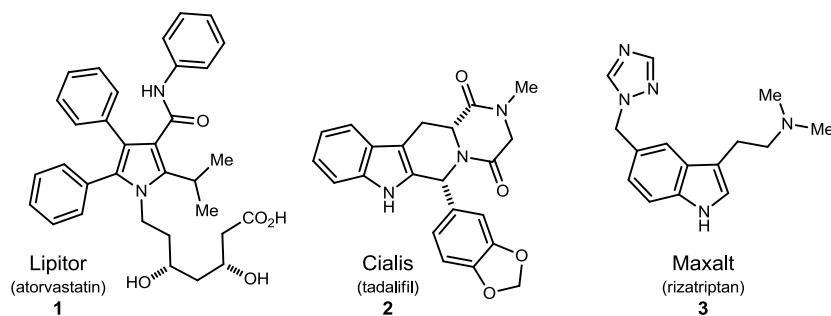
<sup>2</sup> Fattorusso, E. and Tagliatela-Scafati, O. Eds. *Modern Alkaloids. Structure, Isolation, Synthesis and Biology*; Wiley-VCH Verlag GmbH & Co. KGaA: Weinheim, Germany, 2008.

<sup>3</sup> Kochanowska-Karamyan, A. J.; Hamann, M. T. *Chem. Rev.* **2010**, *110*, 4489-4497.

<sup>4</sup> Midas World Review (TM), January 2009-December 2009, IMS Health Incorporated.

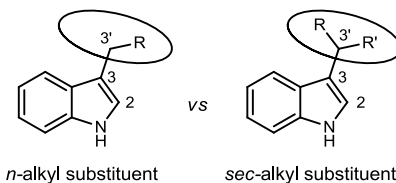


**Figure 1.** Representative Indole- and Pyrrole-Containing Pharmaceuticals in the Top 200 of Sales for the Year 2007



Lipitor (**1**), the top grossing drug for 2007, is a pyrrole containing statin that is used to treat high levels of cholesterol. Cialis (**2**) is an indole-containing drug used to treat erectile dysfunction. Maxalt (**3**) is a selective serotonin reuptake inhibitor (SSRI) that treats the symptoms of migraines. Indole and pyrrole moieties are also present in compounds that demonstrate antiviral, antimicrobial, calcium releasing, enzyme inhibition, and cytotoxic properties, to name but a few.<sup>5</sup>

Indole-containing compounds can be categorized into two structurally related classes based on the substitution at C3: (1) those bearing *n*-alkyl substitution and (2) those bearing *sec*-alkyl substitution.



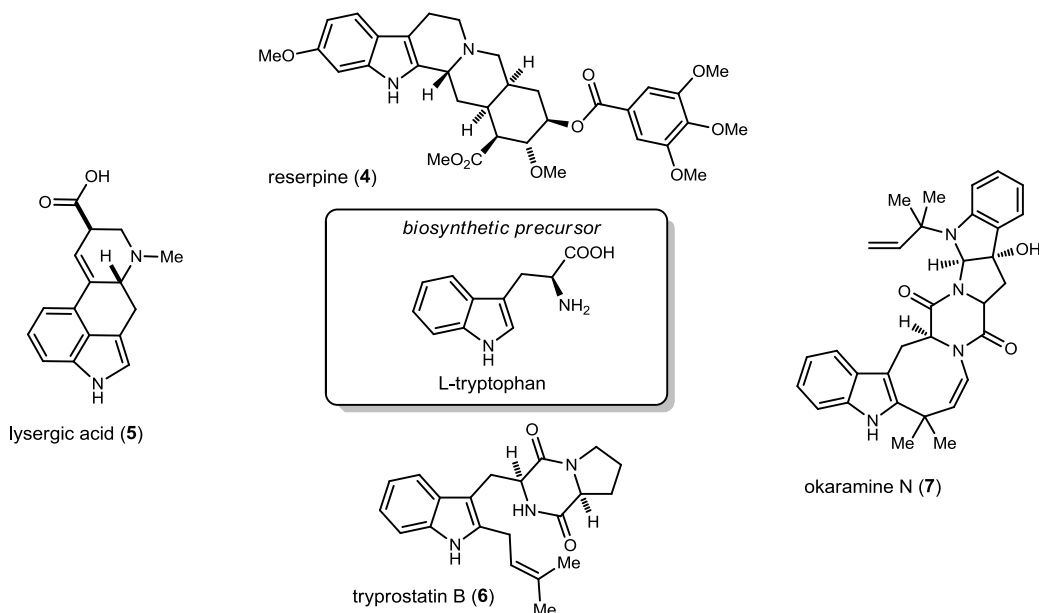
The majority of naturally occurring indole alkaloids contain C3 *n*-alkyl substitution as this fits with their proposed biosynthetic origin from tryptophan (Figure 2). For example, reserpine (**4**), isolated in 1952<sup>6</sup> and synthesized by R. B. Woodward in 1956,<sup>7</sup> was

<sup>5</sup> Gul, W.; Hamann, M. T. *Life Sci.* **2005**, *78*, 442-453.

<sup>6</sup> Muller, J. M.; Schlittler, E.; Bein, H. J. *Experientia*, **1952**, *8*, 338.

recognized for treatment of hypertensive, nervous and mental health disorders. In the same year, Woodward also reported the total synthesis of lysergic acid (**5**), an alkaloid recognized for centuries to have mind altering properties.<sup>8</sup> Danishefsky and coworkers reported the total synthesis of tryprostatin B (**6**) in 1996, a compound targeted as a potential cell cycle inhibitor.<sup>9</sup> E. J. Corey reported the total synthesis of bisindole okaramine N (**7**) in 2003, a natural product with unknown biological properties.<sup>10</sup> This list is not all encompassing and only seeks to demonstrate the complexity and utility of naturally-occurring indole containing compounds. Interest in the synthesis of indole containing compounds continues to grow and is only highlighted in the examples below.

**Figure 2.** Indole Alkaloids with C3 *n*-Alkyl Substitution



<sup>7</sup> Woodward, R. B.; Bader, F. E.; Bickel, H.; Frey, A. J.; Kierstead, R. W. *J. Am. Chem. Soc.* **1956**, *78*, 2023-2025. Woodward, R. B.; Bader, F. E.; Bickel, H.; Frey, A. J.; Kierstead, R. W. *Tetrahedron* **1958**, *2*, 1-57.

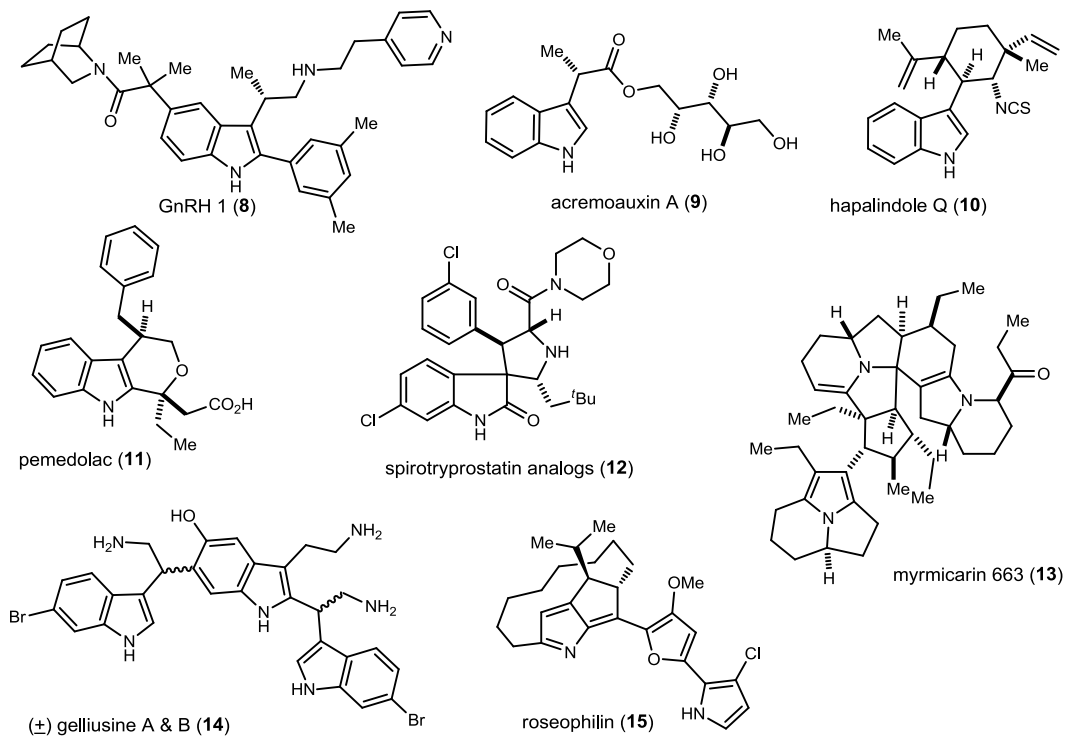
<sup>8</sup> Kornfeld, E. C.; Fornfeldt, E. J.; Kline, G. B.; Mann, M. J.; Morrison, D. E.; Jones, R. G.; Woodward, R. B. *J. Am. Chem. Soc.* **1956**, *78*, 3087-3114.

<sup>9</sup> Depew, K. M.; Danishefsky, S. J.; Rosen, N.; Sepp-Lorenzino, L. *J. Am. Chem. Soc.* **1996**, *118*, 12463-12464.

<sup>10</sup> Baran, P. S.; Guerrero, C. A.; Corey, E. J. *J. Am. Chem. Soc.* **2003**, *125*, 5628-5629.

More recently, indole alkaloids with C3 *sec*-alkyl substitution have emerged as targets of interest (Figure 3).

**Figure 3.** Representative Indole and Pyrrole Heterocycles Bearing Chiral C3 *sec*-Alkyl Substitution



The gonadotropin releasing hormone (GnRH 1, **8**) antagonist developed by Merck<sup>11</sup> and the potent plant-growth inhibitor acremauxin A (**9**)<sup>12</sup> both have a methyl substituent at the 3'-carbon. The potent analgesic pemedolac (**11**) (a close analog of the anti-inflammatory agent etodolac)<sup>13</sup> and the large class of synthetically challenging

<sup>11</sup> Farr, R. N.; Alabaster, R. J.; Chung, J. Y. L.; Craig, B.; Edwards, J. S.; Gibson, A. W.; Ho, G.-J.; Humphrey, G. R.; Johnson, S. A.; Grabowski, E. J. J. *Tetrahedron: Asymmetry* **2003**, *14*, 3503-3515.

<sup>12</sup> Richter, J. M.; Whitefield, B. W.; Maimone, T. J.; Lin, D. W.; Castroviejo, M. P.; Baran, P. S. *J. Am. Chem. Soc.* **2007**, *129*, 12857-12869.

<sup>13</sup> Katz, A. H.; Demerson, C. A.; Shaw, C. C.; Asselin, A. A.; Humber, L. G.; Conway, K. M.; Gavin, G.; Guinosso, C.; Jensen, N. P. *J. Med. Chem.* **1988**, *31*, 1244-1250.

hapalindoles (**10**)<sup>14</sup> are examples of indole alkaloids with more complicated alkyl substituents at the 3-carbon of indoles. Previously isolated and synthesized spirotryprostatin A & B<sup>9</sup> lack substitution at the C3' position; however efforts to exploit the antimetabolic activity of the spirotryprostatin class of compounds resulted in the addition of an aromatic substituent at this position to give potent analogs (**12**).<sup>15</sup> Gelliusines (**14**), isolated from the marine sponge *Orina* sp., are another class of natural products with a chiral 3'-carbon bearing an aryl substituent.<sup>16</sup> There are also a number of compounds with a pyrrole backbone containing *sec*-alkyl substitution, for example, the antibiotic roseophilin (**15**)<sup>17</sup> and the "trimer like" class of myrmicarins (**13**).<sup>18</sup>

These high interest natural products are often in low supply and, as a result, chemical syntheses are developed to make them available for biological testing and derivatization. The synthesis of these complex targets often requires development of new methodologies which in turn, opens the door to a never-ending supply of potential targets. In spite of the significant number of targets containing indole and pyrrole motifs, access to the chiral non-racemic versions is not as well established.

To synthesize these compounds one can envision disconnection between the C3-C3' bond or the C3'-C3'' bond (Figure 4).

---

<sup>14</sup> Richter, J. M.; Ishihara, Y.; Masuda, T.; Whitefield, B. W.; Llamas, T. s.; Pohjakallio, A.; Baran, P. S. *J. Am. Chem. Soc.* **2008**, *130*, 17938-17954.

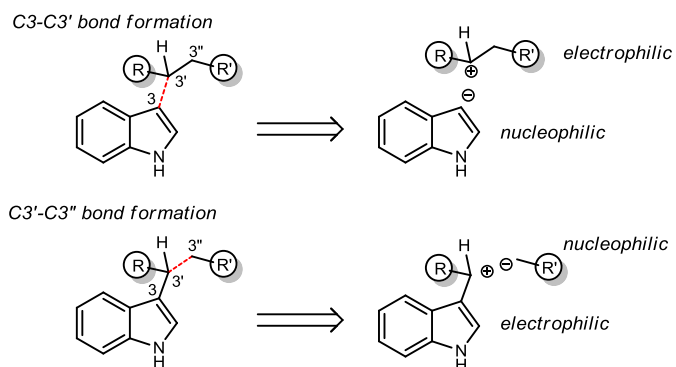
<sup>15</sup> Wang, S.; Ding, K.; Lu, Y.; Nikolovska-Coleska, Z.; Qiu, S.; Wang, G.; Qin, D.; Shangary, S. 2006, p 216 pp.

<sup>16</sup> Bifulco, G.; Bruno, I.; Minale, L.; Riccio, R.; Calignano, A.; Debitus, C. c. *J. Nat. Prod.* **1994**, *57*, 1294-1299.

<sup>17</sup> Kayakawa, Y.; Kawakami, K.; Seto, H.; Furihata, K. *Tetrahedron Lett.* **1992**, *33*, 2701-2704. Fuerstner, A.; Weintritt, H. *J. Am. Chem. Soc.* **1997**, *119*, 2944-2945.

<sup>18</sup> Schröder, F.; Sinnwell, V.; Baumann, H.; Kaib, M.; Francke, W. *Angew. Chem. Int. Ed.* **1997**, *36*, 77-80.

**Figure 4.** Different Disconnections for the Synthesis of Alkyl Indoles



In the forward sense, this would represent a new carbon-carbon bond formation between either an  $sp^3$  and  $sp^2$  center or two  $sp^3$  centers. In terms of nucleophile and electrophile partners, most reactions that have been developed thus far take advantage of either the nucleophilicity of the indole at C3 or the electrophilicity of the indole at C3'. Most of the reactions that will be discussed can be categorized as such: C3-C3' bond formation for nucleophilic indoles and C3'-C3'' for electrophilic indoles.

### ***Nucleophilic Indoles and C3-C3' Bond Formation***

Since its discovery in 1877,<sup>19</sup> the Friedel-Crafts reaction has been one of the most extensively studied carbon-carbon bond forming reactions.<sup>20</sup> Since the first reaction of amyl chloride and aluminum was discovered to give *n*-decane, a variety of nucleophiles and electrophiles have been extensively studied and reviewed.<sup>21</sup> Specifically, our interest is in the products that arise from the Friedel-Crafts alkylation between indole and nitroalkenes, resulting in substituted tryptamine precursors.

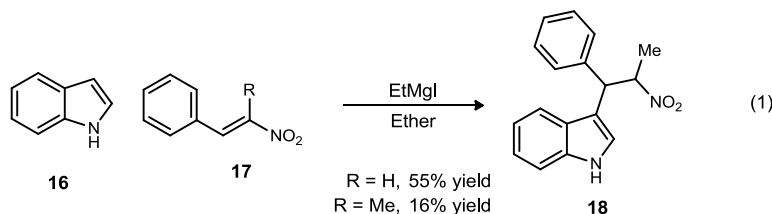
<sup>19</sup> Friedel, P.; Crafts, J. M. *Compt. Rend.* **1877**, *84*, 1392.

<sup>20</sup> A Sci-Finder search of Friedel-Crafts yields over 18,000 references.

<sup>21</sup> Calloway, N. O. *Chem. Rev.* **1935**, *17*, 327-392. Gore, P. H. *Chem. Rev.* **1955**, *55*, 229-281. Groves, J. K. *Chem. Soc. Rev.* **1972**, *1*, 73-97.

The first known report using nitroalkenes as Michael-acceptors was by Noland in 1954 (Scheme 1).<sup>22</sup>

**Scheme 1.** First Reported Use of Nitrostyrenes as Michael Acceptors



Treatment of indole with ethyl magnesium iodide to form the indolemagnesium iodide species, and subsequent addition to the nitroolefin (**17**) gave adduct **18** in good yield (55%). Using more sterically hindered  $\alpha,\beta$ -disubstituted nitrostyrene also gave the desired product, albeit in low yield (16%). Fifty years after this initial report, the Friedel-Crafts reaction between indole and nitrostyrene still draws considerable interest, now for its asymmetric variant catalyzed by both metal- and organo-catalysts.<sup>23</sup>

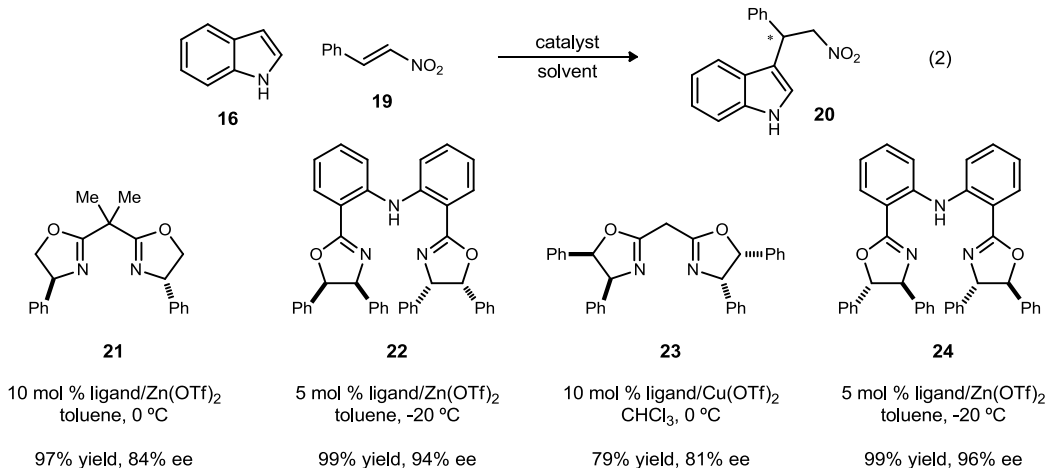
### ***Metal-Catalyzed Friedel-Crafts Reaction between Indole and Nitrostyrene***

A number of Lewis Acid bisoxazoline (BOX) complexes (**21-24**) have been developed to catalyze the enantioselective Friedel-Crafts (FC) reaction of indole and nitrostyrene (Figure 5).

<sup>22</sup> Noland, W. E.; Hartman, P. J. *J. Am. Chem. Soc.* **1954**, *76*, 3227-3228. Noland, W. E.; Christensen, G. M.; Sauer, G. L.; Dutton, G. G. S. *J. Am. Chem. Soc.* **1955**, *77*, 456-457.

<sup>23</sup> Jørgensen, K. A. *Synthesis* **2003**, 1117-1125. Bandini, M.; Melloni, A.; Umani-Ronchi, A. *Angew. Chem. Int. Ed.* **2004**, *43*, 550-556. Poulsen, T. B.; Jørgensen, K. A. *Chem. Rev.* **2008**, *108*, 2903-2915.

**Figure 5.** Chiral BOX-ligands for the Asymmetric Friedel-Crafts Reaction between Indole and Nitrostyrene



In all of the separate reports highlighted above,<sup>24</sup> a variety of Lewis Acids were screened only to reveal that the zinc and copper triflates gave the highest reactivity and selectivity. The addition of a wide range of indole nucleophiles to  $\beta$ -substituted styrene was performed in good yields with these ligands. A small number of other metal-based catalysts (such as SalenAlCl)<sup>25</sup> have had little success in this reaction.

### ***Organocatalyzed Friedel-Crafts Reaction between Indole and Nitrostyrene***

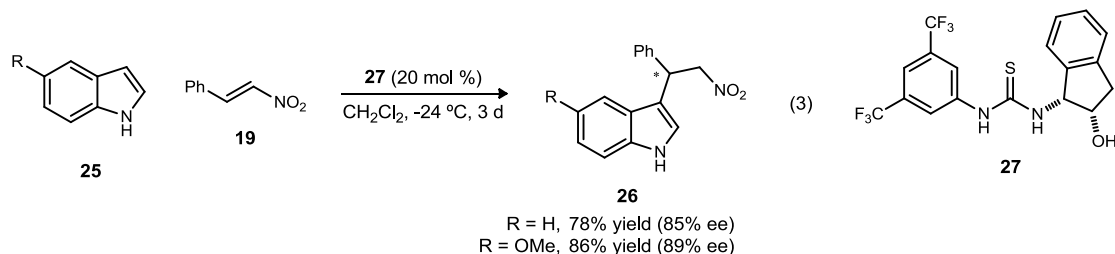
In 2005, Ricci and coworkers reported the first enantioselective organocatalytic version of this transformation using a chiral thiourea (Scheme 2).<sup>26</sup>

<sup>24</sup> Jia, Y.-X.; Zhu, S.-F.; Yang, Y.; Zhou, Q.-L. *J. Org. Chem.* **2005**, *71*, 75-80. Lu, S.-F.; Du, D.-M.; Xu, J. *Org. Lett.* **2006**, *8*, 2115-2118. Singh, P. K.; Bisai, A.; Singh, V. K. *Tetrahedron Lett.* **2007**, *48*, 1127-1129. Liu, H.; Lu, S.-F.; Xu, J.; Du, D.-M. *Chemistry – An Asian Journal* **2008**, *3*, 1111-1121.

<sup>25</sup> Bandini, M.; Garelli, A.; Rovinetti, M.; Tommasi, S.; Umami-Ronchi, A. *Chirality* **2005**, *17*, 522-529.

<sup>26</sup> Herrera, R. P.; Sgarzani, V.; Bernardi, L.; Ricci, A. *Angew. Chem. Int. Ed.* **2005**, *44*, 6576-6579.

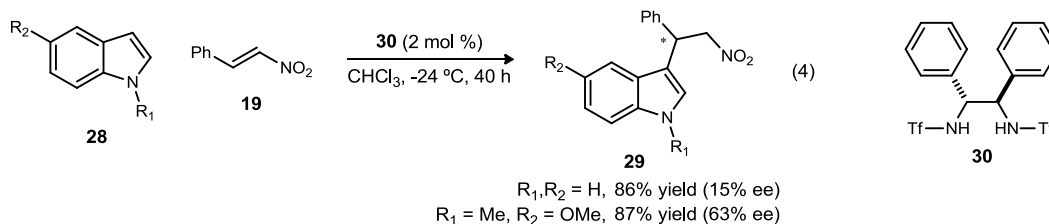
**Scheme 2.** Chiral Thiourea Catalyzed Addition of Indole to Nitrostyrene



Thioureas are known for their bifunctional binding of both the nucleophile and electrophile, with the nitroalkene binding to the thiourea moiety and the indole binding to the alcohol of the catalyst. After a screen of thiourea catalysts, the catalyst derived from indanol (**27**) was found to be the most selective. Reactivity and selectivity increased when an electron donating group (MeO-) was placed on the indole ring. The reaction was tolerant of other aryl rings as the enantioselection saw little change between substrates.

Shortly after the work by Ricci, Jørgensen and coworkers reported their enantioselective Friedel-Crafts reaction using a chiral diamine catalyst (Scheme 3).<sup>27</sup>

**Scheme 3.** Chiral Stilbene Diamine Catalyzed Addition of Indole to Nitrostyrene



Using chiral bis(sulfonamide) stilbene diamine (**30**) as the catalyst, indole addition to nitrostyrene occurred with low enantioselection (15% ee). A methoxy group (R<sub>2</sub>) on the

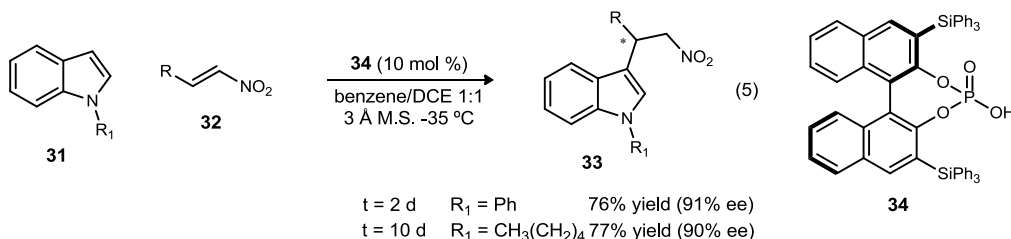
<sup>27</sup> Jørgensen, K. A. *Synthesis* **2003**, 1117-1125.



protected *N*-methyl indole increased the enantioselection dramatically, but the high ee levels obtained by Ricci were not matched.

The use of chiral phosphoric acids to catalyze the Friedel-Crafts addition to nitrostyrenes was first reported in 2008 by Akiyama and coworkers (Scheme 4).<sup>28</sup>

**Scheme 4.** Chiral Phosphoric Acid Catalyzed Addition of Indole to Nitroalkenes



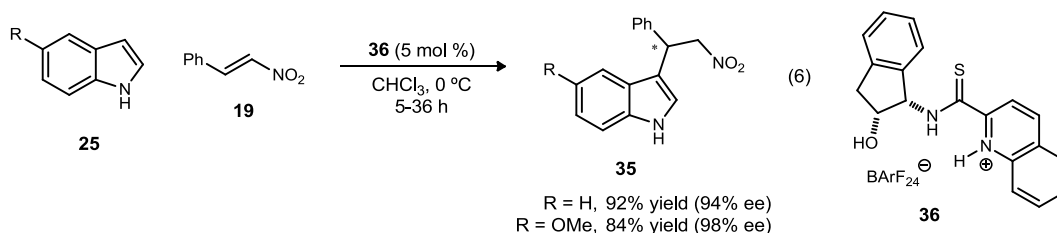
High values of enantioselection were reported for a variety of substrates. Most notably, aliphatic substituted nitroalkenes also gave good yields and high ee despite longer reaction times (10 days). Molecular sieves proved to be essential for conversion in this reaction as very little product (5%), though still with good selectivity (75% ee), was isolated without sieves.

In 2008, the Seidel group had a breakthrough and reported on the use of hydrogen bonding catalysts for the enantioselective Friedel-Crafts reaction (Scheme 5).<sup>29</sup>

<sup>28</sup> Itoh, J.; Fuchibe, K.; Akiyama, T. *Angew. Chem. Int. Ed.* **2008**, *47*, 4016-4018.

<sup>29</sup> Ganesh, M.; Seidel, D. *J. Am. Chem. Soc.* **2008**, *130*, 16464-16465.

**Scheme 5.** Protonated Thioureas as Highly Reactive and Selective Catalysts

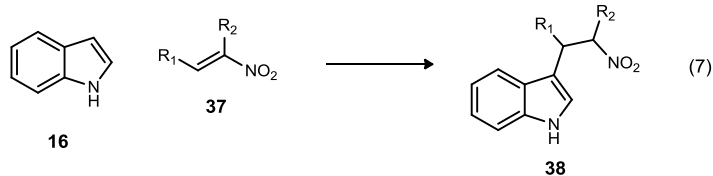


When they used the Ricci thiourea (**27**), the reaction delivered product that was only 36% ee. When the catalyst was protonated with the “BArF acid”, they not only observed acceleration in the reaction rate, but an increase in enantioselection. Further catalyst development led to the development of **36**, which when protonated delivered the standard adduct **35** in 92% ee and 94% ee. The reaction scope was extremely broad, tolerating a variety of substrates at multiple positions on the indole, as well as different substitutions on the nitrostyrene. This reaction is currently the most selective and general for the addition of indole to nitrostyrene for all reported organocatalysts.

***Friedel-Crafts Reaction between Indole and  $\alpha,\beta$ -Disubstituted Nitrostyrenes***

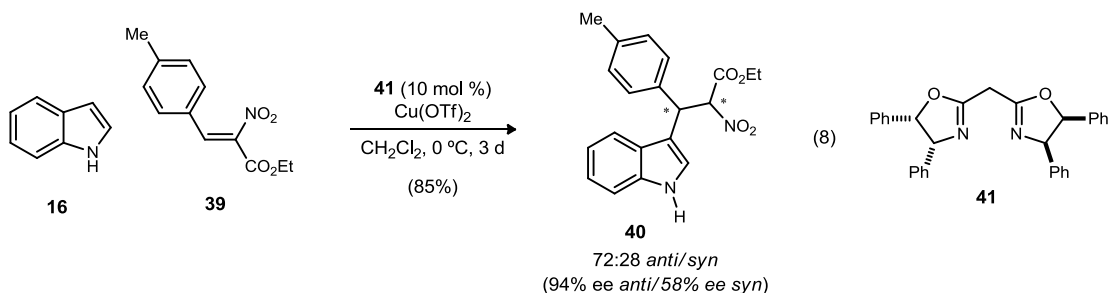
Though significant strides have been made in the enantioselective Friedel-Crafts reaction of indole and  $\beta$ -nitrostyrenes, the enantioselective variant between indole and  $\alpha,\beta$ -disubstituted nitrostyrenes remains unexplored (eq 7). The reported racemic versions often require relatively harsh conditions, resulting in chiral racemic material.<sup>30</sup>

<sup>30</sup> Gore, P. H. *Chem. Rev.* **1955**, *55*, 229-281. Bandini, M.; Melchiorre, P.; Melloni, A.; Umami-Ronchi, A. *Synthesis* **2002**, 1110-1114. Ballini, R.; Clemente, R. R.; Palmieri, A.; Petrini, M. *Adv. Synth. Catal.* **2006**, *348*, 191-196. Kusrkar, R.; Alkobati, N.; Gokule, A.; Chaudhari, P.; Waghchaure, P. *Synth. Commun.* **2006**, *36*, 1075-1081. Kantam, M. L.; Laha, S.; Yadav, J.; Srinivas, P. *Synth. Commun.* **2009**, *39*, 4100-4108. Ye, M.-C.; Yang, Y.-Y.; Tang, Y.; Sun, X.-L.; Ma, Z.; Qin, W.-M. *Synlett* **2006**, 1240-1244. Habib, P. M.; Kavala, V.; Raju, B. R.; Kuo, C.-W.; Huang, W.-C.; Yao, C.-F. *Eur. J. Org. Chem.* **2009**, 4503-4514.



The use of a second activating group (ester) on the nitroolefin has allowed for the synthesis of chiral non-racemic products. The asymmetric Friedel-Crafts reaction between indole and nitroacrylates has been successfully executed using a DiPh-BOX(**41**)-copper triflate complex (Scheme 6).<sup>31</sup>

**Scheme 6.** Enantioselective Friedel-Crafts Alkylation with  $\alpha,\beta$ -Disubstituted Nitroalkenes

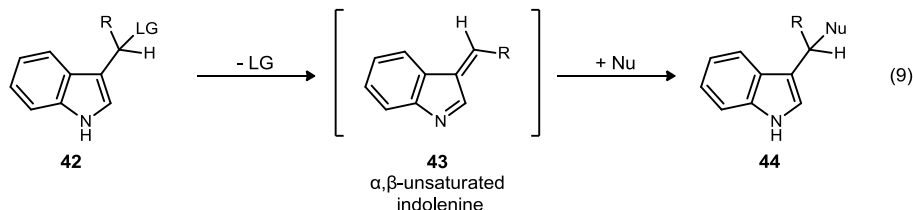


The reaction occurred diastereoselectively (up to 3:1 favoring the *anti*-diastereomer) with the *anti*-diastereomer giving the highest values of enantioselection (94% ee). To the best of our knowledge, this is the first report of an enantioselective addition to  $\alpha,\beta$ -disubstituted nitroolefins, while asymmetric versions where the  $\alpha$ -substituent is non-activating (alkyl, etc.) are nonexistent.

### ***Electrophilic Indole and C3'-C3'' Bond Formation***

Carbon-carbon bond formation also occurs when an electrophilic indole moiety is reacted with a nucleophile. The key intermediate in this step is the  $\alpha,\beta$ -unsaturated indolenine, often formed *in situ* due to its high reactivity (Scheme 7).

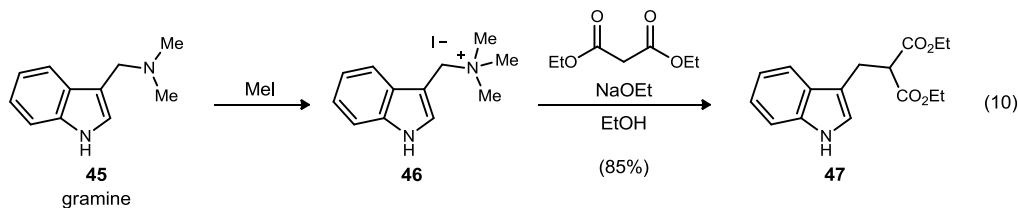
<sup>31</sup> Sui, Y.; Liu, L.; Zhao, J.-L.; Wang, D.; Chen, Y.-J. *Tetrahedron* **2007**, *63*, 5173-5183.

**Scheme 7. Nucleophilic Addition to Indolenines**

Upon treatment of indole **42** with acid or base, elimination of the leaving group reveals the indolenine intermediate (**43**). This highly reactive intermediate can then undergo nucleophilic addition to form a highly functionalized indole (**44**). This sequence has been exploited with a variety of leaving groups and electrophiles.

**Gramine as an Indolenine Precursor**

One of the earliest examples of indolenine formation, reported by Snyder in 1944, was accessed by forming the quaternary ammonium salts of gramine (Scheme 8).<sup>32</sup>

**Scheme 8. Gramine as an Indolenine Precursor**

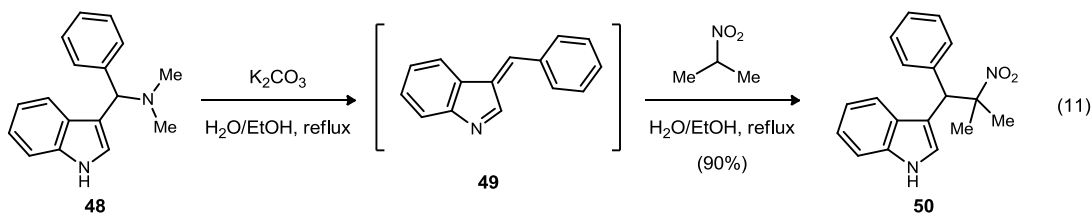
These stable precursors to indolenine are formed by treatment of gramine with methyl iodide to give quaternary ammonium salt **46**. Subsequent treatment with sodium ethoxide and diethyl malonate gave the desired product (**47**) in high yields. This was demonstrated with a variety of malonic ester derivatives as well as indole analogs. The use of gramine

<sup>32</sup> Snyder, H. R.; Smith, C. W.; Stewart, J. M. *J. Am. Chem. Soc.* **1944**, *66*, 200-204.

and other derivatives have been extensively studied and reviewed since this initial report.<sup>33</sup>

A recent example illustrates the use of gramine derivatives in the synthesis of highly substituted tryptamine analogs (Scheme 9).<sup>34</sup>

**Scheme 9.** Addition of Nitroalkanes to Gramine-derived Indolenine Intermediates



Substituted gramine analog (**48**) was refluxed with aqueous potassium carbonate to form the indolenine intermediate (**49**) *in situ* with elimination of dimethylamine. Addition of various nitroalkanes produced substituted tryptamine precursors (**50**) in high yields, though with limited functionality.

### ***Arylsulfonyl Indoles as Indolenine Precursors***

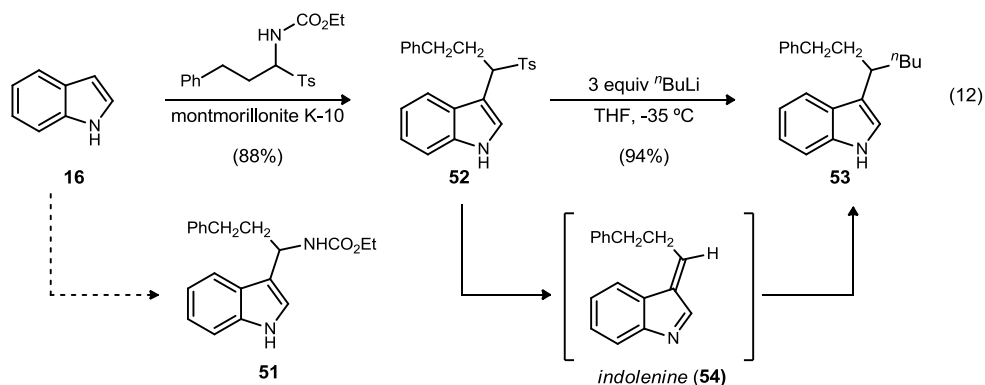
Indolenine formation via other leaving groups, such as halogens and alcohols, has also been explored. However, our interest is focused on the use of arylsulfonyl indoles as stable precursors to indolenines. In 2006, Petrini reported the synthesis and use of 3-arylsulfonylalkyl indoles as indolenine precursors (Scheme 10).<sup>35</sup>

<sup>33</sup> Semenov, B. B.; Granik, V. G. *Pharm. Chem. J.* **2004**, *38*, 287-310.

<sup>34</sup> Semenov, B. B.; Smushkevich, Y. I. *Rus. Chem. Bull.* **2002**, *51*, 185.

<sup>35</sup> Ballini, R.; Palmieri, A.; Petrini, M.; Torregiani, E. *Org. Lett.* **2006**, *8*, 4093-4096.

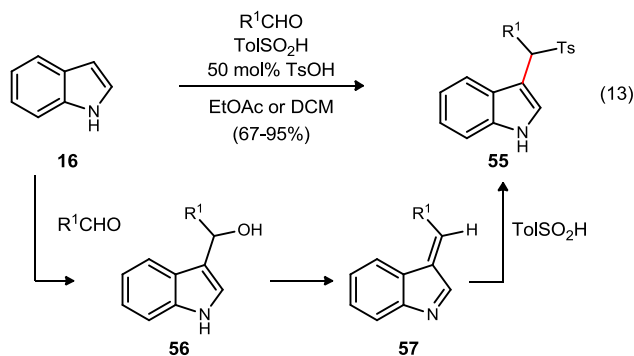
**Scheme 10.** Petrini's Synthesis of Arylsulfonyl Indoles



They envisioned an *in situ* acid-catalyzed aldimine formation with loss of the tosyl group followed by nucleophilic attack of indole to yield **51**. However, the isolated product (**52**) had incorporated the tosyl group instead of the carbamate group. Subsequent addition of three equivalents of butyllithium resulted in elimination to form the indolenine (**54**) and butyllithium addition to give **53** in high yield.

A more direct synthesis of arylsulfonyl indoles was later reported using the desired aldehyde and an arylsulfinic acid under catalytic acid conditions (Scheme 11).<sup>36</sup>

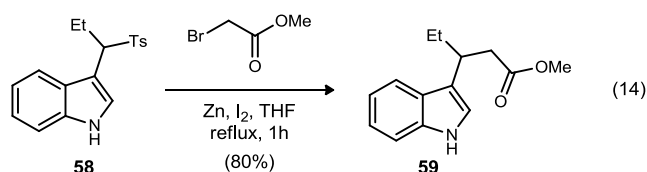
**Scheme 11.** Modified Synthesis of Arylsulfonyl Indoles



<sup>36</sup> Palmieri, A.; Petrini, M. *J. Org. Chem.* **2007**, *72*, 1863-1866.

Under these conditions, it is hypothesized that the indole adds to the aldehyde to form the indolyl alcohol (**56**), which then eliminates the elements of water to form the indolenine intermediate (**57**). The arylsulfonic acid then traps this intermediate affording the arylsulfonyl alkyl indoles (**55**) in good yields. Alternatively, using a second equivalent of indole as the trapping agent yields the bis(indole) compound.<sup>37</sup>

These arylsulfonyl indoles have been used extensively since the initial reports under a variety of reaction conditions.<sup>38</sup> The reaction with Reformatsky-enolates was one of the first applications of these precursors (eq 14).



The  $\alpha$ -bromo ester was treated with zinc metal, iodine, and the arylsulfonyl indole, and refluxed in THF. One equivalent of the Reformatsky-enolate effects the elimination and the second equivalent then adds to the formed indolenine (similar to the alkyl lithium in Scheme 10) to give **59** in good yields.

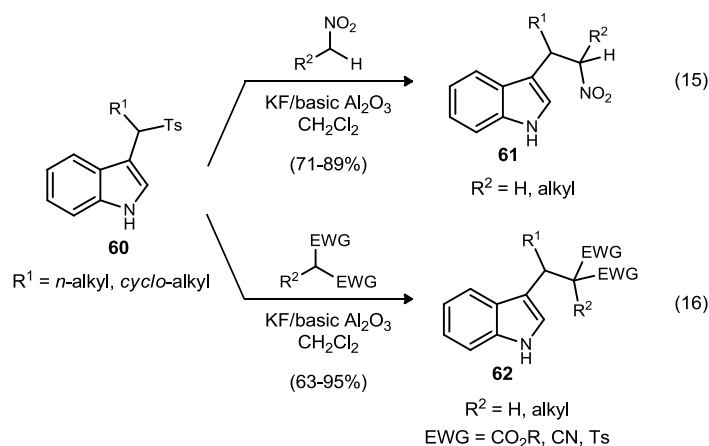
Shortly after this report, the use of an exogenous base eliminated the need for excess nucleophile (Scheme 12).<sup>39</sup>

<sup>37</sup> Deb, M. L.; Bhuyan, P. J. *Tetrahedron Lett.* **2006**, *47*, 1441-1443.

<sup>38</sup> For a review see Palmieri, A.; Petrini, M.; Shaikh, R. R. *Org. Biomol. Chem.* **2010**, *8*, 1259-1270.

<sup>39</sup> Ballini, R.; Palmieri, A.; Petrini, M.; Shaikh, R. *Adv. Synth. Catal.* **2008**, *350*, 129-134.

**Scheme 12.** Additions of Nitroalkanes and Malonates

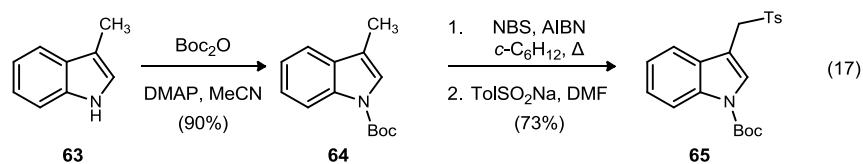
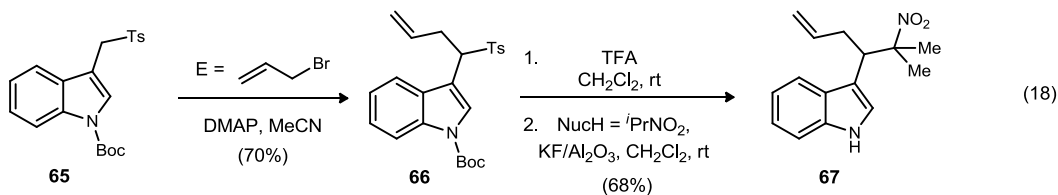


Initial attempts used sodium hydride (not shown) as the exogenous base, and upon heating provided the adducts of type **61** in good yields. However, sodium hydride was not compatible with several functional groups so other exogenous bases were examined. Examination of potassium fluoride on alumina in methylene chloride at room temperature revealed facile elimination to the indolenine and catalyzed addition of the nucleophile. Both primary and secondary nitroalkanes, as well as symmetrical and unsymmetrical malonate derivatives gave the desired products (**61** and **62**) in high yields.

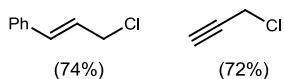
An alternate synthesis of arylsulfonyl alkyl indoles takes advantage of the increased acidity of the  $\alpha$ -proton of sulfonyl groups. The starting indole (**65**) is synthesized in three steps from 3-methylindole by protection of the indole with a Boc group, bromination and nucleophilic attack of the tosylsulfinate (Scheme 13).<sup>40</sup>

<sup>40</sup> Palmieri, A.; Petrini, M.; Shaikh, R. R. *Synlett* **2008**, 1845,1851.

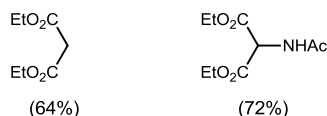
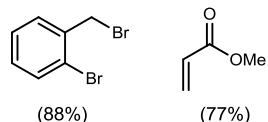


**Scheme 13.** Synthesis of Indole Starting Material for Further Functionalization**Scheme 14.** Double Functionalization of *N*-Boc Protected Indoles

other notable E (yields):



other notable NuCH (yields over 2 steps):

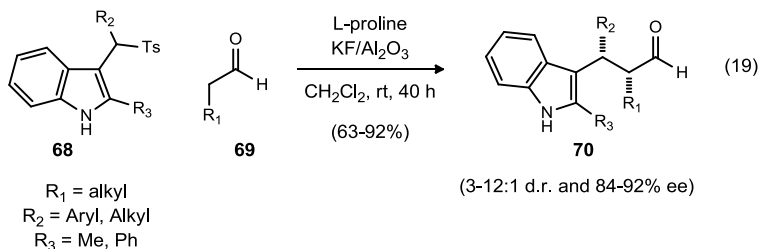


The sulfonyl  $\alpha$ -proton of indole **65** is then deprotonated using DMAP and quenched with an electrophile, providing the protected indole adducts (**66**) in good yields (Scheme 14). Deprotection with TFA and subsequent addition of base and the nucleophile affords the desired doubly functionalized indoles (**67**). This synthetic strategy requires additional synthetic operations than the previously discussed conditions (Scheme 11), but is useful when the aldehydes are not easily obtained or do not react under the previously discussed conditions.

## Enantioselective Additions to Indolenines

One of the first reported instances of indolenine intermediates in asymmetric catalysis is the  $\alpha$ -alkylation of aldehydes by Petrini and coworkers in 2008 (Scheme 15).<sup>41</sup>

**Scheme 15.** Proline-Catalyzed Asymmetric Formal  $\alpha$ -Alkylation of Aldehydes

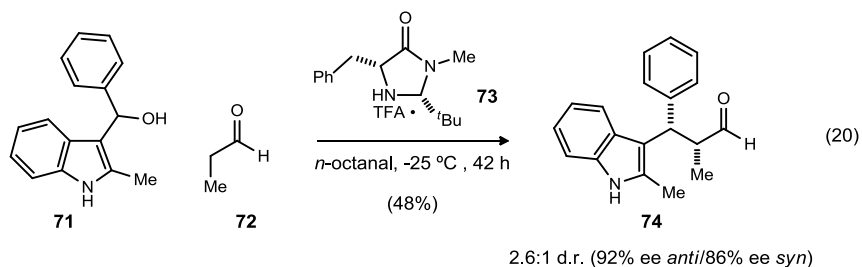


After screening a variety of bases, solvents and catalysts, it was realized that when sulfone **68** was stirred with KF on solid supported alumina, L-proline catalyzed addition of the aldehyde via an enamine intermediate gave good yields of the desired product (**70**) with high diastereo- and enantioselection. This reaction performed best when the  $\alpha$ -substituent (R<sub>1</sub>) of the aldehyde was an alkyl chain, R<sub>2</sub> was an aryl group and R<sub>3</sub> was either methyl or phenyl. The steric bulk at the 2-position proved to be important as enantioselection was almost nonexistent (11% ee) with no substituent (R<sub>3</sub>=H). Petrini and coworkers established this new reaction with acceptable values of enantioselection and reactivity that has since been exploited in other catalytic systems.

Indolyl alcohols were also utilized in this transformation under acidic conditions (Scheme 16).<sup>42</sup>

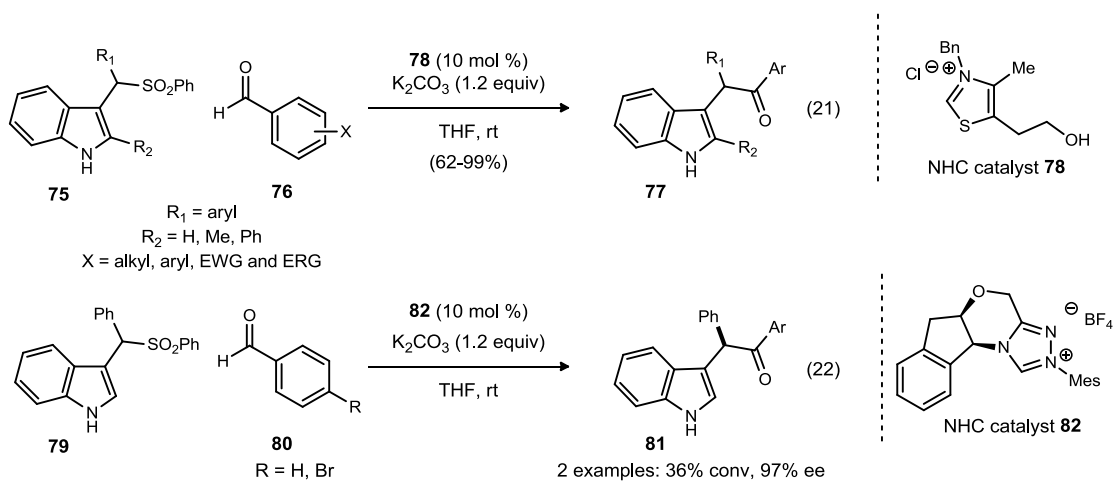
<sup>41</sup> Shaikh, R.; Mazzanti, A.; Petrini, M.; Bartoli, G.; Melchiorre, P. *Angew. Chem. Int. Ed.* **2008**, *47*, 8707-8710.

<sup>42</sup> Cozzi, P.; Benfatti, F.; Zoli, L. *Angew. Chem. Int. Ed.* **2009**, *48*, 1313-1316.

**Scheme 16.** Imidazolidinone Catalyzed Addition of Aldehydes to Indolenine

Catalyzed by imidazolidinone **73**, propionaldehyde (**72**) was added to arylindole **71** with good enantioselectivity and moderate diastereoselection via an enamine addition. The acid promoted elimination of water allowed for the indolenine intermediate to form *in situ* without the need of base, allowing for the compatibility of base-labile functionalities on the starting indoles.

Shortly after the report by Petrini, You and coworkers reported additions to these highly reactive indolenine intermediates using *N*-heterocyclic carbene (NHC) catalysis (Scheme 17).<sup>43</sup>

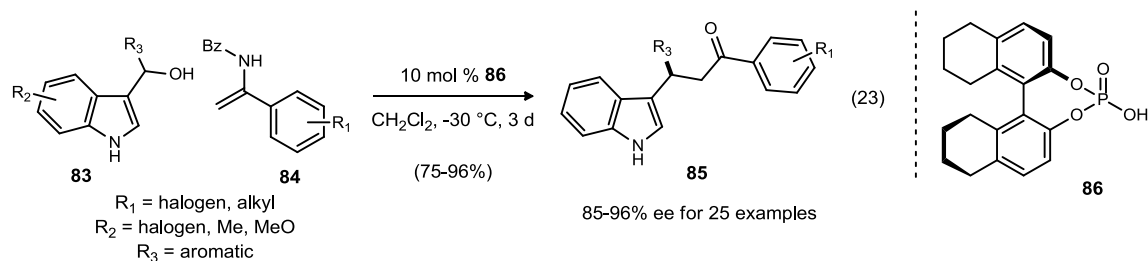
**Scheme 17.** *N*-Heterocyclic Carbene Catalyzed Additions of Aldehydes to Indolenines

<sup>43</sup> Li, Y.; Shi, F. Q.; He, Q. L.; You, S. L. *Org. Lett.* **2009**, *11*, 3182-3185.

The NHC cross-coupling of aryl aldehydes with arylsulfonyl indoles was demonstrated in good yields and high tolerance for a variety of sterically and electronically diverse substrates in both the R<sub>1</sub> and Ar positions. The reaction was not as efficient when either the aldehyde or R<sub>1</sub> was aliphatic (30-50% yields). Of greater interest is their initial exploration into an enantioselective variant. Using NHC catalyst **82**, developed by Rovis and coworkers,<sup>44</sup> the reactions proceeded with high enantioselection but suffered from low conversion. With a more reactive catalyst, this reaction may prove to be a viable method for accessing enantiopure indoles (**81**).

Enantioselectivity can also be obtained using a chiral catalyst to bind to the electrophile through a catalyst/electrophile complex or chelation. Gong and coworkers reported the addition of enamides under chiral Brønsted acidic conditions (Scheme 18).<sup>45</sup>

**Scheme 18.** Enantioselective Alkylation Reaction of Enamides by Chiral Phosphoric Acid Catalysis

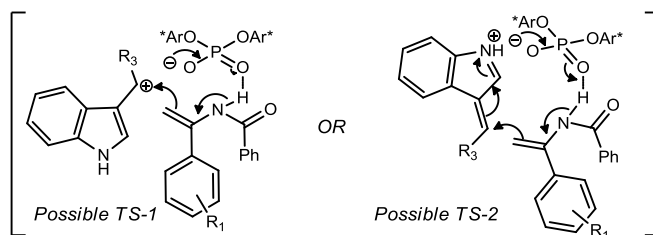


Using chiral phosphoric acid **86**, the addition of enamides (**84**) to indolyl alcohols (**83**) occurred with good enantioselection and yields. Under acidic conditions, the reactive indolenine intermediate is formed with the loss of the elements of water. Most variations

<sup>44</sup> Kerr, M. S.; Read de Alaniz, J.; Rovis, T. *J. Org. Chem.* **2005**, *70*, 5725-5728.

<sup>45</sup> Guo, Q.-X.; Peng, Y.-G.; Zhang, J.-W.; Song, L.; Feng, Z.; Gong, L.-Z. *Org. Lett.* **2009**, *11*, 4620-4623.

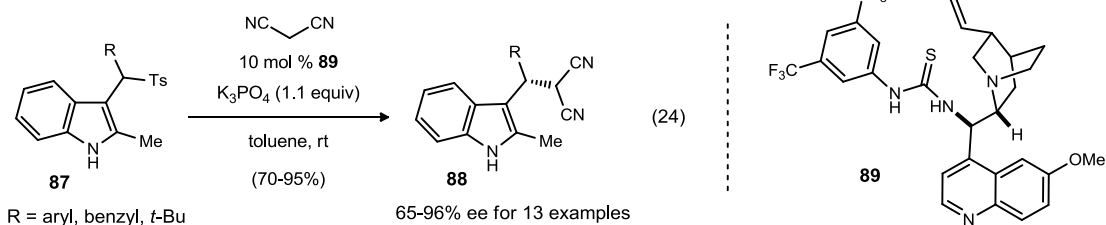
at R<sub>1</sub>, R<sub>2</sub>, and R<sub>3</sub> were well tolerated with the exception of an aliphatic group at R<sub>3</sub> (no desired product was observed). This could be the result of the aliphatic group's inability to stabilize the carbocation proposed in the transition state (TS-1).



The authors propose two transition states or possible modes of binding for the catalyst, accounting for either a stabilized benzylic cation (TS-1) or an  $\alpha,\beta$ -unsaturated indolenine intermediate (TS-2). Both transition states allow for a chiral ion pair to form acting as the point of chiral induction.

In 2010, Zhou and coworkers reported the first use of a chiral Brønsted-base catalyst to promote addition to the highly reactive indolenine intermediate (Scheme 19).<sup>46</sup>

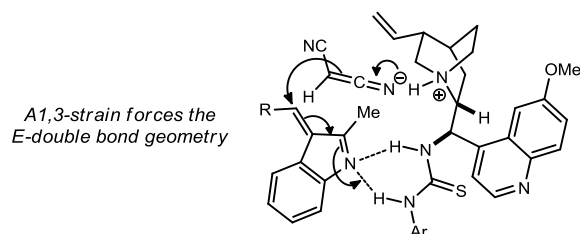
**Scheme 19.** Chiral Brønsted-Base Catalyzed Addition of Malononitriles



The addition of malononitrile proceeded with chiral thiourea **89** (10 mol %) and potassium phosphate in good enantioselection for a variety of aryl indole derivatives. Enantioselection was also observed for benzyl and *tert*-butyl analogs (R position), while

<sup>46</sup> Jing, L.; Wei, J.; Zhou, L.; Huang, Z.; Li, Z.; Wu, D.; Xiang, H.; Zhou, X. *Chem.—Eur. J.* **2010**, *16*, 10955-10958.

no *n*-alkyl derivatives were reported. Further variations in the nucleophile and 2-position were not explored. The presence of the indole 2-methyl might be important for enantioselection because of the influence of steric bulk on the double bond configuration, as seen in the proposed binding model with the *E*-configured double bond.



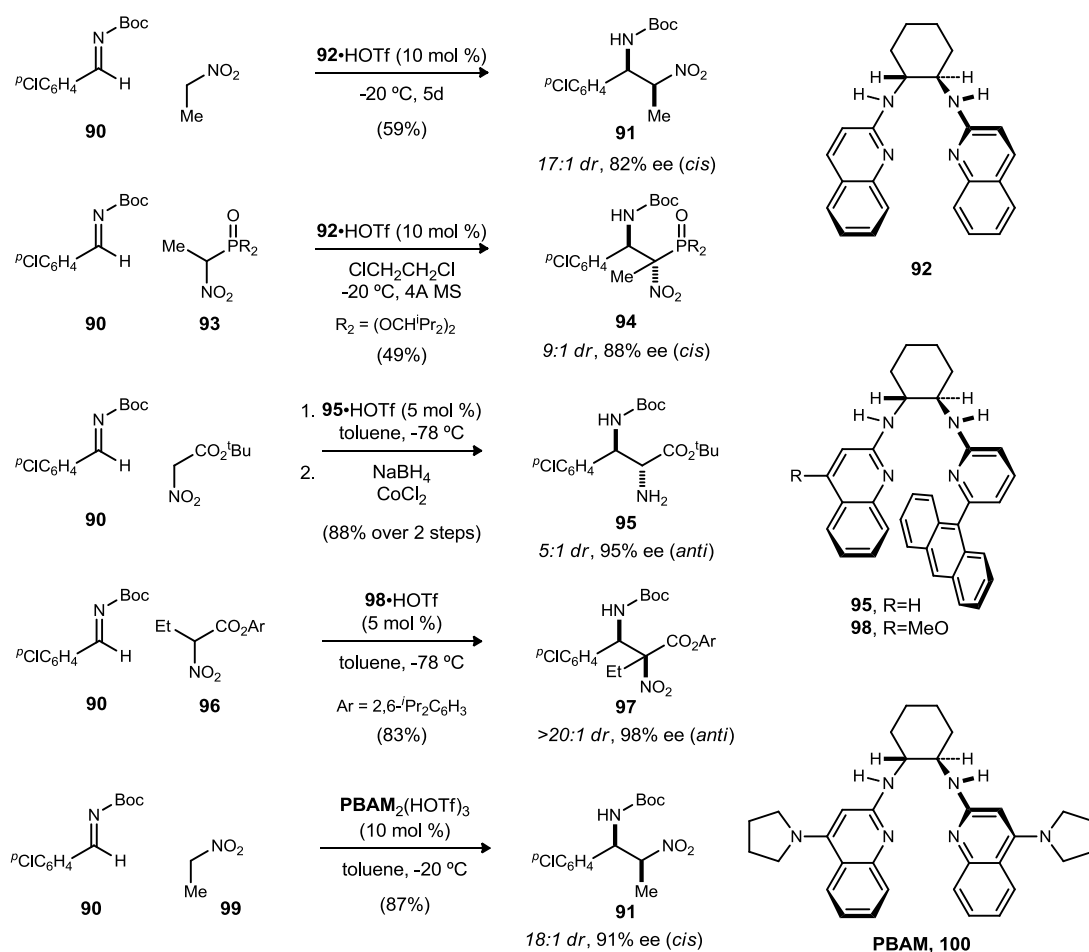
If the methyl group is not present, the double bond may be present as both *E*- and *Z*-isomers, thereby decreasing the enantioselection. Despite the limited substrate scope, this marked the first report of Brønsted base catalyzed enantioselective addition of malononitrile and has further opened avenues to other asymmetric transformations.

## 1.2 Chiral Bisamidine-Promoted Nitroalkane Alkylations

### Previous Work in BAM Catalyzed Additions

Our group has achieved success in the highly enantioselective, Bis(AMidine) (BAM) catalyzed addition of nitroalkanes to imine analogs (Scheme 20).

**Scheme 20.** Enantioselective aza-Henry Additions Using BAM Catalysis



High selectivity has been observed with a variety of nitroalkanes containing different substitutions.<sup>47,48,49,50,51,52</sup> More notably, an increase in reactivity has also been realized from the first generation catalyst <sup>4</sup>H,QuinBAM (**92**)<sup>47</sup> to a more Brønsted basic catalyst H,<sup>4</sup>PyrrolidineQuin-BAM (PBAM, **100**)<sup>52</sup> allowing for additions of simple nitroalkanes in stoichiometric amounts in contrast to the large excess originally needed. The increased reactivity of this catalyst has encouraged us to investigate other combinations of electrophiles and nucleophiles.

### *Preliminary Results from Bisamidine Catalyzed Additions*

Shortly after Petrini reported the L-proline catalyzed alkylation of aldehydes, we began our work on the enantioselective addition of nitroalkanes to indolenine intermediates using our BAM catalysts (Figure 6).

---

<sup>47</sup> Nugent, B. M.; Yoder, R. A.; Johnston, J. N. *J. Am. Chem. Soc.* **2004**, *126*, 3418-3419.

<sup>48</sup> Singh, A.; Yoder, R. A.; Shen, B.; Johnston, J. N. *J. Am. Chem. Soc.* **2007**, *129*, 3466-3467.

<sup>49</sup> Shen, B.; Johnston, J. N. *Org. Lett.* **2008**, *10*, 4397-4400.

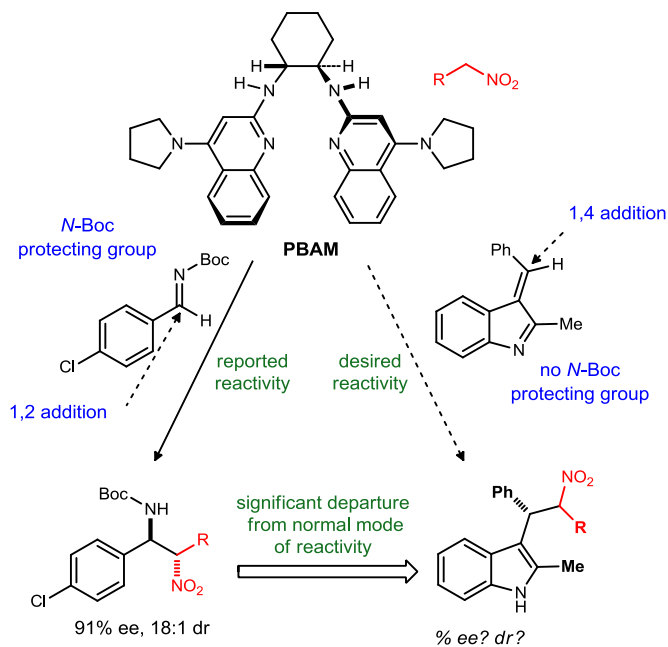
<sup>50</sup> Singh, A.; Johnston, J. N. *J. Am. Chem. Soc.* **2008**, *130*, 5866-5867.

<sup>51</sup> Wilt, J. C.; Pink, M.; Johnston, J. N. *Chem. Commun.* **2008**, 4177-4179.

<sup>52</sup> Davis, T. A.; Wilt, J. C.; Johnston, J. N. *J. Am. Chem. Soc.* **2010**, *132*, 2880-2882.

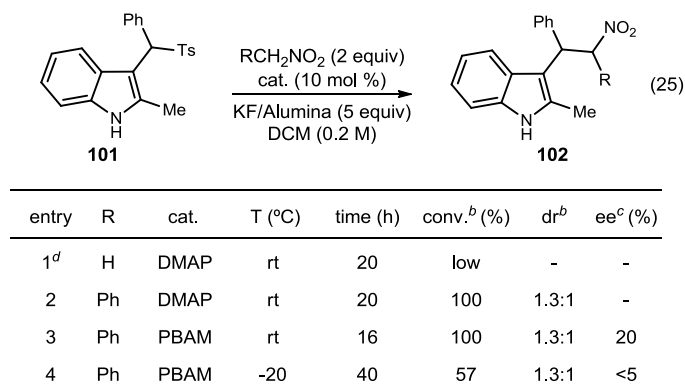


**Figure 6.** Previously Reported BAM Reactivity and Desired Additions of Phenylnitromethane to Indolenine Intermediates



We hypothesized that we could selectively add nitroalkanes in a 1,4-manner if our catalyst provided a chiral proton binding element to the indolenine intermediate. All previous works utilize BAM catalysts for 1,2-additions of nitroalkanes to *N*-Boc aryl aldimines, so expected an amount of optimization to be required.

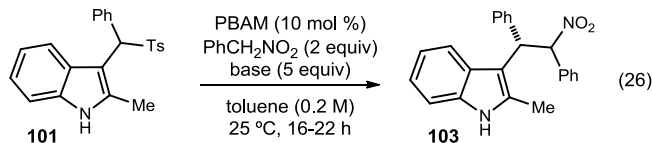
In order to gauge selectivity in the 1,4-additions to indolenines, we initially used the Petrini protocol for a direct comparison (Table 1).<sup>41</sup>

**Table 1.** Reaction Optimization from Petrini's Protocol

<sup>a</sup> All reactions were 0.2 M unless otherwise specified. <sup>b</sup> Conversions and dr measured by <sup>1</sup>H NMR. <sup>c</sup> Enantiomeric excess measured by HPLC using chiral stationary phase. <sup>d</sup> 3 equivalents of MeNO<sub>2</sub> used.

Before the selectivity of the BAM catalysts was examined, the racemic adducts were formed using DMAP, an achiral catalyst deemed similar to PBAM in terms of reactivity. Using nitromethane and phenylnitromethane, progress of the reaction was monitored after stirring overnight, and phenylnitromethane gave full conversion to indole **102** (Table 1, entry 2) while nitromethane gave low conversion (Table 1, entry 1). Thus phenylnitromethane was used as the nucleophile of choice for reaction optimization using PBAM as the chiral Brønsted base. Phenylnitromethane added to indole **101** and gave the desired adduct in 20% ee (Table 1, entry 3). In order to increase selectivity, the reaction was run under cryogenic conditions. However, the conversion and enantioselection of the product dropped dramatically (Table 1, entry 4).

The enantioselectivity (20% ee) observed at room temperature was low but encouraging as this is the first enantioselective 1,4-addition of nitroalkanes using a BAM catalyst. Additionally, this is the first successful use of a substrate lacking an *N*-Boc protecting group for this class of catalysts. The ee was believed to be tunable so we sought other means of increasing the enantioselection (Table 2).

**Table 2.** Further Reaction Optimization

| entry           | cat. | base                                     | T (°C) | conv. (%) | ee (%) |
|-----------------|------|--|--------|-----------|--------|
| 1               | PBAM | KF/Al                                    | rt     | 100       | 60     |
| 2               | PBAM | KF/Al                                    | 10     | 100       | 47     |
| 3               | PBAM | KF/Al                                    | -20    | 48        | 57     |
| 4 <sup>b</sup>  | PBAM | KF/Al                                    | -78    | 40        | 49     |
| 5               | PBAM | KF/Al (2 equiv)                          | rt     | 85        | 35     |
| 6 <sup>c</sup>  | PBAM | -  | rt     | 30        | 33     |
| 7               | -    | KF/Al                                    | rt     | 85        | -      |
| 8 <sup>d</sup>  | -    | K <sub>2</sub> CO <sub>3</sub> (7 equiv) | rt     | 50        | -      |
| 9               | PBAM | K <sub>2</sub> CO <sub>3</sub> (7 equiv) | rt     | 80        | 70     |
| 10 <sup>f</sup> | PBAM | K <sub>2</sub> CO <sub>3</sub> (7 equiv) | rt     | 83        | 78     |

<sup>a</sup> All reactions were performed on a 0.10 mmol scale using 1 equivalent of the indole and run for 16-22 h under the conditions listed. Product was isolated as <1.6:1 dr unless otherwise noted. <sup>b</sup> Reaction ran for 72 h. <sup>c</sup> 20 mol % PBAM used. <sup>d</sup> 1.5 equiv of phenylnitromethane used. <sup>e</sup> Ran at 0.1 M.

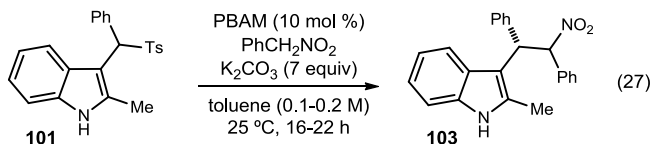
Previously reported BAM catalyzed additions demonstrated higher enantioselection in toluene. We were pleased to see that this reaction was no different as switching the solvent to toluene resulted in a large increase in enantioselection, from 20% to 60% (Table 2, entry 1). The reaction was subjected to cryogenic conditions again, but as observed previously, the enantioselectivity dropped (Table 2, entries 2-4). The poor selectivity at low temperatures is believed to be due to the sluggish elimination step (to be discussed in detail later in the chapter). Decreasing the equivalents of base gave decreased enantioselection (Table 2, entry 5). In order to evaluate the background rate, the reaction was run with PBAM but no exogenous base (Table 2, entry 6). Clearly a full equivalent of base is necessary to effect the elimination of the tosyl group, as is evidenced by poor conversion of starting material. When the reaction was performed with

only KF/Al (Table 2, entry 7) it was realized that KF/Al promoted the elimination as well as the nucleophilic addition. This high background rate would explain the lower enantioselection. As a result, a less reactive inorganic base was sought. Potassium carbonate was chosen and demonstrated lower conversion to product when used as the sole source of base in the reaction (Table 2, entry 8). An increase in ee was observed when using potassium carbonate and PBAM in the reaction (Table 2, entry 9). When the reaction was run under more dilute conditions (0.1 M) we saw a further increase in ee to 78% (Table 2, entry 10). The diastereoselection remained constant throughout reaction optimization (<1.5:1). Traditional efforts to increase the diastereoselection were unsuccessful and will be revisited in future work.

### Reaction Optimization

With the optimal concentration and a satisfactory base in hand the effect of the nucleophile stoichiometry was examined (Table 3).

**Table 3.** Investigations into the Equivalents of PhenylNitromethane



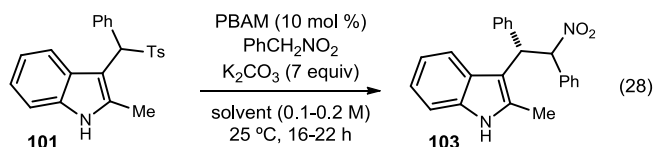
| entry | PNM (equiv) | ee (%) | entry          | PNM (equiv) | ee (%) |
|-------|-------------|--------|----------------|-------------|--------|
| 1     | 2.0         | 78     | 5              | 0.75        | 83     |
| 2     | 1.5         | 78     | 6              | 0.5         | 86     |
| 3     | 1.1         | 79     | 7              | 0.25        | 90     |
| 4     | 1.0         | 81     | 8 <sup>b</sup> | 0.5 + 0.5   | 83     |

<sup>a</sup> All reactions were performed on a 0.10 mmol scale using 1 equivalent of the indole under the conditions listed. Product was isolated as <1.6:1 dr unless otherwise noted. <sup>b</sup> Added in 2 portions after 22 h of stirring.

A clear trend was observed with decreasing amounts of nucleophile (Table 3, entries 1-7). This showed that excess nucleophile has a negative effect on the enantioselection. This may be a reflection of the ratio of catalyst to nucleophile. At higher equivalents (Table 3, entries 1-2) the catalyst may be saturated with nucleophile resulting in increased addition catalyzed by the achiral exogenous base through a non-selective pathway. Therefore, aliquot addition of the nucleophile was performed (Table 3, entry 8) and found to increase the ee slightly. Since the ee was not as high as using only 0.5 equiv (Table 3, entry 6), this suggests that the active catalyst may be more complex than just the nitronate salt.

Though toluene has thus far proved to be the most effective solvent in BAM catalyzed reactions, a thorough solvent screen was conducted (Table 4).

**Table 4.** Phenylnitromethane Addition: Solvent Screen

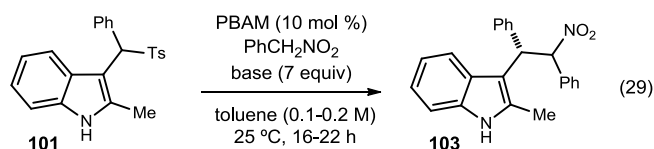


| entry | solvent           | PNM (equiv) | conv. (%) | ee (%) | entry           | solvent                                  | PNM (equiv) | conv. (%) | ee (%) |
|-------|-------------------|-------------|-----------|--------|-----------------|--|-------------|-----------|--------|
| 1     | PhCH <sub>3</sub> | 1.0         | 95        | 81     | 10              | EtOAc                                    | 1.0         | 90        | 30     |
| 2     | PhH               | 1.0         | 85        | 77     | 11              | ether                                    | 1.0         | 37        | 56     |
| 3     | <i>o</i> -xylene  | 1.0         | 100       | 76     | 12              | TBME                                     | 1.0         | 17        | 72     |
| 4     | <i>m</i> -xylene  | 1.0         | 77        | 80     | 13              | THF                                      | 1.1         | 80        | 18     |
| 5     | PhOMe             | 1.5         | 95        | 65     | 14              | <i>c</i> -C <sub>6</sub> H <sub>12</sub> | 1.0         | 27        | 63     |
| 6     | PhCF <sub>3</sub> | 1.1         | 65        | 32     | 15              | MeCN                                     | 1.1         | 95        | 0      |
| 7     | PhNO <sub>2</sub> | 1.0         | 75        | 31     | 16              | DMSO                                     | 1.0         | 100       | 0      |
| 8     | DCE               | 1.0         | 90        | 46     | 17 <sup>b</sup> | H <sub>2</sub> O                         | 1.0         | 90        | 0      |
| 9     | CCl <sub>4</sub>  | 1.0         | 93        | 77     |                 |  |             |           |        |

<sup>a</sup> All reactions were performed on a 0.10 mmol scale using 1 equivalent of the indole and run under the conditions listed. Product was isolated as <1.6:1 dr unless otherwise noted. Enantiomer ratios of major diastereomer (or average of both) measured by HPLC using chiral stationary phase.<sup>b</sup> Reaction ran for 5 d.

A variety of aromatic solvents were examined (Table 4, entries 2-7) and found to give similar enantioselectivities to toluene. Chlorohydrocarbons (Table 4, entries 8-9) gave significantly different values of enantioselection, with carbon tetrachloride giving results similar to toluene. Acyclic and cyclic ethers gave lower enantioselection (Table 4, entries 11-13) with THF giving the lowest at 18% ee. The more polar solvents gave essentially no enantioselection (Table 4, entries 15-17).

**Table 5.** Phenylnitromethane Addition: Exogenous Base Screen



| entry | base                                   | PNM (equiv) | conv. (%)    | ee (%) |
|-------|--|-------------|--------------|--------|
| 1     | K <sub>2</sub> CO <sub>3</sub>         | 1.0         | >85          | 81     |
| 2     | KF/Al                                  | 2.0         | 100          | 60     |
| 3     | KF                                     | 1.5         | 88           | 68     |
| 4     | K <sub>2</sub> CO <sub>3</sub> /sieves | 1.0         | 70           | 75     |
| 5     | K <sub>3</sub> PO <sub>4</sub>         | 1.5         | 30           | 46     |
| 6     | Na <sub>2</sub> CO <sub>3</sub>        | 1.0         | 55           | 63     |
| 7     | NaHCO <sub>3</sub>                     | 1.0         | 25           | -      |
| 8     | NaOH                                   | 1.0         | trace/decomp | -      |

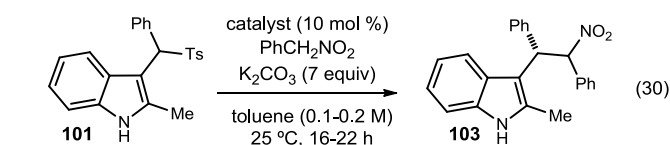
<sup>a</sup> All reactions were performed on a 0.10 mmol scale using 1 equivalent of the indole under the conditions listed. Product was isolated as <1.6:1 dr unless otherwise noted.

A base screen demonstrated that potassium carbonate was still the best inorganic base in this reaction (Table 5, entry 1). KF and KF/Al performed similarly (Table 5, entries 2-3) while the presence of molecular sieves with potassium carbonate led to a decrease in enantioselection (Table 5, entry 4). Sodium bicarbonate (Table 5, entry 7) and sodium hydroxide (Table 5, entry 8) gave low conversion.

### Reaction Optimization: Catalyst Screen

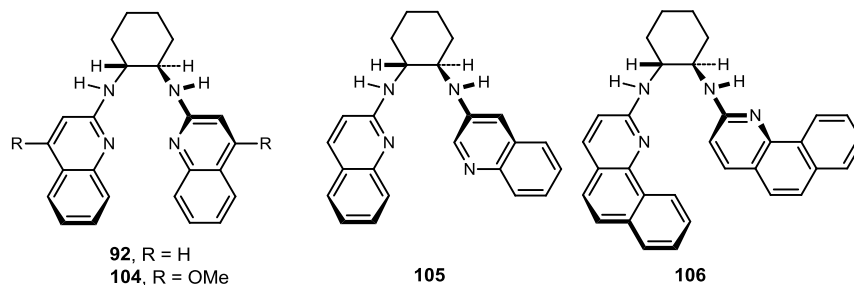
Having determined the optimal stoichiometry (one equivalent of phenylnitromethane), concentration (0.1 M), solvent (toluene) and base (potassium carbonate), a plethora of BAM catalysts from our library were screened (Table 6).

**Table 6.** Catalyst Screen: H,QuinBAM analogs



| entry | catalyst                                    |            | ee (%) |
|-------|---|------------|--------|
| 1     | H,QuinBAM                                   | <b>92</b>  | 56     |
| 2     | H, <sup>2</sup> Quin( <sup>3</sup> Quin)BAM | <b>105</b> | 0      |
| 3     | BenzoQuinBAM                                | <b>106</b> | 0      |
| 4     | <sup>4</sup> MeO-BAM                        | <b>104</b> | 73     |

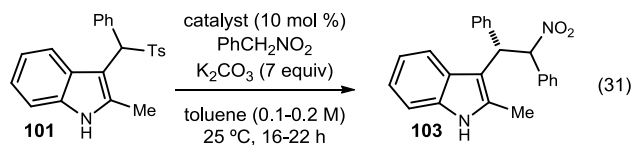
<sup>a</sup> All reactions were performed on a 0.10 mmol scale using 1 equivalent of the indole under the conditions listed. Product was isolated as <1.6:1 dr unless otherwise noted.



The first generation catalyst H,QuinBAM (**92**) catalyzed the addition with good enantioselectivity (56% ee) (Table 6, entry 1). We were surprised to see this as H,QuinBAM has been deemed significantly less basic than PBAM. The unsymmetrical version of H,QuinBAM (**105**, H,<sup>2</sup>Quin(<sup>3</sup>Quin)BAM) and the sterically hindered BenzoQuinBAM (Table 6, entries 2-3) gave no enantioselectivity. The slightly more basic <sup>4</sup>MeO-BAM (**104**) gave increased enantioselection, but did not reach the levels of

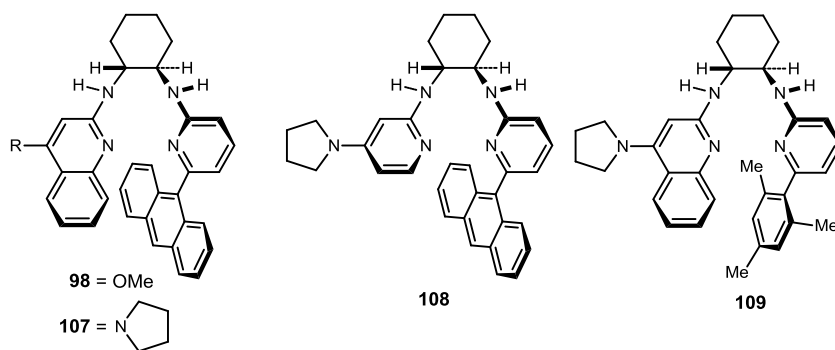
the most basic catalyst PBAM (81% ee). This suggested that increases in catalyst basicity increase the enantioselection (Table 6, entry 4).

**Table 7.** Catalyst Screen: Unsymmetrical PBAM Derivatives



| entry | catalyst                  | ee (%)        |
|-------|---------------------------|---------------|
| 1     | <sup>4</sup> MeO-Anth-BAM | <b>98</b> 35  |
| 2     | Anth-Pyr-PBAM             | <b>108</b> 48 |
| 3     | Anth-PBAM                 | <b>107</b> 55 |
| 4     | Mesityl-PBAM              | <b>109</b> 37 |

<sup>a</sup> All reactions were performed on a 0.10 mmol scale using 1 equivalent of the indole under the conditions listed. Product was isolated as <1.6:1 dr unless otherwise noted.



The unsymmetrical BAM catalysts with bulky substituents on the 6-position of the pyridine (Table 7) have performed very well in other additions,<sup>48,49,50</sup> but performed poorly in this reaction. This is postulated to be due to the steric congestion in the binding pocket.

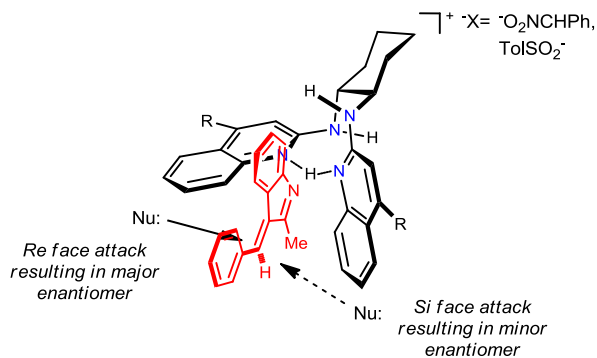
The absolute stereochemistry of the addition products was determined to be of the (*S*)-configuration by chemical correlation (debromination of **138e**).<sup>53</sup> The hypothesized

<sup>53</sup> Debromination of the bromonitromethane adduct was used to match known compound: ref. 26



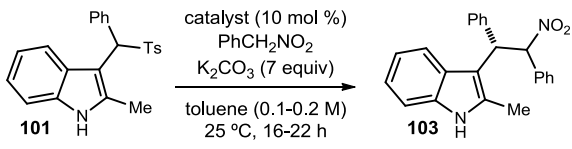
catalyst binding model (Figure 7) is based on previous models of BAM catalysts and imine electrophiles, and accounts for the absolute stereochemistry of the products.<sup>54</sup>

**Figure 7.** Proposed Catalyst Binding Model



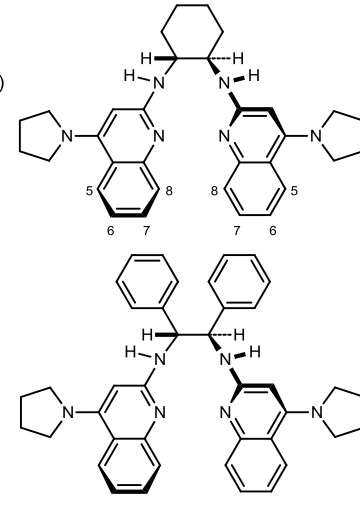
We propose that the electrophile is oriented so that the indole nitrogen is interacting with the chiral proton and the rest of the indole rising out of the pocket. The quinoline ring system of the catalyst would then block attack from the *Si* face. Due to the additional distance between the 1,4-addition site and the chiral pocket (compared to 1,2-addition for an imine), catalysts with more steric influence (extension of quinoline ring versus pocket sterics [Table 7]) were tested in an attempt to further block nucleophilic attack to the *Si* face (Table 8).

<sup>54</sup> Singh, A.; Johnston, J. N. *unpublished results*

**Table 8.** Catalyst Screen: Steric Analogs of PBAM


| entry | catalyst                              |            | ee (%) |
|-------|---------------------------------------|------------|--------|
| 1     | <sup>6,7</sup> (Me) <sub>2</sub> PBAM | <b>110</b> | 77     |
| 2     | <sup>7</sup> iPrPBAM                  | <b>111</b> | 70     |
| 3     | <sup>7</sup> tBuPBAM                  | <b>112</b> | 69     |
| 4     | <sup>7</sup> MeOPBAM                  | <b>113</b> | 40     |
| 5     | <sup>8</sup> MeOPBAM                  | <b>114</b> | 77     |
| 6     | StilbPBAM                             | <b>115</b> | 58/40  |

<sup>a</sup> All reactions were performed on a 0.10 mmol scale using 1 equivalent of the indole under the conditions listed. Product was isolated as <1.6:1 dr unless otherwise noted.



**115**  
StilbPBAM

(32)

**110** = 6,7-Me  
**111** = 7-<sup>i</sup>Pr  
**112** = 7-<sup>t</sup>Bu  
**113** = 7-MeO  
**114** = 8-MeO

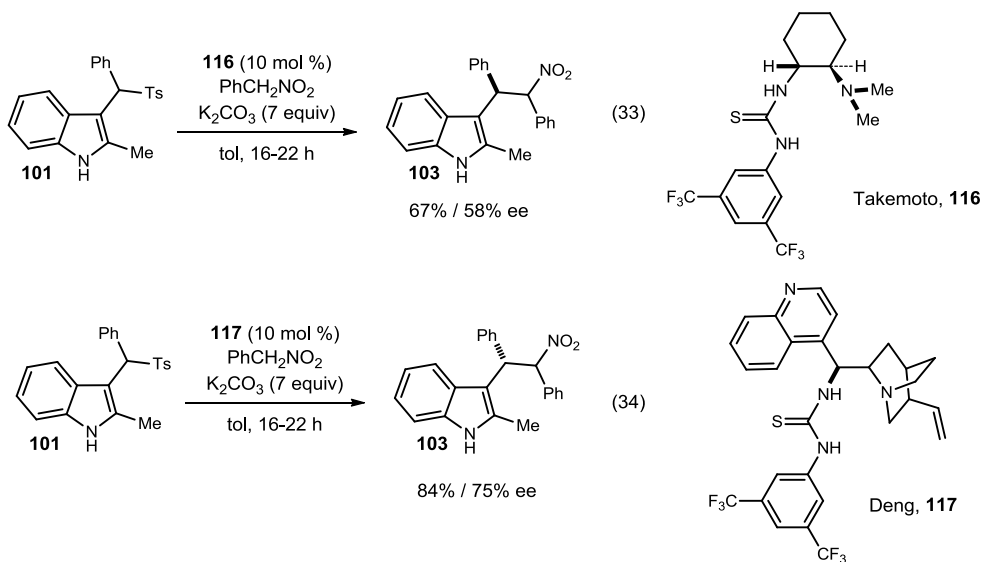
Extending the length of the quinoline ring was found to have little effect on ee. Bulky alkyl substituents at the 7 position of the quinoline ring (Table 8, entries 2-3) gave slightly lower ee than the methyl group (Table 8, entry 1). An electron donating substituent at the 7 position (Table 8, entry 4) gave lower enantioselection than an electron donating substituent at the 8-position (Table 8, entry 5). The influence of substituents at the 8-position is being investigated further. Results in the addition of aryl nitroalkanes to *N*-Boc aryl aldimines show an increase in ee, compared to PBAM, when substitution is at the 8-position.<sup>55</sup> When the catalyst backbone was changed from cyclohexyl diamine to stilbene diamine (StilbPBAM), the enantioselection dropped (Table 8, entry 6). Since the reactivity was the same as PBAM, this drop in enantioselection could be a direct result of a smaller, more hindered pocket.<sup>56</sup>

<sup>55</sup> Davis, T. A.; Johnston, J. N. *Chemical Science* **2011**, 2, 1076-1079. Davis, T. A.; Vara, B. A.; Johnston, J. N. *unpublished results*.

<sup>56</sup> Kim, H.; Yen, C.; Preston, P.; Chin, J. *Org. Lett.* **2006**, 8, 5239-5242.

BAM catalysts have demonstrated similar reactivity and selectivity to the class of chiral thiourea catalysts (Scheme 21).

**Scheme 21.** Catalyst Screen: Thiourea Catalysts



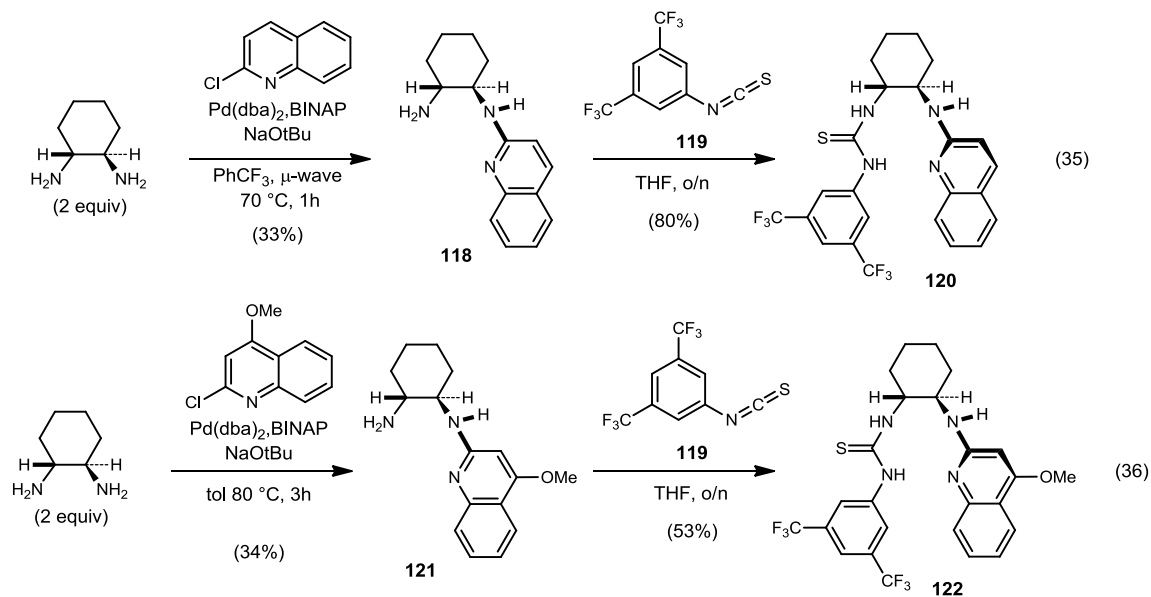
Using the Takemoto catalyst (**116**, eq 32)<sup>57</sup> and the Deng catalyst (**117**, eq 33),<sup>58</sup> good enantioselection was observed. The Takemoto thiourea gave the desired adduct in up to 67% ee and Deng's cinchonidine-based thiourea gave the product in up to 84% ee. This is the first time that a significant difference in enantioselection was observed between the major and minor diastereomers.

Encouraged by the comparable enantioselection to PBAM, the BAM thiourea analogs were synthesized (Scheme 22).

<sup>57</sup> Okino, T.; Hoashi, Y.; Takemoto, Y. *J. Am. Chem. Soc.* **2003**, *125*, 12672-12673.

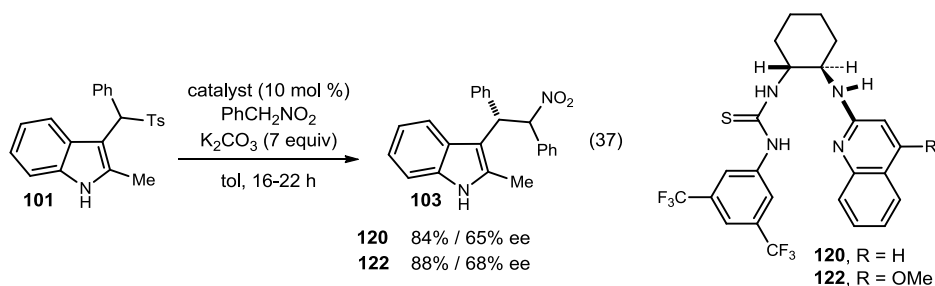
<sup>58</sup> Li, H.; Wang, Y.; Tang, L.; Deng, L. *J. Am. Chem. Soc.* **2004**, *126*, 9906-9907.

**Scheme 22.** Synthesis of UreaBAM Analogs



The quinoline rings were coupled to the *trans*-(*R,R*)-cyclohexyl-diamine under Buchwald-Hartwig type conditions. This occurred in low yields (33-34%) due to the formation of a significant amount of the bis-coupled diamine. In future reactions, this can be avoided using a mono-protected amine, followed by coupling and deprotection. With the mono-coupled diamine in hand, the free amine was treated with one equivalent of the isothiocyanate **119** at room temperature. Both desired catalysts (**120** and **122**) were isolated in acceptable yields (53-80%) and were used in the addition of phenylnitromethane to indole (Scheme 23).

**Scheme 23.** Catalyst Screen: UreaBAM Analogs

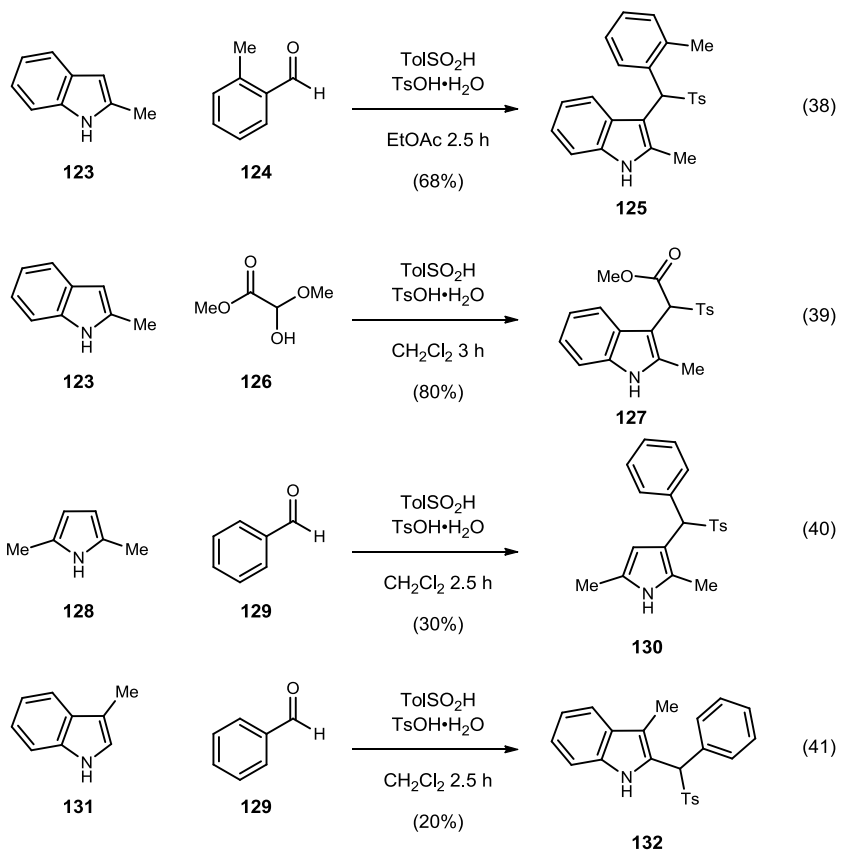


Treatment of indole **101** with the modified Takemoto catalyst resulted in an increase in the enantioselection by about 20%. More interestingly, the enantioselection was inverted from the Takemoto catalyst, even though the diamine backbone remained the same, suggesting a significant change in binding between the catalysts. Adding a methoxy group to the quinoline ring (catalyst **122**) to increase the Brønsted basicity of the catalyst resulted in very small changes in enantioselection, inferring that the amidine participates less in the binding than the thiourea moiety (a steric over electronic influence). Despite the small increase in enantioselection of the UreaBAM catalysts compared to the known catalysts, the average for both diastereomers (78% ee) was still lower than the average for PBAM (81% ee), therefore the thioureas were not pursued further.

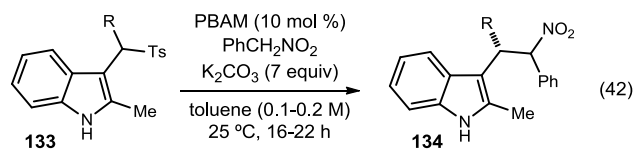
**Reaction Scope: Electrophile Screen**

With highly optimized reaction conditions, a screen of both electronically and sterically diverse electrophiles was completed. Previous indole electrophiles utilized in similar reactions were simple arylsulfonyl indoles. To increase diversity, a larger variety of electrophiles was synthesized using an adaptation of the Petrini protocol (Scheme 24).

**Scheme 24.** Synthesis of a Larger Variety of Electrophiles



The aldehydes were reacted with methyl indole to give a variety of electrophiles [*ortho*-substitution (**125**), methyl ester (**127**), pyrroles (**130**)] isolated in moderate (30%) to good (80%) yields. The arylsulfonyl group was also moved to the 2-position, though the product (**132**) was isolated in low yield (20%). With these new substrates in hand, a thorough electrophile screen commenced (Table 9).

**Table 9.** Reaction Scope: Initial Electrophile Screen

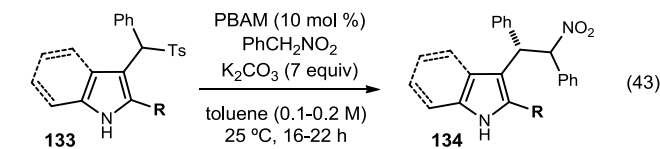
| entry             | R  | 134x       | ee (%) | % yield (% conv) |
|-------------------|--|------------|--------|------------------|
| 1                 | Ph   | <b>103</b> | 81/81  | 78(85)           |
| 2                 | <sup>p</sup> BrC <sub>6</sub> H <sub>4</sub>               | <b>b</b>   | 82/75  | 74(76)           |
| 3                 | <sup>p</sup> MeOC <sub>6</sub> H <sub>4</sub>              | <b>c</b>   | 81/81  | 68(88)           |
| 4                 | <sup>p</sup> F <sub>3</sub> CC <sub>6</sub> H <sub>4</sub> | <b>d</b>   | 84/74  | 71(78)           |
| 5 <sup>c</sup>    | <sup>o</sup> MePh  | <b>e</b>   | 76/70  | 76(95)           |
| 6                 | <sup>2</sup> Furyl   | <b>f</b>   | 53/44  | 69(99)           |
| 7                 | <sup>n</sup> Bu  | <b>g</b>   | 76/74  | 51(56)           |
| 8                 | Me   | <b>h</b>   | 40/40  | (44)             |
| 9 <sup>b</sup>    | CO <sub>2</sub> Me   | <b>i</b>   | 66/47  | 47(52)           |
| 10 <sup>b,c</sup> | CO <sub>2</sub> <sup>t</sup> Bu                            | <b>j</b>   | 65/66  | 55(70)           |

<sup>a</sup> All reactions were performed on a 0.10 mmol scale using 1 equivalent of the indole under the conditions listed. Product was isolated as <1.6:1 dr unless otherwise noted. <sup>b</sup> 3:1 dr observed. <sup>c</sup> 72 h reaction time.

The first array of substrates examined contained additional functionality on the phenyl ring at the indole C3' position. The reaction exhibits good tolerance for both electron donating and electron withdrawing groups (Table 9, entries 2-4). An *ortho*-tolyl results in a drop in reactivity and requires longer reaction times, but the ee is mostly conserved (Table 9, entry 5). Substituting the phenyl ring at C3' with alkyl chains returns the product with good ee (Table 9, entry 7), unlike substitution with a methyl group (Table 9, entry 8). In an attempt to increase the dr by using an ester as a directing group for the nitronate, the methyl ester indole was subjected to the reaction conditions (Table 9, entry 9) and gave good enantioselection with modest dr (3:1). A bulkier ester group was also used, but resulted in similar values of enantioselection and diastereoselection (Table 9, entry 10).

Trying to establish the influence of the indole ring, the next screen varied the substrate at the 2-position of the indole (Table 10).

**Table 10.** Reaction Scope: Variations at the Indole 2-Position



| entry          | R                         | 134x     | ee (%) | % yield<br>(% conv) |
|----------------|---------------------------|----------|--------|---------------------|
| 1              | H                         | <b>k</b> | 39/0   | 65(68)              |
| 2              | Ph                        | <b>l</b> | 74/72  | 49(52)              |
| 3 <sup>b</sup> | CO <sub>2</sub> Me        | <b>m</b> | 0/0    | (<50)               |
| 4 <sup>b</sup> | TMS                       | <b>n</b> | NR     | -                   |
| 5 <sup>b</sup> | 1-Boc, 2-Me               | <b>o</b> | NR     | -                   |
| 6 <sup>b</sup> | PhC(H)SO <sub>2</sub> Tol | <b>p</b> | NR     | -                   |
| 7              | 2,5-Me-Pyrrole            | <b>q</b> | 72/69  | 69(79)              |

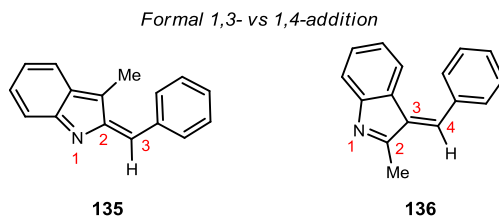
<sup>a</sup> All reactions were performed on a 0.10 mmol scale using 1 equivalent of the indole under the conditions listed. Product was isolated as <1.6:1 dr unless otherwise noted. <sup>b</sup> 72 h reaction time.

When the methyl group of the indole was replaced with a hydrogen (Table 10, entry 1), the enantioselection dropped significantly, suggesting the need for a steric influence at the C2 carbon, possibly influencing the *E/Z* ratio of the indolenine. This same trend was also seen in the initial work by Petrini and coworkers (Scheme 15) and was reaffirmed when a phenyl ring was placed at the C2 (Table 10, entry 2). Hoping to combine the high enantioselectivity of the aromatic indole substrates and the good diastereoselection in the ester substrates (3:1 dr, Table 9, entries 9-10), an ester was placed at the C2 position (Table 10, entry 3). Unfortunately, even after stirring the reaction for days, very little conversion to product was observed suggesting that electron withdrawing groups at the C2 are detrimental to the reactivity and selectivity. In order to set up the indole product for a Hiyama coupling, a TMS group was placed at the 2-position of the indole but did



not yield any product (Table 10, entry 4). Attempts to investigate the effect of a halogen or a boronic acid at the 2-position failed because of the inability to prepare the starting arylsulfonyl indole.

To probe the reaction mechanism and catalyst binding, the *N*-Boc protected indole was synthesized. If the reaction occurred with enantioselection, then the proposed binding model of the chiral proton would have to be reexamined (Figure 7). However, when the indole was *N*-Boc protected, no reaction was seen, even after prolonged reaction times and heating (Table 10, entry 5). Evidently, the *N*-Boc indole was nucleophilic enough to form the starting arylsulfonyl indole (**133o**), but not nucleophilic enough to eliminate the sulfinate group. A final variation of the indole electrophile was envisioned by changing the C3 and C2 substituents (**134p**).

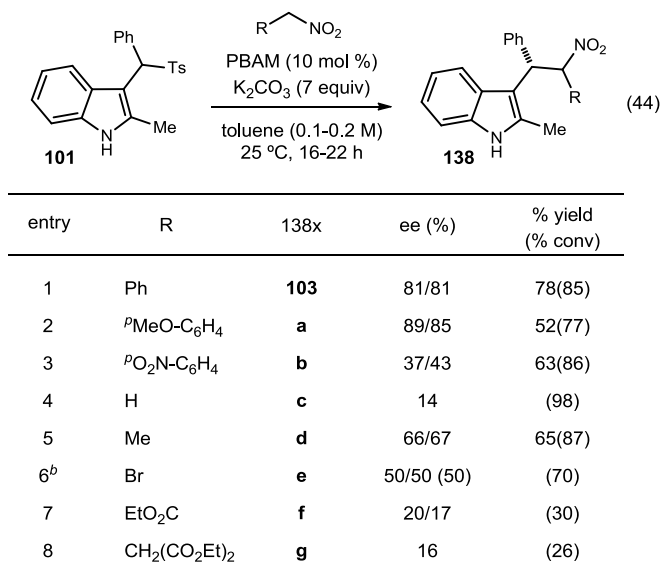


As seen in the figure above, switching the indole substituents would hypothetically bring the reaction site closer to the bound catalyst, and thereby increase ee and possibly influence dr, by formally making it a 1,3-addition (**135**). However, attempts to perform this reaction in multiple solvents with a variety of bases under prolonged reaction time and heat only returned starting material. Finally, removal of the indole aromatic ring to leave a pyrrole analog (Table 10, entry 7) still allowed formation of the adduct with good enantioselection (72% ee).

### Reaction Scope: Nucleophile Screen

BAM catalyzed reactions have historically performed well when the pronucleophile was either a simple or modified nitroalkane. This observation was thoroughly examined in this new reaction (Table 11).

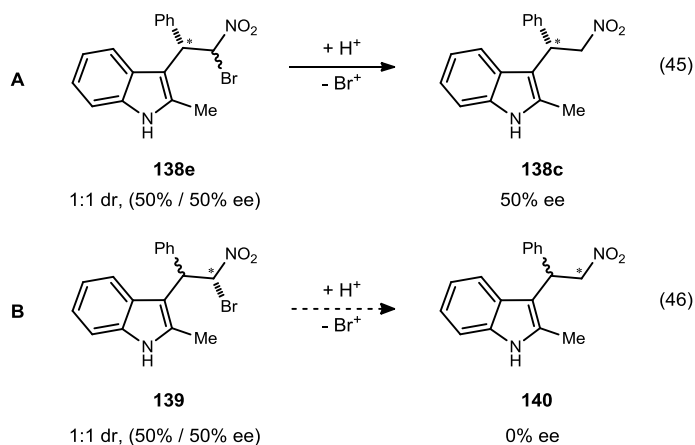
**Table 11.** Nucleophile Screen



<sup>a</sup> All reactions were performed on a 0.10 mmol scale using 1 equivalent of the indole under the conditions listed. Product was isolated as <1.6:1 dr unless otherwise noted. <sup>b</sup> Enantiomeric excess of the debrominated product (PDT:debromo = 4:1)

A variety of aryl nitroalkanes were tested after substantial success with phenylnitromethane. An electron rich substituent on the phenyl ring (Table 11, entry 2) increased the enantioselection, though a slight drop in conversion and yield was observed. A strong electron withdrawing substituent on the phenyl ring resulted in a drastic drop in enantioselection (Table 11, entry 3). This is presumably due to the increased acidity of the  $\alpha$ -proton, allowing for the achiral exogenous base to catalyze the reaction, rather than PBAM. Nitromethane performed very poorly (14% ee) while

nitroethane only saw a small drop in ee from the aryl analogs (Table 11, entry 5). When bromonitromethane was used in the reaction (Table 11, entry 6), the desired product was isolated along with the debrominated product, with equal values of enantioselection (50% ee).



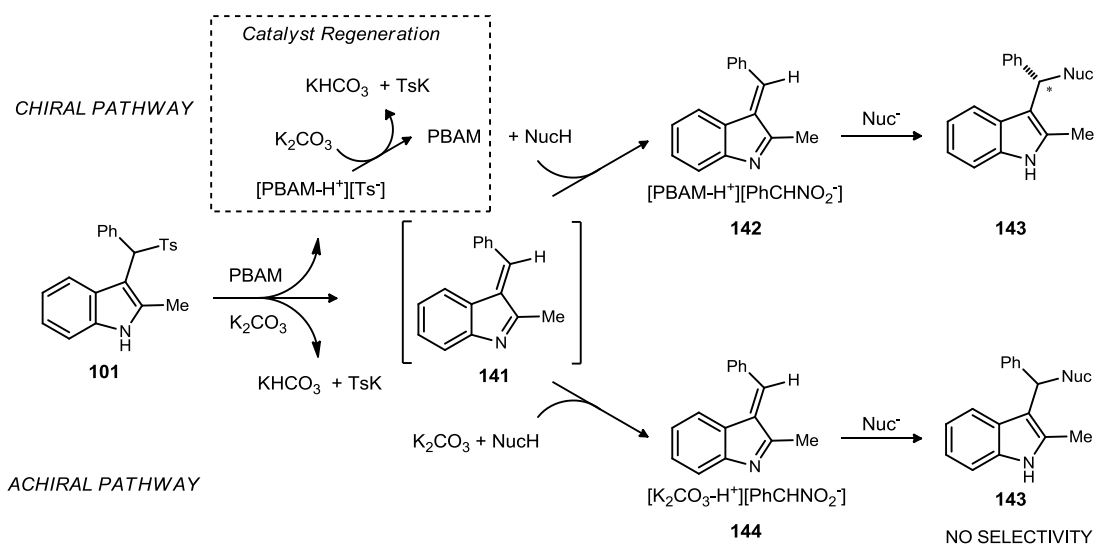
This was our first opportunity to confirm that the products were indeed homochiral at the benzylic carbon, as both diastereomers converged to one enantiomer (**138c**), as observed in equation 44. If the stereocenter was set at the  $\alpha$ -nitro carbon, loss of bromine should return product that was 1:1 in diastereomers to start, with 0% ee (eq 45). Lastly, both  $\alpha$ -nitro esters and malonates (Table 11, entries 7-8) exhibited poor reactivity and low enantioselection.

After a significant amount of optimization and a thorough nucleophile/electrophile screen was completed, further efforts to increase enantioselection were initiated by examining the proposed mechanism.

## Mechanistic Studies and the Development of New Reaction Protocol

When traditional efforts (solvent, base, catalyst, temperature, etc.) to increase enantioselection were exhausted, the proposed mechanism (Figure 8) was reexamined for other routes to increase selectivity.

**Figure 8.** Proposed Mechanism by Chiral and Achiral Routes

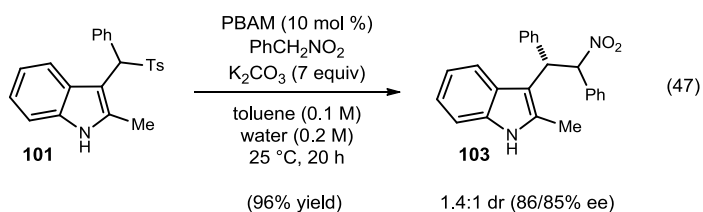


Both PBAM and potassium carbonate are capable of catalyzing the elimination of the sulfonyl group (Table 2, entries 6,8). However, we believe that PBAM catalyzes the elimination at a faster rate to give the indolenine intermediate, even though there is a significant excess of potassium carbonate relative to the catalytic amount of PBAM. Following nucleophile formation (base deprotonation to the nitronate), the addition occurs in either the presence of a chiral complex such as **142**, or an achiral complex such as **144**. When the amount of product that is formed via PBAM catalyzed addition (complex **142**) increases, so does the enantioselection. We also recognize that the active

catalyst may be PBAM with another counter ion, such as sulfinate. Modifications that could influence this shift of selectivity were then investigated.

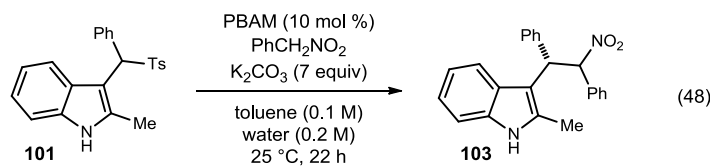
### *Influence of Water in the Reaction*

During the solvent screen, it was determined that the reaction was capable of happening in, or “on water”,<sup>59</sup> with no selectivity (Table 4, entry 17). However, when water was used as a cosolvent with toluene, very encouraging results were observed (eq 46).



A large increase in yield (from 83% to 96%) and moderate increase in enantioselection (from 81% ee to 86% ee) was observed in the test reaction with water as a cosolvent. We then further optimized the reaction with water as a cosolvent (Table 12).

<sup>59</sup> Guo, C.; Song, J.; Luo, S.-W.; Gong, L.-Z. *Angew. Chem. Int. Ed.*, **49**, 5558-5562. Hayashi, Y. *Angew. Chem. Int. Ed.* **2006**, *45*, 8103-8104. Woodward, R. B.; Cava, M. P.; Ollis, W. D.; Hunger, A.; Daeniker, H. U.; Schenker, K. *Tetrahedron* **1963**, *19*, 247-288.

**Table 12.** Reaction Optimization with Water as a Cosolvent

| entry | modification                    | ee (%) | % yield<br>(% conv) |
|-------|---------------------------------|--------|---------------------|
| 1     | 0.2 M H <sub>2</sub> O          | 86/85  | 96                  |
| 2     | 1.0 M H <sub>2</sub> O          | 82/83  | 90                  |
| 3     | 0.1 M H <sub>2</sub> O          | 86/85  | 96                  |
| 4     | 0.2 M toluene                   | 83/82  | 92                  |
| 5     | 0.05 M toluene                  | 85/89  | 84(92)              |
| 6     | Na <sub>2</sub> CO <sub>3</sub> | 84/84  | 97                  |
| 7     | Cs <sub>2</sub> CO <sub>3</sub> | 85/84  | 97                  |
| 8     | KF                              | 61/59  | 50 (52)             |
| 9     | DMAP                            | 28/27  | 83                  |

<sup>a</sup> All reactions were performed on a 0.10 mmol scale using 1 equivalent of the indole under the conditions listed. Product was isolated as <1.6:1 dr unless otherwise noted.

A decrease in enantioselection was observed when the amount of water was decreased (Table 12, entry 2), and a plateau was reached at 0.5 mL (0.2 M) of water (Table 12, entry 3). Small changes were also observed when the amount of toluene was increased and decreased (Table 12, entries 4-5). Other carbonate bases performed similarly when solubilized by water (Table 12, entries 6-7), a change from previously run anhydrous reaction conditions. The other bases tested performed poorly (Table 12, entries 8-9).

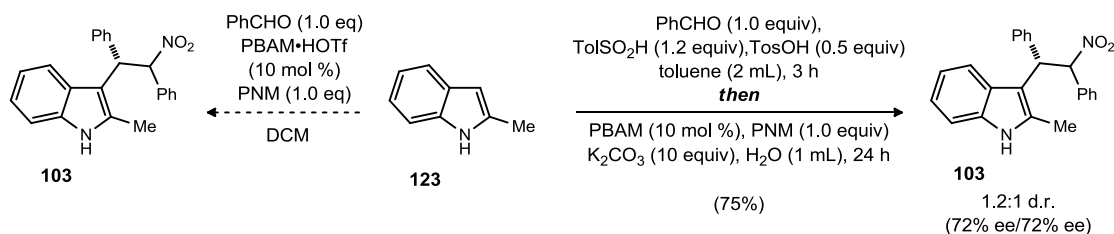
The increase in yield is believed to be a direct result of (a) increased reactivity and (b) solvation of both the inorganic base and the inorganic by-products (sulfinate salts, bicarbonate products, etc.). When the reaction is run without water, the reaction starts as a free stirring reaction of soluble starting materials and heterogeneous base (though not soluble, it does not appear to impede the reaction). As the reaction progresses and the sulfinate group is eliminated as the inorganic salt, the reaction becomes a thick slurry of

non-soluble components. This may hinder efficient dispersion of reaction components, specifically the catalyst, resulting in low conversions and enantioselection. Previously, the workup involved filtering the reaction mixture through silica gel to remove the catalyst, and washing with ethyl acetate to solubilize any product trapped in the solid by-products. The modified reaction workup involved adding water and extracting, followed by silica gel filtration, and gave higher yields.

In addition to elimination of the thick reaction mixture, the increase in enantioselection may also be a result of increasing the interactions between the chiral catalyst and indolenine intermediate, while limiting those of the indolenine with achiral promoters of the reaction. We propose that the starting material, indolenine intermediate and nucleophile remain in the organic layer, promoting addition through the chiral pathway (Figure 8) while limiting the interactions with the large excess of achiral, inorganic that resides primarily in the aqueous layer. This shift towards the chiral pathway is evident with the significant jump in enantioselection.

Knowing that the presence of water was positive, the one-pot formation of the arylsulfonyl indole, indolenine and phenylnitromethane addition was attempted (Scheme 25).

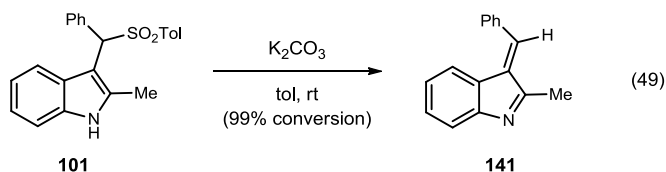
**Scheme 25.** One Pot Addition from 2-Me-Indole



Under acidic conditions (PBAM•HOTf) we attempted to form the indolyl alcohol, which could form the indolenine intermediate with the loss of the elements of water, similar to previously reported work (Scheme 16 and Scheme 18). The phenylnitromethane addition catalyzed by PBAM could then occur. Unfortunately we saw no product formed by this simplified route. However, the arylsulfonyl indole was formed under acidic conditions and water was added with extra potassium carbonate to quench the acid following completion by thin-layer chromatography (TLC). The catalyst and nucleophile were added, and adduct **103** was formed in remarkably good yield and moderate enantioselection (72% ee). This was not investigated further, but remains an option for arylsulfonyl indoles that are difficult to isolate.

### *Preforming the Indolenine Intermediate*

In the proposed reaction mechanism, the slow step of the reaction is the elimination of the sulfinate group. While PBAM may be involved in this step, it makes it less available to catalyze the phenylnitromethane addition. We sought to isolate the intermediate indolenine in order remove the inorganic base from the reaction (the source of chiral-racemic product formation).

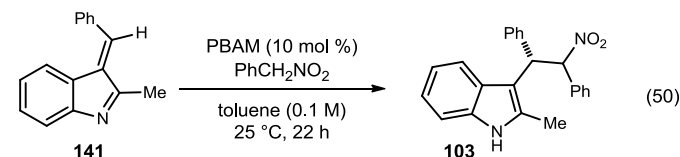


A variety of bases and conditions was used in the elimination to afford the presumed product with consumption of the starting material. This highly reactive intermediate was difficult to purify and characterize with certainty, as the NMR was complicated with



minor impurities and baseline noise. In spite of these issues, the presumed isolated indolenine intermediate was submitted to the reaction conditions (Table 13).

**Table 13.** Phenylnitromethane Addition to Isolated Indolenine Intermediate



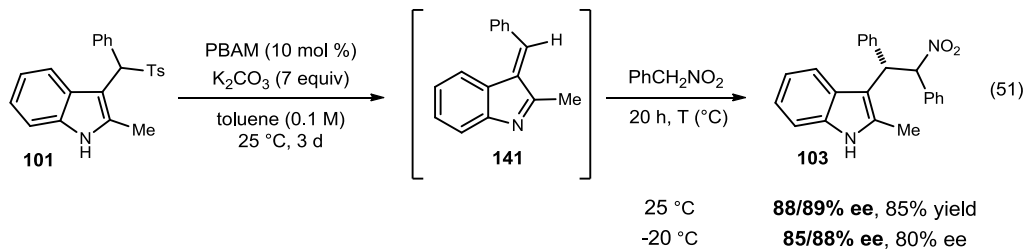
| entry | modification                                  | ee (%) |
|-------|---|--------|
| 1     | 25 °C   | 85/87  |
| 2     | -78 °C  | 79/82  |
| 3     | 25 °C, 7 equiv K <sub>2</sub> CO <sub>3</sub> | 86/88  |

<sup>a</sup> All reactions were performed on a 0.10 mmol scale using 1 equivalent of the indole under the conditions listed. Product was isolated as <1.6:1 dr unless otherwise noted.

When the isolated intermediate was treated with catalyst and the nucleophile, the enantioselectivity increased at both room temperature and under cryogenic conditions. The differences in ee may be a direct result of the inability to properly quantify the amount of electrophile (99% conversion and yield was assumed following intermediate formation) as some may have remained trapped in the heterogeneous base during filtration. More interestingly, when the reaction was also run in the presence of potassium carbonate as well as PBAM, the enantioselection did not change (Table 13, entry 3). This reaffirmed our hypothesis that PBAM catalyzes the elimination and the addition more efficiently than potassium carbonate, subsequently requiring the potassium carbonate for regeneration of PBAM after the elimination step.

Since the isolation of the indolenine intermediate was complicated, not reproducible at times and would not easily translate to other substrates, we attempted to first form the intermediate *in situ* before addition of the nucleophile (Chart 1).

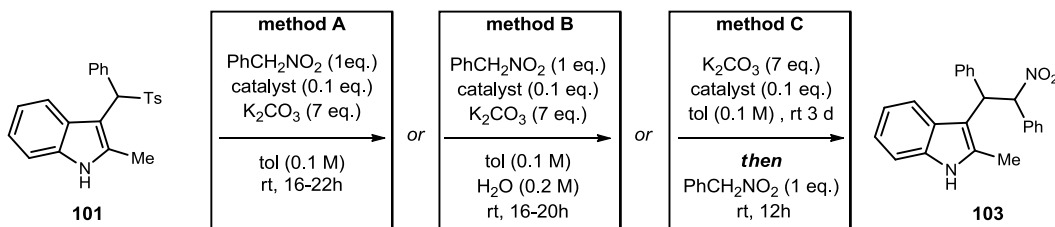
**Chart 1.** Reaction Optimization of *in situ* Indolenine Formation



Since PBAM aids in the elimination step, we were hopeful that combining all reactants except the nucleophile would facilitate the formation of the indolenine intermediate. After three days of stirring, the starting material was consumed and the nucleophile was added. The addition product was isolated in good yield and similar enantioselectivity at both room temperature and -20 °C. The high conversion and enantioselection sharply contrast with the initial attempts under cryogenic conditions, which gave low conversion (48%) and low ee (57% ee) (Table 2, entry 3). Formation of the intermediate without isolation presents a new protocol for enantioselective nitroalkane additions to indolenine intermediates.

### ***Application and Comparison of the Three Reaction Protocols***

With three possible reaction protocols, a selection of catalysts was reexamined and the results were compared across all three methods for each catalyst (Table 14).

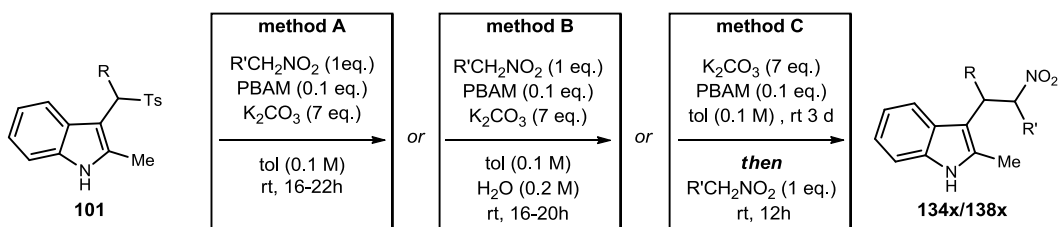
**Table 14.** Comparison of BAM Catalysts in the Three Protocols

| entry | catalyst                |            | A ee (%) | B ee (%) | C ee (%) |
|-------|-------------------------|------------|----------|----------|----------|
| 1     | PBAM                    | <b>100</b> | 81/81    | 86/86    | 89/89    |
| 2     | <sup>4</sup> MeO-BAM    | <b>104</b> | 73       | 81/80    | 69/72    |
| 3     | <sup>7</sup> MeO-PBAM   | <b>113</b> | 40       | 76/61    | 69/66    |
| 4     | <sup>6,7</sup> MeO-PBAM | <b>110</b> | -        | 64/39    | 67/61    |
| 5     | <sup>7</sup> iPr-PBAM   | <b>111</b> | 70       | 83/80    | 78/76    |
| 6     | Deng Thiourea           | <b>117</b> | 75/84    | 74/83    | 50/69    |

<sup>a</sup> All reactions were performed on a 0.10 mmol scale using 1 equivalent of the indole under the conditions listed. Product was isolated as <1.6:1 dr unless otherwise noted.

The catalysts that had performed well in the original method (method A) were tested. The PBAM analogs with methoxy groups at varying positions (Table 14, entries 2-4) generally performed better in the presence of water (method B). The reason for the different values in enantioselectivity for the PBAM analogs when the indolenine intermediate is preformed may be a direct result of the catalyst reactivity. The 7-alkyl PBAM analog also performed better in water (Table 14, entry 5). There was very little change in enantioselection when water was added to the Deng thiourea catalyst, with a slight drop when the indolenine was formed before addition of nucleophile (Table 14, entry 6). Following this brief catalyst screen, it was determined that PBAM remained the best catalyst across all methods.

A selection of substrates was also reexamined and the results were compared across all three methods, with the best highlighted (Table 15).

**Table 15.** Substrate Screen Implementing all Three Methods

| entry | R  | R'  |             | A ee (%) | B ee (%) | C ee (%) |
|-------|--|---|-------------|----------|----------|----------|
| 1     | Ph   | Ph  | <b>103</b>  | 81/81    | 86/86    | 88/89    |
| 2     | <i>p</i> -Br-C <sub>6</sub> H <sub>4</sub>               | Ph  | <b>134b</b> | 82/75    | 87/86    | 88/86    |
| 3     | <i>p</i> -MeO-C <sub>6</sub> H <sub>4</sub>              | Ph  | <b>134c</b> | 81/81    | 85/85    | 87/88    |
| 4     | <i>p</i> -F <sub>3</sub> C-C <sub>6</sub> H <sub>4</sub> | Ph  | <b>134d</b> | 84/74    | 84/76    | 88/78    |
| 5     | 2,5-Me-Pyrrole   | Ph  | <b>134q</b> | 72/69    | 55/54    | 66/58    |
| 6     | <i>n</i> -Bu   | Ph  | <b>134g</b> | 76/74    | 71/70    | 73/59    |
| 7     | CO <sub>2</sub> Me                                       | Ph  | <b>134i</b> | 66/47    | 76/65    | 50/38    |
| 8     | 2-Furyl  | Ph  | <b>134f</b> | 53/44    | 90/79    | 90/81    |
| 9     | Ph   | <i>p</i> -MeO-C <sub>6</sub> H <sub>4</sub> | <b>138a</b> | 89/85    | 87/87    | 90/75    |
| 10    | Ph   | Me  | <b>138d</b> | 66/67    | NR       | 10/10    |

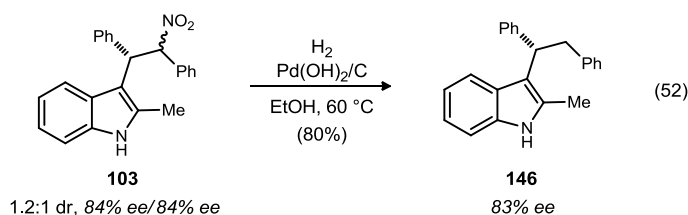
<sup>a</sup> All reactions were performed on a 0.10 mmol scale using 1 equivalent of the indole under the conditions listed. Product was isolated as <1.6:1 dr unless otherwise noted.

All of the aryl analogs performed best when the intermediate was formed before addition of nucleophile (Table 15, entries 1-4, method C), with an average increase of 6% ee from the original method (method A). Certain substrates, such as the pyrrole and aliphatic analogs (Table 15, entries 5-6), exhibited no significant increase in enantioselection with the new methods. Both the ester (Table 15, entry 7) and furyl (Table 15, entry 8) analogs performed better under the semi-aqueous conditions (method B). Interestingly, the furyl analog was the substrate that benefitted most from the new protocol, providing an increase of almost 40% ee from the original method. The *para*-methoxy phenylnitromethane analog saw very little change across the three methods, however there was a large difference in the enantioselection of the diastereomers for method C (Table 15, entry 9, method C). The new methods did not help the enantioselections when

the nucleophile was nitroethane. In fact, reaction progress was severely hindered in water and gave no selectivity with the preformed electrophile (Table 15, entry 10). Overall, for the aryl analogs, method C gave the best enantioselectivity across the board. The data does not support any other trends for predicting the best method for a certain substrate.

### *Nitro Group Modification of the Indole Adducts*

Nitroalkanes offer many opportunities for functionalization through reduction, oxidation and denitration. Using modified conditions for the cleavage of benzylic nitro bonds by Carreira, we attempted to denitrate the phenylnitromethane addition product (eq 52).<sup>60</sup>



Using material with 84% ee for both diastereomers, we successfully denitrated to give **146** with no loss in enantiomeric excess. This confirms that the benzylic carbon is homochiral, as both diastereomers converge to the same enantiomer with good yield. There are a large number of catalysts for the Friedel-Crafts reaction of indole with nitrostyrene, while there are currently no known ways to add indole to stilbene analogs. These denitration products (**146**) represent the products obtained from the enantioselective reaction with stilbene analogs.

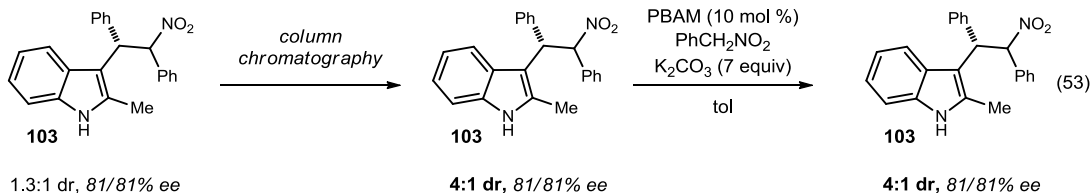
<sup>60</sup> Fessard, T.; Motoyoshi, H.; Carreira, E. *Angew. Chem. Int. Ed.* **2007**, *46*, 2078-2081.

## Future Work

This new reaction is a significant extension of previous work with our BAM catalysts. Through significant reaction optimization and redesign, we were able to increase enantioselectivity from 20% ee to 90% ee in the best cases. More notably, we also realized that water has a positive effect on the reaction, in terms of reactivity, isolation and enantioselection. Further work on this reaction would involve increasing diastereoselection, expanding the scope of nucleophiles and applying this methodology to a target.

Low dr of the final product was observed for all examples (except when the aryl group was an ester group). To determine if this was a result of thermodynamics or kinetics, the isolated product was resubmitted to column chromatography to separate the diastereomers (Scheme 26).

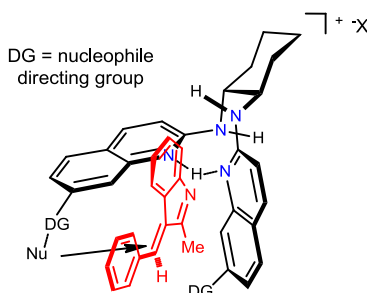
**Scheme 26.** Exposure of High dr Material to Reaction Conditions



Subjecting the high dr product to the reaction conditions returned product with the same dr, suggesting that the low dr was not a result of a thermodynamic equilibrium, but of low selectivity in the addition. This can be rationalized since the nucleophile is so far away from the binding pocket that the catalyst has very little influence on the orientation of the nucleophile, even though facial selectivity is attained (high ee).

One area for further investigation involves installation of a directing group on the catalyst that might orient the attack of the nucleophile while maintaining the quinoline ring responsible for facial selectivity (Figure 9).

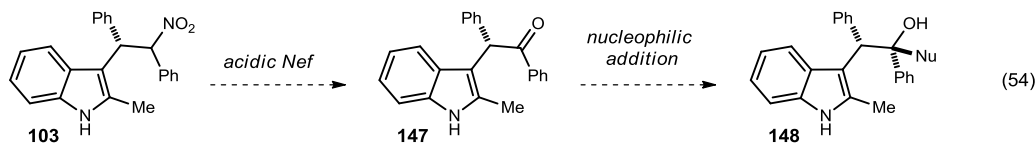
**Figure 9.** Model for Further Catalyst Development



Groups with differing electronics may be able to coordinate with the charged species and orient the nucleophile along a specific trajectory. Other attempts to further block the face by extending the quinoline further may also increase diastereoselection.

In addition to the substrates already synthesized, one could envision conversion of the nitro group to a ketone (Scheme 27).

**Scheme 27.** Further Manipulation of Indole Adducts



Basic Nef conditions may lead to epimerization of the C3' carbon, but an acidic Nef would allow for conversion without epimerization, followed by the diastereoselective addition of a nucleophile. This would allow us to set the C3' stereocenter in high ee and give highly functionalized indole products.

## CHAPTER II

### II. THE ENANTIOSELECTIVE SYNTHESIS OF VNI: A CURE FOR THE NEGLECTED TROPICAL CHAGAS DISEASE<sup>61,62</sup>

#### 2.1 Chagas Disease and the Limitations to Parasite Eradication

##### *Background of Chagas Disease*

Chagas disease, also known as American trypanosomiasis, is a disease that affects 10-12 million people in Latin America and causes over 15,000 deaths each year.<sup>63</sup> Chagas disease is listed as one of the World Health Organization's Neglected Tropical Diseases<sup>64</sup> but human migration has caused the disease to spread to parts of Europe, the United States, Japan, and Australia.<sup>65</sup> This migration of a disease once confined to underrepresented populations and low resource areas has sparked new research into better treatments, as the current options that have been around for decades are not ideal.<sup>63</sup>

Chagas disease is caused by the parasite *Trypanosoma cruzi* and was first discovered by Carlos Chagas in 1909.<sup>63</sup> The significance of this discovery is recognized by the Brazilian 10,000 cruzados banknote (Figure 10).<sup>66</sup>

---

<sup>61</sup> Dobish, M. C.; Villalta, F.; Waterman, M. R.; Lepesheva, G. I.; Johnston, J. N. *Org. Lett.* **2012**, *in press*.

<sup>62</sup> Villalta, F.; Dobish, M. C.; Nde, P. N.; Kleshchenko, Y. Y.; Hargrove, T. Y.; Johnson, C. A.; Waterman, M. R.; Johnston, J. N.; Lepesheva, G. I. *Journal of Infectious Disease*, **2012**, *in press*.

<sup>63</sup> Clayton, J. *Nature*, **465**, S4-S5.

<sup>64</sup> [http://www.who.int/neglected\\_diseases/en/](http://www.who.int/neglected_diseases/en/)

<sup>65</sup> Coura, J. R.; Vinas, P. A. *Nature*, **465**, S6-S7.

<sup>66</sup> <http://www.banknotes.com/br.htm>



**Figure 10.** Brazilian banknote recognizing Carlos Chagas and the life cycle of the deadly parasite.



Carlos Chagas (pictured) determined the clinical manifestations, epidemiology and entire life cycle of the parasite before his death in 1934. In the center of the bill, the blood feeding insect is resting on the human skin. The insect, also known as the kissing bug, bites its host and deposits its feces containing the parasite responsible for the disease. When the host scratches the bite, the parasite is transported into the blood system, and the life cycle of the parasite begins. Though this is the most common transmission vector, other contaminated subjects include crops, food, and drinks, and the parasite can also be passed congenitally from mother to child and through blood transfusions and organ transplantations.<sup>67</sup> The transition from the acute phase to the chronic phase is also pictured in the final stages of the lifecycle with the parasite entering cardiomyocytes.

Clinical Chagas disease is classified into acute and chronic phases.<sup>63</sup> The acute phase begins when the body is first infiltrated by the causative parasite, *T. cruzi*, and it starts multiplying within different organs and tissues. The acute phase often goes unnoticed because of the normally mild, non-specific symptoms: fever, swelling of lymph nodes and tissues, as well as skin lesions and conjunctivitis. However, in a small

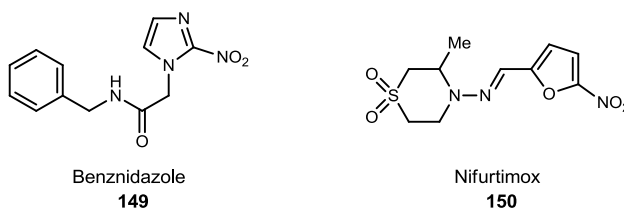
---

<sup>67</sup> Kirchhoff, L. V. *Advances in Parasitology, Vol 75: Chagas Disease, Pt A* 2011, 75, 1-18.

number of acute cases (~0.5%), the symptoms can be severe and lead to death.<sup>68</sup> The acute infection usually lasts 4 to 8 weeks, depending on the parasite burden and host immune system. If the infection is undetected, symptoms usually cease and the parasite then enters the chronic phase, where the parasitemia levels are undetectable by microscopy.

When an acute infection is detected, the drugs that are available to treat the parasite are limited. There are currently two treatments for the acute phase of Chagas disease: benznidazole (**149**) and nifurtimox (**150**), which have been available for over 50 years (Figure 11).<sup>69</sup>

**Figure 11.** Benznidazole and Nifurtimox



These drugs are efficient at treating patients in the early, acute phase with cure rates up to 80% for those completing the 2-3 month dosing regimen. Unfortunately, there are many reasons unrelated to the cell biology for the failure associated with these treatments. Not all areas that are susceptible to parasite transmission have the appropriate infrastructure to administer treatment. In areas where treatment is available, the high cost of these drugs often prevents patients from completing the full treatment, leading to the evolution of

---

<sup>68</sup> Bern, C. *N. Engl. J. Med.* **2011**, *364*, 2527-2534.

<sup>69</sup> Clayton, J. *Nature*, *465*, S12-S15.

drug resistant strains.<sup>70</sup> These drugs also have severe side effects, including skin rashes, nausea, and kidney and liver failure. Nifurtimox has also been shown to cause seizures and other nervous-system disorders, leading to patient noncompliance for a drug that has such a long dosing period. If the parasite is not eradicated in the acute phase, the parasite buries itself into vital organ systems and appears dormant for years or even decades before it manifests itself as a more severe condition.

One in three patients that are not cured in the acute phase will experience the symptoms related to the chronic phase of the disease: abnormal heart rhythm, heart failure, digestive problems, and sudden cardiac death. These symptoms are the result of the parasite infiltrating the vital organs of the patient. These conditions may not present until 5-15 years after infection, after which it is too late to begin treatment of the parasite. There are currently no known treatments for chronic Chagas that lead to complete parasite eradication; only the symptoms from the conditions can be treated. Additionally, the drugs that have been developed for the acute phase have shown very little efficacy in the more problematic chronic stage of the disease. Drug development has been lethargic, as there is insufficient incentive for industrial and commercial development.

### ***Chagas Therapy and Sterol Biosynthesis***

There are currently two approaches to curing Chagas disease: inhibition of protease activity and sterol biosynthesis.<sup>71</sup> It has been demonstrated that proteases are successful druggable targets for some cancers, diabetes, and infectious diseases.<sup>72</sup> The major *T. cruzi* protease cruzain, also known as cruzipain, is found in all phases of the *T. cruzi* lifecycle.

---

<sup>70</sup> Wilkinson, S. R.; Taylor, M. C.; Horn, D.; Kelly, J. M.; Cheeseman, I. *Proc. Natl. Acad. Sci. U. S. A.* **2008**, *105*, 5022-5027.

<sup>71</sup> McKerrow, J. H.; Doyle, P. S.; Engel, J. C.; Podust, L. M.; Robertson, S. A.; Ferreira, R.; Saxton, T.; Arkin, M.; Kerr, I. D.; Brinen, L. S.; Craik, C. S. *Memorias Do Instituto Oswaldo Cruz* **2009**, *104*, 263-269.

<sup>72</sup> Renslo, A. R.; McKerrow, J. H. *Nat. Chem. Biol.* **2006**, *2*, 701-710.

It is believed to be involved in the degradation of proteins from the blood meal of the insect vector. However, the location of the protease changes, depending on the stage of the lifecycle, operating in environments with pH 5.5-7.4. Developing drugs that can exist in both environments can be challenging. This is one of the issues that must be considered when designing therapeutics for cruzain inhibition. Though certain factors need to be considered, cruzain has been validated as a drug target in preclinical experiments.<sup>72</sup>

The other approach is targeting the production of sterols. Sterols are known to be a necessary component of eukaryotic cells, playing key roles in controlling fluidity and permeability of plasma membranes. While some eukaryotic phyla (e.g. insects) have developed the ability to scavenge sterols from exogenous sources for survival, others rely solely on endogenously synthesized sterols. This difference can be critical when considering treatment of certain diseases. In both cases, a sterol deficiency can be lethal to the cell. For example, a close parasitic cousin of *T. cruzi* is *Trypanosoma brucei*, the causative parasite of African sleeping sickness. Since it can scavenge sterols from exogenous sources, shutting down the sterol biosynthesis only slows growth of the parasite. However, because *T. cruzi* relies solely on endogenously produced sterols, shutting down the sterol biosynthesis pathway prevents further replication and is a viable approach to parasite eradication. The inhibition of sterol biosynthesis is also used for the treatment of human infections with fungi.

One of the most efficient and druggable targets in sterol biosynthesis is the sterol 14 $\alpha$ -demethylase (CYP51), a cytochrome P450 monooxygenase that catalyzes oxidative

removal of the 14 $\alpha$ -methyl group from cyclized sterol precursors.<sup>73</sup> CYP51 is present, and conserved in all biological kingdoms, including animal, plants, yeast/fungi, most protozoa and some bacteria. In higher order kingdoms, for example human and other animals, cholesterol serves as a precursor for other biologically important processes, such as production of hormones, nerve tissues, and bile acids, as well as in the conversion to vitamin D.

In *T. cruzi*, the CYP51 that is targeted is important for the conversion of squalene to ergosterol. More specifically, this enzyme is responsible for the three step process that converts eburicol (**M**) to 14 $\alpha$ -demethyl-14-dehydro-eburicol (Figure 12).<sup>74</sup> Each step of the three step process requires a molecule of oxygen, two electrons, and two protons. The methyl is oxidized three times, sequentially, from the alcohol to formic acid, where elimination, or loss of formic acid, yields an olefin. It is both the buildup of toxic methylated sterols and cell membrane damage (lack of ergosterol), that ultimately leads to cell death.<sup>75</sup>

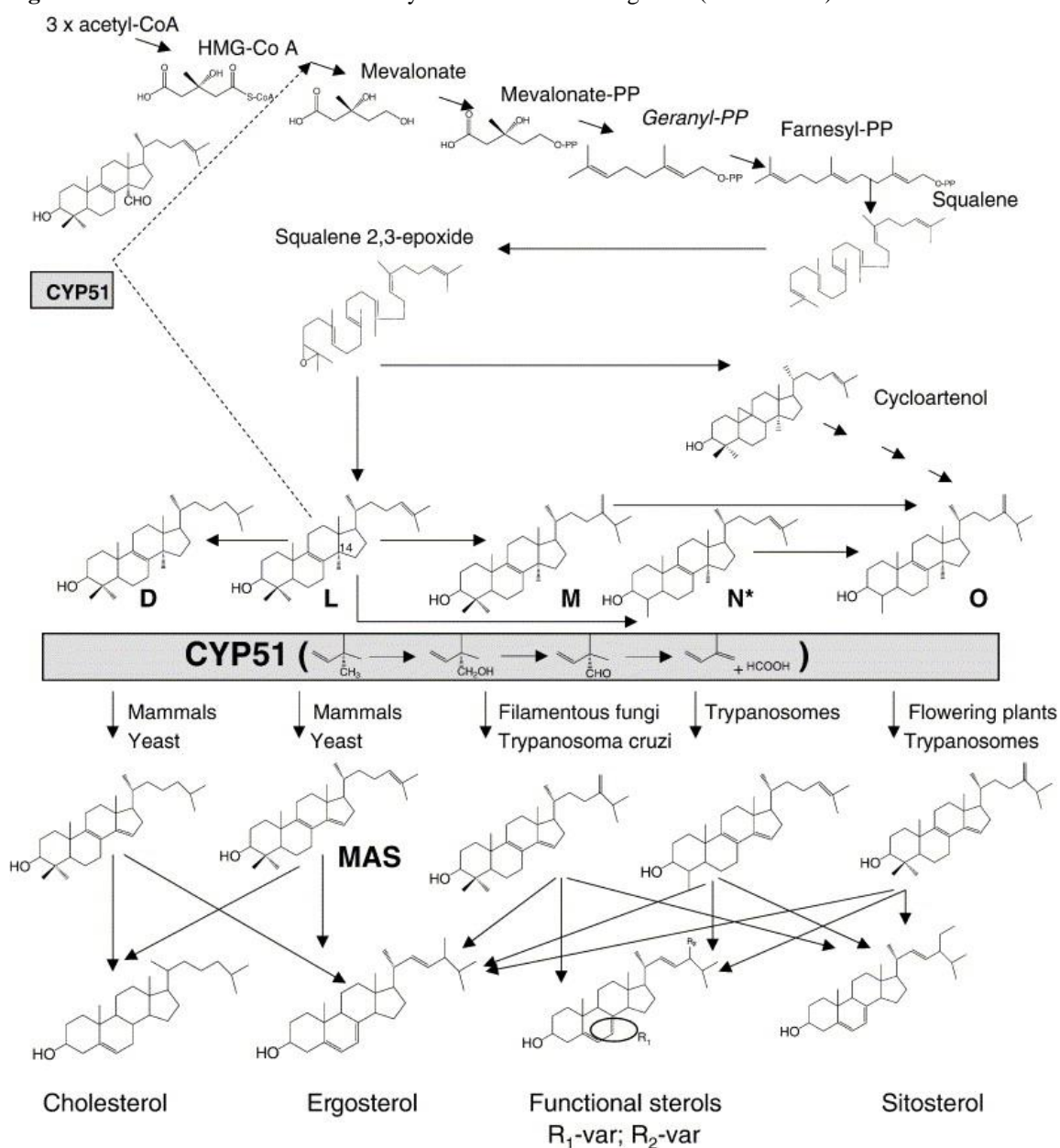
---

<sup>73</sup> Lepesheva, G. I.; Villalta, F.; Waterman, M. R. *Advances in Parasitology, Vol 75: Chagas Disease, Pt A* **2011**, 75, 65-87.

<sup>74</sup> Lepesheva, G. I.; Waterman, M. R. *Biochimica et Biophysica Acta (BBA) - General Subjects* **2007**, 1770, 467-477.

<sup>75</sup> Maertens, J. A. *Clinical Microbiology and Infection* **2004**, 10, 1-10.

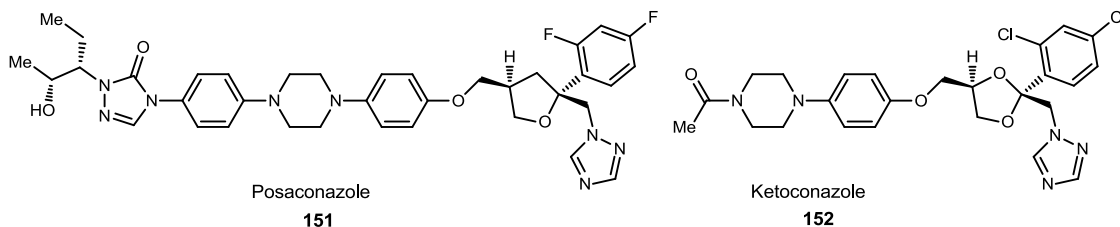
**Figure 12.** CYP51 reaction in sterol biosynthesis across the kingdoms (from ref. 74)



After 40 years of a dry pipeline, recent reports suggest that the antifungal drug posaconazole (**151**) may be effective in the treatment of Chagas disease.<sup>76</sup> Posaconazole, a drug developed by the Schering-Plough Research Institute, showed efficacy in curing both acute and chronic Chagas disease in murine models. In an isolated case in Spain, a

<sup>76</sup> Urbina, J. A.; Docampo, R. *Trends Parasitol.* **2003**, *19*, 495-501.

patient with both lupus and Chagas disease was treated with Posaconazole when conventional methods failed.<sup>69</sup> Though this was done unethically (no scientific basis for treatment) and as a final resort, there was no sign of the parasite three years after treatment, even using the most sensitive of detection techniques. Phase II clinical trials have begun on the use of Posaconazole to treat chronic Chagas disease.



Posaconazole, even if successful in clinical trials, may not be the answer since a course of treatment is estimated to be well over \$1000 per patient. However, posaconazole will validate CYP51 as a druggable target (or mechanism of action) in humans and may open the door for similar compounds that can be more easily attained. Unfortunately, ketoconazole (**152**), a cheaper but similar version of posaconazole, has proven to be drastically less effective in the treatment of benznidazole- and nifurtimox-resistant strains of *T. cruzi*.<sup>77</sup> Drugs with the same mechanism of action, an improved safety profile, and available at low cost are urgently needed.

### ***Industrial Synthesis of Posaconazole***

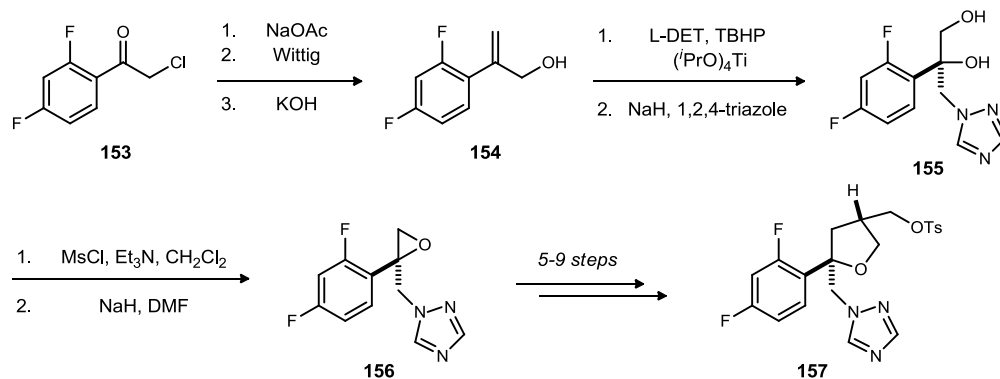
One of the reasons that posaconazole is such a costly treatment is the lengthy and linear sequence. The synthesis of posaconazole, as extracted from available patents, is

---

<sup>77</sup> Molina, J.; Martins-Filho, O.; Brener, Z.; Romanha, A. J.; Loebenberg, D.; Urbina, J. A. *Antimicrob. Agents Chemother.* **2000**, *44*, 150-155.

between 20 and 24 steps. The tricyclic core, which contains two stereocenters, is synthesized in 12-16 steps from achiral ketone **153** (Scheme 28).<sup>78</sup>

**Scheme 28.** Synthesis of Tricyclic Core of Posaconazole



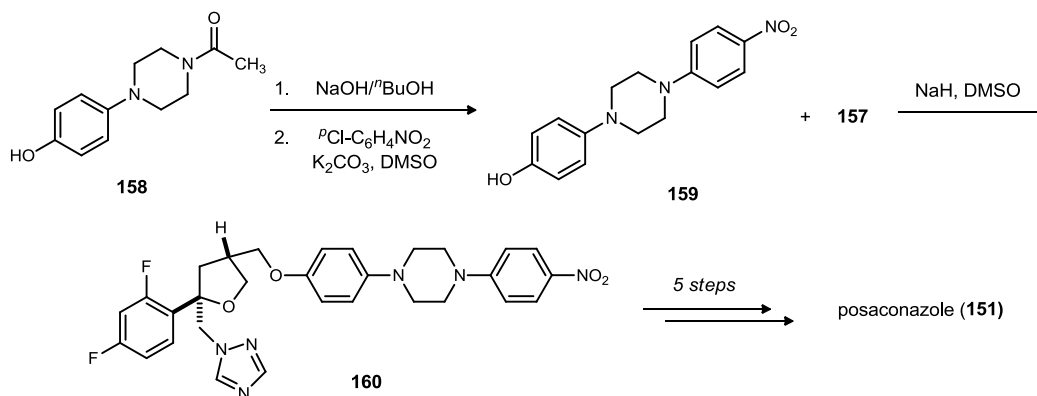
Allyl alcohol **154** is prepared from ketone **153** by a sodium acetate displacement of the chloride, followed by a Wittig reaction and alcohol deprotection. The allyl alcohol is then submitted to the Sharpless epoxidation conditions followed by epoxide ring opening with triazole to give **155** as a single enantiomer. The epoxide is reformed by alcohol mesylation and base promoted cyclization to give epoxide **156**, which is then converted to tricyclic triazole **157** in 5-9 steps.

The tricyclic side chain is synthesized in two steps starting from phenol **158** (Scheme 29).

<sup>78</sup> Saksena, Anil K.; Girijavallabhan, Viyyoor M.; Lovey, Raymond G.; Pike, Russell E.; Wang, Haiyan Liu Yi-tsung Ganguly Ashit K.; Bennett, Frank Tetrahydrofuran Antifungals. WO/95/17407, 29 June 1995.



### Scheme 29. Side Chain Synthesis and Completion of Posaconazole



Hydrolysis of the acetamide portion of bicycle **158** to reveal the secondary amine, followed by reaction of *para*-chloronitrobenzene and potassium carbonate yields the phenol **159**. The sodium salt of phenol **159** displaces the tosyl alcohol to give the main core of posaconazole (**160**). The final heterocycle was formed in five steps to give posaconazole.

### VNI as a Treatment for Chagas Disease

Waterman and Lepesheva at Vanderbilt University have published extensively on the role of 14 $\alpha$ -demethylase cytochrome P450 (CYP51) in sterol biosynthesis<sup>79</sup> and its availability as a druggable target.<sup>80</sup> Specifically, they have published on the 14 $\alpha$ -demethylase (14DM) of the parasites *Trypanosoma cruzi* (TC)<sup>81</sup> and *Trypanosoma brucei*

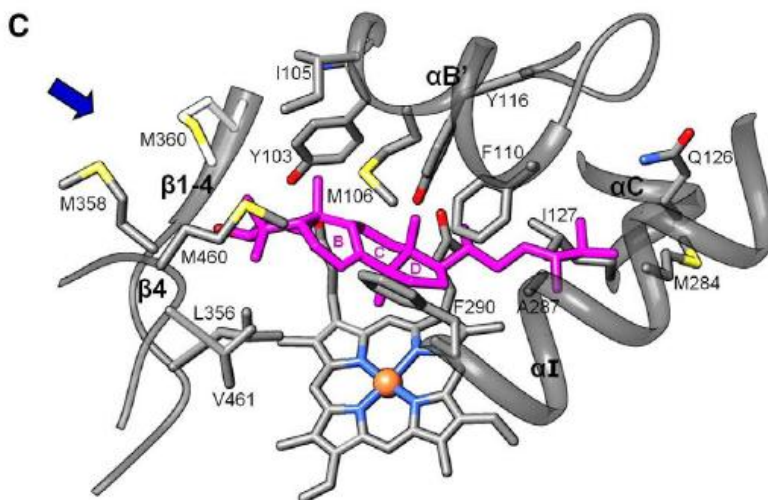
<sup>79</sup> Lepesheva, G. I.; Waterman, M. R. *Biochimica et Biophysica Acta (BBA) - General Subjects* **2007**, *1770*, 467-477.; Konkle, M. E.; Hargrove, T. Y.; Kleshchenko, Y. Y.; von Kries, J. P.; Ridenour, W.; Uddin, M. J.; Caprioli, R. M.; Marnett, L. J.; Nes, W. D.; Villalta, F.; Waterman, M. R.; Lepesheva, G. I. *J. Med. Chem.* **2009**, *52*, 2846-2853.; Lamb, D. C.; Lei, L.; Warrilow, A. G. S.; Lepesheva, G. I.; Mullins, J. G. L.; Waterman, M. R.; Kelly, S. L. *J. Virol.* **2009**, *83*, 8266-8269.

<sup>80</sup> Lepesheva, G.; Hargrove, T.; Kleshchenko, Y.; Nes, W.; Villalta, F.; Waterman, M. *Lipids* **2008**, *43*, 1117-1125.

<sup>81</sup> Lepesheva, G. I.; Ott, R. D.; Hargrove, T. Y.; Kleshchenko, Y. Y.; Schuster, I.; Nes, W. D.; Hill, G. C.; Villalta, F.; Waterman, M. R. *Chem. Biol.* **2007**, *14*, 1283-1293.; Lepesheva, G. I.; Hargrove, T. Y.; Anderson, S.; Kleshchenko, Y.; Futak, V.; Wawrzak, Z.; Villalta, F.; Waterman, M. R. *J. Biol. Chem.* **2010**, *285*, 25582-25590.

(TB),<sup>82</sup> responsible for Chagas disease and African sleeping sickness, respectively. They were able to obtain crystal structures of 14DM from both pathogens in the ligand-free and ligand-bound forms. Using the ligand-free crystal structure of CYP51 from *T. cruzi*, molecular modeling showed the substrate docked in the enzyme cavity (Figure 13).<sup>83</sup>

**Figure 13.** Modeled docking of eburicol in *T. cruzi* CYP51 (from ref. 83)



Eburicol, the sterol precursor that is converted to 14 $\alpha$ -demethyl-14-dehydro-eburicol in the CYP51, is shown in magenta. The blue arrow depicts the proposed entry of the substrate via a hydrophobic channel.

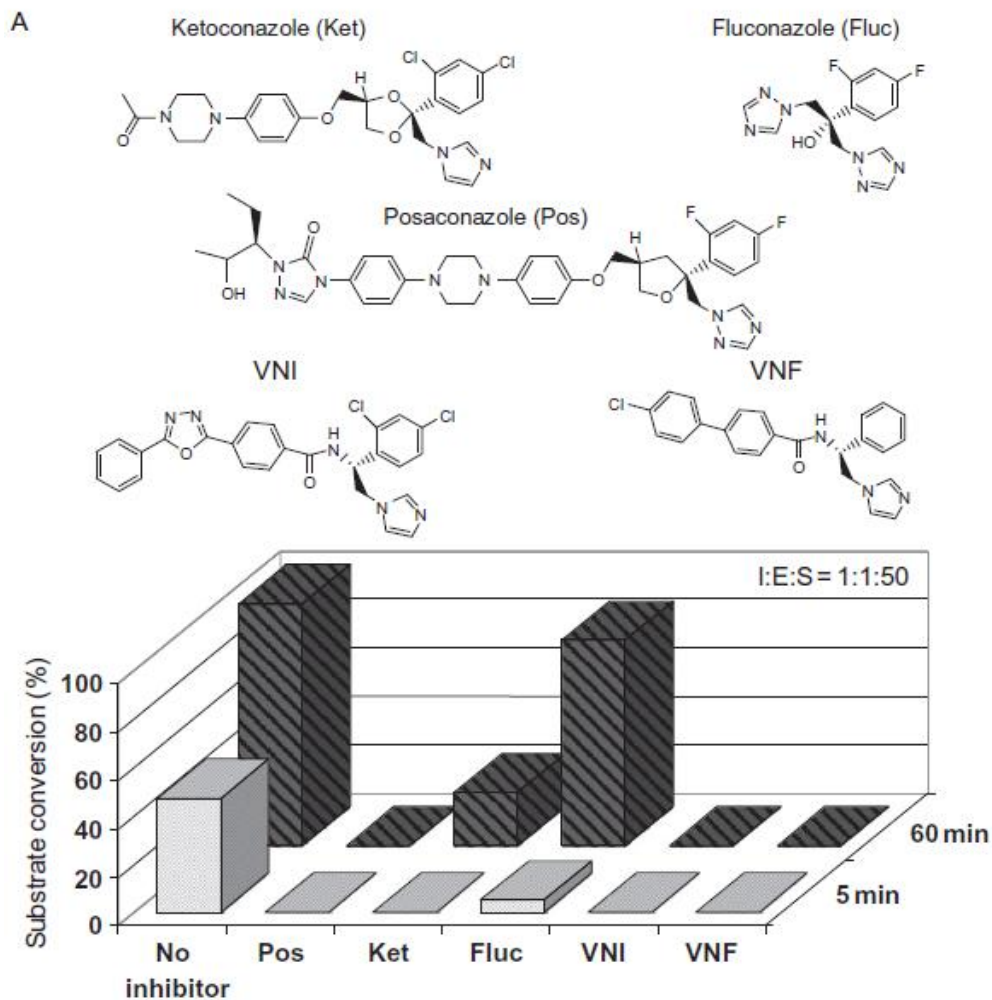
By measuring inhibition of sterol biosynthesis, defined here by the conversion of eburicol to 14 $\alpha$ -demethyl-14-dehydro-eburicol, potential inhibitors could be identified and their co-crystallization with the enzyme could lead to a rational structure-based lead optimization. To test for inhibition, the CYP51 from *T. cruzi* was combined with potential inhibitors, and the production of sterols (14DM activity) was monitored.<sup>81</sup>

<sup>82</sup> Lepesheva, G. I.; Park, H.-W.; Hargrove, T. Y.; Vanhollebeke, B.; Wawrzak, Z.; Harp, J. M.; Sundaramoorthy, M.; Nes, W. D.; Pays, E.; Chaudhuri, M.; Villalta, F.; Waterman, M. R. *J. Biol. Chem.* **2009**, *285*, 1773-1780.

<sup>83</sup> Lepesheva, G. I.; Waterman, M. R. *BBA-Proteins Proteom.* **2011**, *1814*, 88-93.

Initially, common antifungals (posaconazole, fluconazole, ketoconazole) and a selection from a library ofazole-inhibitors from Novartis (Switzerland) were screened (Figure 14).

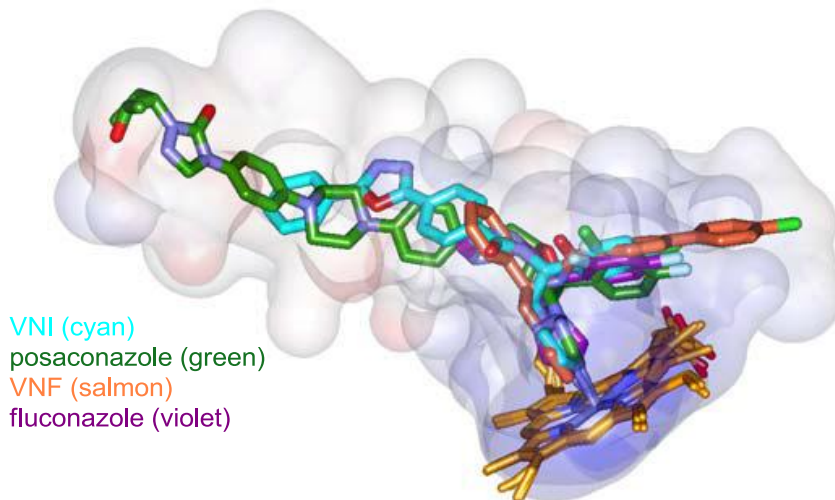
**Figure 14.** Small Molecule Inhibitors of *T. cruzi* CYP51 (from ref. 73)



It was determined that posaconazole (**Pos**), **VNI**, and **VNF** were competent inhibitors of sterol biosynthesis when the ratio of inhibitor:enzyme:substrate was 1:1:50. The other commercial antifungals tested, ketoconazole (**Ket**) and fluconazole (**Fluc**) There was a difference of inhibition between VNI and its enantiomer, with the dextrorotatory having

stronger inhibitory effects (5x more potent). These inhibitors were then cocrystallized with the CYP51 of *T. cruzi* and the crystal structures were overlaid to show the relative orientations in the enzyme cavity (Figure 15).

**Figure 15.** Overlay of Potential Inhibitors of *T. cruzi* CYP51 Crystal Structures (from ref. 81)



They found that posaconazole (green) and **VNI** (cyan) bound in a similar orientation, with the dihaloaryl ring buried deep into the pocket and the azole coordinated to the heme. Additionally, both long chain arms were aligned in the hydrophobic access channel. Interestingly, **VNF** (salmon) is the same configuration of **VNI** but is oriented in the opposite direction.

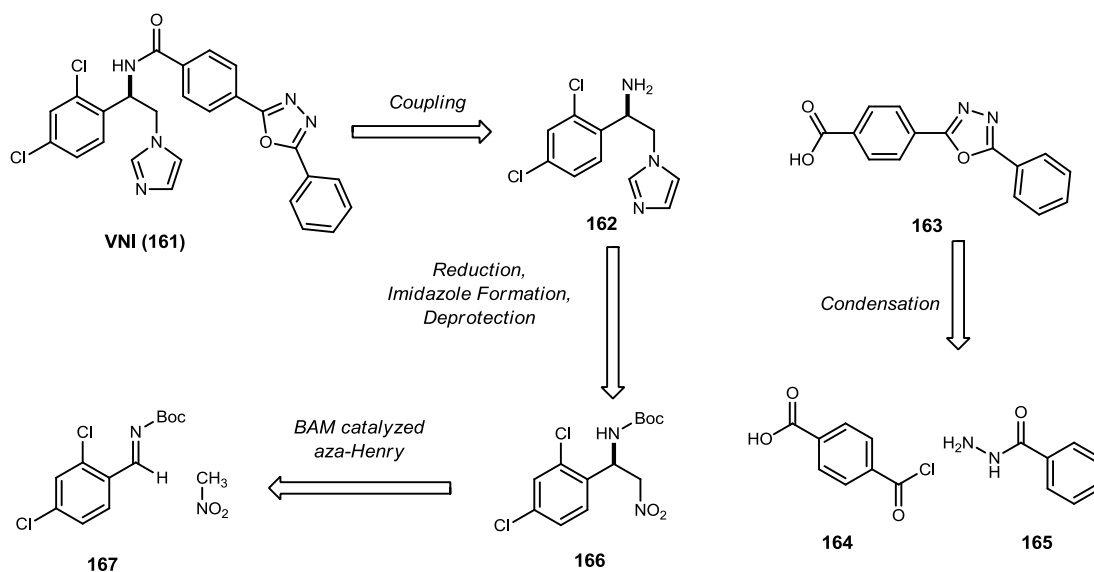
Preliminary results from the Waterman Lab were encouraging: VNI is a potent inhibitor of CYP51 in sterol biosynthesis and VNI binds to the enzyme in a similar fashion to posaconazole. Unfortunately, the compounds from Novartis were obtained in only small amounts, so a new source of VNI was needed to complete further testing.

## 2.2 The Short, Enantioselective Synthesis of VNI

### Background and Project Goals

In 2007, Lepesheva and Waterman identified VNI (**161**) as a potent experimental inhibitor of trypanosomal CYP51.<sup>81</sup> Unfortunately, the initial quantity of VNI was obtained from a nonrenewable source (Novartis library of compounds) and there are no preparative details. Both VNI<sup>84</sup> and its enantiomer were provided for the initial screen, suggesting the racemate was prepared and separated by chiral chromatography. We sought to develop a synthesis that was not only efficient and selective, but easily diversified for other analogs. As illustrated in Scheme 30, our proposed synthesis utilizes a BisAMidine (BAM) catalyzed, enantioselective aza-Henry reaction to set the benzylamine stereocenter.

Scheme 30. Retrosynthetic Analysis of VNI

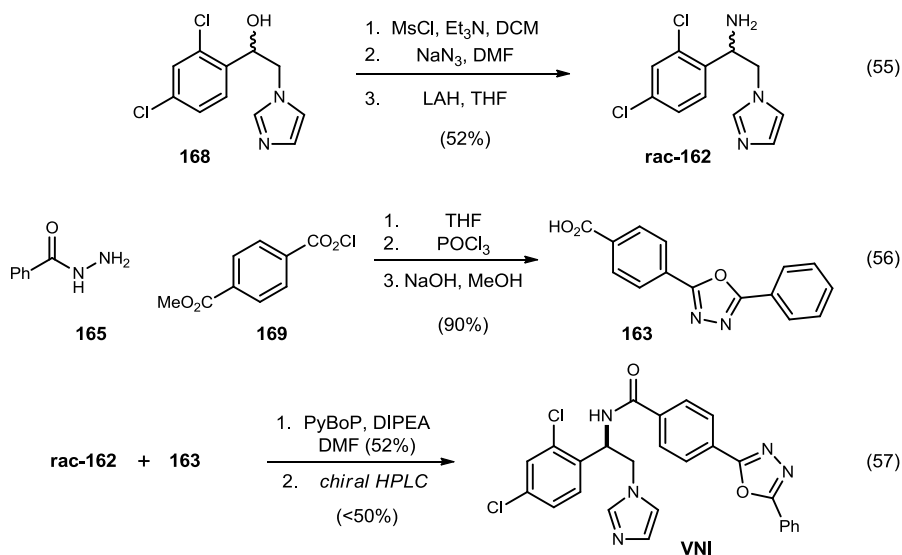


<sup>84</sup> The abbreviation 'VNI' refers specifically to the (*R*)-enantiomer, the more potent inhibitor of CYP51. An X-ray crystal structure of VNI bound to CYP51 has been reported (ref. 81). VNI is the dextrorotatory (+) enantiomer.

First, we envisioned that the amide bond could be formed through a coupling reaction, of chiral amine (**162**) with the appropriate carboxylic acid (**163**). The tricyclic carboxylic acid could be formed via a condensation of 4-(chlorocarbonyl)benzoic acid (**164**) and benzoic hydrazide (**165**). The desired imidazole (**162**) could be formed by a series of condensations with glyoxal, formaldehyde, and ammonia after reduction of the aza-Henry adduct (**166**). To obtain the chiral, non-racemic aza-Henry adduct, we envisioned the addition of nitromethane to the *N*-Boc aryl aldimine (**167**) using a BAM catalyst.

At the same time we began our investigations, the synthesis core at Vanderbilt was contracted to synthesize VNI for further biological testing (Figure 16).<sup>85</sup>

**Figure 16.** Racemic synthesis of VNI and *epi*-VNI



<sup>85</sup> Hargrove, T. Y.; Kim, K.; de Nazaré Correia Soeiro, M.; da Silva, C. F.; da Gama Jaen Batista, D.; Batista, M. M.; Yazlovitskaya, E. M.; Waterman, M. R.; Sulikowski, G. A.; Lepesheva, G. I. *International Journal for Parasitology: Drugs and Drug Resistance* **2012**, *2*, 178-186.

Starting from commercially available racemic alcohol **168**, with the dichloroaryl ring and imidazole already in place, a three step functional group manipulation gave the free amine **rac-162**. The side chain was made through a three step sequence from benzohydrazide (**165**) and monoprotected benzoate **169**. An amide bond forming reaction using PyBoP gave a mixture of VNI and the enantiomer of VNI. The enantiomers were separated by preparative chiral chromatography to give VNI.

Though this route was sufficient for preparation of small quantities of material, this is an inefficient means for synthesis on a large scale, or for the synthesis of other derivatives. The use of chiral chromatography on racemic material is expensive and inefficient, as 50% of the material is discarded. The highly functionalized alcohol that was purchased may not be available for other desired analogs, requiring a new route to obtain a similarly functionalized intermediate. The time and cost of such a route is not conducive to a medicinal chemistry campaign where the goal is to rapidly develop a large library of compounds for biological testing. An enantioselective route from commercially available materials might provide the rapid access to analogs that a medicinal chemistry project needs.

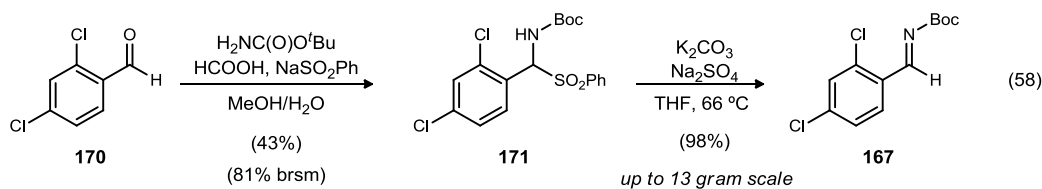
### ***BAM Catalyzed aza-Henry***

The required *N*-Boc aryl aldimine **167** was synthesized using known procedures from the requisite aldehyde (Scheme 31).<sup>86</sup>

---

<sup>86</sup> Kanazawa, A. M.; Denis, J.-N.; Greene, A. E. *J. Org. Chem.* **1994**, *59*, 1238-1240.

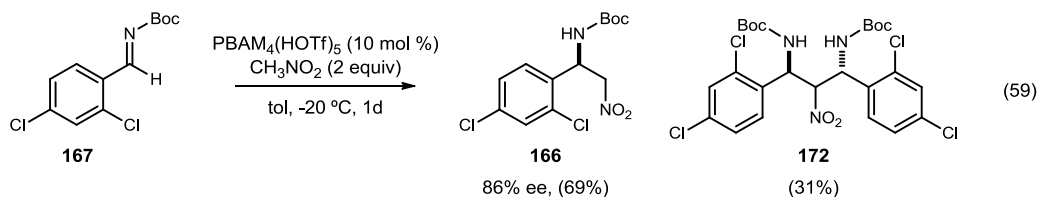
**Scheme 31.** Synthesis of *N*-Boc-2,4-Dichlorobenzaldimine



The commercially available aldehyde was stirred with *tert*-butylcarbamate and benzene sulfinic acid to give  $\alpha$ -amido sulfone **171** in low conversion. We believe the low conversion stemmed from poor solubility of the aldehyde, but were able to recover the starting material and increase the efficiency of our first step. The imine was formed in quantitative yields to give pure imine **167**, with the largest scale yielding 13 grams (48 mmol) of material. The imine was then submitted to the aza-Henry reaction.

We have shown that H,QuinBAM (**92**) can catalyze the addition of simple nitroalkanes to *N*-Boc aryl aldimines when the nitroalkane is used as solvent (56 equiv) and stirred for days.<sup>47</sup> With the development of the more Brønsted-basic catalyst PBAM (**100**), we hoped that the addition could take place with a shorter reaction time using stoichiometric amounts of nucleophile. Recently, it was shown that reaction of aliphatic nitroalkanes with *N*-Boc aryl aldimines is most selective when the triflic acid salt of PBAM [(PBAM)<sub>2</sub>(HOTf)<sub>3</sub>] is used.<sup>52</sup> We used similar conditions for this crucial transformation (Scheme 32).

**Scheme 32.** PBAM Catalyzed aza-Henry Reaction of Nitromethane: A Double Addition

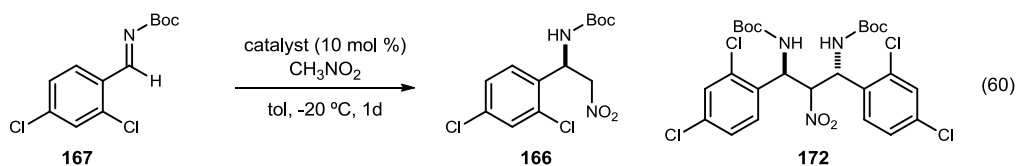




The desired product (**166**) formed with high enantioselection (86% ee) and good yields (74%). Unfortunately, a minor by-product determined to be the double addition product (**172**) was also isolated. When H,QuinBAM was used for nitroalkane additions, negligible amounts of the double addition products were seen, which is most likely due to the decreased reactivity of the catalyst.

To minimize the double addition product and increase enantioselection, different reaction conditions were evaluated (Table 16).

**Table 16.** Reaction Optimization for the PBAM-Catalyzed Addition of Nitromethane



| entry          | catalyst                              | CH <sub>3</sub> NO <sub>2</sub><br>(equiv) | (M) | 166:172<br>(ratio) <sup>b</sup> | ee (%) |
|----------------|---------------------------------------|--|-----|---------------------------------|--------|
| 1              | PBAM <sub>4</sub> (HOTf) <sub>5</sub> | 2  | 0.5 | 69:31                           | 86     |
| 2              | PBAM <sub>4</sub> (HOTf) <sub>5</sub> | 2  | 1.0 | 73:27                           | 90     |
| 3              | PBAM <sub>2</sub> (HOTf) <sub>3</sub> | 2  | 0.5 | 60:40                           | 82     |
| 4              | PBAM(HOTf)                            | 2  | 0.5 | 66:34                           | 79     |
| 5              | PBAM <sub>2</sub> (HOTf) <sub>1</sub> | 2  | 0.5 | 63:37                           | 75     |
| 6              | PBAM <sub>4</sub> (HOTf) <sub>5</sub> | 5  | 0.5 | 79:21                           | 78     |
| 7              | PBAM <sub>4</sub> (HOTf) <sub>5</sub> | 10   | 0.5 | 87:13                           | 80     |
| 8 <sup>c</sup> | PBAM <sub>4</sub> (HOTf) <sub>5</sub> | 93   | -   | >95:5                           | 49     |

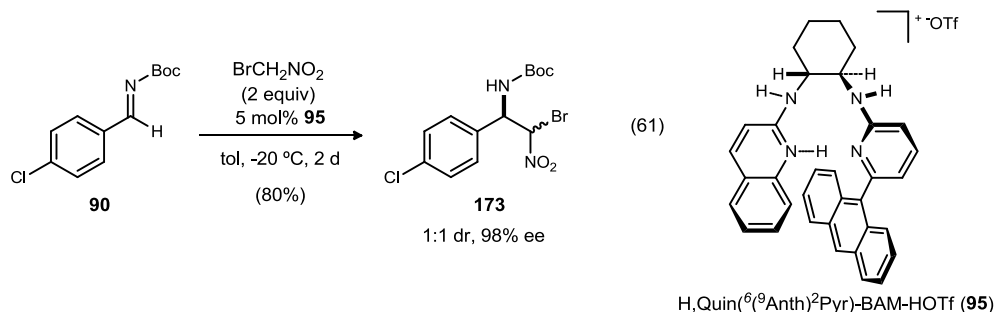
<sup>a</sup> All reactions were performed on a 0.10 mmol scale using 1 equivalent of the imine under the conditions listed. <sup>b</sup> Ratios of product measured by <sup>1</sup>H NMR. <sup>c</sup> Run in nitromethane as solvent.

When the reaction concentration was increased, a slight increase in ee was observed, with nominal change in the ratio (Table 16, entry 2). A screen of catalysts (varying ratios of triflic acid to PBAM) showed very little change in ee or influence in the ratios of mono-addition (**167**) to double addition (**172**) products (Table 16, entries 3-5). An increase in

the equivalents of nitromethane corresponded to an increase in the ratio of **166** to **172** (Table 16, entries 6-8), with a lowering of enantioselection. Use of nitromethane as the solvent (Table 16, entry 8) suppressed the double addition, but enantioselection dropped to 49% ee. Unable to optimize this addition any further, we considered a more hindered nucleophile that could be converted to the same desired intermediate after the enantioselective addition.

In 2010, we reported the addition of bromonitromethane to *N*-Boc aryl aldimines using an unsymmetrical BAM catalyst (Scheme 33).<sup>87</sup>

**Scheme 33.** Bromonitromethane aza-Henry Addition using an Unsymmetrical BAM Catalyst



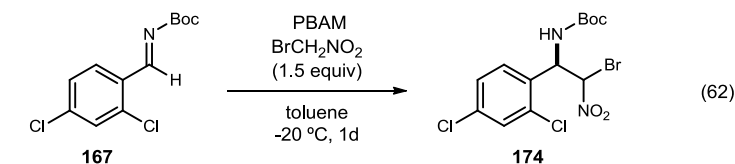
Under these conditions the *para*-chloro adduct **173** was isolated in high yield and 98% ee. Even though the *anti*- and *syn*-diastereomers were isolated as a 1:1 ratio, subsequent experiments showed that they were homochiral at the benzylic carbon. Further optimization showed the more robust catalyst PBAM (**100**) could catalyze the addition of bromonitromethane in higher yields (94%) and enantioselection (99% ee for both diastereomers).<sup>88</sup>

<sup>87</sup> Shen, B.; Makley, D. M.; Johnston, J. N. *Nature* **2010**, *465*, 1027-1032.

<sup>88</sup> Makley, D. M.; Johnston, J. N. *unpublished results*

We hypothesized that the bromine functions as a removable blocking group to slow the double addition, so the addition of bromonitromethane was tested under similar conditions (Table 17).

**Table 17.** Optimization of Bromonitromethane Additions to *N*-Boc-2,4-Dichloroaldimine



| entry          | imine (mmol) | cat. (mol %) | toluene (M) | ee (%) | % yield <sup>b</sup> (% conv) |
|----------------|--------------|--------------|-------------|--------|-------------------------------|
| 1              | 0.1          | 10           | 0.3         | 96/96  | 90                            |
| 2 <sup>c</sup> | 0.1          | 10           | 0.3         | 95/95  | 95                            |
| 3              | 1.0          | 10           | 0.3         | 96/95  | 95                            |
| 4              | 1.0          | 10           | 0.5         | 95/95  | 57 (99)                       |
| 5              | 1.0          | 5            | 0.3         | 96/96  | 85                            |
| 6              | 1.0          | 5            | 0.2         | 96/97  | 90                            |
| 7              | 5.8          | 2            | 0.2         | 95/97  | 83                            |

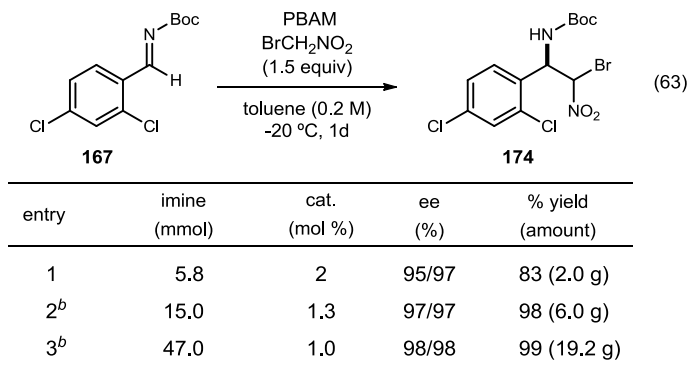
<sup>a</sup> All reactions were performed using 1 equivalent of the imine under the conditions listed. <sup>b</sup> Isolated yields after column chromatography and conversion measured by <sup>1</sup>H NMR. <sup>c</sup> PBAM<sub>2</sub>(HOTf)<sub>3</sub> used as catalyst.

On a small scale, the free base of PBAM (Table 17, entry 1) gave the desired bromonitromethane adduct 174 in marginally higher ee than the triflic acid salt of the catalyst (Table 17, entry 2). The reaction was also concentration dependent, as lower concentrations gave slightly higher values of enantioselection, as well as less debrominated side product **166** (the formal addition of nitromethane). More of the debrominated side product (up to 8%) was seen at higher temperatures and with larger catalyst loadings. This side product may arise from the debromination of the product by the catalyst, as more is present as the catalyst loading increases, rather than a nitromethane impurity in the bromonitromethane. The selectivity for the addition of bromonitromethane appeared robust as the enantiomeric excess was unchanged by slight

variations in the reaction conditions (Table 17, entries 3-6). The catalyst loading was further decreased from 10 mol % to 2 mol %, and the desired product was still delivered in equally high enantioselection. Further scaling up of the reaction was accompanied by a drop in the yield (Table 17, entry 7), which was a result of complications from column chromatography corresponding to incomplete recovery of product.

Attempts were made to complete the reaction on a large scale, testing limits that had not been previously examined with a BAM catalyzed addition (Table 18).

**Table 18.** Large Scale Optimization of BAM Catalyzed aza-Henry



<sup>a</sup> All reactions were performed using 1 equivalent of the imine under the conditions listed. <sup>b</sup> No column after silica filtration to remove catalyst.

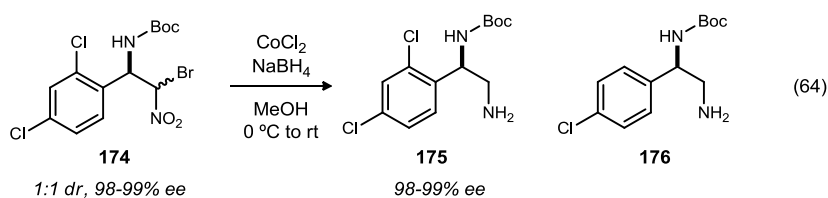
When the reaction was run at three times the scale with a lower catalyst loading, a slight increase in enantioselection of the product was observed (Table 18, entry 2). More importantly, the low level of catalyst loading and larger scale produced the product with greater than 98% purity before column chromatography, leading to an increase in yield (98%). An almost 500 fold increase in scale from initial experiments (from 0.1 mmol scale) returned favorable results (Table 18, entry 3); filtration provided 19.2 grams of analytically and enantiomerically pure product in nearly quantitative yield using only 1 mol % PBAM. The use of this highly reactive organocatalyst (>100 turnovers) in a large

scale preparation to deliver the scaffold is punctuated by the ability to recover and recycle the catalyst without loss of activity. This is the largest PBAM reaction completed in the Johnston group to date and demonstrates the robustness of the transformation for even larger scale applications. With a large amount of enantioenriched aza-Henry adduct (**174**) in hand, the tandem debromination/denitration was performed using a procedure commonly exploited in this group.

### Reduction of the aza-Henry Adduct

In 2008, the group reported the sequential BAM catalyzed addition of nitroacetates and nitro reduction using cobalt chloride and sodium borohydride.<sup>50,89</sup> Using the same conditions, we attempted to reduce the bromonitromethane aza-Henry adduct (Table 19).

**Table 19.** Large-Scale Optimization of One-pot Debromination/Nitro Reduction



| entry | 174 (mmol) | yield (%) <sup>b</sup> | amount |
|-------|------------|------------------------|--------|
| 1     | 1.3        | 75                     | 0.24 g |
| 2     | 6.0        | 55                     | 1.01 g |
| 3     | 46.4       | 52                     | 7.42 g |

<sup>a</sup> All reactions were performed using 1 equivalent of the bromonitromethane adduct under the conditions listed. <sup>b</sup> Isolated yield.

The reaction occurred with high yields (75%) on small scale (Table 19, entry 1) corresponding with isolation of a trace amount of the *ortho*-deschloro adduct **176**. When the reaction scale was increased, the yield of amine **175** decreased (Table 19, entry 2)

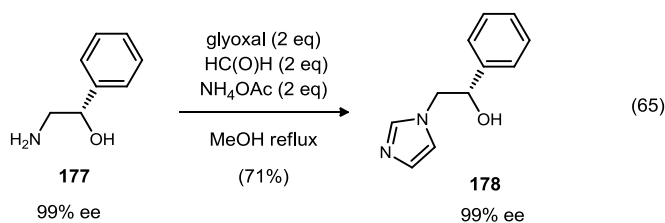
<sup>89</sup> Mechanism: Heinzman, S. W.; Ganem, B. *J. Am. Chem. Soc.* **1982**, *104*, 6801-6802. Osby, J. O.; Heinzman, S. W.; Ganem, B. *J. Am. Chem. Soc.* **1986**, *108*, 67-72.

while the amount of undesired amine **176** increased. The small reduction in yield is attributed to the necessary chromatography separation of two amines that have similar  $R_f$  values. Gratifyingly, at the largest scale we were able to isolate almost 7.5 grams of pure amine **175** (Table 19, entry 3).

### **Imidazole Formation**

To form the imidazole portion of the compound, we looked to work reported by Saigo in 2006 on the synthesis of imidazoles from chiral non-racemic amines (Scheme 34).<sup>90</sup>

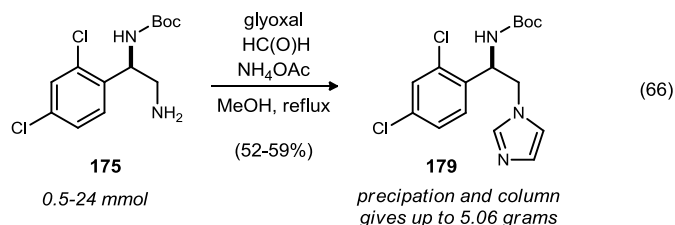
**Scheme 34.** Synthesis of Imidazoles from Chiral Non-Racemic 1,2-Amino Alcohols



Refluxing primary 1,2-amino alcohol **177** in methanol with glyoxal, formaldehyde, and ammonium acetate, resulted in the isolation of enantiopure imidazole **178** in 71% yield. This reaction is valuable because it allows many heterocycles to be accessed from a common amine just by varying the reactants (substituted glyoxals and aldehydes). When these conditions were applied to the VNI 1,2-diamine, we isolated the adduct in moderate, but synthetically useful yields (Scheme 35).

<sup>90</sup> Matsuoka, Y.; Ishida, Y.; Sasaki, D.; Saigo, K. *Tetrahedron* **2006**, *62*, 8199-8206.

**Scheme 35.** Scalable Imidazole Formation from Reduced aza-Henry Adduct



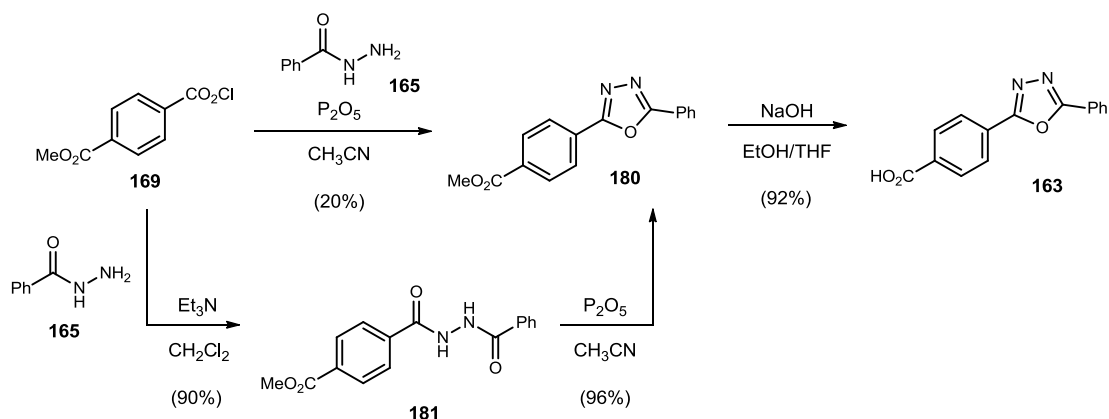
This robust reaction gave similar yields of imidazole **179** on most of the scales tested (from 0.5-24 mmol). Column chromatography often proved difficult because of the poor solubility of the crude reaction mixture in dichloromethane, which may have led to lower recovery of product. The highest yield was obtained on the largest scale reaction, with 49% of the material being recovered by precipitation from dichloromethane with hexanes, and an additional 10% isolated via column chromatography. The enantiomeric excess of imidazole **179** was found to be the same as the starting aza-Henry adduct (**174**), showing that no stereochemical scrambling took place during any of the previous reactions. We then embarked on the synthesis of the carboxylic acid side chain.

***Side Chain Synthesis and Completion of VNI***

It was reported that aryl acid hydrazides and benzoyl chlorides could be condensed to form oxadiazoles (such as **180**) at room temperature under phosphorous pentoxide conditions in excellent yields (>85%).<sup>91</sup> A synthesis was developed for the tri-aryl side chain starting from commercially available starting materials (Scheme 36).

<sup>91</sup> Rostamizadeh, S.; Ghamkhar, S. *Chin. Chem. Lett.* **2008**, *19*, 639-642.

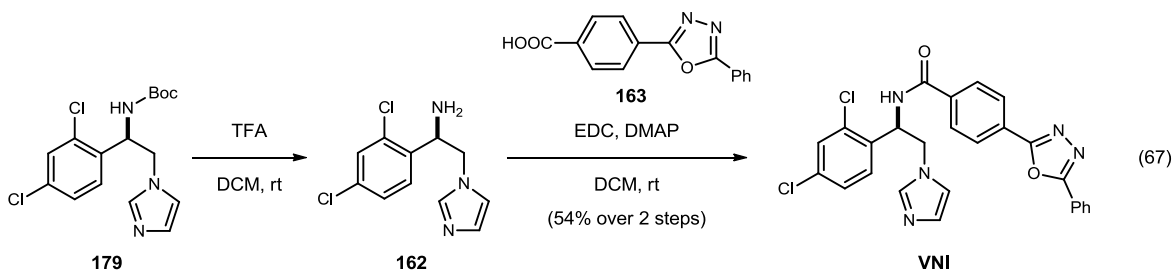
**Scheme 36.** Synthesis of the Tri-Aryl Side Chain.



Unfortunately, using conditions developed for similar substrates, the yields of the oxadiazole (**180**) only reached 20%, which was a fraction of the reported yields. A significant amount of the bisamide **181** was recovered and resubmitted to the reaction conditions to give complete conversion to the desired oxadiazole (**180**). We believe that the bisamide precipitated out of solution and prevented full conversion. In two high yielding steps, the bisamide **181** was formed using triethylamine in 90% yield and the oxadiazole was then formed in >95% yield. Saponification gave the desired carboxylic acid (**163**) in high yields.

With the amine and carboxylic acid portions in hand, all that remained was the coupling to form the desired amide bond (Scheme 37).

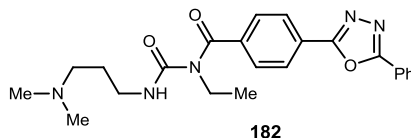
**Scheme 37.** Endgame: The Synthesis of VNI.





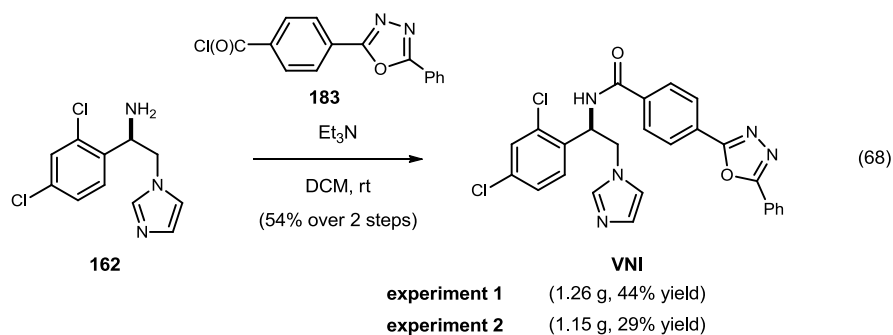
Following *N*-Boc deprotection of amine **179** in quantitative yield, the amine and carboxylic acid were coupled under standard conditions using EDC. The transformation occurred to give VNI in up to 54% yield over two steps, producing 27 mg of product. We were able to develop an assay for the separation of the prepared racemate and aid the Vanderbilt Synthesis Core with their separation needs. Since assignment of absolute configuration to aza-Henry adduct **174** could be made confidently by analogy to numerous BAM-catalyzed reactions, the retention times of VNI prepared by our sequence could be used to identify VNI among the racemate peaks.

We were able to increase the scale of the coupling to obtain 330 mg of VNI (65% yield). However, attempts to increase the scale any further were thwarted by the presence of an unavoidable byproduct, a possible rearrangement product from the EDC and carboxylic acid fragment to the *N*-acylurea **182**.



Our immediate concerns were with the delivery of the compound, so rather than screening numerous other combinations of coupling reagents, we decided to form the amide bond reaction using an acylation of the amine with the requisite acid chloride (**183**) (Scheme 38).

**Scheme 38.** Large Scale Acylation to give VNI



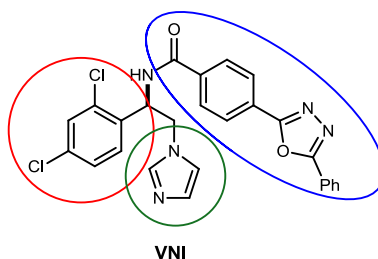
Though we were able to increase the scale of the reaction, delivering grams of VNI in one reaction, the yield (29-44%) and crude purity varied between the reactions. At this point we had reached our target of 4 grams of VNI needed for the initial mouse studies, so further reaction optimization is reserved for second generation routes. To optimize this step, we would look at a number of conditions for the coupling of the carboxylic acid and free amine (e.g. PyBoP<sup>85</sup>).

This highly enantioselective and efficient synthesis, completed on a gram scale, has allowed for the production of enough VNI to complete studies of *T. cruzi* eradication in the murine model. Our first generation route relied heavily on chromatographic purification. Since most of the reactions were scaled and optimized further, we were able to eliminate most columns and use precipitations and filtrations to purify most intermediates. This bodes well for the potential scalability of our route, where our largest scale route required only two chromatographic purifications. Additionally, we have estimated the cost of materials to be less than \$0.10/mg (Appendix I).

## VNI Analog Synthesis

One of the goals of our synthesis was to develop a route that was amenable to further analog development, highlighted in color below (Figure 17).

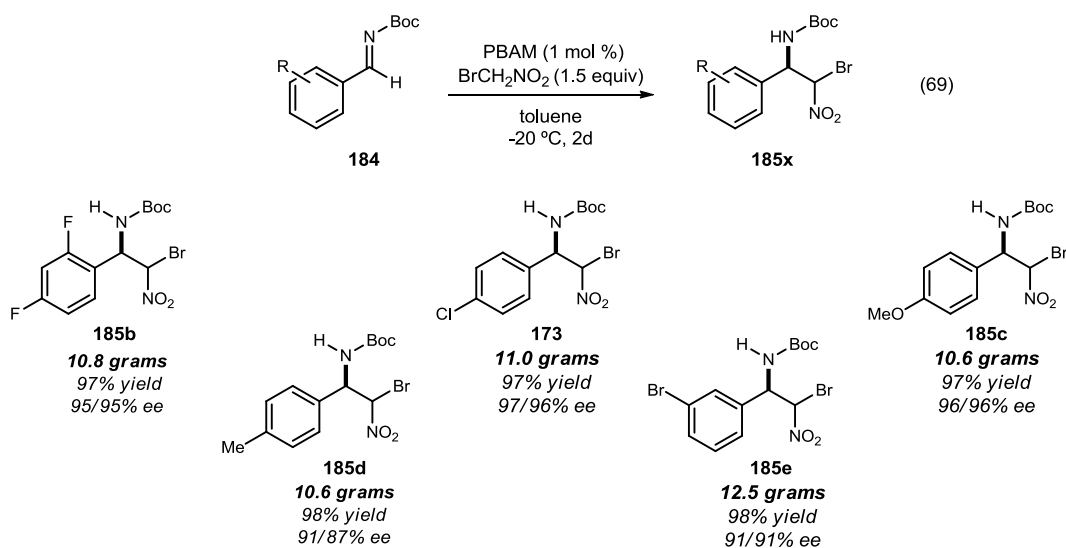
**Figure 17.** Achievable Points of Diversity in the Synthesis of VNI and other Analogs



The aryl ring (circled in red) can be varied using different *N*-Boc-aryl aldimines in the PBAM catalyzed bromonitromethane additions. The imidazole ring (green) can be modified with different functional groups by using substituted glyoxal and formaldehyde equivalents. Other heterocycles can also be accessed from the amine resulting from reduction of the aza-Henry adducts. Finally, any carboxylic acid portion (blue) could conceivably be coupled in the last step of the synthesis, allowing for a quick screen of various analogs.

To demonstrate the generality and scope of the scale of the bromonitromethane additions, we looked at a number of differentially substituted *N*-Boc-aryl aldimines (Chart 2).

**Chart 2.** Large Scale Bromonitromethane Additions to Imines Catalyzed by PBAM.

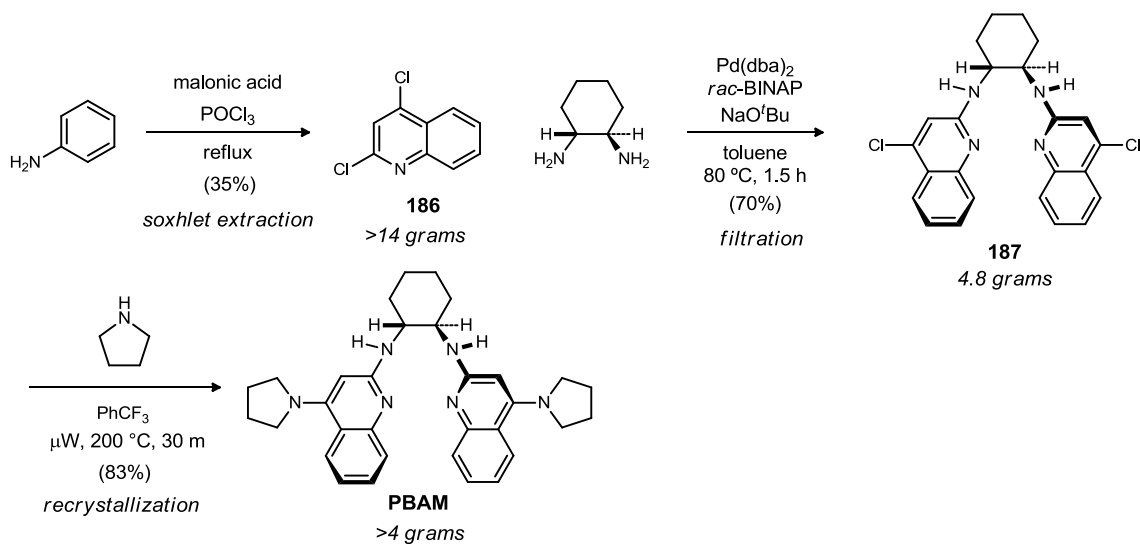


The 2,4-difluorinated analog (**185b**) gave comparable results to the 2,4-dichloro analog of VNI. Removing the *ortho*-chloro (**173**) or installing a *para*-methoxy group (**185c**) returned over 10.5 grams of product in greater than 96% ee for both diastereomers. When a methyl group was in the *para*-position (**185d**) or a bromine was in the *meta*-position (**185e**), a slight drop in enantioselection was observed, but product with greater than 90% ee was recovered. Overall, the additions show that the scalemic scaffold can be quickly accessed, on scale, for a variety of aryl rings.

The use of PBAM on large scale has been advanced by our recent report of an *Organic Syntheses* preparation (Figure 18).<sup>92</sup>

<sup>92</sup> Davis, T. A.; Dobish, M. C.; Schwieter, K. E.; Chun, A. C.; Johnston, J. N. *Org. Synth.* **2012**, *89*, 380-393.

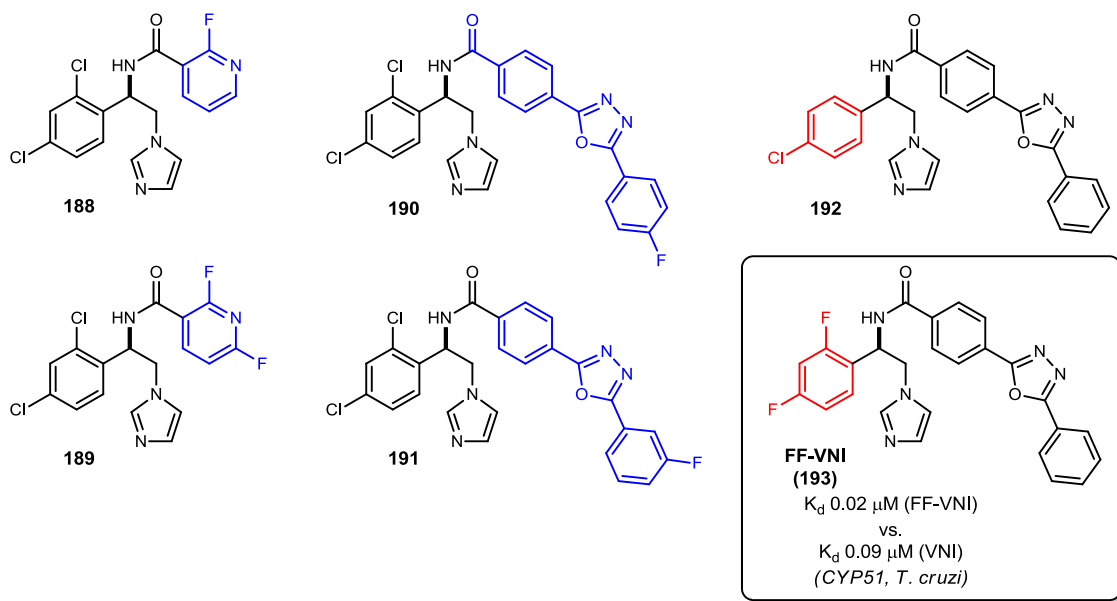
**Figure 18.** *Organic Syntheses* Preparation of PBAM.



Improving on our first generation route, we were able to remove column chromatography at each transformation, replacing them with a hot solvent extraction of quinoline **186**, filtration of  $^4\text{Cl}$ -BAM (**187**), and recrystallization of the final catalyst (**PBAM**). Additionally, two undergraduate students (NSF-REU) aided in the manuscript preparation, demonstrating the straightforwardness of the catalyst synthesis. With this publication, the availability and access to this catalyst has increased as we move forward towards making it commercially available.

To demonstrate the brevity of the route, analogs of VNI were prepared for evaluation (Figure 19).

**Figure 19.** Prepared VNI analogs.



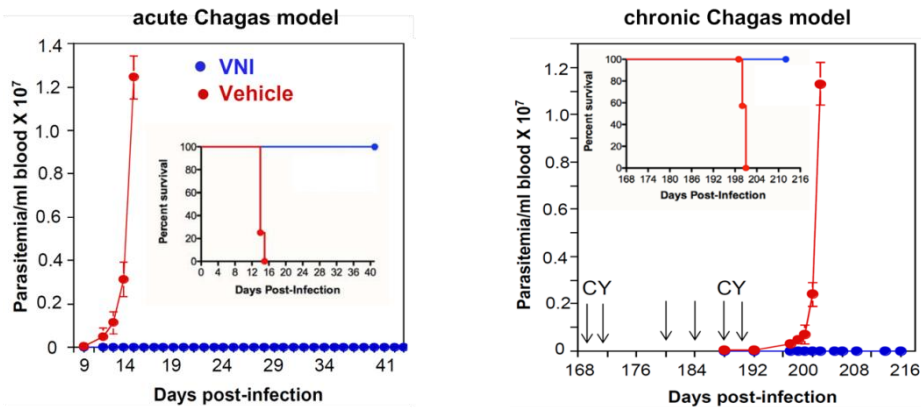
The first analogs made were synthesized by coupling the free amine to fluoro-pyridines in an attempt to both establish the influence of the side chain and possibly slow drug metabolism (**188** & **189**). Slight modifications to the side chain (**190** & **191**) were made to determine the interactions of the substrate access channel. Of the four side chain analogs examined, no significant improvement was observed in the *T. cruzi* CYP51 inhibition assay. The des-chloro-VNI compound **192** (recovered from reduction of **174** in large scale VNI synthesis) was also submitted for testing. The final analog that was synthesized contained a 2,4-difluoroaryl ring in the western portion of the molecule, similar to posaconazole (**151**). The synthesis of **FF-VNI** was completed on large scale and only required a single chromatographic purification in the last step of the synthesis. Gratifyingly, this exchange of chlorines for fluorines on the VNI backbone resulted in a four-fold improvement in binding to the CYP51.<sup>85</sup> (The relative efficacy of CYP51

ligands is estimated through the use of several measurements in addition to  $K_d$ , so VNI still remains the best lead.)

### ***VNI Cures the Murine Model of Acute and Chronic Chagas Disease***

One goal of this project was to provide enough material to establish the curative effect of VNI in a murine model of both the acute and chronic stages of Chagas disease (Figure 20).

**Figure 20.** VNI Eradicates Parasite *in vivo* for Both Phases of Chagas Disease (ref. 62).



For the acute model, two groups of mice were infected with a lethal dose of parasite, and treatment for one group began three days post infection. They were given 25 mg/kg of VNI, twice a day for 30 days, which is a relatively low dose compared to posaconazole (up to 300 mg/kg). Gratifyingly, the parasitological clearance was 100%, with 100% survival of the treated mice while there were no detectable toxic side effects (after VNI-treatment, mice did not lose weight and appeared normal). In the chronic mouse model of Chagas disease, treatment with VNI for 30 days started 90 days post-infection (a small number of parasites), and was followed by six rounds of immunosuppression to induce chronicity. After immunosuppression, all untreated animals visually presented high

parasitemia, whereas all VNI-treated mice showed complete eradication of the parasite. In both the acute and chronic models of the disease, qPCR analysis (Table 20) confirmed parasitological clearance: blood and all tested tissues of the VNI treated animals were free of *T. cruzi*.

**Table 20.** *T. cruzi* Detection by qPCR (ref. 62).

| Chagas disease model | Mice                               | <i>T. cruzi</i> positive animals per group (mean $\pm$ SE of threshold cycle for parasite detection) |                        |                        |                        |                        |
|----------------------|------------------------------------|--|------------------------|------------------------|------------------------|------------------------|
|                      |                                    | Heart  | Muscle                 | Liver                  | Spleen                 | Blood                  |
| Acute                | <i>T. cruzi</i> infected + vehicle | 5/5 (12.40 $\pm$ 0.13)   | 5/5 (12.71 $\pm$ 0.57) | 5/5 (16.26 $\pm$ 0.18) | 5/5 (12.86 $\pm$ 0.20) | 5/5 (14.91 $\pm$ 0.90) |
|                      | <i>T. cruzi</i> infected +VNI      | 0/5 (28.52 $\pm$ 0.53)   | 0/5 (28.82 $\pm$ 0.96) | 0/5 (28.44 $\pm$ 0.71) | 0/5 (28.82 $\pm$ 0.42) | 0/5 (29.52 $\pm$ 0.44) |
|                      | Non-infected                       | 0/5 (28.63 $\pm$ 0.13)   | 0/5 (28.56 $\pm$ 0.20) | 0/5 (28.74 $\pm$ 0.57) | 0/5 (29.36 $\pm$ 0.11) | 0/5 (28.74 $\pm$ 0.10) |
| Chronic              | <i>T. cruzi</i> infected + vehicle | 9/9 (16.64 $\pm$ 0.83)   | 9/9 (12.90 $\pm$ 0.54) | 9/9 (15.02 $\pm$ 0.27) | 9/9 (17.33 $\pm$ 1.09) | 9/9 (14.59 $\pm$ 0.78) |
|                      | <i>T. cruzi</i> infected +VNI      | 0/9 (31.98 $\pm$ 0.81)   | 0/9 (28.12 $\pm$ 0.84) | 0/9 (30.34 $\pm$ 1.74) | 0/9 (31.62 $\pm$ 0.11) | 0/9 (30.31 $\pm$ 1.62) |
|                      | Non-infected                       | 0/9 (28.34 $\pm$ 0.66)   | 0/9 (28.44 $\pm$ 0.70) | 0/9 (29.90 $\pm$ 0.55) | 0/9 (29.69 $\pm$ 0.61) | 0/9 (30.12 $\pm$ 0.57) |

We have demonstrated that VNI, prepared through chemical synthesis, cures acute and chronic Chagas in a murine model of the infection. The low cost of materials highlights the promise that the VNI scaffold can serve as a small molecule therapeutic for a disease endemic to low resource areas. Though VNI is orally bioavailable, non-toxic and has favorable pharmacokinetics, we believe the convergency of our route can deliver straightforward access to derivatives as we move towards a candidate for preclinical testing.



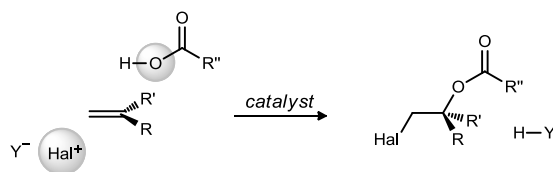
## CHAPTER III

### III. BISAMIDINE CATALYZED ENANTIOSELECTIVE HALOGENATIONS<sup>93,94</sup>

#### 3.1 Enantioselective Halogenations and Asymmetric Organocatalysis

##### *History of Enantioselective Halocarboxylations*

The alkene halocarboxylation reaction was resistant to the application of proven approaches to enantioselective catalysis since its early realization, a shortcoming both unfortunate and notorious considering the practical value of the ester/lactone products.<sup>95</sup>



Reports finally surfaced in 2010, more than 10 years after the first promising results, that enantioselective halogenative addition reactions were possible.<sup>96</sup>

In 1998, Grossman reported the first reagent-controlled enantioselective halolactonization (Scheme 39, eq 70).<sup>97</sup>

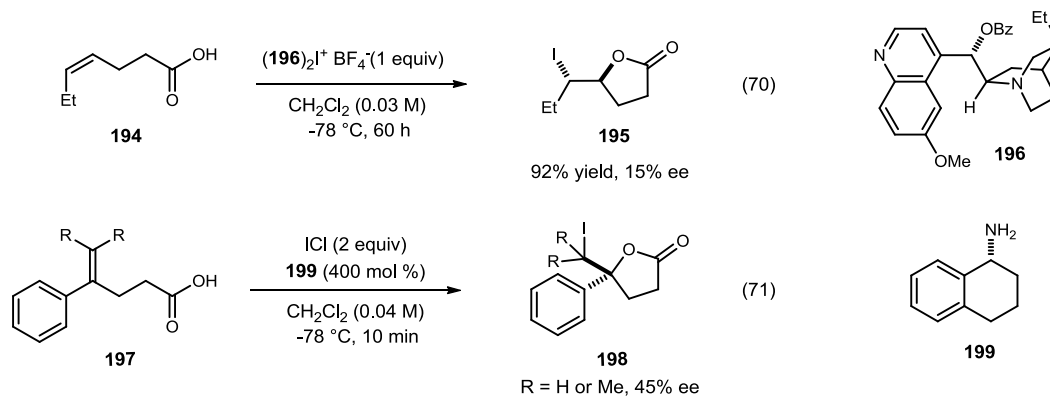
<sup>93</sup> Dobish, M. C.; Johnston, J. N. *J. Am. Chem. Soc.* **2012**, *134*, 6068-6071.

<sup>94</sup> Dobish, M. C.; Johnston, J. N. *unpublished results*.

<sup>95</sup> Hatano, M.; Sugiura, Y.; Akakura, M.; Ishihara, K. *Synlett* **2011**, *2011*, 1247,1250.

<sup>96</sup> Reviews: Chen, G.; Ma, S. *Angew. Chem. Int. Ed.* **2010**, *49*, 8306-8308. Castellanos, A.; Fletcher, S. P. *Chem.--Eur. J.* **2011**, *17*, 5766-5776. Tan, C. K.; Zhou, L.; Yeung, Y.-Y. *Synlett* **2011**, 1335-1339. Hennecke, U. *Chemistry-an Asian Journal* **2012**, *7*, 456-465.

**Scheme 39.** Initial Reports of Enantioselective Halolactonizations using Chiral, Stoichiometric Halogen Complexes.



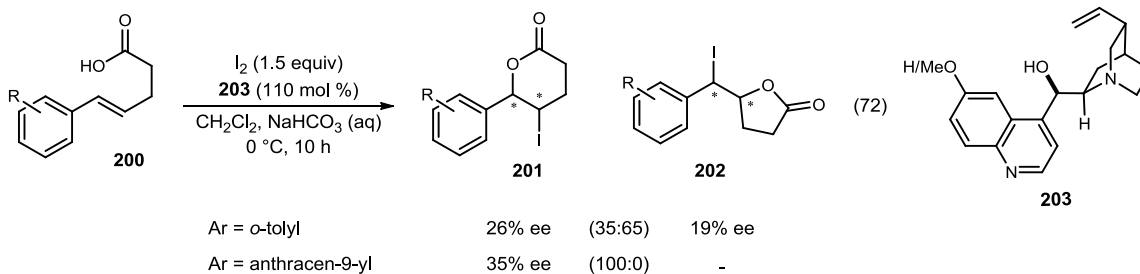
Using dihydroquinidine-halogen complexes  $[(\mathbf{196})_2\text{I}^+\text{BF}_4^-]$ , the iodolactones (**195**) were isolated in up to 7% ee. Most of the amine analogs tested gave racemic lactone, though all was not lost as the chiral amines were able to be recovered. Further dilution of the reaction mixture, gave the lactones in up to 15% ee, a common trend observed in enantioselective halolactonizations. Shortly after this initial report, Wirth reported the use of chiral, primary amines to afford  $\gamma$ -lactones from 1,1-disubstituted acids (Scheme 39, eq 71).<sup>98</sup> Screening a variety of primary amines, they were eventually able to obtain lactone **198** in up to 45% ee using chiral amine **199**. Gratifyingly, it was general for a variety of electronically diverse aromatic rings as well as tetrasubstituted olefins, though aliphatic analogs produced only the racemate.

Looking to expand on the work of Grossman, Gao further investigated the use of cinchona based alkaloids as stoichiometric, chiral halogen equivalents in reagent-controlled asymmetric iodolactonizations (Scheme 40).

<sup>97</sup>Grossman, R. B.; Trupp, R. J. *Can. J. Chem.* **1998**, *76*, 1233-1237.

<sup>98</sup> Haas, J.; Piguel, S.; Wirth, T. *Org. Lett.* **2001**, *4*, 297-300. Haas, J.; Bissmire, S.; Wirth, T. *Chem.--Eur. J.* **2005**, *11*, 5777-5785.

**Scheme 40.** Cinchona Based Chiral Iodine Sources in Enantioselective Iodolactonization.



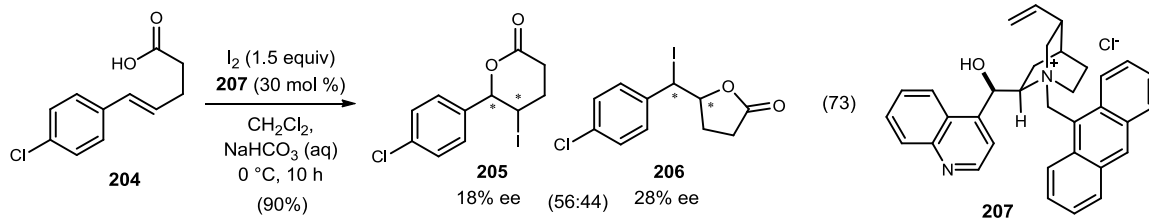
The use of 1,2-disubstituted olefinic acids (**200**) gives both  $\gamma$ - and  $\delta$ -lactones, requiring control of both regio- and enantioselectivity. Under these conditions, the results of the reaction proved to be very dependent on the catalyst used and aromatic ring of the acid. The highest enantioselectivity (19% ee) for the  $\gamma$ -lactone (5-*exo*) was obtained with the *ortho*-tolyl analog of **202** (though it only forming in a 2:1 diastereoselective ratio). When the more sterically congested anthracenyl-analog of the olefinic acid was used, the resulting reaction gave only the  $\delta$ -lactone (6-*endo*, **201**) in the highest enantioselection observed (35%). In most cases, amine **203** used at 110 mol % loading was recovered with about a 90% recovery. Though the values of enantioselection were low, this publication and results helped to further the first organocatalytic halolactonization.

### ***Substoichiometric, catalytic halocyclizations***

While the work with stoichiometric chiral halogen reagents in lactonizations was limited, Gao published the first substoichiometric, catalytic halolactonization of *trans*-5-aryl-4-pentenoic acids in the presence of iodine and 30 mol % of ligand (Scheme 41).<sup>99</sup>

<sup>99</sup> Wang, M.; Gao, L. X.; Mai, W. P.; Xia, A. X.; Wang, F.; Zhang, S. B. *J. Org. Chem.* **2004**, *69*, 2874-2876.

**Scheme 41.** First Catalytic, Enantioselective Halolactonization with a Chiral Ammonium Derived from Cinchonidine.

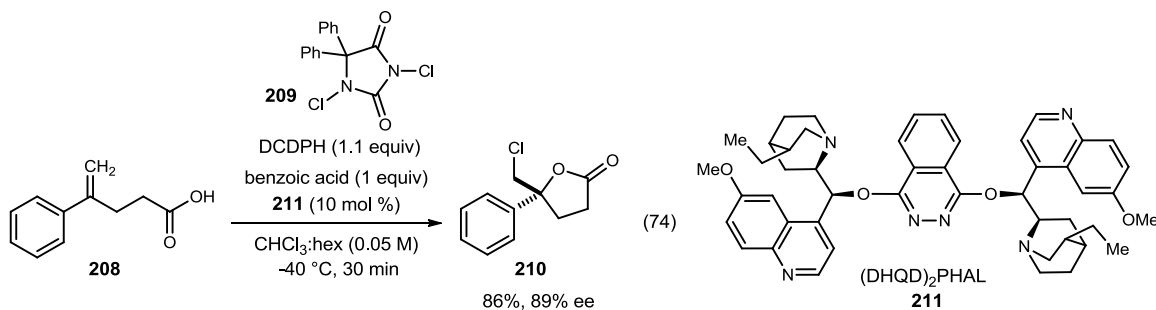


Using a chiral non racemic, quaternary ammonium salt derived from cinchonidine, a mixture of the  $\gamma$ - lactone (**206**) and  $\delta$ -lactone (**205**) was isolated. Catalyst and substrate manipulation gave a variety of endo-/exo- and enantioselectivities. The highest observed selectivity was 42% ee (for the product formed in a minor amount). Though low enantioselectivities were observed, this was the first time that a substoichiometric catalyst was used with some success.

### Highly Enantioselective, Organocatalytic Halocyclizations

Finally in 2010, Borhan published the first highly enantioselective and substoichiometric chlorolactonization (Scheme 42).<sup>100</sup>

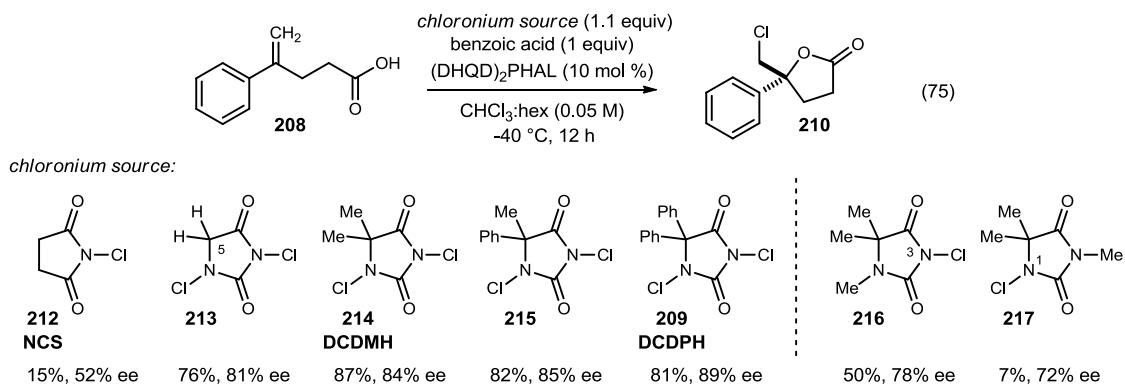
**Scheme 42** Enantioselective Chlorolactonization Reported by Borhan.



<sup>100</sup> Whitehead, D. C.; Yousefi, R.; Jaganathan, A.; Borhan, B. *J. Am. Chem. Soc.* **2010**, *132*, 3298-3300.

Using low catalyst loadings of (DHQD)<sub>2</sub>PHAL (10 mol %), a stoichiometric amount of benzoic acid, and dichlorodiphenylhydantoin (DCDPH, **209**) in an optimal mixture of chloroform and hexanes (1:1), the  $\gamma$ -lactone **210** was obtained in up to 90% ee. For a select number of substrates, decreasing the catalyst loading to 1 mol % gave relatively similar levels of enantioselection and yield, though with slightly diminished values (~3% ee). They also examined a variety of substituted hydantoin sources (Scheme 43).

**Scheme 43.** Effect of Halogen Source on Enantioselection and Yield.

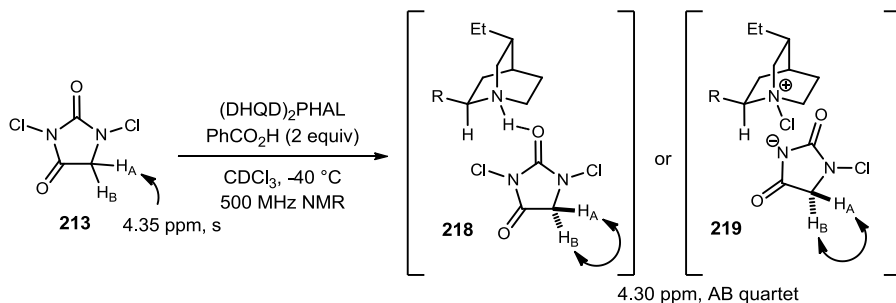


During reaction optimization, a trend emerged that highlighted the structural features of the chloronium source. The enantioselectivity increased as the steric bulk at the C5 position increased. For example, the diphenyl analog **209** (DCDPH) performed significantly better than the dihydrogen analog (**213**). Additional testing with the mono-methylated hydantoins (**216** and **217**) revealed that the chlorine on N1 does not readily transfer, giving only 7% product. They hypothesized that the electronic nature of the chlorinated nitrogen (N1) helps to activate the chlorine at N3 for transfer. This was further investigated with other substituents having similar electronic profiles.<sup>101</sup> The

<sup>101</sup> Yousefi, R.; Whitehead, D. C.; Mueller, J. M.; Staples, R. J.; Borhan, B. *Org. Lett.* **2011**, *13*, 608-611.

authors proposed two possible modes of binding using  $^1\text{H}$  NMR studies of a 1:1 mixture of catalyst and hydantoin (Figure 21).

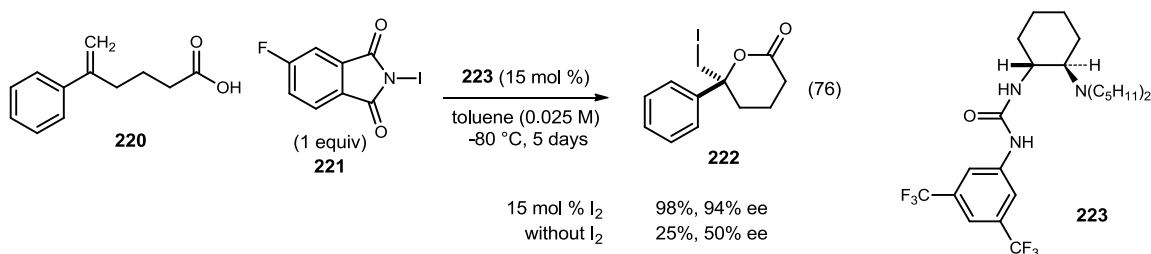
**Figure 21.** Proposed Mode of Binding in Enantioselective Chlorolactonization.



When the two were mixed together, an AB quartet was observed, suggesting the two components could form a complex or tight-ion pair. Though the mechanism was not further examined, this publication served as the floodgate for the field of enantioselective halolactonizations, as other research groups quickly followed suit and investigated a variety of catalyst systems and halogen sources.

Shortly after Borhan's report, Jacobsen revealed the tertiary aminourea-catalyzed enantioselective iodolactonization (Scheme 44).<sup>102</sup>

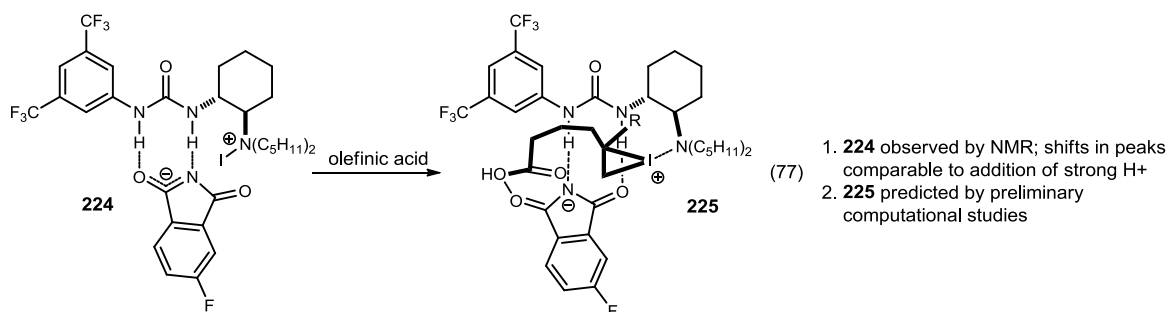
**Scheme 44.** Urea/iodine Catalyzed Enantioselective Iodocyclization of  $\delta$ -Unsaturated Acids.



<sup>102</sup> Veitch, G. E.; Jacobsen, E. N. *Angew. Chem. Int. Ed.* **2010**, *49*, 7332-7335.

Following a large screen of iodine sources, including NIS (95% yield, 92% ee), DIDMH (5% yield, 60% ee), and other substituted phthalimides, *N*-iodo-4-fluorophthalimide (**221**) was determined to be the most optimal source of I<sup>+</sup>. Surprisingly, an equimolar amount of iodine relative to the urea catalyst was necessary for high levels of enantioselection and yield. The authors speculate that the combination of the *N*-iodoimides and iodine in the presence of a protic acid, reveal the active (presumably more selective) triiodide cation. The triiodide then facilitates transfer of the I<sup>+</sup> source to the tertiary amine, regenerating iodine in the catalytic cycle. This is also observed in their proposed mechanism and transition state (Figure 22).

**Figure 22.** Proposed Transition State and Mechanism for Enantioselective Iodolactonization.

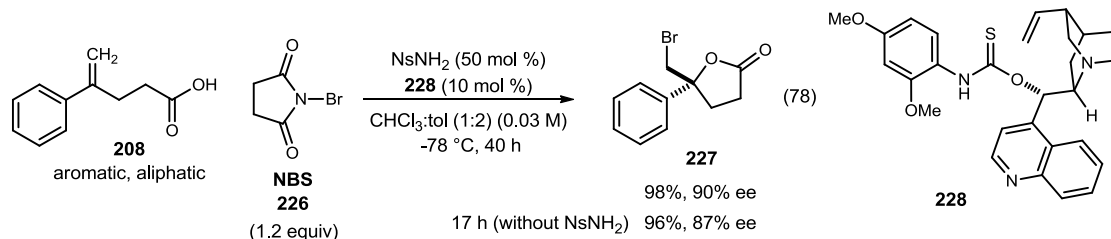


The authors speculate that the fluoro-phthalimide **221** and I<sub>2</sub> react to form the triiodide, which then transfers an I<sup>+</sup> to the catalyst, regenerating I<sub>2</sub> to continue the catalytic cycle. The proposed complex **224** was observed by NMR, as the shifts were characteristic to the combination of catalyst **223** with a strong acid. There is also computational support for the intermediacy of the tertiary amino-iodonium ion complex **225** when combined with the olefinic acid. A screen of approximately 10 substrates was completed using 15 mol% of the urea catalyst (**223**), delivering product in varying enantioselection (48% to 96%) after stirring at -80 °C for 5 days.

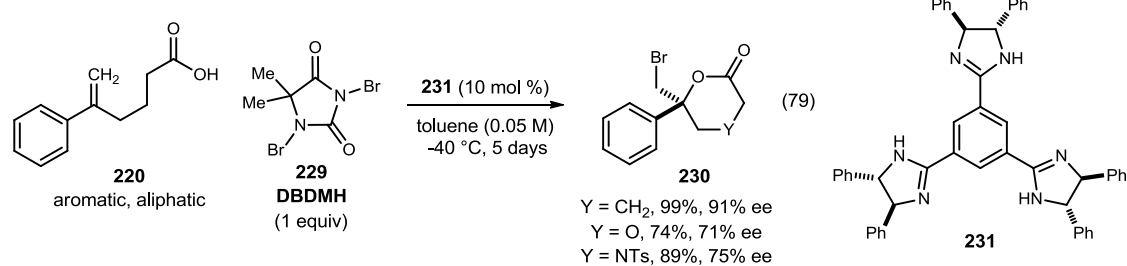
Almost simultaneously, Yeung<sup>103</sup> and Fujioka<sup>104</sup> reported on the asymmetric bromolactonizations using an amino-thiocarbamate catalyst (**228**) and C<sub>3</sub>-symmetric chiral trisimidazoline (**231**) respectively (Figure 23).

**Figure 23.** First Catalytic and Highly Enantioselective Bromolactonizations.

**Yeung's  $\gamma$ -Bromolactonization**



**Fujioka's  $\delta$ -Bromolactonization**



Both groups were able to synthesize the adducts with good levels of enantioselection (up to 93% ee) and yield. For Yeung, the nosylamine was deemed necessary, even though a small increase in enantioselection (3% ee) was observed for the standard substrate, along with prolonged reaction times. They also completed a screen of catalysts to determine the importance of each functionality (thiocarbamate vs. thiourea or carbamate, -NH vs. -NMe, etc). The large reaction scope of aliphatic and aromatic acids (>20 examples) was impressive, returning the lactones in 41-93% ee. Fujioka, similar to Borhan, used the

<sup>103</sup> Zhou, L.; Tan, C. K.; Jiang, X.; Chen, F.; Yeung, Y.-Y. *J. Am. Chem. Soc.* **2010**, *132*, 15474-15476.

<sup>104</sup> Murai, K.; Matsushita, T.; Nakamura, A.; Fukushima, S.; Shimura, M.; Fujioka, H. *Angew. Chem. Int. Ed.* **2010**, *49*, 9174-9177, S9174/1-S9174/129.



halohydrantoin to obtain the highest levels of enantioselection (up to 91% ee) when 10 mol % of the chiral trisimidazoline was used. Additionally, they showed the tolerance of other heteroatoms in the lactone ring. Both also demonstrated that the reactions with NIS and NCS gave low yields and enantioselection.

The Yeung laboratory has reported on a number of halocyclization reactions since their seminal publication (Figure 24). Using quinidine derived aminothiocarbamate catalysts, they were able to complete the bromoaminocyclizations of 1,1-disubstituted<sup>105</sup> and 1,2-disubstituted<sup>106</sup> olefins, bromolactonizations of *trans*- and *cis*-olefins,<sup>107</sup> and the synthesis of 3,4-dihydroisocoumarin analogs.<sup>108</sup>

---

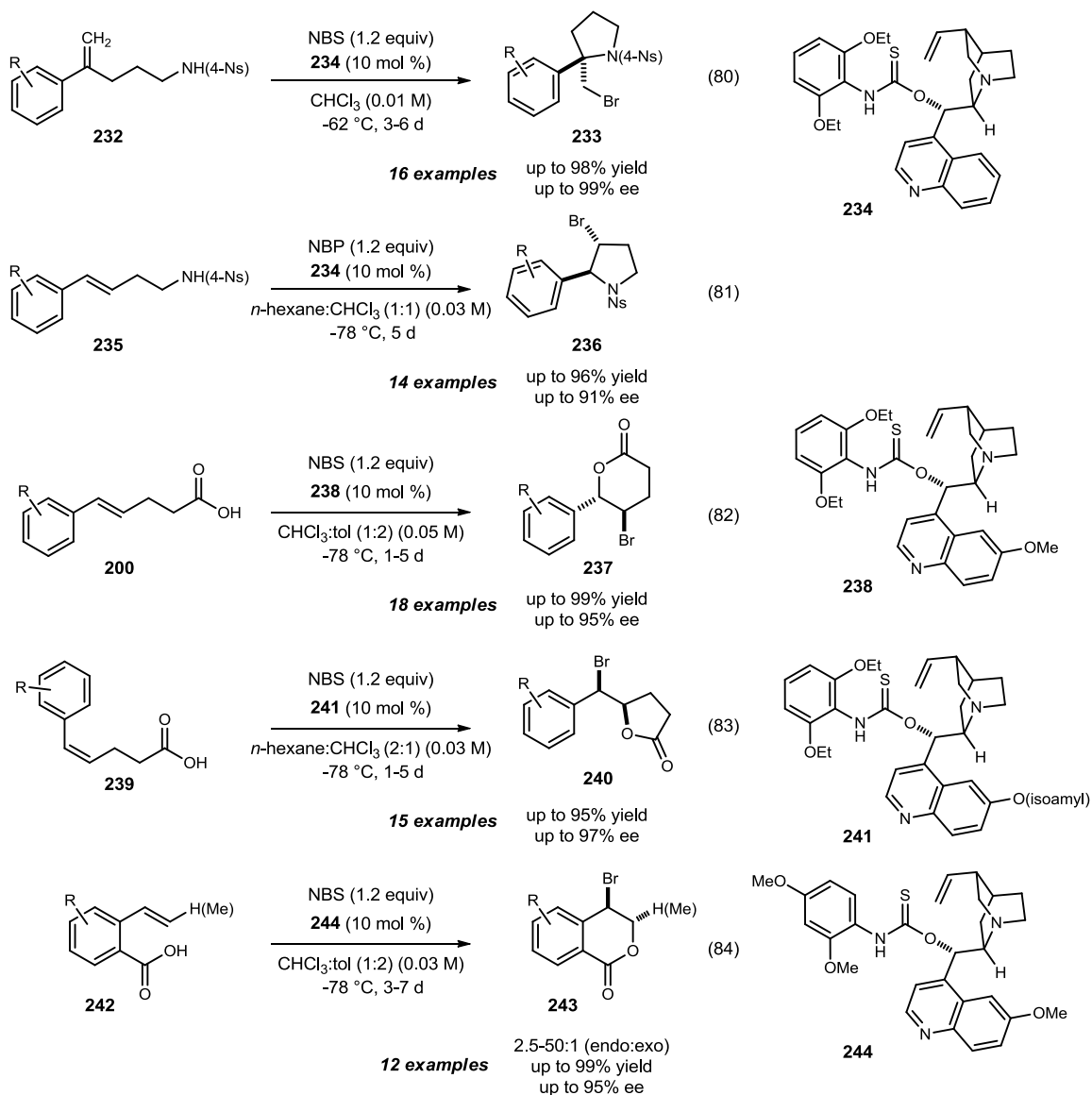
<sup>105</sup> Zhou, L.; Chen, J.; Tan, C. K.; Yeung, Y.-Y. *J. Am. Chem. Soc.* **2011**, *133*, 9164-9167.

<sup>106</sup> Chen, J.; Zhou, L.; Yeung, Y.-Y. *Org. Biomol. Chem.* **2012**, *10*, 3808-3811.

<sup>107</sup> *trans*-olefins: Tan, C. K.; Zhou, L.; Yeung, Y.-Y. *Org. Lett.* **2011**, *13*, 2738-2741. *cis*-olefins: Tan, C. K.; Le, C.; Yeung, Y.-Y. *Chem. Commun.* **2012**, *48*, 5793-5795.

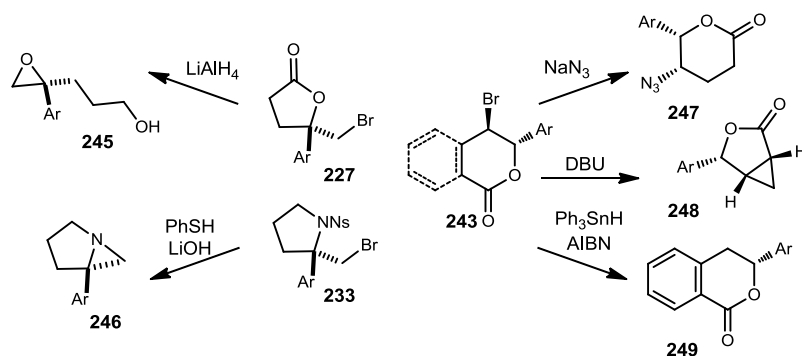
<sup>108</sup> Chen, J.; Zhou, L.; Tan, C. K.; Yeung, Y.-Y. *J. Org. Chem.* **2011**, *77*, 999-1009.

**Figure 24.** Enantioselective Bromocyclization Work from the Yeung Laboratory.



Characteristics of all the transformations were high levels of enantioselection and yield. Additionally, a number of synthetically useful transformations for all of the bromolactone products have been demonstrated (Figure 25).

**Figure 25.** Synthetically Useful Transformations of Products from Halocyclization Reactions.



These reactions, specifically with 1,1-disubstituted acids, served as precursors to a variety of other enantioselective halocyclization reactions, reported by the same groups and opened the door for advances by other research groups.

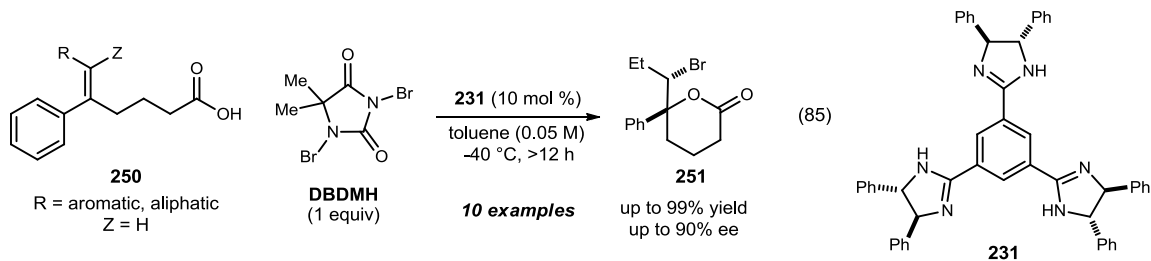
### *Current limitations in enantioselective halocyclizations*

While a number of different reaction conditions for a variety of halogens and olefinic acids have been investigated, a few limitations to the methodology are apparent. Most of the reactions work well with disubstituted olefins (1,1- and 1,2-), while tri- and tetra-substituted olefins have limited representation. Additionally, there appears to be significant differences between halogens that prevent obstacles to the development of a “one size fits all” catalyst system, as most reports state that other halogens performed poorly under their specific reaction conditions.

Very recently, the Fujioka lab reported on the highly enantioselective bromolactonization of tri- and tetrasubstituted olefins using their previously reported trisimidazoline (Scheme 45).<sup>109</sup>

<sup>109</sup> Murai, K.; Nakamura, A.; Matsushita, T.; Shimura, M.; Fujioka, H. *Chemistry – A European Journal* **2012**, *18*, 8448-8453.

**Scheme 45.** Fujioka Bromolactonization of Tri- and Tetra-substituted Olefins.

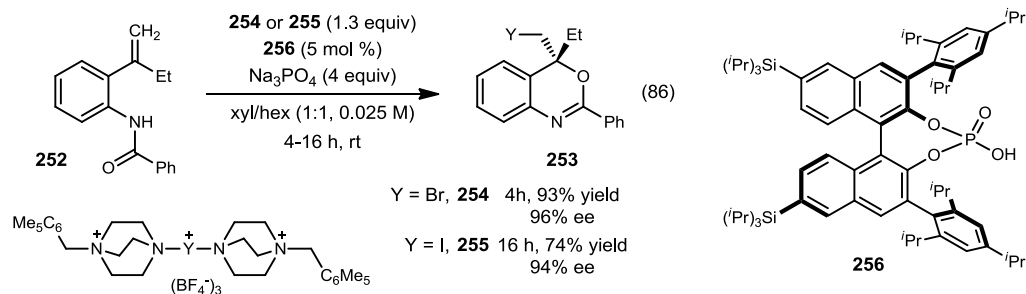


A number of substrates were examined, all isolated in 76-90% ee. As expected, only the *exo*-lactone (6- over 7-membered ring) product was isolated, though they did not examine the use of the nor-homolog which would have compared 5- over 6-membered ring selectivity. The tetrasubstituted olefinic acid (R = Me and Z = Me) was isolated in 85% ee and 65% yield, an encouraging result for such a hindered substrate. They also determined that the facial delivery of the bromine was the same for both the *Z*-olefin (in 88% ee) and the *E*-olefin (in 47% ee), as debromination gave the same product with the same absolute configuration. This also suggests that the *Z*-olefin is the preferred geometry for the trisimidazoline catalyzed bromolactonization.

One of the more impressive solutions for the use of different halogens in the same system was recently reported by the Toste group (Scheme 46).<sup>110</sup>

<sup>110</sup> Wang, Y.-M.; Wu, J.; Hoong, C.; Rauniyar, V.; Toste, F. D. *J. Am. Chem. Soc.* **2012**, *134*, 12928-12931.

**Scheme 46.** Tailored Cationic Halogenating Reagents in Halocyclization Reactions.



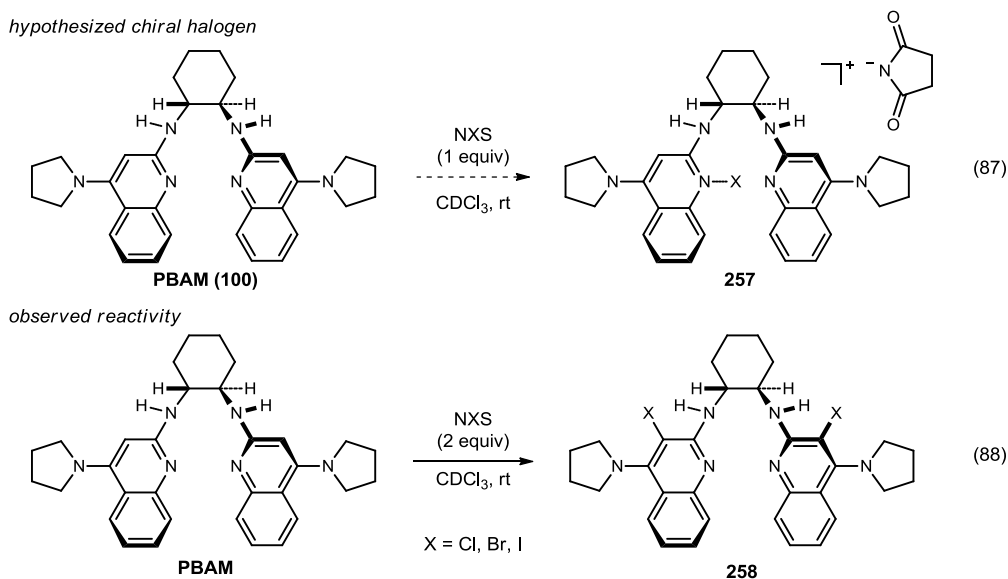
Amides (**252**) were exposed to the reaction conditions (5 mol % of catalyst **256** at room temperature) to provide bromo-benzoxazines (**253**) in high yield and enantioselection. A variety of substrates, including trisubstituted olefins and oxygen/nitrogen functional groups, were well tolerated. It is hypothesized that the halogen source remains insoluble until it reacts with the chiral phosphate, rendering it active and affording enantioselective delivery of the halogen. This tuning of the halogen source allows for the same reaction to be completed using iodine (**255**), instead of bromine, with little loss in enantioselectivity.

## 3.2 Bisamidine Catalyzed Enantioselective Iodolactonization

### Preliminary Results

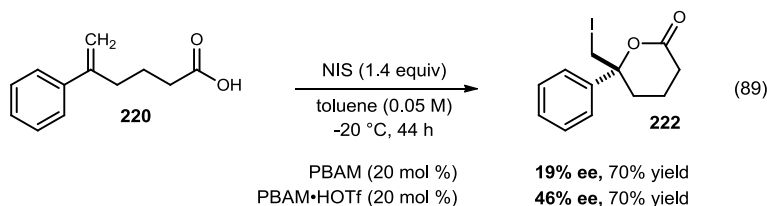
Having demonstrated the use of bisamidine catalysis to effect transformations using a chiral proton complex, we sought similar electrophiles that could be rendered chiral through bisamidine catalysis. We first combined a BAM ligand and an electrophilic source of halogen, seeking evidence for halogen complexation by  $^1\text{H}$  NMR (Figure 26).

**Figure 26.** Proposal for Bisamidine and Electrophilic Halogen Complexation.

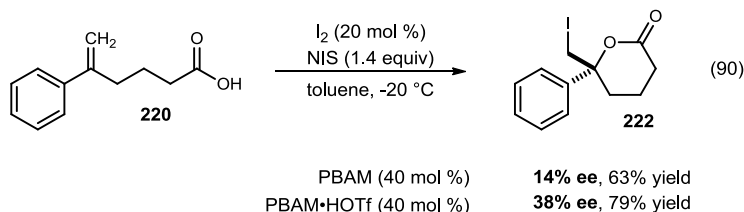


By combining PBAM (**100**) and 1 equivalent of *N*-iodosuccinimide in  $\text{CDCl}_3$ , we hoped to observe a symmetrical shift in the catalyst signals (eq 87), representing an averaged structure that is complexing the halogen. Unfortunately, we only saw desymmetrization of the catalyst. An additional equivalent of the *N*-halosuccinimide returned symmetry to the catalyst (eq 88). It was determined that instead of halogen complexation, electrophilic aromatic substitution led to halogenation of the C3 and C3' positions. Unfortunately, the

catalysts were not stable to column chromatography. Though shifts in the  $^1\text{H}$  NMR suggesting complexation (without reaction) between the halogen and catalyst were not observed, we thought catalyst modification may be slower or thwarted at colder temperatures. To test the feasibility of a BAM•halogen system as a chiral halogen source, the iodolactonization of 1,1-disubstituted acids was examined (eq 89).



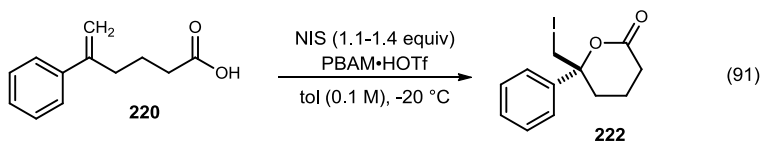
Starting with conditions similar to those of Jacobsen (Scheme 44) reported earlier, both the free base of PBAM and the triflic acid salt of PBAM (PBAM•HOTf) gratifyingly imparted selectivity, in 19% and 46% ee respectively. We were initially surprised that the catalyst:acid salt gave higher enantioselection, though this may be rationalized through acid activation of the succinimide (to be discussed in detail in upcoming sections). Furthermore, the difference in enantioselection between the free base and acid salt highlighted a variable in the reaction that could be easily modified (acid equivalents, types of acids, etc.). Attempting to increase the enantioselection and reactivity, a catalytic amount of iodine was added in an attempt to form the triiodide species (eq 90).



The extra iodine activation did not help the reaction; instead, it slightly decreased the enantioselectivity. The extra iodine may increase the rate of the background (nonselective) reaction. Satisfied the reaction did not need additional iodine activation, we looked to further examine other reaction parameters that may have an influence on the enantioselection and yield.

Though toluene has previously given the best results for BAM reactions, 1,2-dichloroethane has given similar selectivities in some reactions. A variety of chlorinated solvents were tested, resulting in high yields (>95%) but low selectivity (<10% ee). Moving forward with toluene, we then looked at the effect the amount of catalyst present may have on the reaction (Table 21).

**Table 21.** Initial Catalyst Loading Studies with PBAM.



| entry | cat. (mol %) | time (h) | % yield    | ee (%) |
|-------|--------------|----------|------------|--------|
| 1     | 20           | 44       | 89         | 48     |
| 2     | 10           | 22       | 87         | 54     |
| 3     | 5            | 40       | 73         | 50     |
| 4     | 2            | 96       | 45         | 46     |
| 5     | 0            | 48       | <16% conv. | -      |

<sup>a</sup>All reactions were performed on a 0.10 mmol scale using 1 equivalent of the carboxylic acid under conditions listed.

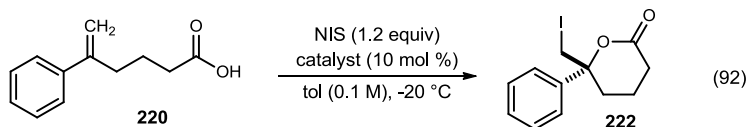
Decreasing the catalyst loading from 20 to 10 mol % showed a favorable increase in enantioselection (entry 2). Further drops in the loading of catalyst (entries 3-4) only slowed the reaction and returned product with lower enantioselection (50% and 46% ee). We hypothesized that the uncatalyzed background reaction may be competing and



contributing to the low enantioselection. However, running the reaction with no catalyst at -20 °C showed very little conversion by <sup>1</sup>H NMR after 48 hours of stirring (entry 5). These results may suggest that there are multiple pathways to the product, while the optimal control is achieved when 10 mol % of catalyst is used.

To further examine the role of the achiral acid in the catalyst system, different equivalents of the PBAM:acid salts were examined (Table 22).

**Table 22.** Role of Triflic Acid Equivalents.



| entry          | catalyst                              | time (h) | % yield | ee (%) |
|----------------|---------------------------------------|----------|---------|--------|
| 1 <sup>b</sup> | PBAM                                  | 44       | 70      | 19     |
| 2              | PBAM <sub>2</sub> (HOTf)              | 22       | 52      | 35     |
| 3              | PBAM(HOTf)                            | 22       | 87      | 54     |
| 4              | PBAM <sub>4</sub> (HOTf) <sub>5</sub> | 22       | 48      | 50     |
| 5              | PBAM <sub>2</sub> (HOTf) <sub>3</sub> | 22       | 26      | 41     |
| 6              | PBAM(HOTf) <sub>2</sub>               | 22       | 19      | 19     |

<sup>a</sup> All reactions were performed on a 0.10 mmol scale using 1 equivalent of the carboxylic acid under conditions listed. <sup>b</sup> 20 mol % catalyst loading used.

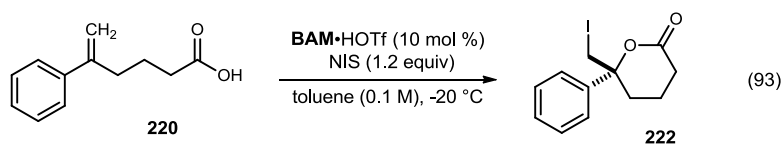
The catalyst PBAM<sub>2</sub>HOTf (entry 2), where there are two equivalents of BAM to each equivalent of acid, lies on the continuum between the free base (entry 1) and 1:1 salt (entry 3) for selectivity. This suggests the catalyst may exist independently of each other, half as the free base and half as the 1:1 salt. Further increasing the equivalents of BAM to acid (1:2) had a negative effect on the enantioselection (entry 6) to 19% ee. Though we have previously demonstrated that higher ratios of acid relative to BAM<sup>52</sup> can significantly influence diastereoselectivity (with small influence on enantioselectivity), we did not observe any trends for this system, as the 1:1.25 and 1:1.5 gave similar results

to the 1:1 salt. It was quickly determined that the optimal ratio of BAM to acid was the 1:1 salt.

### Catalyst and Achiral Acid Screen

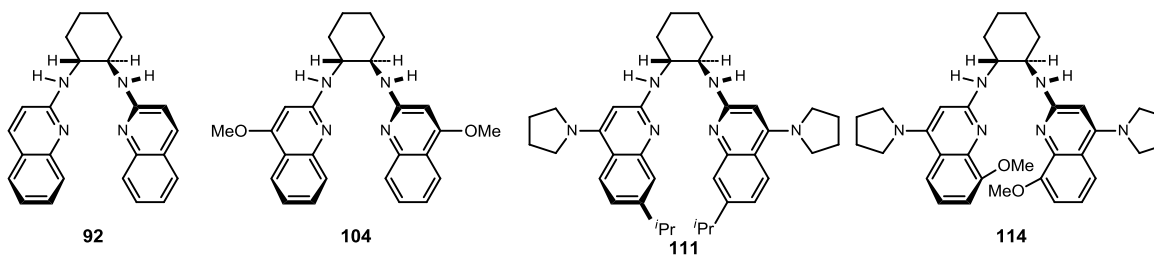
Surveying a small and diverse selection of other BAM catalysts at our disposal, we began a screen of catalysts and counterions (Table 23).

**Table 23.** Catalyst Screen of BAM-Triflic Acid Salts.



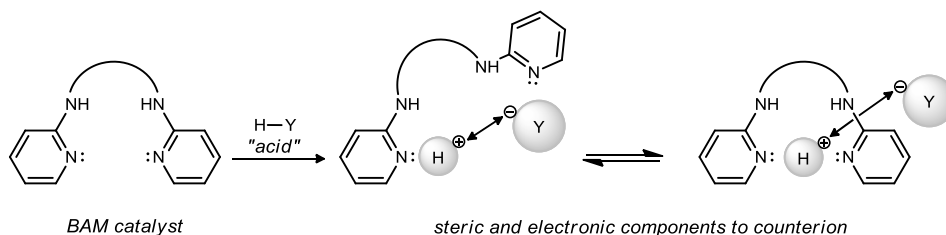
| entry | BAM                             | time (h) | % yield | ee (%) |
|-------|---------------------------------|----------|---------|--------|
| 1     | PBAM                            | 22       | 87      | 54     |
| 2     | H,QuinBAM <b>92</b>             | 48       | 45      | 13     |
| 3     | <sup>4</sup> MeOBAM <b>104</b>  | 48       | 19      | 0      |
| 4     | <sup>7i</sup> PrPBAM <b>111</b> | 22       | 45      | 36     |
| 5     | <sup>8</sup> MeOPBAM <b>114</b> | 22       | >95     | 40     |

<sup>a</sup>All reactions were performed on a 0.10 mmol scale using 1 equivalent of the carboxylic acid under conditions listed.



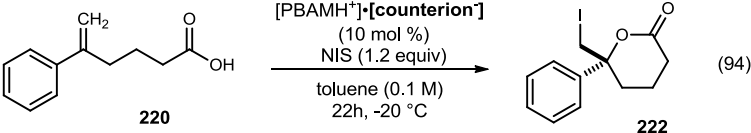
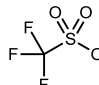
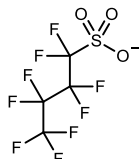
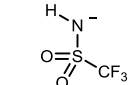
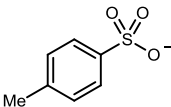
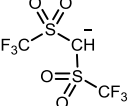
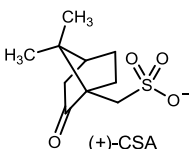
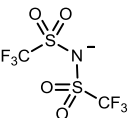
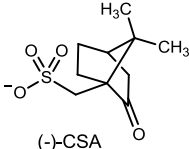
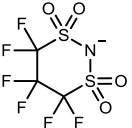
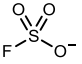
The less basic catalysts H,QuinBAM (**92**) and <sup>4</sup>MeOBAM (**104**) gave very low enantioselection (entries 2-3), while the sterically hindered <sup>7i</sup>PrPBAM (**111**) and sterically hindered/electron rich <sup>8</sup>MeOPBAM (**114**) gave no improvement in the enantioselection. Both the basicity of the catalyst and sterically available nature of the chiral pocket appears to be necessary for high enantioselection.

In addition to the Brønsted basic catalyst, modification of the strong acid used to form the chiral proton complex can be varied. Though the proton would remain unchanged, the achiral counterion can be “modified” electronically or sterically. Use of a



stronger acid encourages a more dissociated counterion, potentially changing the orientation of the amidine rings in the chiral pocket. In the same way, increasing the bulk of the achiral counterion may also influence the cavity size while functioning as a blocking element, offering a more selective catalyst-acid system. A large screen of achiral counterions, from their requisite acids, was tested in this system (Chart 3).

**Chart 3.** Catalyst Screen of BAM-Protic Acid Salts.

|  |   | (94)          |    |  |              |
|--|---|---------------|----|--|--------------|
| 1  | — (SM)  | 19% ee (70%)  | 8  |    | 53% ee (87%) |
| 2  | Cl <sup>-</sup>   | 59% ee (>95%) | 9  |    | 49% ee (45%) |
| 3  | Br <sup>-</sup>   | 43% ee (>95%) | 10 |    | 24% ee (95%) |
| 4  |    | 20% ee (90%)  | 11 |    | 75% ee (94%) |
| 5  |    | 29% ee (41%)  | 12 |   | 84% ee (90%) |
| 6  |   | 29% ee (35%)  | 13 |  | 82% ee (74%) |
| 7  |  | 40% ee (35%)  |    |  |              |

<sup>a</sup> All reactions were performed on a 0.10 mmol scale using 1 equivalent of the carboxylic acid under conditions listed.

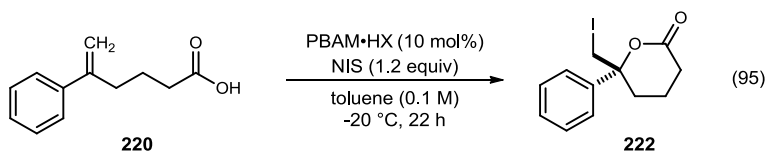
<sup>b</sup> 20 mol % catalyst loading and reaction time of 44 h.

Starting with the HCl and HBr salts of PBAM (entries 2-3), we were surprised to see that these counterions gave relatively good levels of enantioselection compared to triflic acid. Switching to sulfonate counterions, derived from relatively weaker sulfonic acids, gave lower enantioselection than triflic acid (entries 4-6). For the weaker acids, we consider that starting carboxylate (entry 1), present in much higher amounts, may be a competitive counterion when the acid strengths are similar. The enantioselection is also similar to the selectivities observed when the free base of PBAM was used, furthering the hypothesis of counterion competition. The fluorosulfonates, analogous to triflic acid, (entries 7-9) all

gave relatively similar enantioselection. It appeared that the strength of the acid was not the only determining factor in the enantioselection. However, when we looked at bistrifluoromethanesulfonamide (entry 12), we saw a significant increase to 84% ee. The less acidic trifluoromethanesulfonamide (entry 10) gave enantioselection similar to the free base of PBAM. Additionally, the carbon acid analog (entry 11) gave higher enantioselection than triflic acid, but lower than sulfonimide, while a cyclic triflimide counterion (entry 13) showed no significant increase in enantioselection or yield. The response of enantioselection to counterions with varying electronic and steric character suggests that the role of the achiral counterion, despite its presence down to 1 mol % (see below), is not simply to provide a resting state for the catalyst but instead to affect the catalyst reactivity and structure directly as it interacts with the substrate.

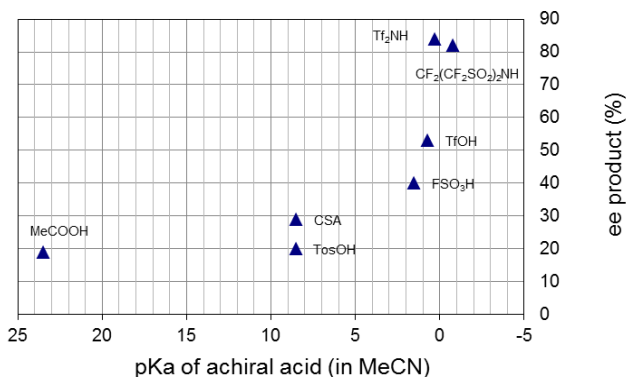
Cognizant of the electronic and steric component each counterion presented, we wanted to look for trends that may help guide further reaction optimization. The enantioselection of the product was plotted against the strength of the acid (Chart 4).

**Chart 4.** The pK<sub>a</sub> Values of Achiral Acids used in BAM Catalyzed Iodolactonizations.



| achiral acid   | pKa MeCN |        | pKa H <sub>2</sub> O | pKa DCE | % ee product |
|--|----------|--------|----------------------|---------|--------------|
|  | expt.    | calc.* |                      |         |              |
| MeCOOH   | 23.5     |        | 4.76                 |         | 19           |
| CSA  | 8.5      |        | -2.7                 |         | 29           |
| TosOH  | 8.5      |        | -2.7                 |         | 20           |
| FSO <sub>3</sub> H                                   |          | 1.5    |                      | -10.5   | 40           |
| TfOH   |          | 0.7    | -14                  | -11.4   | 53           |
| Tf <sub>2</sub> NH                                   |          | 0.3    |                      | -11.9   | 84           |
| CF <sub>2</sub> (CF <sub>2</sub> SO <sub>2</sub> )NH |          | -0.8   |                      | -13.1   | 82           |
| TfNH <sub>2</sub>                                    |          |        | 6.3                  |         | 24           |

\*calculated based on experimentally determined values in DCE



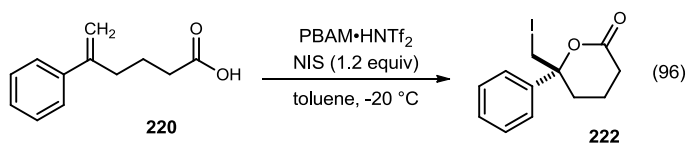
Unfortunately, not all of the pK<sub>a</sub> values of the acids are known in the same solvent. The pK<sub>a</sub> values of the acids in MeCN are either known experimentally or extrapolated from the pK<sub>a</sub> measurement in dichloroethane.<sup>111</sup> It appears that the enantioselection of the product slightly increases as the acid strength increases, plateauing at triflic acid. However, the results with triflic acid, triflimide, and the cyclic triflimide, which are all relatively equal in acid strength, show significant variation in the enantioselection. Though a direct relationship (albeit not linear) is evident between achiral acid pK<sub>a</sub> and enantioselection, it is unclear whether these values hold more useful predictive value. We

<sup>111</sup> Kütt, A.; Rõdima, T.; Saame, J.; Raamat, E.; Mäemets, V.; Kaljurand, I.; Koppel, I. A.; Garlyauskayte, R. Y.; Yagupolskii, Y. L.; Yagupolskii, L. M.; Bernhardt, E.; Willner, H.; Leito, I. *J. Org. Chem.* **2011**, *76*, 391-395.

have measured the  $pK_a$ 's of various BAM-HX salts, but have not found this information to be terribly helpful.<sup>112</sup> This may not be surprising since it is an attempt to correlate a thermodynamic measurement to a kinetically-controlled phenomenon. It appears that the role of the counterion in influencing enantioselection may be a combination of acid strength and sterics, where an appropriately dissociated and sterically defined counterion is necessary for highest levels of enantioselection. With this new phenomenon of enantioselection being so dramatically altered by an achiral counterion, we wanted to reexamine other reaction parameters that were previously investigated with the PBAM•HOTf catalyst system.

We sought to establish optimal parameters of the reaction with the new catalyst system, by again looking at the catalyst loading and reaction concentration (Table 24).

**Table 24.** Optimization Studies and Reaction Parameter Limits for PBAM•HNTf



| entry | cat. (mol %) | tol [M] | time (h) | % yield | ee (%) |
|-------|--------------|---------|----------|---------|--------|
| 1     | 10           | 0.1     | 22       | 94      | 81     |
| 2     | 20           | 0.1     | 22       | >95     | 76     |
| 3     | 15           | 0.1     | 22       | 94      | 81     |
| 4     | 5            | 0.1     | 46       | 84      | 82     |
| 5     | 10           | 0.2     | 22       | >95     | 81     |
| 6     | 10           | 0.05    | 22       | 74      | 90     |
| 7     | 10           | 0.025   | 46       | >95     | 90     |

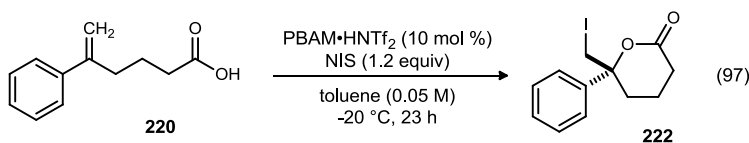
<sup>a</sup>All reactions were performed on a 0.10 mmol scale using 1 equivalent of the carboxylic acid under conditions listed.

<sup>112</sup> Hess, A. S.; Yoder, R. A.; Johnston, J. N. *Synlett* **2006**, 147-149.

As we had observed before with the triflic acid salt of PBAM, doubling the catalyst loading decreased the enantioselectivity of the reaction slightly (entry 2), while the difference between 15, 10, and 5 mol % was not significant. As expected, yields increased with greater catalyst loadings, suggesting that the reactions at lower catalyst loadings did not go to completion. Running the reaction at higher concentration (entry 5) resulted in increased yields while giving similar levels of enantioselection. Gratifyingly, decreasing the concentration to 0.05 M gave an increase in selectivity to 90% ee (entry 6). Further decreasing the concentration returned the product in similar enantioselection, suggesting a plateau for the concentration effect (entry 7).

A significant number of reactions have very precise parameters, or a small operating window for delivering maximum efficiency, for example small amounts of water might drastically change a reaction mechanism or pathway.<sup>59</sup> In an attempt to establish the maximum operating parameters, the amount of NIS, water content, and acid equivalents were examined (Table 25).



**Table 25.** Study of Operating Parameters for the Iodolactonization Reaction.

| entry | deviation from standard conditions                  | % yield | ee (%) |
|-------|---|---------|--------|
| 1     | none  | 90      | 84     |
| 2     | 0.6 equiv. NIS                                      | 42      | 81     |
| 3     | 2.4 equiv. NIS                                      | >95     | 83     |
| 4     | 1.2 equiv I <sub>2</sub>                            | 38      | 0      |
| 5     | wet toluene   | 90      | 80     |
| 6     | molecular sieves                                    | 94      | 68     |
| 7     | PBAM <sub>4</sub> (HNTf <sub>2</sub> ) <sub>3</sub> | 77      | 83     |
| 8     | PBAM <sub>4</sub> (HNTf <sub>2</sub> ) <sub>5</sub> | 84      | 76     |

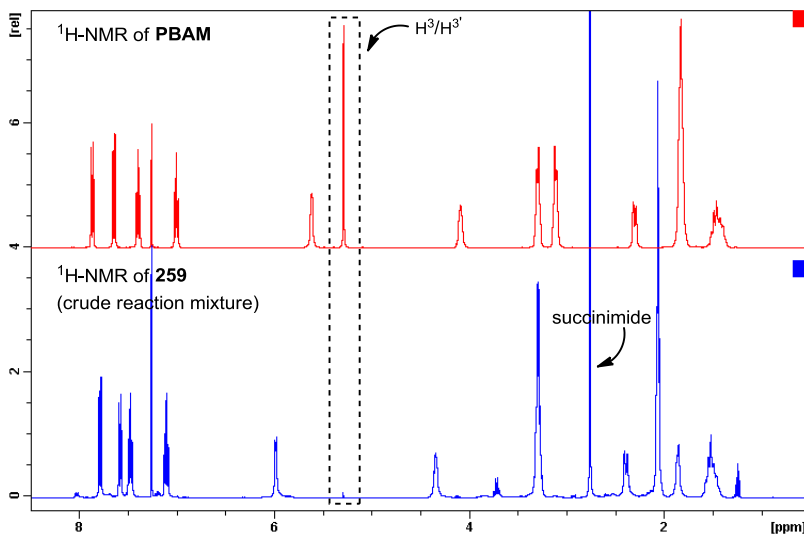
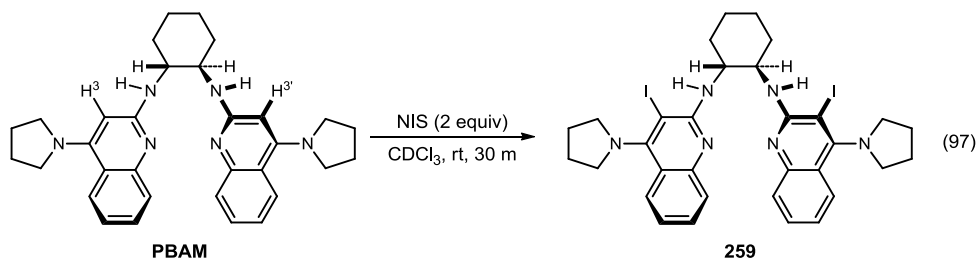
<sup>a</sup>All reactions were performed on a 0.10 mmol scale using 1 equivalent of the carboxylic acid under conditions listed.

When the amount of NIS was limited in the reaction (0.6 equivalents), a small drop in the enantioselection and yield was observed (entry 2), while increasing the amount of NIS to 2.4 equivalents did not decrease enantioselection (entry 3). We believe this lends to the observation that the background reaction is very slow in comparison to the catalyzed, enantioselective pathway. We also confirmed that when iodine is used, only racemic product is isolated in low yield (entry 4). Small amounts of water in the reaction do not influence enantioselection (entry 5) while the presence of molecular sieves sharply decreases the enantioselection (entry 6), possibly due to the decreased efficiency in stirring. Small variations in the equivalents of the counterion (entries 7-8) were tolerated, as there was little dependence on the exact ratio. The reaction so far proves to be relatively tolerant of water and excess NIS, while the highest selectivity can be attributed to a careful balance of the reaction concentration and catalyst loading.

Prior to this point, reactions were completed with an additional quantity of NIS (2 equivalents of NIS/1 equivalent of catalyst) in the reaction to correct for possible

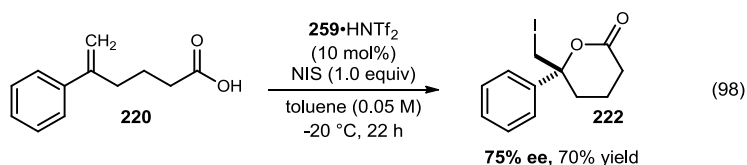
iodination of the catalyst, as observed in initial experiments (Figure 26). Furthering this hypothesis, when 0.6 equivalents of NIS was used, the product was only isolated in 40% yield. This suggests that 0.2 equivalents of the NIS are consumed in other parts of the reaction. If the catalyst is iodinated under the reaction conditions, it is also necessary to determine which of the catalysts is most selective and active. To test this, PBAM was combined with 2 equivalents total of NIS at room temperature (Figure 27).

**Figure 27.** Evidence by NMR of PBAM Iodination.



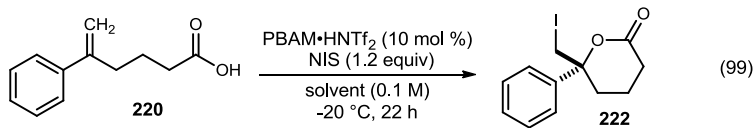
Evidence of the di-iodination was gathered using <sup>1</sup>H NMR by monitoring the disappearance of the quinoline singlet at the 3/3' position. When one equivalent of NIS was added, a mixture of the non-/mono-/di-iodinated ligands was observed. After the

addition of a second equivalent, all three merged to the presumed di-iodinated ligand **259**. The di-iodinated ligand was also observed by HRMS [(ESI): Exact mass calcd for  $C_{32}H_{37}I_2N_6$   $[M+H]^+$  759.1169, found 759.1134.] Unfortunately, attempts to purify this catalyst via flash column chromatography only returned impure material. Following a sodium thiosulfate and subsequent sodium hydroxide wash, the unpurified catalyst was immediately combined with 1 equivalent of bistriflimide to give the putative di-iodinated catalyst (**259**•HNTf<sub>2</sub>) which was submitted to the standard reaction conditions (eq 98).



After stirring for 22 hours under normal reaction conditions at -20 °C with **259**•HNTf<sub>2</sub>, 75% ee material was recovered in 70% yield, which can be compared to 84% ee and 90% yield for PBAM•HNTf<sub>2</sub> (not pretreated with NIS as above). The lower selectivity observed may be a result of the impurities that arise from the unpurified catalyst. Nevertheless, the reactivity and selectivity observed were only a small deviation from the ligand not pretreated with NIS, demonstrating that the active catalyst may exist anywhere on the iodinated ligand continuum (non-, mono-, or di-iodinated). With these observations, we moved forward using an excess of NIS relative to the catalyst for all reactions. Additionally, other reports for enantioselective halo-functionalization use an excess of the halogenating agents, possibly representing catalyst modification.

A solvent screen was then completed with the new catalyst system to probe the association that the solvent and achiral counterion may have on each other, with the ultimate goal of increasing enantioselection (Table 26).

**Table 26.** Solvent Screen with PBAM•HNTf<sub>2</sub> as the Optimal Catalyst.

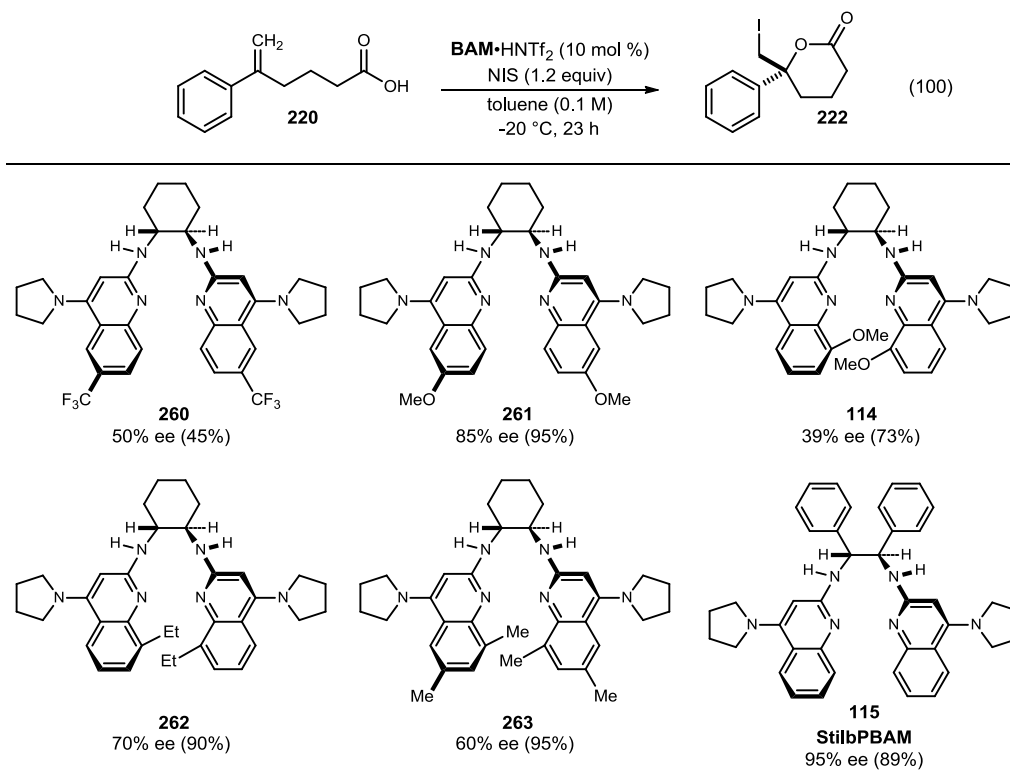
| entry | solvent                         | % yield | ee (%) |
|-------|---------------------------------|---------|--------|
| 1     | toluene                         | 90      | 84     |
| 2     | CHCl <sub>3</sub>               | 94      | 38     |
| 3     | MeNO <sub>2</sub>               | >95     | -5     |
| 4     | DME                             | 33      | 0      |
| 5     | acetone                         | >95     | 0      |
| 6     | toluene/CHCl <sub>3</sub> (3/1) | >95     | 79     |

<sup>a</sup>All reactions were performed on a 0.10 mmol scale using 1 equivalent of the carboxylic acid under conditions listed.

Unfortunately, none of the solvents tested increased the enantioselection of the adduct (entries 2-5). This may be due to the more favorable solubility profile for the reaction, which in turn increases the background rate. However, when a mixture of toluene and chloroform (3:1) was used, a slight drop in enantioselection to 79% was observed (entry 6). This method of using a mixture of solvents could help to increase starting material solubility if some are only partially soluble in toluene.

To further validate and exploit the observed achiral counterion effect, a diverse set of pyrrolidine-derived BAM catalysts from our library was reexamined (Chart 5).

**Chart 5.** Screen of Electronically and Sterically Diverse Pyrrolidine Bisamidine Ligands.

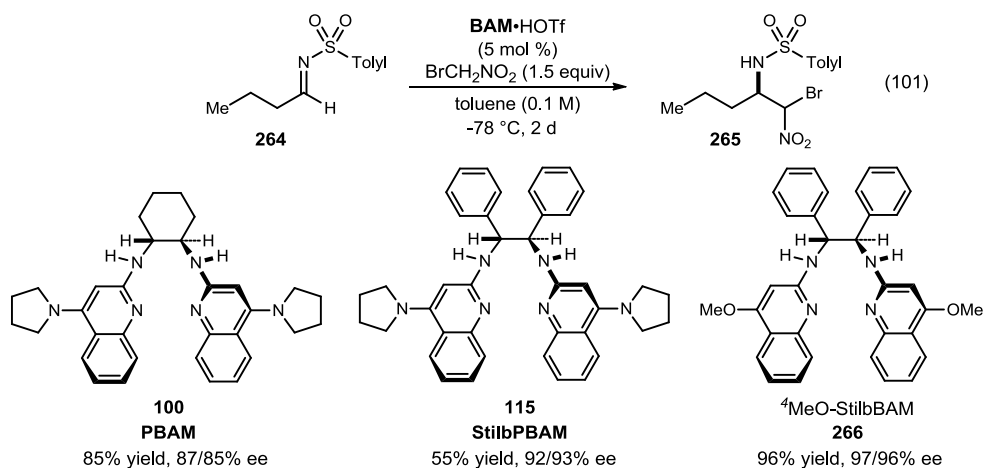


<sup>a</sup>All reactions were performed on a 0.10 mmol scale using 1 equivalent of the carboxylic acid under conditions listed.

The triflimide salts of the catalysts were easily synthesized by mixing equimolar amounts of triflimidic acid and the BAM free base in DCM, followed by removal of the solvent *in vacuo*. The more electron deficient analog <sup>6</sup>F<sub>3</sub>C-PBAM (**260**) showed lower reactivity and selectivity, while increasing the electron density with a methoxy group at the same position (<sup>6</sup>MeO-PBAM, **261**) gave the adduct in high enantioselection and yields (85% ee, 95% yield). As previously observed, <sup>8</sup>MeO-PBAM (**114**) severely diminished the catalyst's selectivity by disrupting the chiral pocket and delivering the product in 39% ee. In addition to the steric congestion <sup>8</sup>MeO-PBAM contributes, the electronic congestion also is pertinent, as <sup>8</sup>Et-PBAM (**262**) gave vastly better selectivity (70% ee). Sterically, the ethyl group and methoxy group are similar in size, but the difference in the electronics of the group may play a role in the enantioselection. Interestingly,

<sup>6,8</sup>Me-PBAM (**263**) gave the adduct in lower enantioselection (60% ee) than <sup>8</sup>Et-PBAM. However, when StilbPBAM (**115**), derived from stilbene diamine instead of cyclohexane diamine, was used high yield (89%) and a large increase in selectivity to 95% ee was observed. This catalyst was initially developed for the enantioselective additions of nitroalkanes to aliphatic imines (Scheme 47).<sup>113</sup>

**Scheme 47.** Bromonitromethane Additions to Aliphatic Imines.



It was hypothesized that the smaller NCCN dihedral angle of the stilbene diamine ( $52^\circ$ ) relative to cyclohexane diamine ( $69^\circ$ ) may offer a smaller pocket for the aliphatic electrophile to bind.<sup>114</sup> Though StilbPBAM gave promising results (55% yield, 92/93% ee), the optimal catalyst has since been identified as the less Brønsted basic <sup>4</sup>MeO-StilbBAM (**266**), delivering the aza-Henry adduct in >95% yield and >96% ee for both diastereomers. These adducts can be further manipulated to useful amide products by applying the Umpolung Amide Synthesis previously developed in our group.<sup>87</sup>

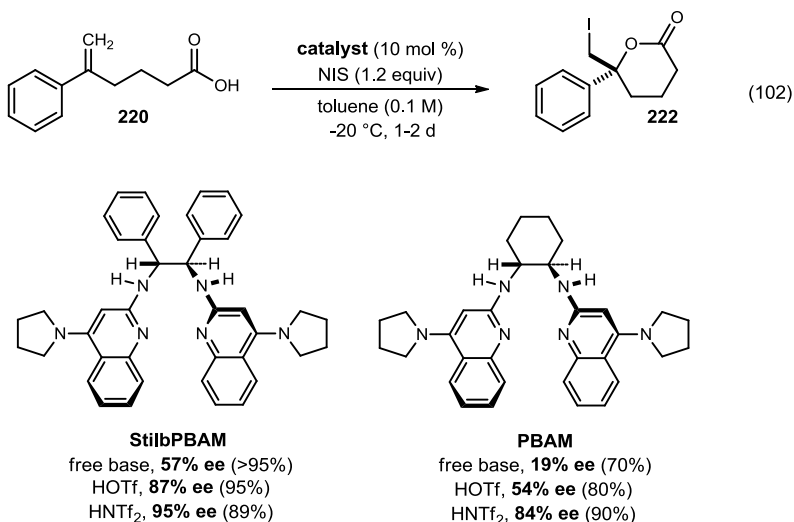
<sup>113</sup> Schweiter, K. E.; Dobish, M. C.; Singh, A. S.; Johnston, J. N. *unpublished results*

<sup>114</sup> Calculations of NCCN dihedral angle from: Kim, H.; Yen, C.; Preston, P.; Chin, J. *Org. Lett.* **2006**, *8*, 5239-5242.

### *StilbPBAM: A More Reactive and Selective Catalyst*

To further validate the effect of the stilbene diamine backbone for the iodolactonization reaction, we submitted the free base and triflic acid salts of the catalyst to the reaction conditions (Chart 6).

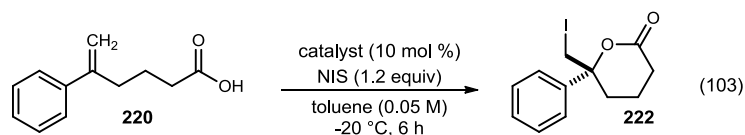
**Chart 6.** StilbPBAM and PBAM Comparison: Effect of Diamine Backbone on Enantioselection



StilbPBAM in its free base form delivered the lactone **222** in 57% ee, while its triflic acid salt delivered product in 87% ee and 95% yield. These trends for the counterions were also observed for PBAM, suggesting that the influence of the backbone is a real effect and can be exploited for further increase in enantioselection.

In previous halofunctionalization reports, a stoichiometric amount of acid was needed to maintain high reactivity and selectivity. Experiments were completed to determine the optimal ratio of chiral catalyst to achiral acid (Table 27).

**Table 27.** Changing the Ratio of the Chiral, Brønsted Basic Catalyst to the Achiral Acid.



| entry | catalyst   | % yield | ee (%) |
|-------|--|---------|--------|
| 1     | StilbPBAM  | 99      | 57     |
| 2     | StilbPBAM <sub>2</sub> (HNTf <sub>2</sub> ) <sub>1</sub> | 76      | 83     |
| 3     | StilbPBAM•HNTf <sub>2</sub>                              | >95     | 96     |
| 4     | StilbPBAM <sub>2</sub> (HNTf <sub>2</sub> ) <sub>3</sub> | 91      | 96     |
| 5     | StilbPBAM <sub>1</sub> (HNTf <sub>2</sub> ) <sub>2</sub> | <50     | <5     |

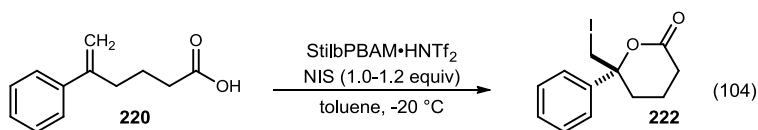
<sup>a</sup>All reactions were performed on a 0.10 mmol scale using 1 equivalent of the carboxylic acid under conditions listed.

The reaction with the 2:1 catalyst (chiral base:achiral acid) gave the adduct in 76% yield and 83% ee (entry 2). As expected, the selectivity of the reaction lies somewhere on the continuum between the free base and 1:1 salt, as there is approximately 50% of each catalyst in solution. The reactivity for the 1:2 catalyst complex (entry 5) was sluggish and returned nearly racemic material. For the 2:1 catalyst complex, we hypothesize that both basic nitrogen sites are protonated rendering the catalyst inactive. Alternatively, very little change was observed when the 1:1.5 salt was used (entry 4). This may be due to the fact that there is still 5 mol % of the active catalyst available while the other 5 mol % is inactive. This is additional evidence that the achiral acid is important in the transition state and doesn't function to only provide a resting state for the catalyst, as an excess shuts down all reactivity.

Further reaction optimization with the ligand revealed an interesting trend in catalyst loading (Table 28).



**Table 28.** Final Reaction Optimization of the Most Selective Catalyst System.



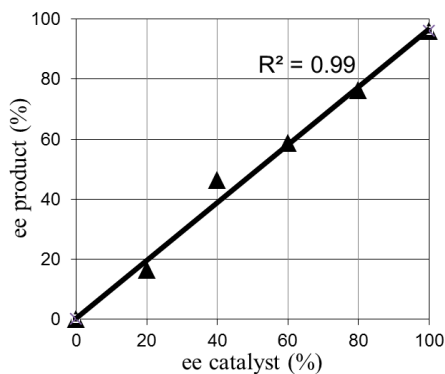
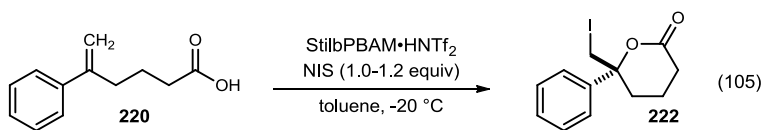
| entry | cat. (mol %) | (M)  | time (h) | % yield | ee (%) |
|-------|--------------|------|----------|---------|--------|
| 1     | 10           | 0.1  | 3        | 89      | 95     |
| 2     | 10           | 0.05 | 4        | 98      | 96     |
| 3     | 5            | 0.05 | 6        | >99     | 97     |
| 4     | 2            | 0.05 | 36       | 95      | 98     |
| 5     | 1            | 0.05 | 72       | 79      | 97     |
| 6     | 1            | 0.1  | 120      | 82      | 96     |

<sup>a</sup>All reactions were performed on a 0.10 mmol scale using 1 equivalent of the carboxylic acid under conditions listed.

Running the reaction under more dilute conditions delivered the adduct (**222**) in slightly higher yield and similar enantioselection (entry 2). Further decreasing the catalyst loading (entries 3-5) required longer reaction times, but a slight increase in enantioselection was observed when the catalyst loading was lowered to 2 mol %. Running the reaction at 1 mol % catalyst loading (entries 5-6) delivered highly enantioenriched material, independent of the reaction concentration. This effect of increase in enantioselection with decrease in catalyst loading provides some interesting insight to the reaction mechanism, possibly suggesting that there may be multiple catalysts involved in the most selective transition state.

To probe whether the lower catalyst loading was a result of higher polymorphs of the catalyst, we completed a nonlinear effect study (Graph 1).

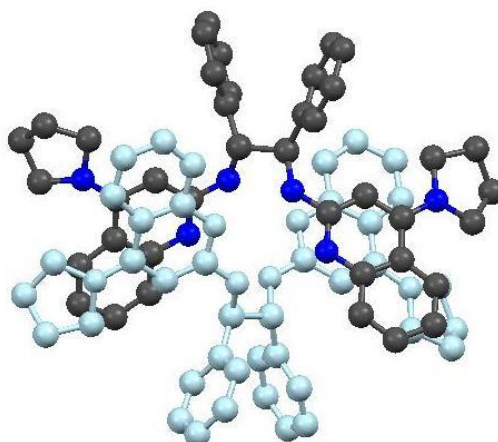
**Graph 1.** StilbPBAM Nonlinear Effect.



When catalysts with varying enantioselection (20%, 40%, 60%, 80% ee) were used (0.05 M, 10 mol % StilbPBAM•HNTf<sub>2</sub>), a non-linear effect was not observed ( $R^2=0.99$ ).<sup>115</sup> Of course, this does not preclude the possibility of dimers/oligomers, as they may not have significantly different reactivity relative to their homochiral counterparts. The dimeric nature of the free base StilbPBAM in the solid state was observed in a crystal structure obtained during purification (Figure 28).

<sup>115</sup> Satyanarayana, T.; Abraham, S.; Kagan, H. B. *Angew. Chem. Int. Ed.* **2009**, *48*, 456-494.

**Figure 28.** Crystal structure of StilbPBAM dimer.

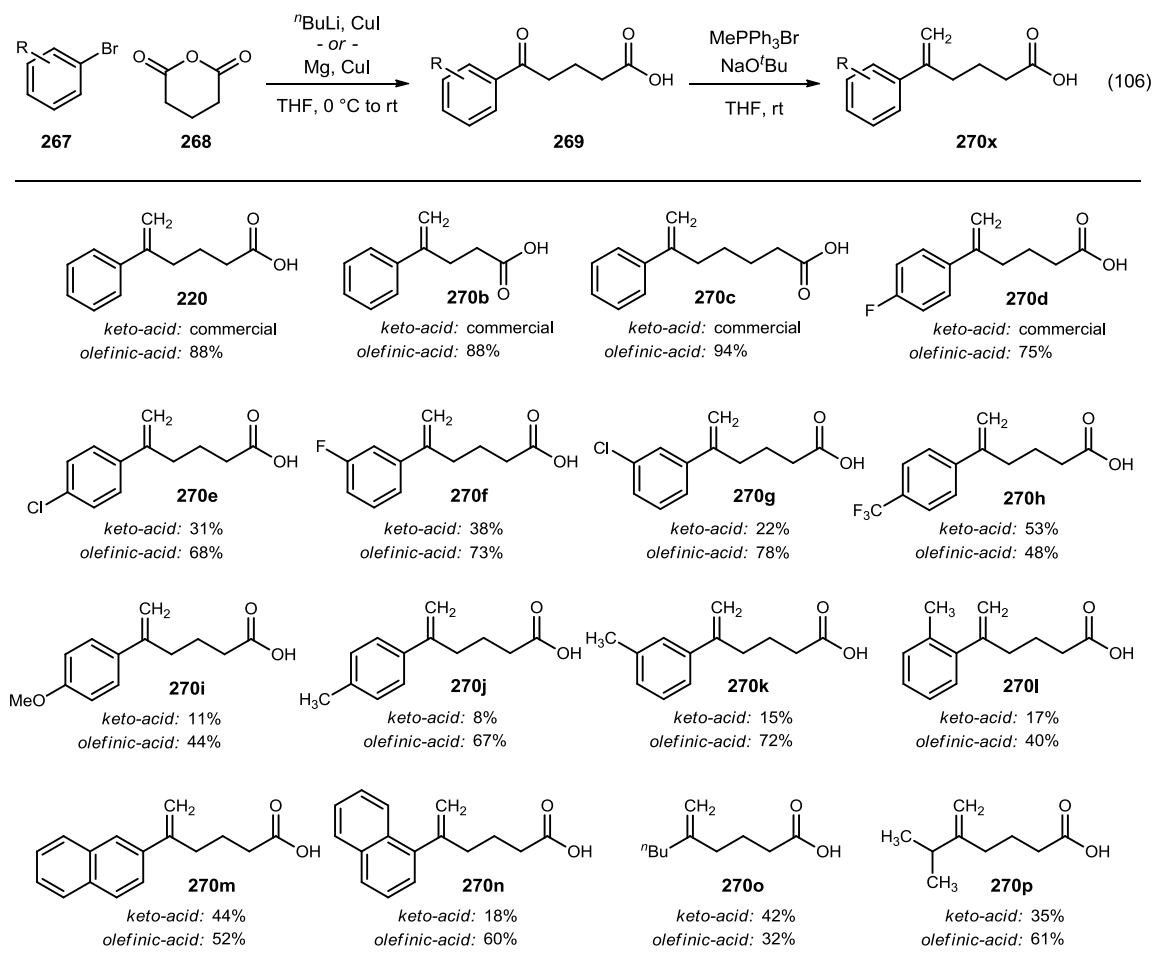


One molecule of catalyst is highlighted in gray (carbon) and blue (nitrogen), while the other molecule is light blue for clarity. Though the solid state of the catalyst is not a direct representation of the catalyst in solution, it presents possible interactions that may be observed in solution. Interestingly, the dihedral angles (NCCN) of both molecules of catalyst were measured to be  $62^\circ$  and  $69^\circ$ , larger than the  $52^\circ$  that was previously calculated for this diamine in another system.<sup>56</sup> This increased flexibility in the diamine backbone may be the reason for the increase in reactivity and enantioselectivity.

#### ***Substrate Scope for 1,1-Disubstituted Olefinic Acids***

Before a full substrate scope could be examined in this transformation, the synthesis of the starting materials needed to be completed, as not all of the keto-acids were readily available (Chart 7).

**Chart 7.** Synthesis of Desired Olefinic Acids for Idolactonization.



The opening of glutaric anhydride with organocuprates to give the desired ketoacids was carried out using a modified procedure from Rovis<sup>116</sup> and Ishihara.<sup>117</sup> The use of the organocuprate was incorporated to minimize the double addition, which results in an undesired alcohol. The yields for this step are variable (from 8-53%), but most were run only once and in some instances the yield was sacrificed for purity. The ketoacids were then submitted to the Wittig reaction with much better success. Most of the yields to form the olefin were over 70%, while the lower yields were a result of semipure starting

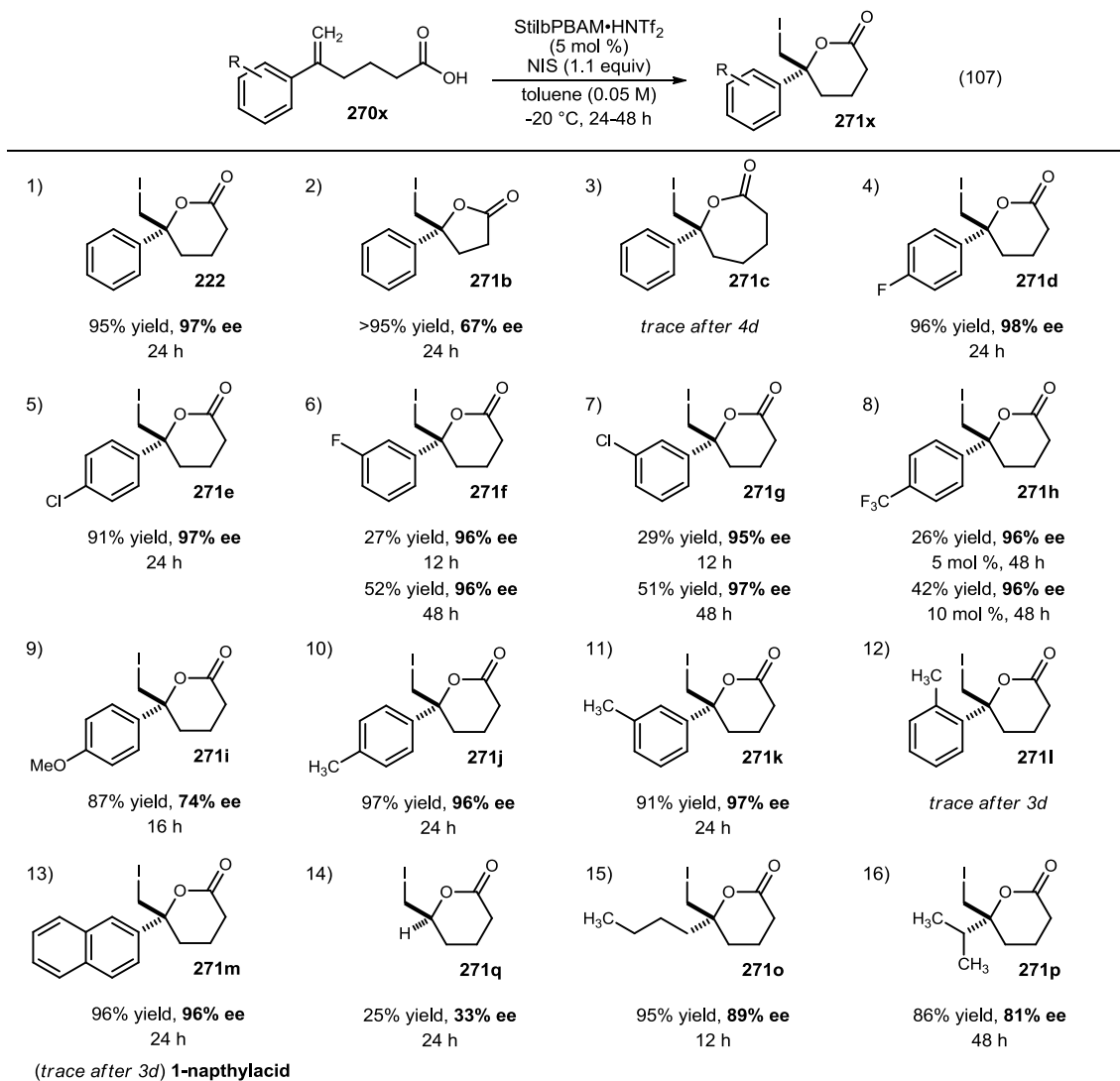
<sup>116</sup> Lee, E. E.; Rovis, T. *Org. Lett.* **2008**, *10*, 1231-1234.

<sup>117</sup> Uyanik, M.; Yasui, T.; Ishihara, K. *Bioorg. Med. Chem. Lett.* **2009**, *19*, 3848-3851.

ketoacid or incomplete conversion. Further optimization could increase the yields for both steps, but the route provided enough material (from inexpensive starting materials) to establish a substrate scope.

Though previous experiments demonstrated the reactivity of the iodolactonization using only 1 mol % catalyst, initial experiments for the substrate screen established that 5 mol % catalyst loading was most general across the board (Chart 8).

**Chart 8.** Substrate Scope in Enantioselective Iodolactonization of 1,1-Disubstituted Acids.



<sup>a</sup>All reactions were performed on a 0.10 mmol scale using 1 equivalent of the carboxylic acid under conditions listed.

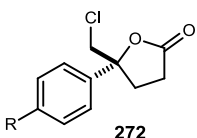
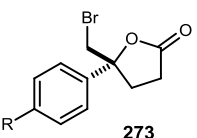
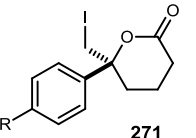
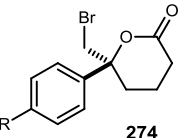
Encouraged by the results with the formation of the  $\delta$ -lactone, we first looked at variations in the ring size. Removing one carbon from the chain gave the  $\gamma$ -lactone (**271b**) with low enantioselection (67% ee), possibly due to a more reactive species and background reaction. Conversely, the addition of a carbon (desired  $\epsilon$ -lactone) severely hindered reactivity, giving only trace product (**271c**) after four days of stirring, though the racemic product formed with only slightly diminished reactivity. Halogens at the *para*-position (**271d** and **271e**) returned product with high enantioselection and yield. However, moving both halogens to the *meta*-position (**271f** and **271g**) severely hindered the reaction progress, stalling after 48 hours of stirring, but still maintaining the high selectivity (96 and 97% ee). A similar trend in reactivity and selectivity was observed with the *para*-trifluoromethyl analog (**271h**), as product was recovered in 96% ee and only 42% yield (low conversion). Running the same reaction with a higher catalyst loading only slightly increased the yields, while giving the same selectivity. The reactivity was recovered when the electron withdrawing substituent was replaced with an electron donating substituent (MeO-) to give lactone **271i** in higher yields (87%) but with lower enantioselection (74% ee). Methyl substituents at the *para*- and *meta*-position (**271j** and **271k**) returned product that was >91% yield and >96% ee, while no difference in reactivity was observed, a stark contrast to the *meta*-halogen substrates. Moving the methyl group one position to the sterically encumbering position completely stymied the reactivity, as only a trace amount of the desired lactone (**271l**) was observed after three days of stirring. The same drop in reactivity was observed with the 1-naphthyl analog (**271n**), but reactivity was restored for the 2-naphthyl lactone **271m**, as product was

isolated in 96% yield and 96% ee. The aliphatic analogs performed well if the olefin was doubly substituted. Commercially available 6-hexenoic acid was significantly less selective, affording the desired lactone (**271q**) with only 33% ee. The *n*-butyl derivative (**271o**) was isolated with 95% yield and 89% ee, while increasing the steric bulk to the isopropyl derivative provided lactone **271p** in 86% yield and 81% ee. Though the scope improves on the previously reported iodolactonizations, further optimization on some of the lower performing substrates was necessary.

### Lower performing substrate optimization

The *para*-methoxy analog produced product in 74% ee under standard conditions, which still represents a large increase from previously reported examples (Figure 29).

**Figure 29.** The Problematic *para*-Methoxy Substrate.

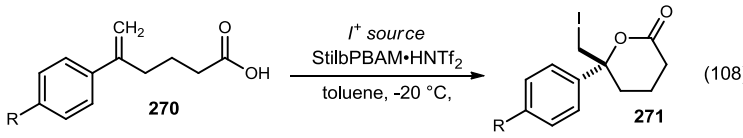
|   |   |  |   |                           |
|---|---|--|---|---------------------------|
|  |  |  |  |                           |
| R = -H  | 86% yield, <b>89% ee</b>  | 98% yield, <b>90% ee</b>   | 87% yield, <b>94% ee</b>  | 99% yield, <b>91% ee</b>  |
| R = -OMe  | 99% yield, <b>&lt;5% ee</b>   | 67% yield, <b>28% ee</b>   | 91% yield, <b>48% ee</b>  | 74% yield, <b>80% ee*</b> |
|   | ref. X(Borhan)  | ref. X(Yeung)  | ref. X(Jacob)   | ref. X(Fuji)              |
|   |   |  |   | *modified procedure       |

In the (DHQD)<sub>2</sub>PHAL catalyzed chlorolactonization,<sup>100</sup> the *para*-methoxy substrate **272** was obtained in quantitative yield and essentially no enantioselectivity. The authors hypothesized that the *para*-methoxy substrate promotes the chloronium ring opening, while the closure of the acid occurs independently of the catalyst. This higher rate of background reaction was also observed for the  $\gamma$ -bromolactonization<sup>103</sup> and  $\delta$ -iodolactonization.<sup>102</sup> One successful approach to increasing the enantioselectivity for *para*-substituted electron rich acids was demonstrated in the trisimidazoline catalyzed  $\delta$ -

bromolactonization.<sup>104</sup> The authors decreased the temperature from -40 °C to -78 °C and added extra halonium source to deliver the adduct in 74% yield and 80% ee [where the standard substrate (R=H) was isolated in 99% yield and 91% ee].

We investigated different reaction conditions in an attempt to increase the selectivity for the *para*-methoxy substrate (Table 29).

**Table 29.** Increasing Enantioselection for the Lactonization for the *para*-Methoxy Acid.



| entry | R    | I <sup>+</sup> (equiv) | mol % | (M)   | time (h) | % yield | ee (%) |
|-------|------|------------------------|-------|-------|----------|---------|--------|
| 1     | MeO- | NIS (1.1)              | 5     | 0.05  | 16       | 87      | 74     |
| 2     | MeO- | NIS (1.05)             | 2     | 0.05  | 3        | 58      | 63     |
| 3     | MeO- | NIS (1.3)              | 15    | 0.05  | 0.5      | 70      | 72     |
| 4     | MeO- | NIS (1.1)              | 5     | 0.025 | 2        | 58      | 69     |
| 5     | H-   | DIDMH (1.1)            | 5     | 0.05  | 6        | 89      | 92     |
| 6     | H-   | DIDMH (0.6)            | 5     | 0.05  | 6        | 85      | 96     |
| 7     | MeO- | DIDMH (0.6)            | 5     | 0.05  | 2        | 84      | 85     |

<sup>a</sup> All reactions were performed on a 0.10 mmol scale using 1 equivalent of the carboxylic acid under conditions listed.

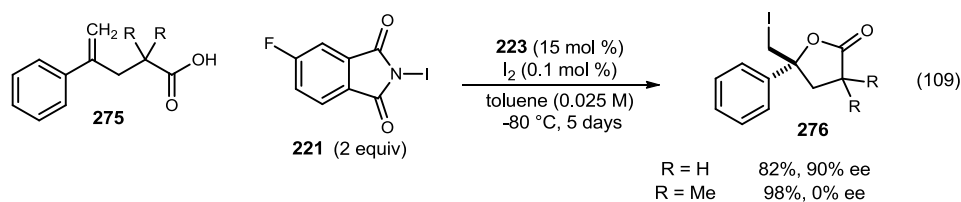
Decreasing the catalyst loading to 2 mol % (entry 2) was ineffective while increasing the catalyst loading to 15 mol % (entry 3) gave similar results at 70% yield and 72% ee. Running the reaction more dilute did not increase the enantioselection (entry 4). We then looked at other commercial sources of I<sup>+</sup>. Unfortunately, the commercial availability for sources of electrophilic iodine are limited, while there are a number of available sources of chlorine and bromine (Cl<sup>+</sup>>Br<sup>+</sup>>>>I<sup>+</sup>). Of the milder sources, 1,3-diiodo-5,5-dimethylhydantoin (DIDMH) was previously explored by Jacobsen (with added iodine) to give the lactone in 5% yield and 60% ee. In our system with the standard olefinic acid



(Ar = Ph) and using 1.1 equivalents of DIDMH (entry 5), we recovered product in 89% yield and 92% ee, a slight drop from NIS. Since DIDMH has two equivalents of I<sup>+</sup>, decreasing the equivalents to 0.6 (entry 6) increased the enantioselection to 96% ee, similar to the optimal conditions with NIS. Gratifyingly, switching the source of iodine from NIS to DIDMH for the *para*-methoxy substrate (entry 7) increased the enantioselection to 85% ee without a loss in yield. This selectivity is one of the highest reported for a *para*-methoxy acid thus far.

The pentenoic acid substrate also proved problematic for Jacobsen in the initial report.<sup>102</sup> Two observations were made when looking at the pentenoic acid, or nor-homolog, derivatives (Scheme 48).

**Scheme 48.** Jacobsen's Modification of Conditions for Pentenoic Acid Derivatives.

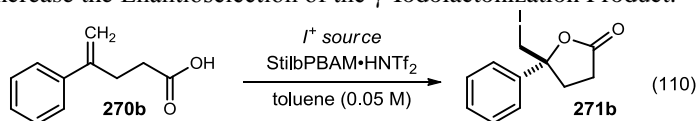


When their initial conditions using 15 mol % of iodine additive were applied, the adduct (**276**) was obtained in 86% yield and only 31% ee. Decreasing the amount of iodine additive to 0.1 mol % gave the adduct in 45% yield and 90% ee. The low yield was corrected when an additional equivalent of the *N*-iodo-4-fluorophthalimide (**221**) was added. It was believed that the low enantioselectivity was a result of the more reactive lactone formation. This was confirmed when the *gem*-dimethyl analog was submitted to the reaction and the product formed in 0% ee. Additionally, the pentenoic acid analog

was isolated in the opposite absolute configuration as the hexenoic acid analogs, suggesting a slightly different model for enantioinduction.

We sought to increase the enantioselection by looking at similar reaction optimization without dramatic changes in reaction conditions (Table 30).

**Table 30.** Attempts to Increase the Enantioselection of the  $\gamma$ -Iodolactonization Product.



| entry | $I^+$ | cat. (mol %) | T (°C) | time (h) | % yield | ee (%) |
|-------|-------|--------------|--------|----------|---------|--------|
| 1     | NIS   | 5            | -20    | 24       | >95     | 67     |
| 2     | NIS   | 10           | -78    | 96       | 60      | 70     |
| 3     | DIDMH | 5            | -20    | 3        | 89      | 58     |

<sup>a</sup>All reactions were performed on a 0.10 mmol scale using 1 equivalent of the carboxylic acid under conditions listed.

Earlier experiments that probed the catalyst loading and reaction concentration using PBAM·HNTf<sub>2</sub> as a catalyst (not listed) were not fruitful. Similar experiments with StilbPBAM were completed to determine the role the catalyst may have on the substrate. Decreasing the reaction temperature to -78 °C (entry 2) slightly increased enantioselection to 70% ee, while sacrificing time (4 days) and yield (60%). Unfortunately, using DIDMH did not increase enantioselection for the  $\gamma$ -lactone (entry 3), delivering product in 89% yield and 58% ee. It is still believed that the background rate is the primary source of low enantioselection. An interesting observation is that the same sense of enantioselection was observed, suggesting that the mechanism for the  $\gamma$ -lactone is very similar to that of the  $\delta$ -lactone formation.

## Mechanistic Observations

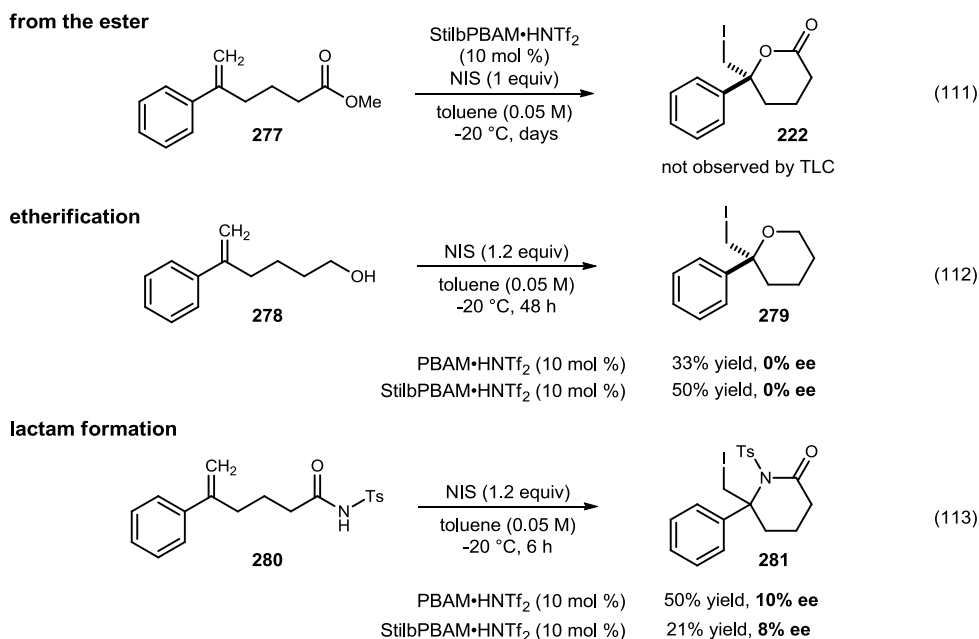
A few observations about the bisamidine catalyzed enantioselective iodolactonization reaction have been made thus far:

1. The acidity *and* sterics of the achiral counterion both influence enantioselection.
2. Lower catalyst loadings (to 1 mol %) and more dilute concentrations (0.05M) give product with higher enantioselection.
3. A non-linear effect has not yet been observed.
4. The BAM:HNTf<sub>2</sub> ratio (1:1) is important to maintaining enantioselection, where a 1:2 ratio delivers product as the racemate.

The influence of the solvent and reaction conditions on the enantioselection has been extensively studied, in addition to the catalyst system. One component that has not been fully explored is the starting carboxylic acid.

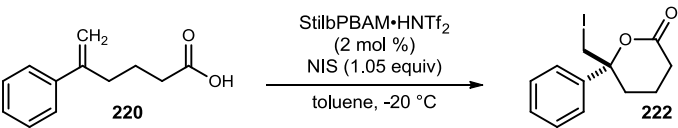
To determine the importance of the carboxylic acid in the reaction, different functional groups were investigated in the iodocyclization reaction (Chart 9).

**Chart 9.** BAM Catalyzed Cyclizations of other Functional Groups.



Attempts were made to access the lactone directly from ester **277**, though no conversion of the ester was observed by TLC (eq 111). Using a better leaving group such as the *tert*-butyl ester may better facilitate product formation. The alcohol, using both PBAM and StilbPBAM, gave the etherification product **279**, but as racemic material. The lactam **281** was formed in low yield and with low selectivity, with neither BAM catalyst showing a preference. This suggests that the carboxylic acid is necessary for enantioselection, possibly through a pre-coordination with the catalyst prior to iodine delivery.

Early on in the study, minor observations suggested that the enantioselection may change as the reaction progresses. To probe this, we wanted to look at the enantiomeric excess of the product as a function of reaction time. Initial experiments using 2 mol % of catalyst were quenched at 1, 2, 4, and 24 hours. However, significant conversion ( $^1\text{H}$  NMR) to product was observed at just 1 hour, and it was realized that quenches at earlier time points were needed. Additionally, monitoring reaction completion by  $^1\text{H}$  NMR was inconsistent due to the partial solubility of the starting material in the aqueous layer (existing as sodium salt) after the sodium thiosulfate quench. The reactions were set up again on a 0.2 mmol scale and quenched at 15 minute intervals for the first hour, then at 2 and 4 hours, while one was allowed to reach full conversion after three days (Table 31).

**Table 31.** Monitoring Enantiomeric Excess over Reaction Progress.


| entry | quench (min) | isolated yield (mg) | isolated yield (%) | ee (%) | ( <i>R</i> )-lactone (mg) <sup>b</sup> | ( <i>S</i> )-lactone (mg) <sup>b</sup> |
|-------|--------------|---------------------|--------------------|--------|--|--|
| 1     | 15           | 6.1                 | 9                  | 80     | 5.5                                    | 0.6                                    |
| 2     | 30           | 8.2                 | 13                 | 86     | 7.6                                    | 0.6                                    |
| 3     | 45           | 10.1                | 16                 | 88     | 9.5                                    | 0.6                                    |
| 4     | 60           | 11.9                | 19                 | 90     | 11.3                                   | 0.6                                    |
| 5     | 120          | 14.6                | 23                 | 93     | 14.1                                   | 0.5                                    |
| 6     | 240          | 21.7                | 34                 | 96     | 21.2                                   | 0.5                                    |
| 7     | 4,320        | 57.4                | 91                 | 98     | 56.8                                   | 0.6                                    |

<sup>a</sup> The reaction was performed on a 0.20 mmol scale (0.05 M) using 1 equivalent of the carboxylic acid. Reactions were quenched by the addition of sodium thiosulfate.

<sup>b</sup> Amounts of each enantiomer were calculated using ee and isolated yield.

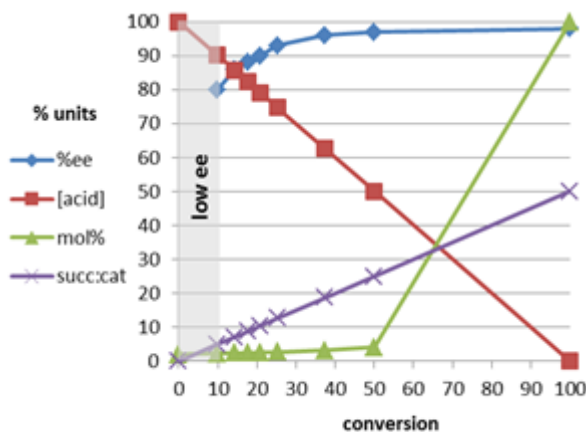
Interestingly, we saw that the enantiomeric excess of the product increased as the reaction progressed. Further calculations (using the isolated yield and enantioselection of each reaction) showed the amount of each lactone enantiomer present and suggested that all of the minor enantiomer (*S*-configuration) was produced in the first 15 minutes of the reaction! In other words, the reaction that occurs after the first 15 minutes returns product that is >99% ee. There are few explanations that can account for this behavior, but intrigued by this phenomenon, we attempted to isolate the variable.

As the reaction progresses, there are variables that are dynamic and may contribute to the drastic change in enantioselection observed from the beginning to end of the reaction.

1. **Acid concentration** changes as starting material is consumed.
2. **Catalyst loading** increases from an initial concentration of 2 mol % (cat **115**).
3. **Succinimide** (N-H) is not available or limited for the first few catalyst turnovers.
4. **Product** concentration is the inverse of the olefinic acid concentration.

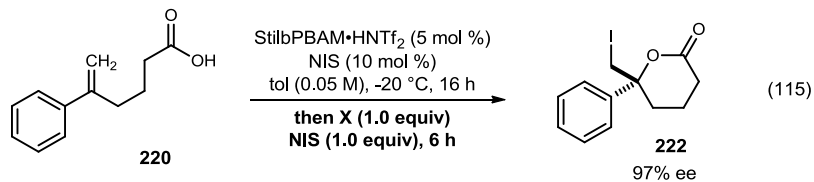
We wanted to only look at changes in the first 10% of the reaction (gray area), which become evident when plotted as a function of conversion (Graph 2).

**Graph 2.** Mapping Out Reaction Progress and Variables that Change Most in First 10% of Reaction.

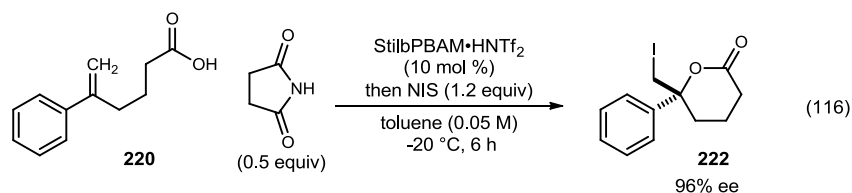


The graph shows that in the first 10% of the reaction, there is little change in the amount of olefinic acid available (100% to 90%) and in catalyst loading (2 mol % to 2.2 mol %). For the first catalyst turnovers, succinimide concentration is low, as the catalyst:succinimide ratio is 2:0. At 10% conversion, the ratio decreases to 2:10 (catalyst:succinimide), presenting a very different combination of reagents. Another component that undergoes significant change is the product, which is not present for the first catalyst turnovers in the reaction.

Experiments were completed to determine the influence of succinimide on the reaction. First the catalyst (5 mol %) and NIS (10 mol %) were stirred for 16 hours at -20 °C, to represent the course of a reaction (eq 115).



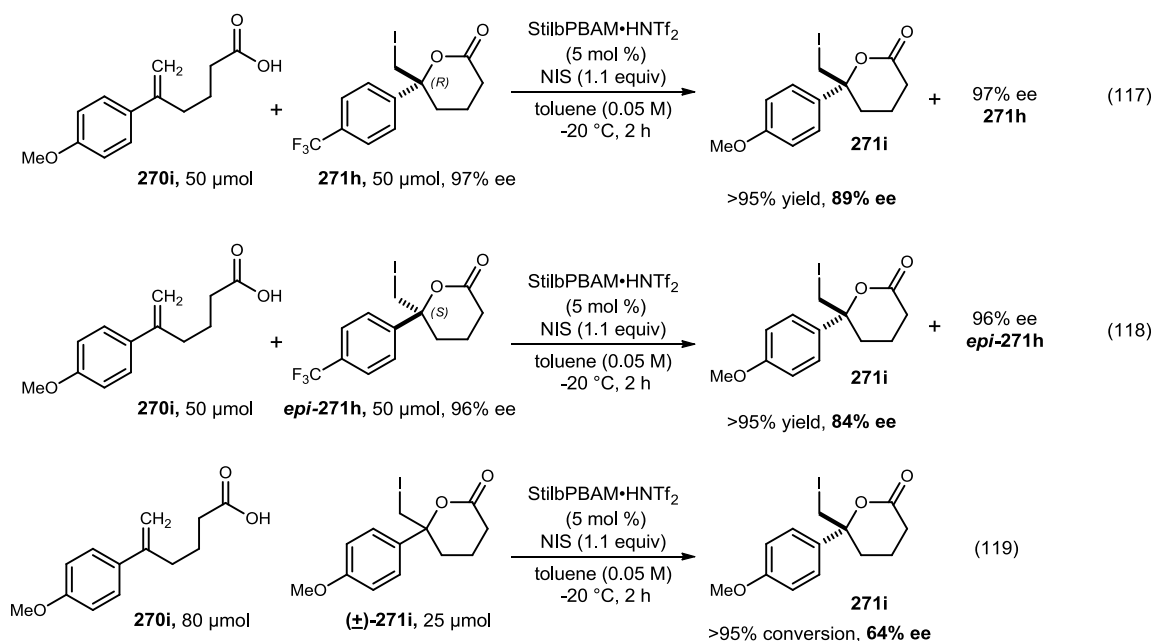
If the catalyst is modified or other interactions are necessary, this allows time for those to occur. After adding the starting acid and remainder of NIS (1.0 equiv), material was isolated in 97% ee, which was similar to normal conditions. Second, a reaction was completed with 50 mol % of succinimide (representing the 50% conversion mark) and this resulted in no change in enantioselection (eq 116).



This suggests that the coproduct succinimide has little influence on enantioselection in the reaction. Other reactions completed with depleted (0.6 equiv) or excess (2.4 equiv) NIS showed little change in enantioselection. Having thoroughly investigated the role of NIS and succinimide, we looked at the role the product may have on enantioselection.

The first turnover of catalyst takes place without any product present (0:1, product:ligand), where the fifth turnover of the catalyst is completed with approximately a 5:1 ratio of product:ligand. To simulate this, the reaction was spiked with an iodolactone product (Chart 10).

**Chart 10.** Role of the Product in Influencing Enantioselection.



To ensure an accurate calculation of enantioselection, we used a different lactone than what would arrive from the starting acid, as well as one that would not overlap in the HPLC assay. Gratifyingly, one of our more problematic substrates (*para*-methoxy) and best substrates (*para*-trifluoromethyl) paired nicely for ease of HPLC analysis as all four enantiomers were separated. This allowed us to complete the reaction without having to separate the two lactones. Under our standard conditions, we were able to obtain the *para*-methoxy adduct (**271i**) in 74% ee. Surprisingly, when we combined the starting acid (**270i**) and the *para*-trifluoromethyliodolactone (**271h**), we saw a significant increase in enantioselection for the *para*-methoxylactone **271i** to 89%. When the reaction was completed with the opposite enantiomer of the *para*-trifluoromethyliodolactone (*epi*-**271h**), we saw a similar influence on enantioselection, returning the product in 84% ee. The reaction was also done in the presence of *rac*-**271i**, where the product was determined to form in 84% ee (after calculations). This influence of the product on the

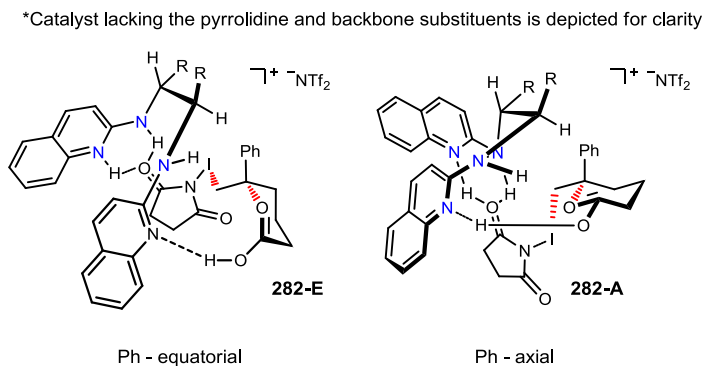


most selective pathway paves the way for additional research into the involvement of the product in the transition state. Additionally, a thorough investigation into the lactone's simplest functionality, the ester, may reveal a more general additive that can be used to increase enantioselection for this, and other reactions.

### ***Development of Reagent-Substrate Assembly Models for Enantioselection***

The catalyst is bifunctional, acting as both a Brønsted acid and a Brønsted base. Although these experiments clearly outline a conceptually unique catalyst system with practical importance, the catalyst-reagent-substrate assemblies depicted in Figure 30 illustrate two possible models for enantioselection.

**Figure 30.** Proposed Reagent-Substrate Assemblies.



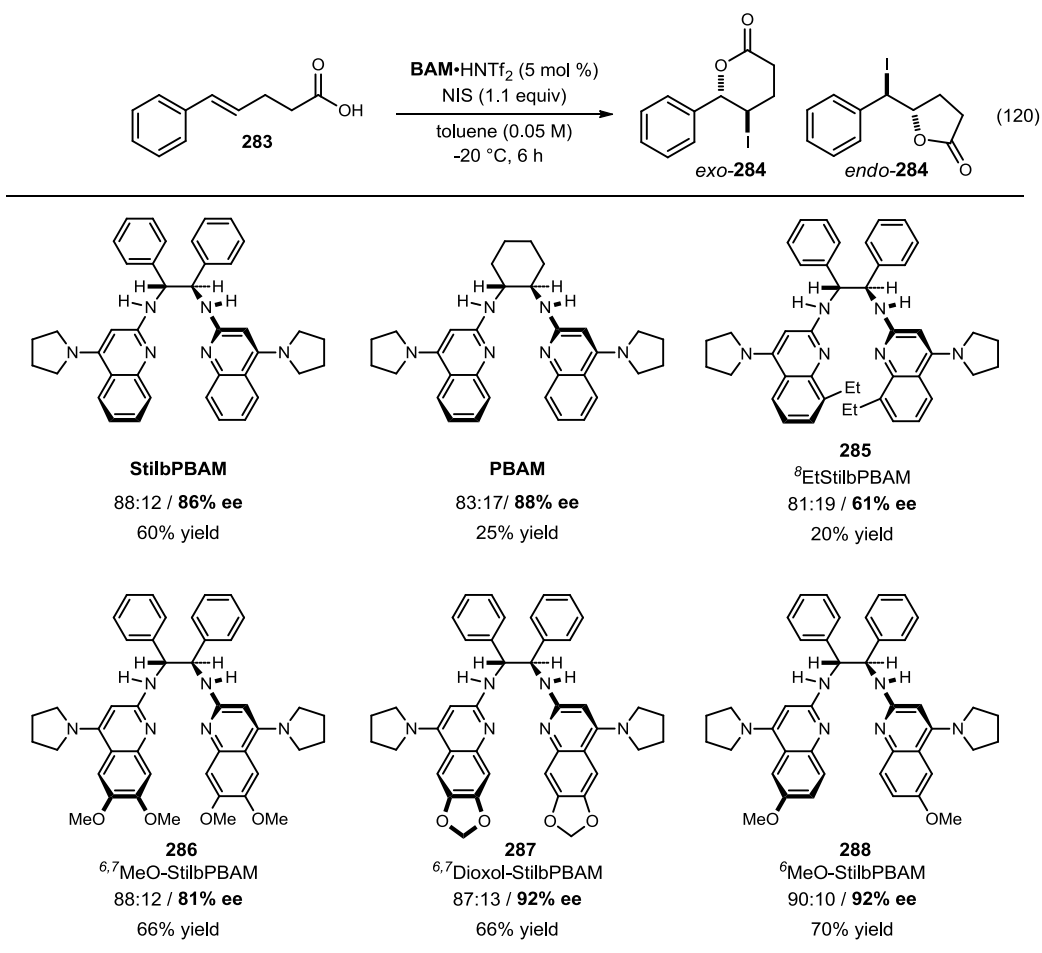
The assumptions common to each of these include: 1) *anti*-addition to the alkene, 2) a 1:1:1:1 complex of  $\text{Tf}_2\text{NH}$ :chiral ligand:NIS:substrate, 3) a coplanar arrangement between the quinolinium ring and NIS based on double hydrogen bonding to the NIS carbonyl, and 4) orientation of the iodine toward the chiral backbone. It is almost certain that a linear relationship along the succinimide-iodine-alkene axis does not exist, but twisting of the quinolinium ring toward the interior would help. Each of these assemblies

also hypothesizes a hydrogen bond (or ion pair) between the quinoline and the substrate carboxylic acid, supported by the necessity of the carboxylic acid for high selectivity. It is also possible that this pre-coordination of the carboxylate is important for high facial selectivity in the iodine delivery step. Assembly **282-E** depicts the substrate orientation with an equatorial placement of the phenyl, whereas **282-A** differs primarily by the axial orientation of the phenyl. No specific orientation of the counterion is depicted relative to the substrate, but it may provide either a more enveloped pocket or provide helpful hydrogen bond acceptor contacts. Each of these assemblies leads to the observed enantiomer but are not exclusive of alternatives. Although we can't establish exactly the reason for the achiral counterion control or enantioinduction, we do identify and characterize the unique composition and behavior of the catalyst system described as an important first step.

#### *Application to endo-Iodolactonization*

Having demonstrated the 6-exo-iodocyclization of 1,1-disubstituted  $\delta$ -unsaturated acids and equipped with a knowledge of the subtleties this reaction offers, we sought to apply it to 1,2-disubstituted  $\gamma$ -unsaturated acids. Using this class of acids, two lactones can form, either in a 5-exo or 6-endo fashion. We sought a catalyst system that would not only deliver the desired adduct in high enantiomeric excess, but also with high regioselectivity.

Initial reaction optimization was completed on this system using our BisAMidine library of catalysts (Table 32).

**Table 32.** Catalyst Screen for *endo*-Iodolactonization.

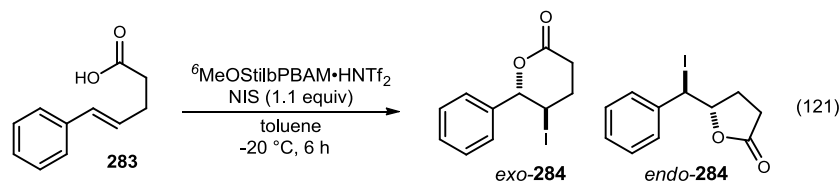
<sup>a</sup>All reactions were performed on a 0.10 mmol scale using 1 equivalent of the carboxylic acid under conditions listed. Isolated yields are a mixture of *endo*- and *exo*-lactone products (6:5).

The previously optimized conditions were first applied at -20 °C using StilbPBAM (**115**) as the catalyst in toluene (0.05 M). A mixture (88:12) of the  $\delta$ - and  $\gamma$ -lactone **284** was isolated in 60% yield, while the *endo*-lactone formed in 88% ee and the *exo*-lactone formed in <30% ee. Unfortunately, the  $\gamma$ -lactone enantiomers did not consistently resolve by chiral HPLC and could not be determined with certainty. However, enantioselection is clearly low (less than 30% in most cases). The slight preference (2:1) for the *endo*-lactone was also observed when DMAP was used for the racemic reaction. PBAM gave similar selectivities for the *endo*-/*exo*-lactones, with the major lactone isolated in 88% ee,

but the catalyst was significantly less reactive. A variety of stilbene derived BAM catalysts were synthesized and screened in the reaction. When <sup>8</sup>Et-StilbPBAM (**285**) was used, a sharp drop in reactivity and enantioselectivity was observed, with product isolated in 20% yield and 61% ee. We hypothesize that this steric bulk blocks the chiral pocket and slows the reaction while crowding the binding pocket which decreases the enantioselection. The more electron rich catalyst, <sup>6,7</sup>MeOStilbPBAM (**286**), presented the desired adduct in 66% yield and 81% ee. The electronically similar, but sterically less hindered <sup>6,7</sup>Dioxol-StilbPBAM (**287**) gave the product in 92% ee and 66% yield. Gratifyingly, when the methoxy or oxygen substituent at the 7-position was removed (<sup>6</sup>MeO-StilbPBAM, **288**), we isolated the product in 70% yield and 92% ee for the major lactone which formed as a 90:10 ratio.

Using the optimal <sup>6</sup>MeO-StilbPBAM catalyst, other reaction parameters were examined (Table 33).

**Table 33.** Reaction Optimization for the *endo*-Iodolactonization.



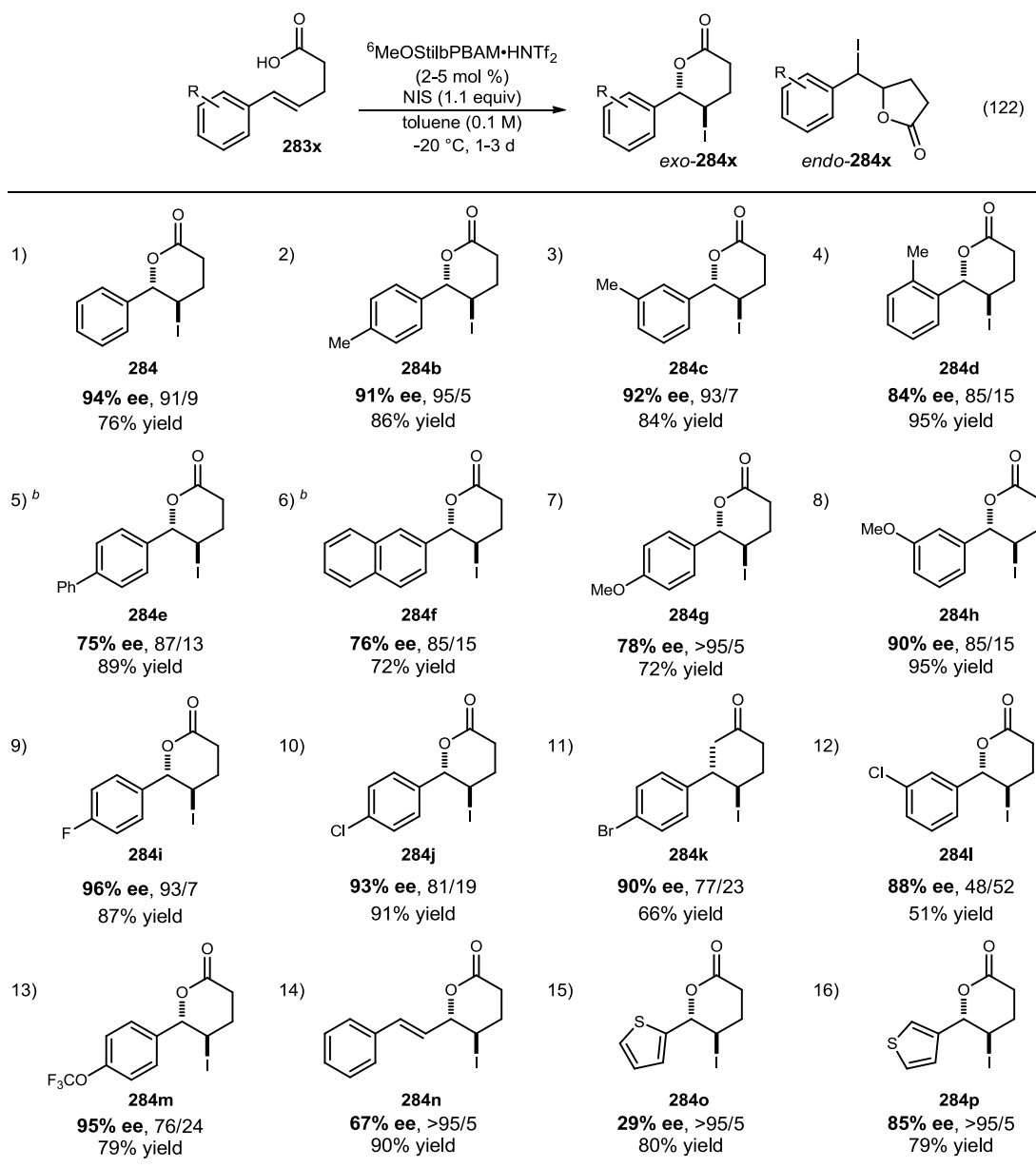
| entry | cat. (mol %) | NIS (equiv) | (M)  | T (°C) | time (h) | yield (%) | A:B   | A% ee |
|-------|--------------|-------------|------|--------|----------|-----------|-------|-------|
| 1     | 5            | 1.1         | 0.05 | -20    | 6        | 66        | 90:10 | 92    |
| 2     | 5            | 1.1         | 0.1  | -20    | 24       | 83        | 88:12 | 93    |
| 3     | 5            | 1.1         | 0.1  | -78    | 96       | trace     | -     | -     |
| 4     | 0            | 1.1         | 0.1  | -20    | 24       | trace     | -     | -     |
| 5     | 10           | 1.2         | 0.1  | -20    | 24       | 76        | 84:16 | 89    |
| 6     | 2            | 1.05        | 0.1  | -20    | 24       | 76        | 91:9  | 94    |

<sup>a</sup>All reactions were performed on a 0.10 mmol scale using 1 equivalent of the carboxylic acid under conditions listed.

Increasing the concentration of the reaction corresponded to an increase in the yield, with no loss in enantioselection (entry 2). Attempts to further increase the enantioselection by running the reaction at -78 °C only returned trace amounts of product (entry 3). The reaction was run in  $d_8$ -toluene at -20 °C without catalyst (entry 4) to establish if there is a significant background rate, possibly accounting for the low selectivity of the *exo*-lactone. No product was observed, possibly due to the limited solubility of NIS without the catalyst present. Further increasing the catalyst loading to 10 mol % led to a decrease in enantioselection (entry 5), while decreasing the catalyst loading to 2 mol % was favorable (entry 6), delivering the major product in 94% ee, with a 91:9 ratio of the *endo*:*exo*-lactone.

To assess the generality of the reaction, a substrate scope of varying electronics and sterics was completed (Chart 11).

**Chart 11.** Substrate Scope for the *endo*-Iodolactonization.



<sup>a</sup> All reactions were performed on a 0.10 mmol scale using 1 equivalent of the carboxylic acid under conditions listed using 2 or 5 mol % catalyst loading. Yields are isolated yields of both regioisomers. Ratios of the *endo*- to *exo*-lactone were measured by <sup>1</sup>H NMR. <sup>b</sup> Reaction run in a toluene/trifluorotoluene (4/1) mixture.

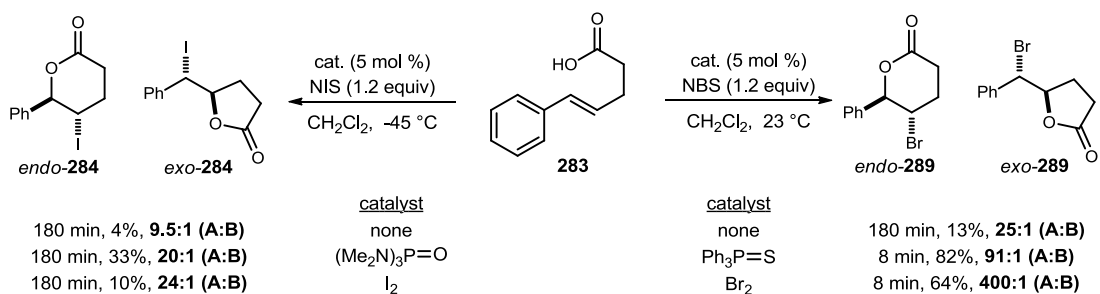
Methyl groups were tolerated at all positions of the aromatic ring (entries 2-4) with very little difference in yield or selectivity between the *para*- and *meta*-substituted rings (91% and 92% ee). The *ortho*-methyl analog gave the lactone (**284d**) in slightly lower enantioselection (84% ee), but good yield after 3 days of stirring, a stark contrast to the

result with 1,1-disubstituted olefins (trace product after days of stirring). This may result from catalyst-NIS binding to the homobenzylic carbon instead of the benzylic carbon, making the *ortho*-position substitution less cumbersome. The starting acids of the *para*-phenyl and 2-naphthyl were very insoluble in toluene and returned very little product (entries 5-6). However, when they were run in a toluene/trifluorotoluene mixture (4/1), both the *para*-phenyl lactone (**284e**) and the 2-naphthyl lactone (**284f**) were isolated in good yield (89% and 72% yield) and moderate enantioselection (75% ee and 76% ee). (Reactions run in only trifluorotoluene returned product that was significantly lower in enantioselection.) The enantioselection for the electron rich rings was heavily dependent on the position of the substituent, as the *para*-methoxy gave lactone **284g** in 78% ee and 72% yield (entry 7) while the *meta*-methoxy gave lactone **284h** in 90% ee and 95% yield (entry 8). For the *para*-methoxy analog, none of the  $\gamma$ -lactone was observed by  $^1\text{H}$  NMR, a trend observed with other electron rich aromatic rings. The *para*-halogenated rings maintained high levels of enantioselection (entries 9-11), but were slower and produced variable amounts of the  $\gamma$ -lactone. The *para*-fluoro lactone **284i** (entry 9) was isolated in 87% yield (93/7) and 96% ee, while the *para*-chloro lactone **284j** (entry 10) was isolated in 91% yield (81/19) and 93% ee. The decrease in enantioselection and *endo*-/*exo*- ratio continued with the *para*-bromo lactone **284k** (entry 11), isolated in 66% yield and 90% ee for the major lactone while producing 23% of the undesired lactone. When the chlorine was moved to the *meta*-position, the  $\delta$ - and  $\gamma$ -lactone **284l** were both produced equally (entry 12). Fortunately, the *endo*-lactone **284l** was still enriched with one enantiomer (88% ee). The solubility of the starting *meta*-chloro acid and the *meta*-chloro product might have played a role in the low lactone ratio. The *para*-trifluoromethoxy acid

delivered lactone **284m** in 79% yield and 95% ee (entry 13), the highest for any of the substrates. The cinnamyl lactone **284n** (entry 14) and 2-thiophene lactone **284o** (entry 15) performed similarly to the *para*-methoxy analog, delivering the adducts in lower enantioselection (67% and 29%, respectively) and only one regioisomer. Surprisingly, moving the sulfur one position (**284p**, entry 16) increased enantioselection to 85%, while still producing only the desired isomer in 79% yield. Pleased with the scope and enantioselection for the *endo*-lactone, we wanted to further investigate the driving force for the *exo*-lactone formation.

Throughout our studies we saw that the regioselectivity of the product, though >85% in most cases, was dependent on the aromatic ring of the acid. The electron rich rings gave mostly the *endo*-lactone. Additionally, as the halogens moved from fluorine to bromine, the amount of *exo*-lactone production also increased. Based on the work of Denmark, it has been suggested that these systems allow for catalyst control of the *endo*-/*exo*-product formation (Scheme 49).<sup>118</sup>

**Scheme 49.** Lewis Base Catalysis and Control of *endo*-/*exo*-Selectivity in Halolactonizations



When acid **283** was combined with NIS in dichloromethane, the ratio of lactones **284** was 25:1. Adding Ph<sub>3</sub>P=S as a catalyst increased the ratio to 91:1, while Br<sub>2</sub> increased the

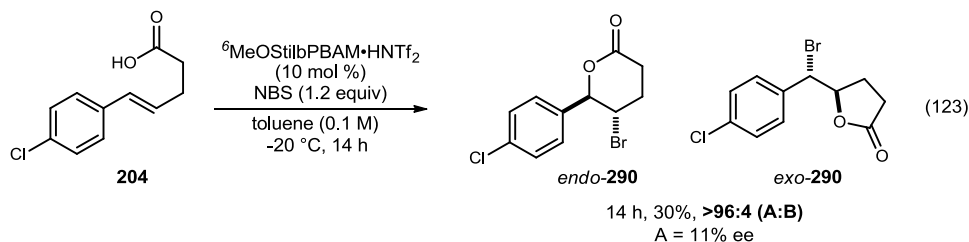
<sup>118</sup> Denmark, S. E.; Burk, M. T. *Proc. Natl. Acad. Sci. U. S. A.* **2010**, *107*, 20655-20660.



ratio of lactone **289** to 400:1. Running the same reaction with NIS in dichloromethane at -45 °C, significantly less control was observed when only NIS was used (9.5:1). Using  $(\text{Me}_2\text{N})_3\text{P}=\text{O}$  as a catalyst imparted some selectivity for the *endo*-lactone, though it was not much different from using only  $\text{I}_2$ . Though the catalyst imparts some control over the regioselectivity, it is also apparent that the halonium source also plays a role, with NBS offering more opportunity for control. This was also demonstrated in the *endo*-bromolactonization by Yeung where most examples gave exclusively the *endo*-lactone.<sup>107</sup>

To assess our catalyst system in the bromolactonizations, we combined the *para*-chloroacid **204** with NBS under the standard BAM conditions (Scheme 50).

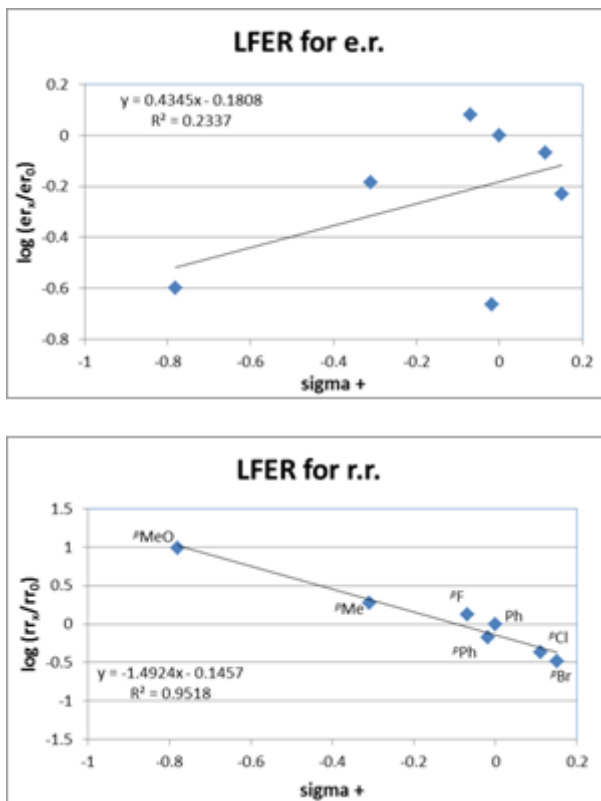
**Scheme 50.** BAM Catalyzed *endo*-Bromolactonization.



The resulting bromo-lactone **290** from the bisamidinium catalyst formed as the *endo*-lactone (>96:4 by  $^1\text{H}$  NMR analysis of crude reaction mixture) while the iodo-lactone **284j** was isolated as an 81:19 mixture of lactones (Chart 11, entry 10). Unfortunately, the bromolactone was isolated with very low enantioselection (11%), lending credibility to the hypothesis that the catalyst/reagent systems are not general for all halonium sources. This also suggests that NBS, when used as the halonium source, imparts some preference for the *endo*-lactone.

To further quantify the effect the electronics of the aromatic ring have on the reaction, Hammett plots were constructed to assess both enantioselection and regioselection for the *trans*-1,2-disubstituted olefins (Graph 3).

**Graph 3.** Hammett Plots for Enantiomeric Ratio and Regioisomeric Ratio.



When the enantiomeric ratio of seven *para*-substituted lactones were plotted against the functional group  $\sigma^+$  values, no correlation was observed ( $R^2 = 0.23$ ). Though this data does not provide a quantitative statement about the electronic effects, it does suggest that a carbocation is not involved in the enantiodetermining step of lactone formation. This is contrary to the work of Borhan, where they gathered evidence for a carbocation

intermediate in the chlorolactonization.<sup>119</sup> The lack of trend may also be due to other factors that are not considered, such as solubility of starting materials and products. However, we believe that for most cases, the catalyst is overriding the electronic effects of the aromatic ring for the enantiodetermining step (halogen delivery).

More interestingly, when the regioisomeric ratio was plotted against  $\sigma^+$  values, a linear free energy relationship for the points was evident. The more electron rich analog (*para*-methoxy **284g**) showed trace amounts of the *exo*-lactone by <sup>1</sup>H NMR while the *para*-bromo lactone **284k** delivered the highest amount of *exo*-lactone for the series. The negative  $\rho$ -value (slope) supports a carbocation-like intermediate in the course of the reaction, even more specifically, the regioidetermining step. This also contributes to the hypothesis that the *exo/endo*-selectivity is more dependent on the halogen source and electronics of the aromatic ring than lies under control of the catalyst.

Further mechanistic studies and catalyst optimization may reveal strategies to control the *endo/exo*-selectivity, as well as allow for enantiocontrol in the *exo*-lactone formation.

---

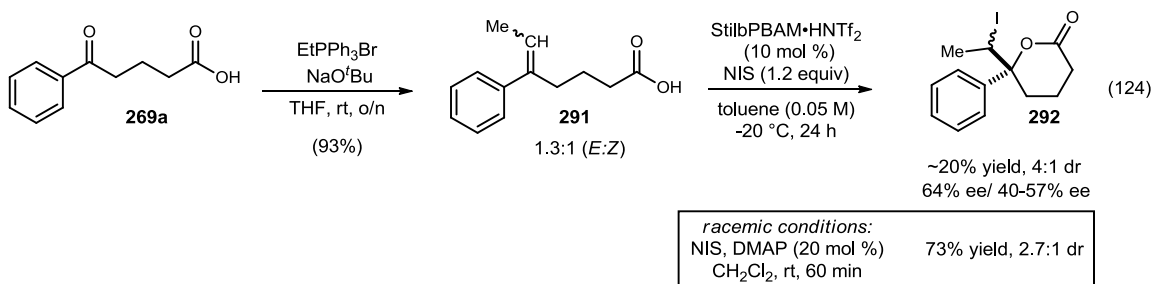
<sup>119</sup> Yousefi, S. R. Mechanistic Insights into the Origin of Enantioselectivity of the Organocatalytic Asymmetric Chlorolactonization. Ph.D. Thesis, Michigan State University, 2012.

## Future Work

### Tri- and Tetra-Substituted Olefinic Acids

Applying this methodology to tri- and tetra-substituted olefins has been briefly explored (Scheme 51).

**Scheme 51.** Initial Attempts to Study Tri-Substituted Olefinic Acids.



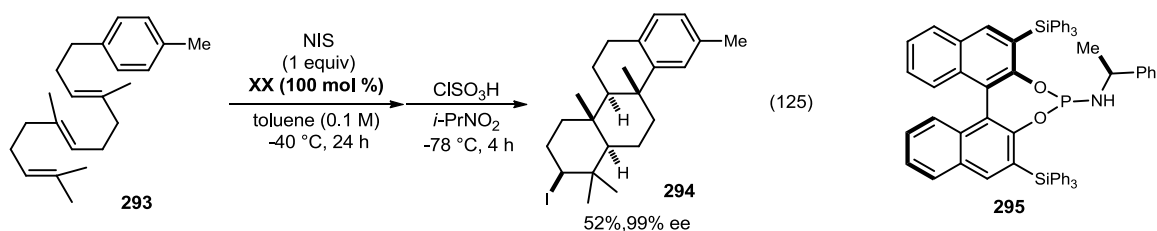
Unfortunately, the tetra-substituted olefin could not be synthesized from **269a** under a variety of Wittig conditions. The tri-substituted olefin (**291**) was synthesized in high yield but with low *E*:*Z* selectivity (~1.3:1). This mixture of olefins was then submitted to the reaction conditions to deliver iodolactone **292** in low yield (20% ee) and moderate ee (40-64% ee). Though selectivity was seen, it appears that one olefin undergoes a faster cyclization, as the starting material was isolated as an enriched mixture of olefins. A more reactive system may be able to deliver the adducts in higher yields while tuning the catalyst pocket could increase the enantioselection.

### Cascade Reactions

In 2007, Ishihara reported on the use of chiral non-racemic, nucleophilic phosphoramidites as promoters of enantioselective polycyclizations (Scheme 52).<sup>120</sup>

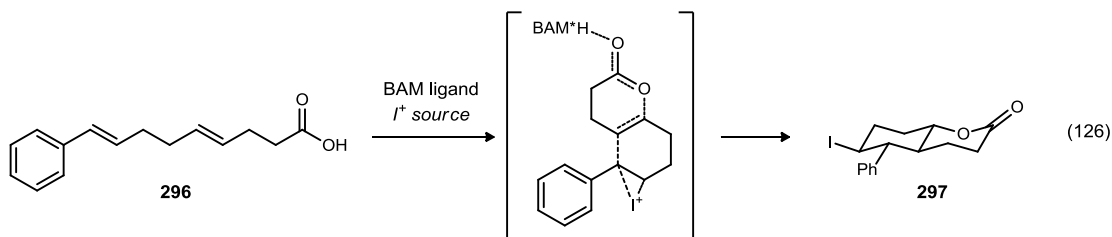
<sup>120</sup> Sakakura, A.; Ukai, A.; Ishihara, K. *Nature* **2007**, *445*, 900-903.

**Scheme 52.** Ishihara's Enantioselective Halocyclization of Polyprenoids.



They hypothesized that instead of activating the halogen source using a Lewis acid, they could activate NIS with a chiral nucleophile to give enantioselective delivery of a halogen (NBS performed poorly). When NIS was combined with a phosphoramidite of type **295** a number of polyenes were cyclized to the tricyclic compounds. The use of chlorosulfonic acid was used to ensure full completion at the final cyclization (between aromatic ring and final double bond). Perhaps one of the more impressive examples was accomplished with 4-(homofarnesyl)toluene (**293**), to give the tetracyclic compound (**294**) in 52% yield and 99% ee. Though elegant, one of the drawbacks is the use of 100 mol % of the chiral promoter. The use of substoichiometric catalyst (a chiral phosphonous acid) was demonstrated in the protocyclization of 2-geranylphenols using a chiral Lewis base assisted Brønsted acid catalyst system.<sup>121</sup>

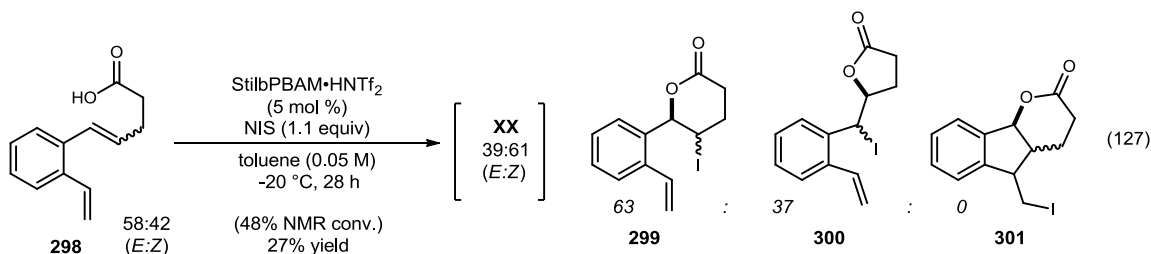
We envision that a cyclization may also be accomplished using our chiral proton catalyst–NIS reagent system by extending the olefinic acid by one unit.



<sup>121</sup> Sakakura, A.; Sakuma, M.; Ishihara, K. *Org. Lett.* **2011**, *13*, 3130-3133.

However, one of the immediate drawbacks of this approach is the synthesis of the starting di-olefinic acid **296**. While we were exploring this synthesis, we also looked at a simpler system, using an *ortho*-olefin styrene analog, knowing that similar olefins were previously activated by our BAM-NIS catalyst system (Scheme 53).

**Scheme 53.** Initial Attempts at a Cascade Reaction: Looking for Double Ring Closure.



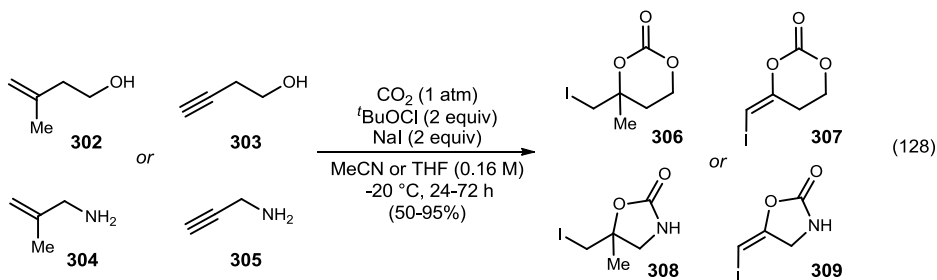
The starting olefin was made using a Wittig reaction from 2-formylstyrene. Unfortunately, it was isolated as 1.4:1 ratio of a mixture of olefins. Submitting acid **298** to the reaction conditions only produced the mono-cyclic ring products **299** and **300**. By analysis of the <sup>1</sup>H NMR, no bis-closure (**301**) was seen. Other factors may have contributed to the lack of cascade, but further efforts to make **297** may reveal that it is a suitable substrate for this system.

### *Enantioselective capture of carbon dioxide*

Realization that the carboxylic acid functionality is crucial for enantioselectivity, we sought to extend it to carbonic acids. A quick literature search confirmed that as starting materials, these are not easily isolated due to stability concerns. We envisioned

forming the carbonate *in situ* with an alcohol and carbon dioxide. Fortunately, this has been previously demonstrated (Scheme 54).<sup>122</sup>

**Scheme 54.** Carbon Dioxide Capture Using Alcohols and Amines.

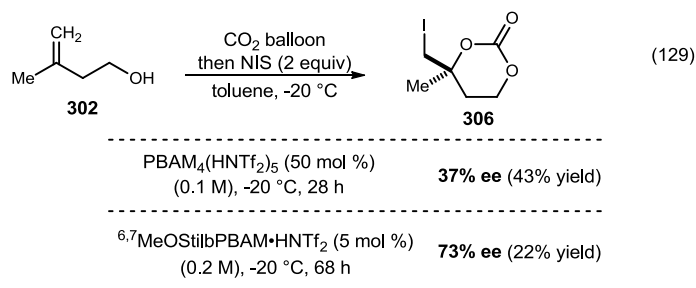


Minakata has reported on the trapping of olefinic and propargylic alcohols and amines by forming  $t\text{BuOI}$  *in situ* (from  $\text{NaI}$  and  $t\text{BuOCl}$ ) under relatively neutral reaction conditions. They acknowledge that the equilibrium for carbon dioxide trapping heavily favors the starting materials, but iodination of the carbonic acid intermediate changes the equilibrium to favor the products. High yields and conversions were reported for most substrates while other iodine reagents ( $\text{IPy}_2\text{BF}_4$ ,  $\text{NIS}$ ,  $\text{I}_2$ , etc.) did not provide the desired product.

No enantioselective variant of the above reaction has been reported, so we sought to carry out a similar reaction using our chiral proton catalyst-NIS reagent system (Scheme 55).

<sup>122</sup> Minakata, S.; Sasaki, I.; Ide, T. *Angew. Chem. Int. Ed.* **2010**, *49*, 1309-1311. Takeda, Y.; Okumura, S.; Tone, S.; Sasaki, I.; Minakata, S. *Org. Lett.* **2012**, *14*, 4874-4877.

**Scheme 55.** Preliminary Results for the Enantioselective Iodocarboxylation of Homoallylic Alcohols.



Combining 3-methyl-butene-1-ol (**302**) in toluene with (PBAM)<sub>4</sub>(HNTf<sub>2</sub>)<sub>5</sub> under an atmosphere of carbon dioxide, the desired adduct was isolated in 37% ee and 43% yield. Further reaction optimization was completed with a visiting undergraduate researcher from Kalamazoo College.<sup>123</sup> A number of experiments looking at conversion, yield and enantioselectivity were completed. One of the most promising results came when <sup>6,7</sup>MeOStilbPBAM•HNTf<sub>2</sub> (5 mol %) was used in the reaction, delivering product in moderate enantiomeric excess (73% ee) but low yield (22%). Additionally, the observed yield and conversion were variable between reactions; it was hypothesized that one contributing factor is the timing of the introduction of CO<sub>2</sub>. Though more reaction optimization needs to be completed (to increase yields and enantioselection), this work serves as a framework to build the methodology.

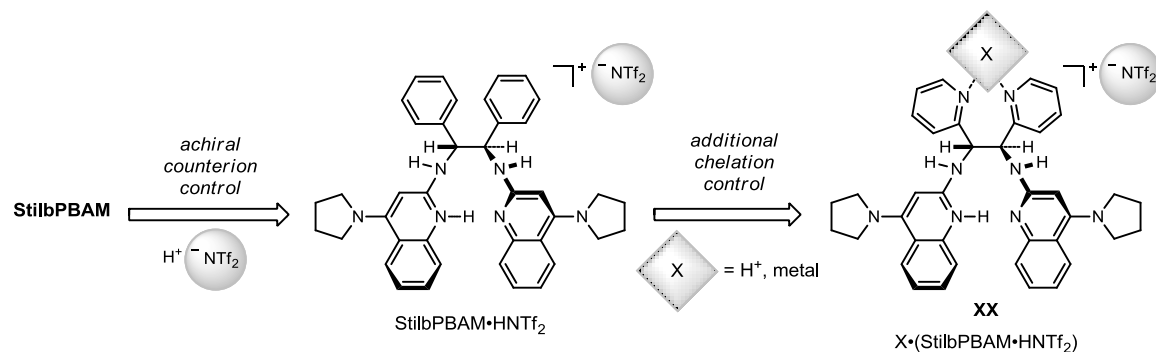
#### *Additional modes of catalyst binding*

The observed effect of the enantiocontrol imparted by the achiral counterion is in fact very interesting. However, the influence of a relatively dissociated achiral counterion in a transition state is reason to explore modifications outside of the chiral pocket (Figure 31).

<sup>123</sup> Dobish, M. C.; Wang, W.; Johnston, J. N. *unpublished results*.



**Figure 31.** Catalyst Modification Leading to Additional Chelation Control in Diamine Backbone.



We envision making the stilbene derived catalyst from the commercially available bis-pyridine stilbene diamine (2- or 3-substituted). The addition of additives which differ in sterics and electronics while chelating with the pyridine rings can in turn modify the catalyst pocket. This approach may lead to a more selective system in other transformations where the size and electronics of the chiral pocket need to be tuned.

## CHAPTER IV

### IV. EXPERIMENTALS

Glassware was flame-dried under vacuum for all non-aqueous reactions. All reagents and solvents were commercial grade and purified prior to use when necessary. Tetrahydrofuran (THF), dichloromethane (CH<sub>2</sub>Cl<sub>2</sub>) and toluene was dried by passage through a column of activated alumina as described by Grubbs.<sup>124</sup> This was done to accurately quantitate the amount of water in each reaction. All organic layers collected from extractions were dried over MgSO<sub>4</sub> unless otherwise indicated.

Thin layer chromatography (TLC) was performed using glass-backed silica gel (250 μm) plates and flash chromatography utilized 230–400 mesh silica gel from Sorbent Technologies. UV light, and/or the use of potassium iodoplatinate and potassium permanganate solutions were used to visualize products.

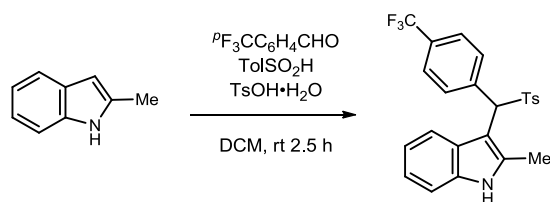
IR spectra were recorded on a Nicolet Avatar 360 spectrophotometer and are reported in wavenumbers (cm<sup>-1</sup>). All compounds were analyzed as neat films on a NaCl plate (transmission). Nuclear magnetic resonance spectra (NMR) were acquired on a Bruker DRX-500 (500 MHz), Bruker AV-400 (400 MHz) or Bruker AV II-600 (600 MHz) instrument. Chemical shifts are measured relative to residual solvent peaks as an internal

---

<sup>124</sup> Pangborn, A. B.; Giardello, M. A.; Grubbs, R. H.; Rosen, R. K.; Timmers, F. J. *Organometallics* **1996**, *15*, 1518-1520.

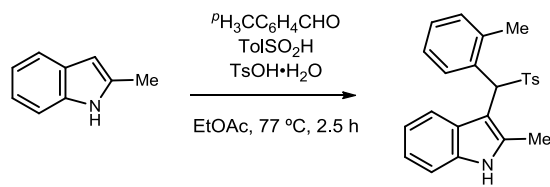
standard set to  $\delta$  7.26 and  $\delta$  77.0 for  $\text{CDCl}_3$  and  $\delta$  2.50 and  $\delta$  39.5 for  $d_6$ -DMSO. Mass spectra were recorded on a Thermo Electron Corporation MAT 95XP-Trap mass spectrometer by use of chemical ionization (CI), electron impact ionization (EI) or electrospray ionization (ESI) by the Indiana University Mass Spectrometry Facility. A post-acquisition gain correction was applied using sodium formate or sodium iodide as the lock mass. Optical rotations were measured on a Perkin Elmer-341 polarimeter. Chiral HPLC analysis was conducted on an Agilent 1100 series instrument using the designated ChiralPak column.

**General Procedure for Arylsulfonylalkyl Indoles:**<sup>125</sup> 2-Methylindole (0.42 g, 3.2 mmol), toluenesulfinic acid (0.56 g, 3.6 mmol) and toluenesulfonic acid monohydrate (0.29 g, 1.5 mmol) were combined in a round-bottomed flask and suspended in ethyl acetate or CH<sub>2</sub>Cl<sub>2</sub> (10 mL). The aldehyde (3.0 mmol) was added and the pot stirred for 2.5 h. The reaction was quenched with satd aq NaHCO<sub>3</sub> (7 mL), extracted with solvent, dried (Na<sub>2</sub>SO<sub>4</sub>) and passed through a plug of decolorizing carbon and Celite. Concentration provided crude material that could be purified by flash column chromatography.

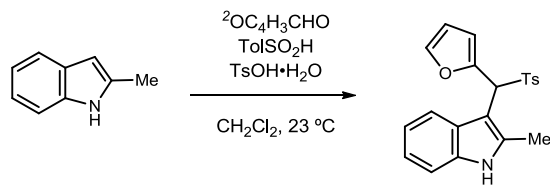


**2-Methyl-3-(tosyl(4-(trifluoromethyl)phenyl)methyl)-1H-indole (133d).** 2-Me-indole (420 mg, 3.20 mmol) and *para*-(trifluoromethyl)benzaldehyde (522 mg, 3.00 mmol) were combined in CH<sub>2</sub>Cl<sub>2</sub> according to the general procedure. Precipitation from CH<sub>2</sub>Cl<sub>2</sub> with hexanes yielded a yellow solid (1.2 g, 95%). IR (film) 3372, 2918, 1618 cm<sup>-1</sup>; <sup>1</sup>H NMR (400 MHz, CDCl<sub>3</sub>) δ 7.98 (br s, 1H), 7.92 (d, *J* = 8.3 Hz, 2H), 7.32 (d, *J* = 7.9 Hz, 1H), 7.59 (d, *J* = 8.3 Hz, 2H), 7.41 (d, *J* = 8.3 Hz, 2H), 7.22 (d, *J* = 7.8 Hz, 1H), 7.15-7.09 (m, 2H), 7.06 (d, *J* = 8.1 Hz, 2H), 5.66 (s, 1H), 2.33 (s, 3H), 2.02 (s, 3H); <sup>13</sup>C NMR (100 MHz, CDCl<sub>3</sub>) ppm 144.4, 137.2, 135.6, 135.5, 135.0, 130.3, 129.1, 128.6, 126.9, 125.3, 125.3, 121.8, 120.9, 120.3, 110.4, 103.7, 69.0, 21.5, 11.9; HRMS (ESI): Exact mass calcd for C<sub>24</sub>H<sub>21</sub>F<sub>3</sub>NO<sub>2</sub>S [M+H]<sup>+</sup> 444.1245, found 444.1256.

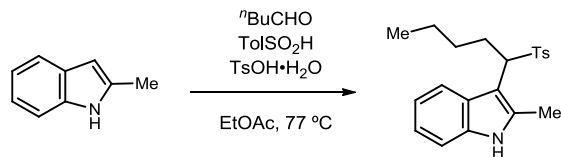
<sup>125</sup> Adapted from: Palmieri, A.; Petrinì, M. *J. Org. Chem.* **2007**, *72*, 1863-1866.



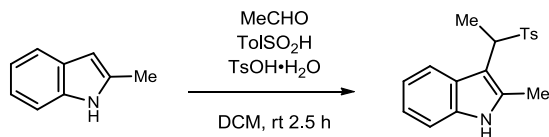
**2-Methyl-3-(*o*-tolyl(tosyl)methyl)-1H-indole (133e).** 2-Me-indole (420 mg, 3.20 mmol) and *ortho*-tolualdehyde (360 mg, 3.00 mmol) were combined in ethyl acetate and refluxed for 2.5 h according to the general procedure. Flash column chromatography (SiO<sub>2</sub>, 10-33% ethyl acetate in hexanes) yielded a tan solid (790 mg, 68%).  $R_f = 0.2$  (20% EtOAc/hexanes); IR (film) 3341, 3055, 1460 cm<sup>-1</sup>; <sup>1</sup>H NMR (400 MHz, CDCl<sub>3</sub>)  $\delta$  8.54 (d,  $J = 7.7$  Hz, 1H), 7.85 (br s, 1H), 7.61 (d,  $J = 7.9$  Hz, 1H), 7.48 (d,  $J = 8.2$  Hz, 2H), 7.35-7.29 (m, 1H), 7.21-7.17 (m, 2H), 7.10 (d,  $J = 8.0$  Hz, 2H), 7.09-7.04 (m, 2H), 7.00-6.99 (m, 1H), 5.67 (s, 1H), 2.35 (s, 3H), 2.07 (s, 3H), 2.06 (s, 3H); <sup>13</sup>C NMR (100 MHz, CDCl<sub>3</sub>) ppm 144.2, 136.8, 136.1, 135.5, 134.8, 132.2, 130.9, 129.2, 129.2, 128.9, 127.9, 127.7, 125.9, 121.3, 120.0, 119.8, 110.2, 103.4, 65.9, 21.5, 19.7, 12.1; HRMS (ESI): Exact mass calcd for C<sub>24</sub>H<sub>23</sub>NNaO<sub>2</sub>S [M+Na]<sup>+</sup> 412.1347, found 412.1356.



**3-(Furan-2-yl(tosyl)methyl)-2-methyl-1H-indole (133f).** 2-Me-indole (420 mg, 3.20 mmol) and 2-furaldehyde (288 mg, 3.00 mmol) were combined in CH<sub>2</sub>Cl<sub>2</sub> according to the general procedure. The tan solid was used without further purification (930 mg, 85%). IR (film) 3366, 1595 cm<sup>-1</sup>; <sup>1</sup>H NMR (600 MHz, CDCl<sub>3</sub>) δ 8.03 (s, 1H), 7.69 (d, *J* = 8.0 Hz, 1H), 7.44-7.43 (m, 3H), 7.22 (d, *J* = 8.0 Hz, 1H), 7.12-7.10 (m, 3H), 7.05 (dd, *J* = 8.0, 8.0 Hz, 1H), 6.67 (d, *J* = 3.4 Hz, 1H), 6.38 (dd, *J* = 3.2, 1.8, 1H), 5.67 (s, 1H), 2.35 (s, 3H), 2.12 (s, 3H); <sup>13</sup>C NMR (150 MHz, CDCl<sub>3</sub>) ppm 146.1, 144.3, 143.0, 135.8, 135.3, 135.0, 129.1, 128.9, 127.1, 121.6, 121.0, 120.0, 111.9, 110.8, 110.2, 102.0, 64.5, 21.6, 11.9; HRMS (CI): Exact mass calcd for C<sub>21</sub>H<sub>18</sub>NO<sub>3</sub>S [M-H]<sup>-</sup> 366.1002, found 366.1019.

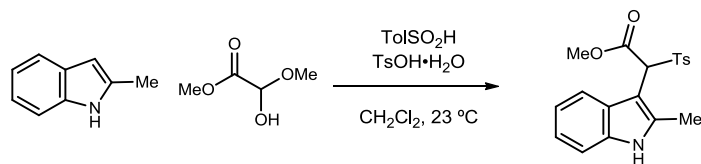


**2-Methyl-3-(1-tosylpentyl)-1H-indole (133g).** 2-Me-indole (420 mg, 3.20 mmol) and valeraldehyde (258 mg, 3.00 mmol) were combined in ethyl acetate and refluxed according to the general procedure. Flash column chromatography (SiO<sub>2</sub>, 10-30% ethyl acetate in hexanes) yielded a tan solid (700 mg, 62%).  $R_f = 0.3$  (20% EtOAc/hexanes); IR (film) 3352, 2958, 1461 cm<sup>-1</sup>; <sup>1</sup>H NMR (400 MHz, CDCl<sub>3</sub>)  $\delta$  7.92 (br s, 1H), 7.63 (d,  $J = 7.5$  Hz, 1H), 7.37 (d,  $J = 7.6$  Hz, 2H), 7.23 (d,  $J = 7.7$  Hz, 1H), 7.10-7.03 (m, 4H), 4.20 (d,  $J = 8.0$  Hz, 1H), 2.56-2.45 (m, 2H), 2.38 (s, 3H), 1.87 (s, 3H), 1.34-1.17 (m, 4H), 0.80 (t,  $J = 7.0$  Hz, 3H); <sup>13</sup>C NMR (100 MHz, CDCl<sub>3</sub>) ppm 143.9, 135.8, 135.1, 129.1, 128.9, 121.3, 120.7, 119.9, 110.3, 103.0, 65.6, 29.3, 25.4, 22.3, 21.5, 13.8, 11.2; HRMS (CI): Exact mass calcd for C<sub>21</sub>H<sub>25</sub>NNaO<sub>2</sub>S [M+Na]<sup>+</sup> 378.1504, found 378.1516.

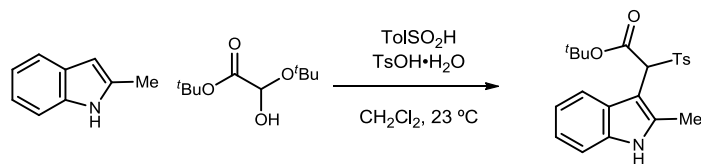


**2-methyl-3-(1-tosylethyl)-1H-indole (133h).** See general procedure for aryl-indoles. Trituration from DCM with hexanes yielded a yellow solid (200 mg, 22%); IR (film) 3348, 3054, 2917, 2849, 1596 cm<sup>-1</sup>; <sup>1</sup>H NMR (400 MHz, DMSO) δ 10.96 (br s, 1H), 7.54 (d, *J* = 7.7 Hz, 1H), 7.44 (d, *J* = 8.0 Hz, 2H), 7.28 (d, *J* = 8.0 Hz, 2H), 7.23 (d, *J* = 7.9 Hz, 1H), 6.99 (dd, *J* = 7.2, 7.7 Hz, 1H), 6.91 (dd, *J* = 7.5, 7.3 Hz, 1H), 4.67 (q, *J* = 7.0 Hz, 1H), 2.34 (s, 3H), 1.95 (s, 3H), 1.77 (d, *J* = 7.2 Hz, 3H); <sup>13</sup>C NMR (100 MHz, DMSO) 143.8, 136.0, 135.2, 135.1, 129.3, 128.4, 120.2, 119.8, 118.6, 112.8, 110.6, 102.8, 58.4, 54.9, 21.0, 13.0, 11.2 ppm; HRMS (ESI): Exact mass calcd for C<sub>18</sub>H<sub>19</sub>NO<sub>2</sub>S [M+Na]<sup>+</sup> 336.1034, found 336.1041.

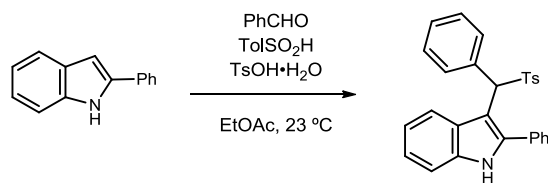




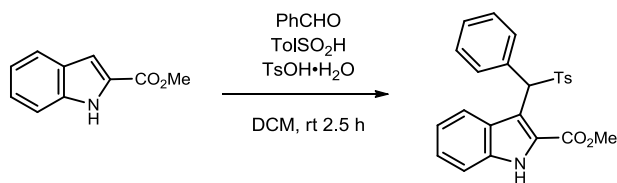
**Methyl 2-(2-methyl-1H-indol-3-yl)-2-tosylacetate (133i).** 2-Me-indole (420 mg, 3.20 mmol) and methyl 2-hydroxy-2-methoxyacetate (360 mg, 3.00 mmol) were combined in CH<sub>2</sub>Cl<sub>2</sub> according to the general procedure. Flash column chromatography (SiO<sub>2</sub>, 10-50% ethyl acetate in hexanes) yielded an off-white solid (850 mg, 80%).  $R_f = 0.3$  (50% EtOAc/hexanes); IR (film) 3385, 2953, 1743 cm<sup>-1</sup>; <sup>1</sup>H NMR (400 MHz, CDCl<sub>3</sub>)  $\delta$  8.29 (br s, 1H), 7.53 (d,  $J = 8.2$  Hz, 2H), 7.39 (d,  $J = 8.1$  Hz, 1H), 7.21 (d,  $J = 8.1$  Hz, 1H), 7.12 (d,  $J = 8.1$  Hz, 2H), 7.08-7.05 (m, 1H), 6.97-6.93 (m, 1H), 5.30 (s, 1H), 3.74 (s, 3H), 2.36 (s, 3H), 2.14 (s, 3H); <sup>13</sup>C NMR (100 MHz, CDCl<sub>3</sub>) ppm 165.9, 144.9, 136.9, 134.8, 134.4, 129.7, 129.2, 126.9, 121.6, 120.2, 119.6, 110.4, 99.0, 68.6, 52.9, 21.6, 11.7; HRMS (ESI): Exact mass calcd for C<sub>19</sub>H<sub>19</sub>KNO<sub>4</sub>S [M+K]<sup>+</sup> 396.0672, found 396.0678.



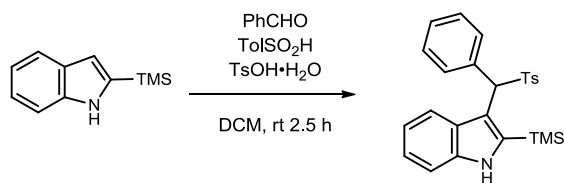
***tert*-Butyl 2-(2-methyl-1H-indol-3-yl)-2-tosylacetate (133j).** 2-Me-indole (420 mg, 3.20 mmol) and *tert*-butyl 2-oxoacetate (390 mg, 3.00 mmol) were combined in  $\text{CH}_2\text{Cl}_2$  according to the general procedure. Flash column chromatography ( $\text{SiO}_2$ , 20% ethyl acetate in hexanes) yielded a colorless solid (390 mg, 33%).  $R_f = 0.2$  (33% EtOAc/hexanes); IR (film) 3379, 2978, 1734  $\text{cm}^{-1}$ ;  $^1\text{H}$  NMR (400 MHz,  $\text{CDCl}_3$ )  $\delta$  8.04 (br s, 1H), 7.53 (d,  $J = 8.2$  Hz, 2H), 7.49 (d,  $J = 8.1$  Hz, 1H), 7.22 (d,  $J = 8.2$  Hz, 1H), 7.13 (d,  $J = 8.1$  Hz, 2H), 7.09-7.06 (m, 1H), 6.98-6.94 (m, 1H), 5.20 (s, 1H), 2.36 (s, 3H), 2.21 (s, 3H), 1.45 (s, 9H);  $^{13}\text{C}$  NMR (100 MHz,  $\text{CDCl}_3$ ) ppm 164.3, 144.6, 136.9, 134.9, 134.9, 129.5, 129.1, 121.3, 120.0, 119.8, 110.4, 99.1, 83.6, 69.9, 27.8, 21.5, 11.7; HRMS (ESI): Exact mass calcd for  $\text{C}_{22}\text{H}_{26}\text{NO}_4\text{S}$   $[\text{M}+\text{H}]^+$  400.1583, found 400.1574.



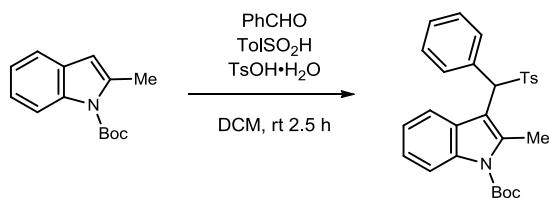
**2-Phenyl-3-(phenyl(tosyl)methyl)-1H-indole (133I).** 2-Phenyl-indole (618 mg, 3.20 mmol) and benzaldehyde (318 mg, 3.00 mmol) were combined in ethyl acetate according to the general procedure. The solid that precipitated before workup was washed with ethyl acetate to provide the desired product as a brown solid (690 mg, 53%). IR (film) 3338, 3058, 1494  $\text{cm}^{-1}$ ;  $^1\text{H}$  NMR (400 MHz,  $\text{CDCl}_3$ )  $\delta$  8.27-8.26 (m, 1H), 8.10 (s, 1H), 7.80 (dd,  $J = 7.3, 1.8$ , 2H), 7.40-7.30 (m, 7H), 7.25-7.22 (m, 2H), 7.19 (d,  $J = 8.2$  Hz, 2H), 7.00-6.98 (m, 2H), 6.95 (d,  $J = 8.0$  Hz, 2H), 5.79 (s, 1H), 2.33 (s, 3H);  $^{13}\text{C}$  NMR (100 MHz,  $\text{CDCl}_3$ ) ppm 143.7, 139.4, 135.9, 133.0, 131.3, 130.2, 128.9, 128.8, 128.7, 128.5, 128.4, 128.3, 126.9, 123.6, 122.7, 120.7, 110.8, 105.2, 70.0, 21.5; HRMS (CI): Exact mass calcd for  $\text{C}_{28}\text{H}_{24}\text{NO}_2\text{S}$   $[\text{M}+\text{H}]^+$  438.1522, found 438.1501.



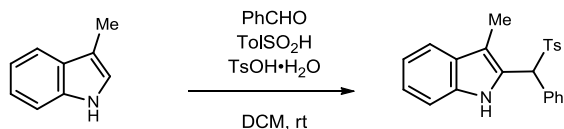
**methyl 3-(phenyl(tosyl)methyl)-1H-indole-2-carboxylate (133m).** See general procedure for aryl-indoles. Flash column chromatography (SiO<sub>2</sub>, 20% ethyl acetate in hexanes) yielded a white solid (330 mg, 27%);  $R_f = 0.21$  (33% EtOAc/hexanes); IR (film) 3337, 2360, 2341, 1706  $\text{cm}^{-1}$ ; <sup>1</sup>H NMR (400 MHz, CDCl<sub>3</sub>) d 9.00 (br s, 1H), 8.43 (d,  $J = 8.3$  Hz, 1H), 7.69-7.66 (m, 2H), 7.51 (d,  $J = 8.2$  Hz, 2H), 7.36-7.21 (m, 6H), 7.15 (s, 1H), 7.12 (d,  $J = 8.1$  Hz, 2H), 3.76 (s, 3H), 2.35 (s, 3H); <sup>13</sup>C NMR (100 MHz, CDCl<sub>3</sub>) 161.3, 144.2, 135.8, 135.8, 133.1, 130.1, 129.0, 128.7, 128.4, 128.2, 126.2, 125.9, 125.0, 124.8, 121.5, 115.6, 111.9, 67.0, 51.8, 21.6 ppm; HRMS (ESI): Exact mass calcd for C<sub>24</sub>H<sub>21</sub>NO<sub>4</sub>S [M+Na]<sup>+</sup> 442.1089, found 442.1089.



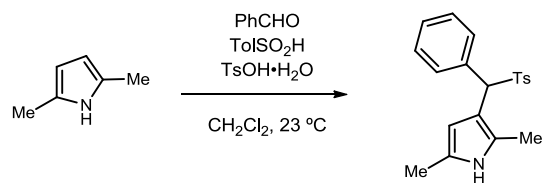
**3-(phenyl(tosyl)methyl)-2-(trimethylsilyl)-1H-indole (133n).** See general procedure for aryl-indoles. Flash column chromatography (SiO<sub>2</sub>, 5-10-15% ethyl acetate in hexanes) and a crystallization yielded a white crystalline solid (50 mg, 8%);  $R_f = 0.37$  (20% EtOAc/hexanes); IR (film) 3381, 3063, 2954, 1597, 1494 cm<sup>-1</sup>; <sup>1</sup>H NMR (400 MHz, CDCl<sub>3</sub>) δ 8.47-8.44 (m, 1H), 8.06 (br s, 1H), 7.67-7.65 (m, 2H), 7.44 (d,  $J = 8.2$  Hz, 2H), 7.36-7.34 (m, 1H), 7.30-7.22 (m, 5H), 7.08 (d,  $J = 8.1$  Hz, 2H), 5.73 (s, 1H), 2.33 (s, 3H), 0.21 (s, 9H); <sup>13</sup>C NMR (100 MHz, CDCl<sub>3</sub>) 144.1, 138.7, 138.2, 135.9, 133.4, 130.4, 129.2, 129.0, 128.3, 128.3, 127.3, 123.7, 122.8, 120.5, 116.7, 110.9, 73.0, 21.5, -0.67 ppm; HRMS (ESI): Exact mass calcd for C<sub>25</sub>H<sub>27</sub>NO<sub>2</sub>SSi [M+K]<sup>+</sup> 472.1169, found 472.1149.



***tert*-butyl 2-methyl-3-(phenyl(tosyl)methyl)-1*H*-indole-1-carboxylate (133o).** See general procedure for aryl-indoles. Flash column chromatography (SiO<sub>2</sub>, 10-20% ethyl acetate in hexanes) yielded an orange solid (323 mg, 20%);  $R_f = 0.27$  (20% EtOAc/hexanes); IR (film) 2979, 2933, 1733, 1458 cm<sup>-1</sup>; <sup>1</sup>H NMR (400 MHz, CDCl<sub>3</sub>) δ 8.06 (d,  $J = 8.3$  Hz, 1H), 7.77 (d,  $J = 7.9$  Hz, 1H), 7.70 (dd,  $J = 7.9, 2.2$  Hz, 2H), 7.47 (d,  $J = 8.2$  Hz, 2H), 7.34-7.31 (m, 3H), 7.25-7.22 (m, 1H), 7.17 (d,  $J = 7.43$  Hz, 1H), 7.14-7.11 (m, 2H), 5.75 (s, 1H), 2.36 (s, 3H), 2.25 (s, 3H), 1.65 (s, 9H); <sup>13</sup>C NMR (100 MHz, CDCl<sub>3</sub>) 150.1, 144.4, 137.7, 135.8, 135.7, 132.6, 129.5, 129.2, 128.7, 128.5, 128.2, 127.7, 123.7, 122.7, 121.4, 114.9, 111.4, 84.3, 68.8, 28.2, 21.5, 13.9 ppm; HRMS (ESI): Exact mass calcd for C<sub>28</sub>H<sub>29</sub>NO<sub>4</sub>S [M+Na]<sup>+</sup> 498.1715, found 498.1723.

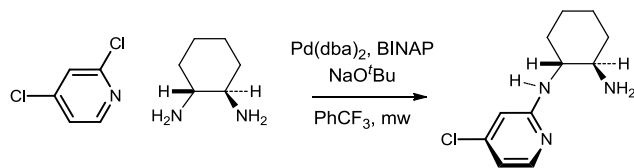


**3-methyl-2-(phenyl(tosyl)methyl)-1H-indole (133p).** 3-Methylindole (420 mg, 3.2 mmol), toluenesulfonic acid (560 mg, 3.6 mmol), toluenesulfonic acid monhydrate (290 mg, 1.5 mmol) were combined in a round bottom flask and suspended in dichloromethane (10 mL). The benzaldehyde (320 mg, 3.0 mmol) was added and the pot was stirred for 4 h. The reaction was quenched with sat aq NaHCO<sub>3</sub> (7 mL), extracted with dichloromethane, dried over Na<sub>2</sub>SO<sub>4</sub> and passed through a plug of decolourising carbon and Celite to give a brown solid. Flash column chromatography (SiO<sub>2</sub>, 10-20% ethyl acetate in hexanes) yielded a gray solid (230 mg, 21%); *R<sub>f</sub>* = 0.3 (16% EtOAc/hexanes); IR (film) 3395, 3060, 2919, 1597, 1494, 1455 cm<sup>-1</sup>; <sup>1</sup>H NMR (400 MHz, CDCl<sub>3</sub>) δ 9.15 (s, 1H), 7.59 (dd, *J* = 7.3, 3.5 Hz, 2H), 7.53 (d, *J* = 8.2, 2H), 7.44 (dd, *J* = 7.8, 2.1 Hz, 2H), 7.36-7.35 (m, 3H), 7.23 (t, *J* = 7.8 Hz, 1H), 7.14 (d, *J* = 8.1 Hz, 2H), 7.10 (t, *J* = 7.8 Hz, 1H), 5.61 (s, 1H), 2.36 (s, 3H), 2.95 (s, 3H); <sup>13</sup>C NMR (100 MHz, CDCl<sub>3</sub>) 144.9, 136.2, 134.9, 131.7, 129.8, 129.5, 128.8, 128.4, 127.9, 124.9, 122.8, 119.4, 118.9, 112.6, 111.3, 67.9, 21.6, 8.1 ppm; HRMS (ESI): Exact mass calcd for C<sub>23</sub>H<sub>21</sub>NO<sub>2</sub>SK [M+K]<sup>+</sup> 414.0930, found 414.0931.

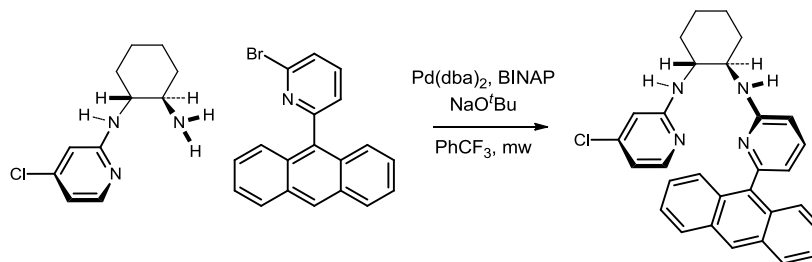


**2,5-Dimethyl-3-(phenyl(tosyl)methyl)-1H-pyrrole (133q).** 2,5-Dimethylpyrrole (304 mg, 3.20 mmol) and benzaldehyde (318 mg, 3.00 mmol) were combined in  $\text{CH}_2\text{Cl}_2$  according to the general procedure. Flash column chromatography ( $\text{SiO}_2$ , 20-33% ethyl acetate in hexanes) yielded a tan solid (300 mg, 30%).  $R_f = 0.2$  (20% EtOAc/hexanes); IR (film) 3368, 2923, 1597  $\text{cm}^{-1}$ ;  $^1\text{H}$  NMR (400 MHz,  $\text{CDCl}_3$ )  $\delta$  7.66 (br s, 1H), 7.56-7.53 (m, 2H), 7.48 (d,  $J = 8.2$ , 2H), 7.31-7.27 (m, 3H), 7.14 (d,  $J = 8.1$  Hz, 2H), 6.26 (d,  $J = 2.0$  Hz, 1H), 5.10 (s, 1H), 2.37 (s, 3H), 2.20 (s, 3H), 1.89 (s, 3H);  $^{13}\text{C}$  NMR (100 MHz,  $\text{CDCl}_3$ ) ppm 143.8, 135.6, 134.1, 130.0, 129.0, 128.9, 128.4, 128.1, 126.0, 125.9, 110.2, 106.6, 69.7, 21.5, 12.9, 10.6; HRMS (ESI): Exact mass calcd for  $\text{C}_{20}\text{H}_{21}\text{KNO}_2\text{S}$   $[\text{M}+\text{K}]^+$  378.0930, found 378.0937.

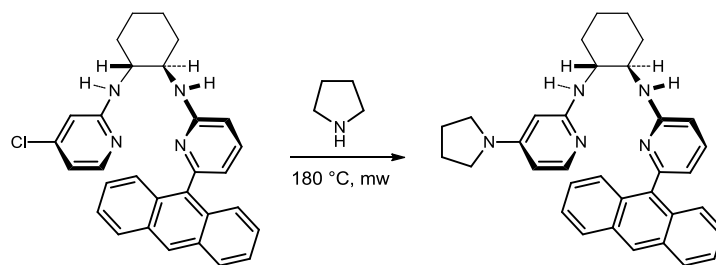




**(1R,2R)-N<sup>1</sup>-(4-chloropyridin-2-yl)cyclohexane-1,2-diamine (108SI).** A flame dried microwave vessel (10-20 mL) was charged with Pd(dba)<sub>2</sub> (58 mg, 0.10 mmol), *rac*-BINAP (125 mg, 0.200 mmol) and NaO<sup>t</sup>Bu (1.44 g, 15.0 mmol) in a glove box. To the vessel was added cyclohexyl diamine (1.98 g, 10.0 mmol), 2,4-chloropyridine (740 mg, 5.00 mmol) and PhCF<sub>3</sub> (10 mL), followed by heating in a Biotage Initiator at 70 °C for 30 min. The reaction was filtered through Celite and concentrated to afford a crude brown oil. Flash column chromatography (SiO<sub>2</sub>, 3-10-25% MeOH in DCM) yielded a tan solid (0.66 g, 58%); R<sub>f</sub> = 0.18 (10% MeOH/DCM); IR (film) 3258 (br), 2931, 2857, 1593, 1513, 1480 cm<sup>-1</sup>; <sup>1</sup>H NMR (400 MHz, CDCl<sub>3</sub>) d 7.92 (d, *J* = 5.5 Hz, 1H), 6.54 (dd, *J* = 5.5, 1.7 Hz, 1H), 6.46 (d, *J* = 1.5 Hz, 1H), 4.60 (d, *J* = 8.8 Hz, 1H), 3.38-3.29 (m, 1H), 2.55 (ddd, *J* = 10.1, 10.1, 4.1 Hz, 1H), 2.09-1.97 (m, 4H), 1.75-1.73 (m, 2H), 1.41-1.12 (m, 4H); <sup>13</sup>C NMR (100 MHz, CDCl<sub>3</sub>) ppm 160.0, 149.1, 144.9, 116.5, 107.0, 58.3, 56.1, 35.0, 32.7, 25.3, 25.0; HRMS (ESI): Exact mass calcd for C<sub>11</sub>H<sub>17</sub>ClN<sub>3</sub> [M+H]<sup>+</sup>, 226.1111, found 226.1107.

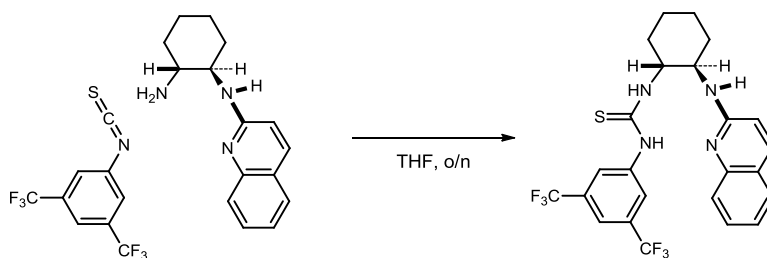


**(1R,2R)-N<sup>1</sup>-(6-(anthracen-9-yl)pyridin-2-yl)-N<sup>2</sup>-(4-chloropyridin-2-yl)cyclohexane-1,2-diamine (<sup>4</sup>Cl-108).** A flame dried microwave vessel (2-5 mL) was charged with Pd(dba)<sub>2</sub> (5 mg, 0.009 mmol), *rac*-BINAP (10 mg, 0.016 mmol) and NaOtBu (29 mg, 0.30 mmol) in a glove box. To the vessel was added mono-protected diamine (45 mg, 0.20 mmol), 2-(anthracenyl)-6-bromopyridine (66 mg, 0.20 mmol) and PhCF<sub>3</sub> (1.5 mL), followed by heating in a Biotage Initiator at 80 °C for 40 min, 100 °C for 15 min, 120 °C for 30 min and 140 °C for 30 min (to be optimized at a later time). The reaction was filtered through Celite/Silica and concentrated to afford a crude brown oil. Flash column chromatography (SiO<sub>2</sub>, 10-20% EtOAc in Hexanes) yielded a yellow solid (79 mg, 83%); R<sub>f</sub> = 0.39 (20% EtOAc in Hexanes); IR (film) 3051, 2930, 2855, 1592, 1500, 1454 cm<sup>-1</sup>; <sup>1</sup>H NMR (400 MHz, CDCl<sub>3</sub>) δ 8.53 (s, 1H), 8.08-8.05 (m, 2H), 7.86 (d, *J* = 5.5 Hz, 1H), 7.79 (d, *J* = 8.4 Hz, 1H), 7.74 (d, *J* = 8.8 Hz, 1H), 7.55-7.45 (m, 4H), 7.39 (m, 1H), 6.73 (d, *J* = 6.9 Hz, 1H), 6.44 (d, *J* = 8.3 Hz, 1H), 6.38 (dd, *J* = 5.5, 1.7 Hz, 1H), 5.86 (d, *J* = 1.4 Hz, 1H), 5.64 (d, *J* = 6.5 Hz, 1H), 4.67 (d, *J* = 7.5 Hz, 1H), 3.88-3.80 (m, 1H), 3.71-3.63 (m, 1H), 2.20-2.16 (m, 2H), 1.78-1.65 (m, 2H), 1.46-1.27 (m, 5H), 1.12-1.02 (m, 1H); <sup>13</sup>C NMR (100 MHz, CDCl<sub>3</sub>) ppm 159.1, 158.7, 155.8, 148.5, 143.7, 137.2, 136.2, 131.4, 129.9, 129.8, 128.4, 128.3, 127.0, 127.7, 126.3, 126.1, 125.3, 125.3, 125.0, 115.7, 112.2, 107.9, 106.9, 57.2, 54.3, 33.2, 32.1, 24.9, 24.4; HRMS (ESI): Exact mass calcd for C<sub>30</sub>H<sub>28</sub>ClN<sub>4</sub> [M+H]<sup>+</sup> 479.2002, found 479.1993.



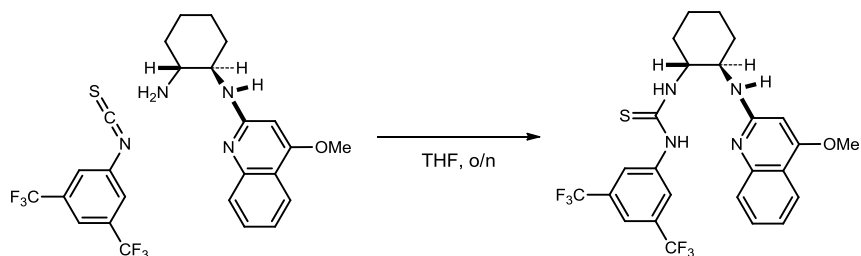
**(1*R*,2*R*)-*N*<sup>1</sup>-(6-(anthracen-9-yl)pyridin-2-yl)-*N*<sup>2</sup>-(4-(pyrrolidin-1-yl)pyridin-2-yl)cyclohexane-1,2-diamine (108).** A solution of catalyst (192 mg, 0.400 mmol) and

pyrrolidine (0.8 mL, 8 mmol) in a microwave vessel was heated in a Biotage Initiator at 180 °C for 2 h, diluted with DCM, and washed with sat aq Na<sub>2</sub>CO<sub>3</sub>, water and Brine. Flash column chromatography (SiO<sub>2</sub>, 0.5/3-10 % acetic acid/MeOH in DCM) yielded a solid that was washed with 3M NaOH and dried to give a yellow solid (0.13 g, 63%); IR (film) 2927, 2852, 1606, 1522, 1484, 1458 cm<sup>-1</sup>; <sup>1</sup>H NMR (400 MHz, CDCl<sub>3</sub>) δ 8.48 (s, 1H), 8.02 (d, *J* = 8.5, 2H), 7.86 (d, *J* = 8.8, 1H), 7.82 (d, *J* = 9.0, 1 H), 7.78 (d, *J* = 6.0, 1H), 7.49 (t, *J* = 7.8, 1H), 7.45-7.41 (m, 2H), 7.38-7.33 (m, 2H), 6.67 (d, *J* = 7.0, 1H), 6.43 (d, *J* = 8.4, 1H), 5.85 (dd, *J* = 6.0, 2.0, 1H), 5.51 (d, *J* = 6.7, 1H), 5.25 (d, *J* = 1.8, 1H), 4.46 (d, *J* = 5.3, 1H), 3.82-3.74 (m, 1H), 3.70-3.63 (m, 1H), 3.15 (t, *J* = 6.56, 4H), 2.34-2.32 (m, 1 H), 2.15-2.12 (m, 1 H), 1.95-1.90 (m, 4H), 1.67-1.24 (m, 8H); <sup>13</sup>C NMR (100 MHz, CDCl<sub>3</sub>) ppm 159.6, 158.9, 155.9, 153.2, 147.7, 137.0, 136.7, 131.6, 130.4, 130.0, 128.4, 128.3, 127.1, 126.9, 125.4, 125.3, 125.1, 125.0, 115.5, 106.7, 99.79, 88.53, 56.3, 55.1, 47.0, 33.0, 32.7, 29.8, 25.4, 24.9, 24.6; HRMS (ESI): Exact mass calcd for C<sub>34</sub>H<sub>36</sub>N<sub>5</sub> [M+H]<sup>+</sup> 514.2971, found 514.2957.

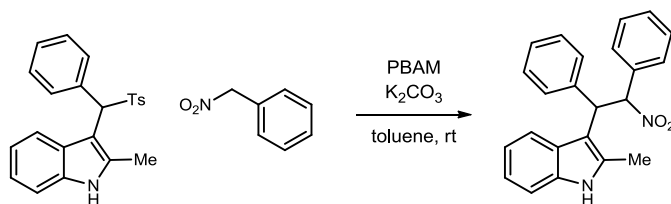


**ThioureaBAM (120) [(1-(3,5-bis(trifluoromethyl)phenyl)-3-((1*R*,2*R*)-2-(quinolin-2-**

**ylamino)cyclohexyl)thiourea].** A round bottomed flask fitted with a stir bar was charged with the mono-quinoline diamine (100 mg, 414  $\mu\text{mol}$ ), THF (2 mL) and 3,5-trifluoromethyl-phenylisothiocyanate (76  $\mu\text{L}$ , 414  $\mu\text{mol}$ ) was added slowly. The reaction was stirred at room temperature for 16 h. The reaction mixture was concentrated to an oil. Flash column chromatography ( $\text{SiO}_2$ , 10-20-40% ethyl acetate in hexanes) of the residue yielded a white solid (0.17 g, 80%).  $R_f = 0.3$  (20% EtOAc in Hexanes);  $[\alpha]_D^{20} +360$  ( $c$  0.54,  $\text{CHCl}_3$ ); IR (film) 3271, 3049, 2936, 2860, 1619, 1532, 1472  $\text{cm}^{-1}$ ;  $^1\text{H}$  NMR (400 MHz,  $\text{CDCl}_3$ )  $\delta$  8.91 (br s, 1H), 7.76 (d,  $J = 8.8$  Hz, 1H), 7.56 (d,  $J = 7.9$  Hz, 1H), 7.45 (br s, 1H), 7.39 (br s, 2H), 7.20 (dd,  $J = 7.5, 7.5$  Hz, 1H), 7.16 (br s, 1H), 6.57 (d,  $J = 8.8$  Hz, 1H), 4.80 (br s, 1H), 4.23 (br s, 2H), 2.56 (br s, 1H), 2.22-2.04 (m, 2H), 1.82 (br s, 2H), 1.47 (br s, 4H);  $^{13}\text{C}$  NMR (150 MHz,  $\text{CDCl}_3$ ) 180.6, 156.5, 145.5, 139.9, 138.1, 132.0 (q,  $^2J_{CF} = 28.2$  Hz,  $-\text{CF}_3$ ), 130.3, 127.8, 125.1, 123.1, 123.0, 122.8 (q,  $^1J_{CF} = 273$  Hz,  $-\text{CF}_3$ ), 122.3, 117.8, 113.1, 62.2, 54.3, 32.8, 31.6, 25.0, 24.3 ppm;  $^{19}\text{F}$  NMR (376 MHz,  $\text{CDCl}_3$ ) -61.2; HRMS (ESI): Exact mass calcd for  $\text{C}_{24}\text{H}_{23}\text{F}_6\text{N}_4\text{S}$   $[\text{M}+\text{H}]^+$  513.1548, found 513.1552.



**<sup>4</sup>MeO-ThioureaBAM (122) 1-(3,5-bis(trifluoromethyl)phenyl)-3-((1R,2R)-2-((4-methoxyquinolin-2-yl)amino)cyclohexyl)thiourea**. A round bottomed flask fitted with a stir bar was charged with the mono-quinoline diamine (220 mg, 810  $\mu$ mol), THF (3 mL) and 3,5-trifluoromethyl-phenylisothiocyanate (165  $\mu$ L, 900  $\mu$ mol) was added slowly. The reaction was stirred at room temperature for 2 days. The reaction mixture was concentrated to an oil. Flash column chromatography (SiO<sub>2</sub>, 10-20-40% ethyl acetate in hexanes) of the residue yielded a yellow solid (0.23 g, 53%).  $R_f = 0.3$  (5% MeOH in DCM);  $[\alpha]_D^{20} +187$  ( $c$  0.71 CHCl<sub>3</sub>); IR (film) 3149, 2937, 2859, 1623, 1533, 1467 cm<sup>-1</sup>; <sup>1</sup>H NMR (400 MHz, CDCl<sub>3</sub>)  $\delta$  9.25 (br s, 1H), 7.92 (d,  $J = 4.3$  Hz, 1H), 7.45 (br s, 2H), 7.38 (br s, 1H), 7.17 (dd,  $J = 7.5, 7.5$  Hz, 2H), 5.87 (br s, 1H), 4.83 (br s, 1H), 4.19 (br s, 2H), 3.92 (s, 3H), 2.56 (br s, 1H), 2.07 (br s, 2H), 1.81 (br s, 2H), 1.44 (br s, 4H); <sup>13</sup>C NMR (150 MHz, CDCl<sub>3</sub>) 180.7, 163.3, 157.7, 145.3, 140.2, 131.8 (q, <sup>2</sup> $J_{CF} = 33.4$  Hz, -CF<sub>3</sub>), 130.9, 127.5, 124.2, 122.9 (q, <sup>1</sup> $J_{CF} = 273$  Hz, -CF<sub>3</sub>), 122.5, 122.2, 117.5, 90.2, 61.6, 55.7, 54.7, 32.3, 31.4, 24.8, 24.3 ppm; <sup>19</sup>F NMR (376 MHz, CDCl<sub>3</sub>) -61.2; HRMS (ESI): Exact mass calcd for C<sub>25</sub>H<sub>25</sub>F<sub>6</sub>N<sub>4</sub>OS [M+H]<sup>+</sup> 543.1653, found 543.1663.



**2-Methyl-3-(2-nitro-1,2-diphenylethyl)-1H-indole (103). General Procedure (Method**

**A):** To a flame dried vial equipped with a stir bar was added the sulfone (38 mg, 0.10 mmol), PBAM (5.1 mg, 0.010 mmol) and potassium carbonate (96 mg, 0.70 mmol). The solid was suspended in toluene (1 mL) with stirring and phenylnitromethane (14 mg, 0.10 mmol) was added immediately. The mixture was stirred for 22 hours before dilution with water and extraction with ethyl acetate. The organic layer was filtered through silica gel, concentrated and determined to be 1.2:1 dr by NMR. Flash column chromatography (SiO<sub>2</sub>, 10-20% ethyl acetate in hexanes) yielded a yellow-pink solid (28 mg, 78%). The major diastereomer was determined to be 81% ee and the minor diastereomer was determined to be 81% ee by chiral HPLC analysis (see HPLC data below).

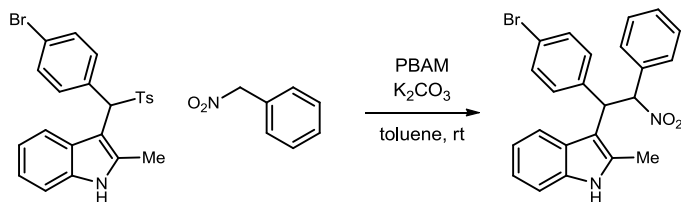
**Method B:** To a vial equipped with a stir bar was added the sulfone (38 mg, 0.10 mmol), PBAM (5.1 mg, 0.010 mmol) and potassium carbonate (96 mg, 0.70 mmol). The solid was suspended in toluene (1 mL) and water (500 μL) with stirring and phenylnitromethane (14 mg, 0.10 mmol) was added immediately. The mixture was stirred for 22 hours before dilution with water and extraction with ethyl acetate. The organic layer was filtered through silica gel, concentrated and determined to be 1.4:1 dr by NMR. Flash column chromatography (SiO<sub>2</sub>, 10-20% ethyl acetate in hexanes) yielded a yellow-pink solid (34 mg, 95%). The major diastereomer was determined to be 86% ee and the minor diastereomer was determined to be 86% ee by chiral HPLC analysis (see HPLC data below).

**Method C:** To a flame dried vial equipped with a stir bar was added the sulfone (36 mg, 0.10 mmol), PBAM (5 mg, 0.01 mmol) and potassium carbonate (96 mg, 0.70 mmol). The solid was suspended in toluene (1 mL) and stirred for 3 days. Phenylnitromethane (14 mg, 0.10 mmol) was added and stirred for 16 hours before dilution with water and extraction with ethyl acetate. The organic layer was filtered through silica gel, concentrated and determined to be 1.25:1 dr by NMR. Flash column chromatography (SiO<sub>2</sub>, 10-20% ethyl acetate in hexanes) yielded a yellow-pink solid (33 mg, 93%). The major diastereomer was determined to be 88% ee and the minor diastereomer was determined to be 89% ee by chiral HPLC analysis (see HPLC data below).

Chiral HPLC analysis (Chiralcel IA, 8% EtOH/hexanes, 1 mL/min,  $t_r(d_2e_1, \text{minor}) = 9.3$  min,  $t_r(d_2e_2, \text{minor}) = 10.7$  min,  $t_r(d_1e_1, \text{major}) = 13.0$  min,  $t_r(d_1e_2, \text{major}) = 14.8$  min);  $R_f = 0.3$  (25% EtOAc/hexanes); IR (film) 3411, 2922, 1552 cm<sup>-1</sup>; HRMS (ESI): Exact mass calcd for C<sub>23</sub>H<sub>21</sub>N<sub>2</sub>O<sub>2</sub> [M+H]<sup>+</sup> 357.1603, found 357.1607. ***d*<sub>1</sub>, major:** (85% ee)  $[\alpha]_D^{20} -31$  (*c* 0.20, CHCl<sub>3</sub>); <sup>1</sup>H NMR (600 MHz, CDCl<sub>3</sub>)  $\delta$  7.66 (dd, *J* = 6.1, 1.9 Hz, 1H), 7.59 (s, 1H), 7.52 (d, *J* = 7.4, 2H), 7.39 (d, *J* = 7.1 Hz, 2H), 7.30 (dd, *J* = 7.9, 7.6 Hz, 2H), 7.21-7.15 (m, 4H), 7.12-7.11 (m, 1H), 7.06-7.02 (m, 2H), 6.68 (d, *J* = 12.2 Hz, 1H), 5.34 (d, *J* = 12.2 Hz, 1H), 2.29 (s, 3H); <sup>13</sup>C NMR (150 MHz, CDCl<sub>3</sub>) ppm 140.2, 135.2, 133.8, 131.8, 129.5, 128.8, 128.4, 127.6, 127.3, 127.1, 121.1, 119.6, 118.7, 110.5, 109.3, 93.1, 46.8, 29.7, 12.2; ***d*<sub>2</sub>, minor:** (recrystallized, 94% ee)  $[\alpha]_D^{20} -66$  (*c* 0.10, CHCl<sub>3</sub>); <sup>1</sup>H NMR (600 MHz, CDCl<sub>3</sub>)  $\delta$  7.83 (s, 1H), 7.77 (dd, *J* = 5.9, 3.1 Hz, 1H), 7.61 (dd, *J* = 7.0, 3.5 Hz, 2H), 7.34-7.33 (m, 3H), 7.24-7.23 (m, 1H), 7.18 (d, *J* = 7.5 Hz, 2H), 7.11-7.07 (m, 4H), 7.02 (dd, *J* = 7.3, 7.3 Hz, 1H), 6.68 (d, *J* = 12.2 Hz, 1H), 5.38 (d, *J* = 12.2 Hz, 1H),

2.57 (s, 3H);  $^{13}\text{C}$  NMR (150 MHz,  $\text{CDCl}_3$ ) ppm 138.9, 135.4, 133.6, 132.4, 129.8, 128.9, 128.5, 128.4, 128.3, 126.7, 126.5, 121.2, 119.8, 118.8, 110.7, 110.0, 93.5, 46.4, 12.3.

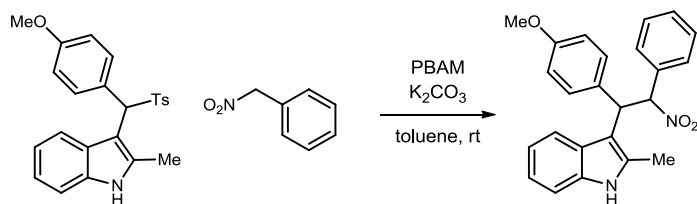




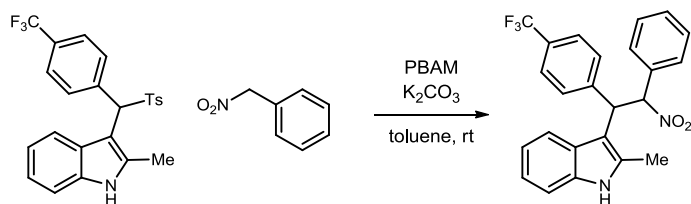
**3-(1-(4-Bromophenyl)-2-nitro-2-phenylethyl)-2-methyl-1H-indole (134b).** Sulfone (45 mg, 0.10 mmol) and phenylnitromethane (14 mg, 0.10 mmol) were combined and stirred for 22 hours according to the general procedure. Flash column chromatography (SiO<sub>2</sub>, 10-20% ethyl acetate in hexanes) yielded the title compound (32 mg, 74%).  $R_f = 0.3$  (20% EtOAc/hexanes); chiral HPLC analysis (Chiralcel IA, 10% IPA/hexanes, 1 mL/min,  $t_r(d_{1e1}, \text{major}) = 14.0$  min,  $t_r(d_{1e2}, \text{major}) = 18.2$  min,  $t_r(d_{2e1}, \text{minor}) = 16.1$  min,  $t_r(d_{2e2}, \text{minor}) = 32.1$  min); IR (film) 3408, 3059, 2924, 1552 cm<sup>-1</sup>; <sup>1</sup>H NMR (600 MHz, CDCl<sub>3</sub>)<sup>126</sup> **d<sub>1</sub>, major**  $\delta$  7.85-7.05 (14H), 6.61 (d,  $J = 12.2$  Hz, 1H), 5.34 (d,  $J = 12.2$  Hz, 1H), 2.55 (s, 3H); **d<sub>2</sub>, minor**  $\delta$  7.85-7.05 (14H), 6.62 (d,  $J = 12.1$  Hz, 1H), 5.29 (d,  $J = 12.1$  Hz, 1H), 2.27 (s, 3H); <sup>13</sup>C NMR (150 MHz, CDCl<sub>3</sub>)<sup>127</sup> ppm 139.3, 138.0, 135.4, 135.2, 133.5, 133.3, 132.6, 131.9, 131.4, 130.2, 130.0, 129.6, 129.1, 129.0, 128.5, 128.4, 127.5, 126.5, 121.4, 121.3, 121.0, 120.4, 119.9, 119.8, 118.5, 118.4, 110.8, 110.6, 109.3, 108.7, 93.2, 92.9, 46.4, 45.8, 12.2, 12.1; HRMS (ESI): Exact mass calcd for C<sub>23</sub>H<sub>20</sub>BrN<sub>2</sub>O<sub>2</sub> [M+H]<sup>+</sup> 435.0708, found 435.0687.

<sup>126</sup> Due to isolation as a mixture of diastereomers, overlapping peaks in the aromatic region are not listed individually, but are listed as a number of hydrogens over a range (ppm). Peaks that could be assigned to their respective diastereomer with confidence are listed with proper integration and splitting. Please see spectra in Supporting Information II.

<sup>127</sup> Due to isolation as a mixture of diastereomers, all carbons are listed and are not assigned to one specific diastereomer. Please see spectra in Supporting Information II.

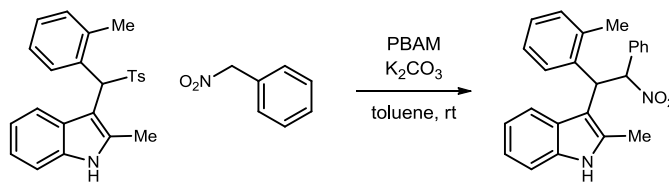


**3-(1-(4-Methoxyphenyl)-2-nitro-2-phenylethyl)-2-methyl-1H-indole (134c).** Sulfone (39 mg, 0.10 mmol) and phenylnitromethane (14 mg, 0.10 mmol) were combined and stirred for 22 hours according to the general procedure. Flash column chromatography (SiO<sub>2</sub>, 10-20% ethyl acetate in hexanes) yielded the title compound (26 mg, 68%). *R<sub>f</sub>* = 0.3 (20% EtOAc/hexanes); chiral HPLC analysis (Chiralcel IA, 10% EtOH/hexanes, 1 mL/min, *t<sub>r</sub>*(*d*<sub>1</sub>*e*<sub>1</sub>, major) = 10.5 min, *t<sub>r</sub>*(*d*<sub>1</sub>*e*<sub>2</sub>, major) = 11.9 min, *t<sub>r</sub>*(*d*<sub>2</sub>*e*<sub>1</sub>, minor) = 13.6 min, *t<sub>r</sub>*(*d*<sub>2</sub>*e*<sub>2</sub>, minor) = 18.6 min); IR (film) 3410, 3032, 2932, 1610 cm<sup>-1</sup>; <sup>1</sup>H NMR (600 MHz, CDCl<sub>3</sub>) **d**<sub>1</sub>, **major** δ 7.67 (d, *J* = 7.6 Hz, 1H), 7.58 (br s, 1H), 7.44 (d, *J* = 8.7 Hz, 2H), 7.41 (d, *J* = 7.0 Hz, 2H), 7.22-7.02 (6H), 6.83 (d, *J* = 8.7 Hz, 2H), 6.65 (d, *J* = 7.1 Hz, 1H), 5.29 (d, *J* = 12.0 Hz, 1H), 3.74 (s, 3H), 2.27 (s, 3H); **d**<sub>2</sub>, **minor** δ 7.81 (br s, 1H), 7.77-7.76 (m, 1H), 7.62-7.60 (m, 2H), 7.35-7.34 (m, 3H), 7.22-7.02 (5H), 6.63-6.61 (m, 3H) 5.32 (d, *J* = 12.6 Hz, 1H), 3.64 (s, 3H), 2.52 (s, 3H); <sup>13</sup>C NMR (150 MHz, CDCl<sub>3</sub>) ppm 158.4, 157.9, 135.4, 135.2, 133.8, 133.7, 132.4, 132.3, 131.7, 131.0, 129.8, 129.5, 128.9, 128.4, 128.4, 127.6, 126.7, 121.1, 1121.0, 119.7, 119.6, 118.8, 118.7, 114.2, 113.7, 110.7, 110.5, 110.1, 109.5, 93.8, 93.6, 55.2, 55.0, 46.1, 45.7, 12.2, 12.1; HRMS (ESI): Exact mass calcd for C<sub>24</sub>H<sub>23</sub>N<sub>2</sub>O<sub>3</sub> [M+H]<sup>+</sup> 387.1709, found 387.1693.

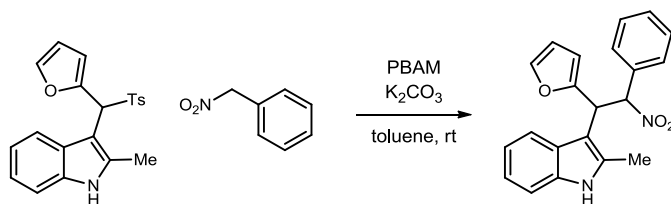


**2-Methyl-3-(2-nitro-2-phenyl-1-(4-(trifluoromethyl)phenyl)ethyl)-1H-indole (134d).**

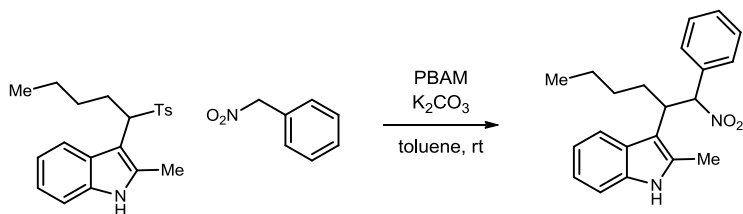
Sulfone (42 mg, 0.10 mmol) and phenylnitromethane (14 mg, 0.10 mmol) were combined and stirred for 22 hours according to the general procedure. Flash column chromatography (SiO<sub>2</sub>, 10-20% ethyl acetate in hexanes) yielded the title compound (30 mg, 71%).  $R_f = 0.3$  (20% EtOAc/hexanes); chiral HPLC analysis (Chiralcel IA, 8% EtOH/hexanes, 1 mL/min,  $t_r(d_{2e_1}, \text{minor}) = 8.2$  min,  $t_r(d_{2e_2}, \text{minor}) = 9.6$  min,  $t_r(d_{1e_1}, \text{major}) = 10.4$  min,  $t_r(d_{1e_2}, \text{major}) = 13.3$  min); IR (film) 3408, 1619 cm<sup>-1</sup>; <sup>1</sup>H NMR (600 MHz, CDCl<sub>3</sub>) ***d*<sub>1</sub>, major**  $\delta$  7.64-7.04 (14H), 6.69 (d,  $J = 12.0$  Hz, 1H), 5.39 (d,  $J = 12.0$  Hz, 1H), 2.29 (s, 3H); ***d*<sub>2</sub>, minor**  $\delta$  7.90 (br s, 1H), 7.72-7.71 (m, 1H), 7.64-7.04 (12H), 6.68 (d,  $J = 12.0$  Hz, 1H), 5.45 (d,  $J = 12.0$  Hz, 1H), 2.56 (s, 3H); <sup>13</sup>C NMR (150 MHz, CDCl<sub>3</sub>) ppm 144.3, 143.0, 135.4, 135.2, 133.4, 133.1, 132.8, 132.1, 130.2, 129.7, 129.4, 129.2, 129.1, 128.8, 128.5, 128.3, 127.6, 127.5, 126.4, 125.8, 125.8, 125.3, 125.3, 121.5, 121.4, 120.0, 119.9, 118.4, 118.3, 110.9, 110.7, 109.0, 108.3, 93.1, 92.6, 46.7, 46.1, 12.2, 12.1; HRMS (ESI): Exact mass calcd for C<sub>24</sub>H<sub>20</sub>F<sub>3</sub>N<sub>2</sub>O<sub>2</sub> [M+H]<sup>+</sup> 425.1477, found 425.1485.



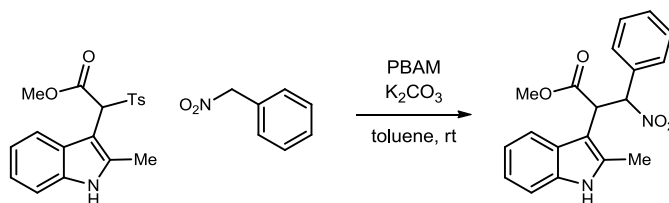
**2-Methyl-3-(2-nitro-2-phenyl-1-(*o*-tolyl)ethyl)-1*H*-indole (134e).** Sulfone (37 mg, 0.10 mmol) and phenylnitromethane (14 mg, 0.10 mmol) were combined and stirred for 72 hours according to the general procedure. Flash column chromatography (SiO<sub>2</sub>, 10-20% ethyl acetate in hexanes) yielded the title compound (28 mg, 76%).  $R_f = 0.4$  (20% EtOAc/hexanes); chiral HPLC analysis (Chiralcel IA, 10% EtOH/hexanes, 1 mL/min,  $t_r(d_{1e1}, \text{major}) = 11.2$  min,  $t_r(d_{2e1}, \text{minor}) = 13.0$  min,  $t_r(d_{2e2}, \text{minor}) = 14.0$  min,  $t_r(d_{1e2}, \text{major}) = 16.6$  min; IR (film) 3409, 2922, 1552 cm<sup>-1</sup>; <sup>1</sup>H NMR (600 MHz, CDCl<sub>3</sub>) ***d*<sub>1</sub>, major**  $\delta$  7.86-7.01 (14H), 6.64 (d,  $J = 12.0$  Hz, 1H), 5.26 (d,  $J = 12.0$  Hz, 1H), 2.30 (s, 3H), 2.03 (s, 3H); ***d*<sub>2</sub>, minor**  $\delta$  7.86-7.01 (14H), 6.72 (d,  $J = 12.1$  Hz, 1H), 5.52 (d,  $J = 12.1$  Hz, 1H), 2.52 (s, 3H), 2.26 (s, 3H); <sup>13</sup>C NMR (150 MHz, CDCl<sub>3</sub>) ppm 137.6, 136.7, 136.2, 135.4, 135.1, 134.1, 133.3, 132.9, 132.7, 131.4, 131.0, 129.7, 129.3, 128.9, 128.4, 128.3, 128.0, 127.2, 126.9, 126.8, 126.4, 125.9, 125.3, 124.8, 121.1, 120.9, 119.5, 119.4, 118.8, 110.5, 110.3, 107.6, 106.3, 94.2, 92.0, 44.0, 41.5, 20.0, 19.8, 12.4, 12.1; HRMS (ESI): Exact mass calcd for C<sub>24</sub>H<sub>21</sub>N<sub>2</sub>O<sub>2</sub> [M-H]<sup>-</sup> 369.1603, found 369.1596.



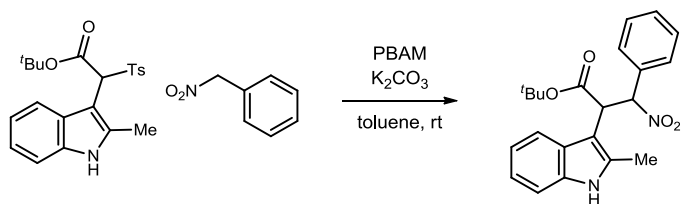
**3-(1-(Furan-2-yl)-2-nitro-2-phenylethyl)-2-methyl-1H-indole (134f).** Sulfone (35 mg, 0.10 mmol) and phenylnitromethane (14 mg, 0.10 mmol) were combined and stirred for 22 hours according to the general procedure. Flash column chromatography (SiO<sub>2</sub>, 10-20% ethyl acetate in hexanes) yielded the title compound (24 mg, 69%).  $R_f = 0.2$  (25% EtOAc/hexanes); chiral HPLC analysis (Chiralcel IA, 5% EtOH/hexanes, 1 mL/min,  $t_r(d_1e_1, \text{major}) = 11.8$  min,  $t_r(d_1e_2, \text{major}) = 13.5$  min,  $t_r(d_2e_1, \text{minor}) = 15.5$  min,  $t_r(d_2e_2, \text{minor}) = 16.5$  min); IR (film) 3408, 2923, 1553 cm<sup>-1</sup>; <sup>1</sup>H NMR (600 MHz, CDCl<sub>3</sub>) ***d*<sub>1</sub>, major**  $\delta$  7.86 (br s, 1H), 7.84-7.82 (m, 1H), 7.64-7.05 (9H), 6.52 (d,  $J = 11.8$  Hz, 1H), 6.07 (dd,  $J = 3.2, 1.9$  Hz, 1H), 5.90 (d,  $J = 3.2$  Hz, 1H), 5.40 (d,  $J = 11.8$ , 1H), 2.54 (s, 3H); ***d*<sub>2</sub>, minor**  $\delta$  7.64-7.05 (10H), 7.60 (br s, 1H), 6.46 (d,  $J = 11.8$  Hz, 1H), 6.29 (dd,  $J = 3.2, 2.0$  Hz, 1H), 6.25 (d,  $J = 3.2$  Hz, 1H), 5.39 (d,  $J = 11.7$ , 1H), 2.19 (s, 3H); <sup>13</sup>C NMR (150 MHz, CDCl<sub>3</sub>) ppm 153.0, 151.6, 141.8, 141.6, 135.3, 135.1, 133.4, 133.3, 133.0, 132.5, 129.9, 129.5, 128.8, 128.5, 128.3, 128.1, 127.4, 126.8, 126.7, 121.3, 121.2, 119.8, 119.6, 118.9, 118.8, 110.6, 110.4, 110.4, 110.1, 107.7, 107.3, 106.8, 106.5, 92.5, 92.0, 40.9, 29.7, 12.0, 11.9; HRMS (ESI): Exact mass calcd for C<sub>21</sub>H<sub>19</sub>N<sub>2</sub>O<sub>3</sub> [M+H]<sup>+</sup> 347.1396, found 347.1401.



**2-Methyl-3-(1-nitro-1-phenylhexan-2-yl)-1H-indole (134g).** Sulfone (36 mg, 0.10 mmol) and phenylnitromethane (14 mg, 0.10 mmol) were combined and stirred for 22 hours according to the general procedure. Flash column chromatography (SiO<sub>2</sub>, 10-20% ethyl acetate in hexanes) yielded the title compound (17 mg, 51%).  $R_f = 0.5$  (20% EtOAc/hexanes); chiral HPLC analysis (Chiralcel IA, 2% IPA/hexanes, 1 mL/min,  $t_r(d_1e_1, \text{major}) = 17.3$  min,  $t_r(d_1e_2, \text{major}) = 19.2$  min,  $t_r(d_2e_1, \text{minor}) = 24.1$  min,  $t_r(d_2e_2, \text{minor}) = 29.2$  min); IR (film) 3407, 2955, 1549 cm<sup>-1</sup>; <sup>1</sup>H NMR (600 MHz, CDCl<sub>3</sub>) **d<sub>1</sub>, major**  $\delta$  7.55 (br s, 1H), 7.48-7.08 (9H), 6.03 (d,  $J = 9.9$  Hz, 1H), 3.86 (br s, 1H), 2.17 (br s, 1H) 2.09 (s, 3H), 1.76-0.99 (5H), 0.79 (t,  $J = 7.2$  Hz, 3H); **d<sub>2</sub>, minor**  $\delta$  7.82 (br s, 1H), 7.69 (dd,  $J = 7.6, 2.3$  Hz, 2H), 7.65 (d,  $J = 7.5$  Hz, 2H), 7.48-7.08 (5H), 6.03 (d,  $J = 9.9$  Hz, 1H), 3.86 (br s, 1H), 2.45 (s, 3H) 1.85 (br s, 1H), 1.76-0.99 (5H), 0.67 (t,  $J = 7.2$  Hz, 3H); <sup>13</sup>C NMR (150 MHz, CDCl<sub>3</sub>) ppm 135.4, 134.3, 134.0, 129.9, 129.1, 129.1, 128.3, 128.1, 127.5, 121.0, 120.9, 119.3, 118.5, 110.8, 110.6, 95.3, 95.2, 42.7, 41.5, 30.8, 29.6, 29.2, 22.4, 22.2, 13.9, 13.8, 11.7; HRMS (ESI): Exact mass calcd for C<sub>21</sub>H<sub>25</sub>N<sub>2</sub>O<sub>2</sub> [M+H]<sup>+</sup> 337.1916, found 337.1917.

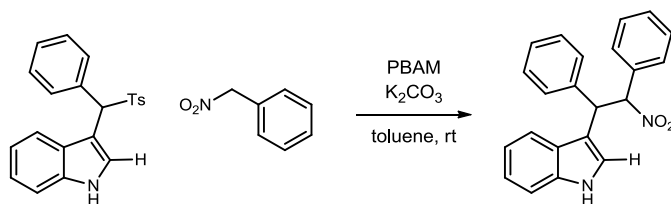


**Methyl 2-(2-methyl-1H-indol-3-yl)-3-nitro-3-phenylpropanoate (134i).** Sulfone (36 mg, 0.10 mmol) and phenylnitromethane (14 mg, 0.10 mmol) were combined and stirred for 22 hours according to the general procedure. Flash column chromatography (SiO<sub>2</sub>, 10-20% ethyl acetate in hexanes) yielded the title compound (16 mg, 47%).  $R_f = 0.2$  (20% EtOAc/hexanes); chiral HPLC analysis (Chiralcel IA, 5% IPA/hexanes, 1 mL/min,  $t_r(d_2e_1, \text{minor}) = 19.0$  min,  $t_r(d_1e_1, \text{major}) = 20.2$  min,  $t_r(d_2e_2, \text{minor}) = 22.0$  min,  $t_r(d_1e_2, \text{major}) = 25.2$  min); IR (film) 3399, 2952, 2922, 1735, 1554 cm<sup>-1</sup>; **d<sub>1</sub>, major:** <sup>1</sup>H NMR (400 MHz, CDCl<sub>3</sub>)  $\delta$  7.97 (br s, 1H), 7.88-7.85 (m, 1H), 7.75-7.73 (m, 2H), 7.47-7.44 (m, 3H), 7.28-7.24 (m, 1H), 7.18-7.13 (m, 2H), 6.48 (d,  $J = 11.8$  Hz, 1H), 5.02 (d,  $J = 11.8$  Hz, 1H), 3.46 (s, 3H), 2.53 (s, 3H); <sup>13</sup>C NMR (100 MHz, CDCl<sub>3</sub>) ppm 169.7, 135.2, 134.6, 133.1, 130.2, 129.1, 128.2, 126.4, 121.6, 120.2, 118.8, 110.6, 103.4, 90.7, 52.2, 47.1, 11.8; HRMS (ESI): Exact mass calcd for C<sub>19</sub>H<sub>17</sub>N<sub>2</sub>O<sub>4</sub> [M-H]<sup>-</sup> 337.1188, found 337.1180.

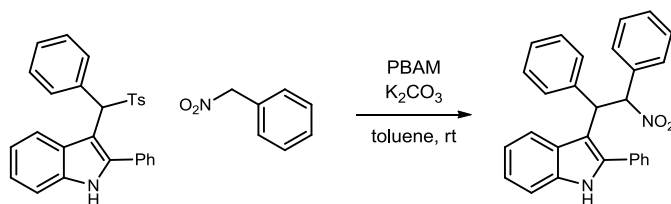


**tert-Butyl 2-(2-methyl-1H-indol-3-yl)-3-nitro-3-phenylpropanoate (134j).** Sulfone (38 mg, 0.10 mmol) and phenylnitromethane (14 mg, 0.10 mmol) were combined and stirred for 72 hours according to the general procedure. Flash column chromatography (SiO<sub>2</sub>, 10-20% ethyl acetate in hexanes) yielded the title compound (21 mg, 55%).  $R_f = 0.4$  (20% EtOAc/hexanes); chiral HPLC analysis (Chiralcel IA, 2% IPA/hexanes, 1 mL/min,  $t_r(d_2e_1, \text{minor}) = 26.5$  min,  $t_r(d_2e_2, \text{minor}) = 30.4$  min,  $t_r(d_1e_1, \text{major}) = 46.0$  min,  $t_r(d_1e_2, \text{major}) = 57.7$  min); IR (film) 3403, 2979, 1722, 1556 cm<sup>-1</sup>; <sup>1</sup>H NMR (600 MHz, CDCl<sub>3</sub>) ***d*<sub>1</sub>, major**,  $\delta$  7.92 (br s, 1H), 7.91-7.89 (m, 1H), 7.75-7.73 (m, 2H), 7.47-7.08 (6H), 6.39 (d,  $J = 11.8$  Hz, 1H), 4.93 (d,  $J = 11.8$  Hz, 1H), 2.55 (s, 3H), 1.13 (s, 9H); ***d*<sub>2</sub>, minor**,  $\delta$  7.66 (br s, 1H), 7.47-7.08 (9H), 6.30 (d,  $J = 11.8$  Hz, 1H), 4.71 (br s, 1H), 2.02 (s, 3H), 1.42 (s, 9H); <sup>13</sup>C NMR (150 MHz, CDCl<sub>3</sub>) ppm 168.1, 133.6, 130.1, 128.9, 128.5, 128.4, 121.4, 121.3, 119.9, 119.1, 110.5, 103.9, 90.7, 82.2, 48.6, 27.8, 27.6; HRMS (ESI): Exact mass calcd for C<sub>22</sub>H<sub>24</sub>N<sub>2</sub>NaO<sub>4</sub> [M+Na]<sup>+</sup> 403.1634, found 403.1623.

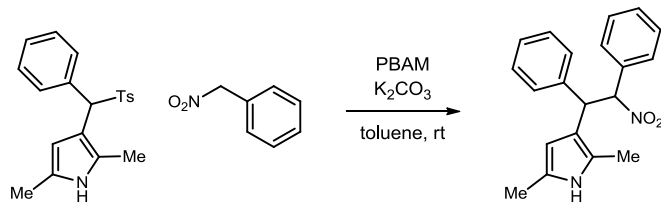




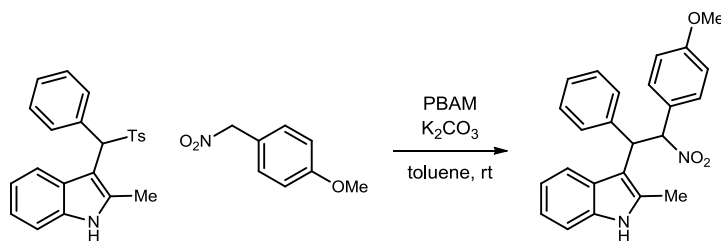
**3-(2-Nitro-1,2-diphenylethyl)-1H-indole (134k).** Sulfone (34 mg, 0.10 mmol) and phenylnitromethane (14 mg, 0.10 mmol) were combined and stirred for 22 hours according to the general procedure. Flash column chromatography (SiO<sub>2</sub>, 10-20% ethyl acetate in hexanes) yielded the title compound (22 mg, 65%).  $R_f = 0.2$  (20% EtOAc/hexanes); chiral HPLC analysis (Chiralcel IA, 15% EtOH/hexanes, 1 mL/min,  $t_r(d_{2e1}, \text{minor}) = 9.9$  min,  $t_r(d_{1e1}, \text{major}) = 12.4$  min,  $t_r(d_{2e2}, \text{minor}) = 14.4$  min,  $t_r(d_{1e2}, \text{major}) = 16.2$  min); IR (film) 3419, 1549 cm<sup>-1</sup>; <sup>1</sup>H NMR (600 MHz, CDCl<sub>3</sub>) ***d*<sub>1</sub>, major**  $\delta$  8.13 (br s, 1H), 7.59-6.99 (15H), 6.18 (d,  $J = 12.0$  Hz, 1H), 5.39 (d,  $J = 11.9$  Hz, 1H); ***d*<sub>2</sub>, minor**  $\delta$  7.90 (br s, 1H), 7.59-6.99 (14H), 6.84 (d,  $J = 1.5$  Hz, 1H), 6.30 (d,  $J = 12.1$  Hz, 1H), 5.42 (d,  $J = 12.0$  Hz, 1H); <sup>13</sup>C NMR (150 MHz, CDCl<sub>3</sub>) ppm 139.9, 138.4, 136.2, 133.2, 129.8, 129.7, 128.8, 128.8, 128.7, 128.6, 128.3, 128.2, 128.1, 127.9, 127.5, 126.9, 126.5, 122.6, 122.4, 121.7, 120.2, 119.8, 119.7, 119.0, 118.9, 115.6, 111.2, 111.0, 95.6, 95.0, 47.3, 46.1; HRMS (ESI): Exact mass calcd for C<sub>22</sub>H<sub>18</sub>N<sub>2</sub>NaO<sub>2</sub> [M+Na]<sup>+</sup> 365.1266, found 365.1273.



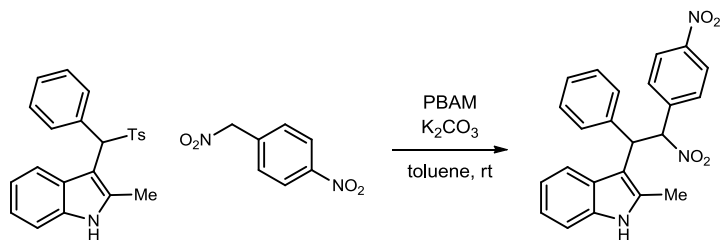
**3-(2-Nitro-1,2-diphenylethyl)-2-phenyl-1H-indole (134I)**. Sulfone (44 mg, 0.10 mmol) and phenylnitromethane (14 mg, 0.10 mmol) were combined and stirred for 72 hours according to the general procedure. Flash column chromatography (SiO<sub>2</sub>, 10-20% ethyl acetate in hexanes) yielded the title compound (20 mg, 49%).  $R_f = 0.5$  (20% EtOAc/hexanes); chiral HPLC analysis (Chiralcel IA, 10% EtOH/hexanes, 1 mL/min,  $t_r(d_{2e1}, \text{minor}) = 8.4$  min,  $t_r(d_{2e2}, \text{minor}) = 11.5$  min,  $t_r(d_{1e1}, \text{major}) = 13.6$  min,  $t_r(d_{1e2}, \text{major}) = 26.4$  min; IR (film) 3409, 3062, 1552 cm<sup>-1</sup>; <sup>1</sup>H NMR (600 MHz, CDCl<sub>3</sub>) ***d*<sub>1</sub>, major**  $\delta$  8.13-7.01 (20H), 6.74 (d,  $J = 12.0$  Hz, 1H), 5.43 (d,  $J = 12.0$  Hz, 1H); ***d*<sub>2</sub>, minor**  $\delta$  8.13-7.01 (20H), 6.63 (d,  $J = 12.0$  Hz, 1H), 5.42 (d,  $J = 12.0$  Hz, 1H); <sup>13</sup>C NMR (150 MHz, CDCl<sub>3</sub>) ppm 140.4, 139.2, 136.9, 136.9, 136.0, 135.8, 133.6, 133.3, 132.6, 132.2, 129.7, 129.3, 129.1, 129.1, 128.9, 128.8, 128.8, 128.7, 128.6, 128.6, 128.5, 128.4, 128.3, 128.3, 128.2, 127.8, 127.7, 127.2, 126.7, 126.7, 122.3, 122.1, 120.3, 120.3, 120.2, 120.1, 111.4, 111.2, 110.5, 109.8, 93.9, 93.9, 47.4, 46.6; HRMS (ESI): Exact mass calcd for C<sub>28</sub>H<sub>23</sub>N<sub>2</sub>O<sub>2</sub> [M+H]<sup>+</sup> 419.1760, found 419.1750.



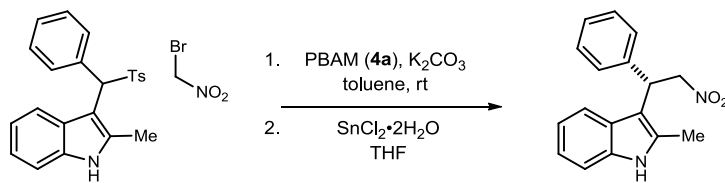
**2,5-Dimethyl-3-(2-nitro-1,2-diphenylethyl)-1H-pyrrole (134q).** Sulfonamide pyrrole (34 mg, 0.10 mmol) and phenylnitromethane (14 mg, 0.10 mmol) were combined and stirred for 22 hours according to the general procedure. Flash column chromatography (SiO<sub>2</sub>, 10-20% ethyl acetate in hexanes) yielded the title compound (22 mg, 69%).  $R_f = 0.4$  (20% EtOAc/hexanes); chiral HPLC analysis (Chiralcel IA, 5% EtOH/hexanes, 1 mL/min,  $t_r(d_2e_1, \text{minor}) = 9.9$  min,  $t_r(d_2e_2, \text{minor}) = 11.1$  min,  $t_r(d_1e_1, \text{major}) = 12.1$  min,  $t_r(d_1e_2, \text{major}) = 18.1$  min); IR (film) 3428, 1652, 1646 cm<sup>-1</sup>; <sup>1</sup>H NMR (600 MHz, CDCl<sub>3</sub>) ***d*<sub>1</sub>, major**  $\delta$  7.51-7.00 (m, 11H), 6.11 (d,  $J = 11.9$  Hz, 1H), 5.66 (d,  $J = 2.2$  Hz, 1H), 4.83 (d,  $J = 11.9$  Hz, 1H), 2.04 (s, 3H), 1.90 (s, 3H); ***d*<sub>2</sub>, minor**  $\delta$  7.51-7.00 (m, 11H), 6.08 (d,  $J = 11.9$  Hz, 1H), 5.98 (d,  $J = 1.1$  Hz, 1H), 4.88 (d,  $J = 11.9$  Hz, 1H), 2.21 (s, 3H), 2.18 (s, 3H); <sup>13</sup>C NMR (150 MHz, CDCl<sub>3</sub>) ppm 141.1, 139.9, 133.9, 133.5, 129.4, 129.4, 128.8, 128.6, 128.4, 128.3, 128.1, 127.3, 127.0, 126.4, 125.8, 125.7, 122.8, 122.5, 117.4, 116.0, 104.2, 103.6, 95.7, 95.5, 47.2, 47.1, 13.1, 13.0, 10.9, 10.8; HRMS (ESI): Exact mass calcd for C<sub>20</sub>H<sub>21</sub>N<sub>2</sub>O<sub>2</sub> [M+H]<sup>+</sup> 321.1603, found 321.1604.



**3-(2-(4-Methoxyphenyl)-2-nitro-1-phenylethyl)-2-methyl-1H-indole (138a).** Sulfone (38 mg, 0.10 mmol) and aryl nitromethane (17 mg, 0.10 mmol) were combined and stirred for 22 hours according to the general procedure. Flash column chromatography (SiO<sub>2</sub>, 10-20% ethyl acetate in hexanes) yielded the title compound (20 mg, 52%).  $R_f = 0.3$  (25% EtOAc/hexanes); chiral HPLC analysis (Chiralcel IA, 8% EtOH/hexanes, 1 mL/min,  $t_r(d_{2e1}, \text{minor}) = 13.4$  min,  $t_r(d_{2e2}, \text{minor}) = 15.0$  min,  $t_r(d_{1e1}, \text{major}) = 19.7$  min,  $t_r(d_{1e2}, \text{major}) = 27.3$  min); IR (film) 3409, 2925, 1609, 1549 cm<sup>-1</sup>; <sup>1</sup>H NMR (600 MHz, CDCl<sub>3</sub>) ***d*<sub>1</sub>, major**  $\delta$  7.68 (d,  $J = 7.5$  Hz, 1H), 7.61 (br s, 1H), 7.52 (d,  $J = 7.5$  Hz, 2H), 7.35 (d,  $J = 8.7$  Hz, 2H), 7.28 (dd,  $J = 7.6, 7.6$  Hz, 2H), 7.20-7.17 (m, 1H), 7.12-7.09 (m, 1H), 7.08-7.01 (m, 2H), 6.67 (d,  $J = 8.7$  Hz, 2H), 6.66-6.63 (m, 1H), 5.32 (d,  $J = 12$  Hz, 1H), 3.68 (s, 3H), 2.33 (s, 3H), <sup>1</sup>H NMR (600 MHz, CDCl<sub>3</sub>); ***d*<sub>2</sub>, minor**  $\delta$  7.81 (br s, 1H), 7.75 (dd,  $J = 4.8, 3.0$  Hz, 1H), 7.55 (d,  $J = 8.7$  Hz, 2H), 7.21 (dd,  $J = 6.1, 3.0$  Hz, 1H), 7.20-7.17 (m, 2H), 7.12-7.09 (m, 4H), 7.08-7.01 (m, 1H), 6.85 (d,  $J = 8.7$  Hz, 2H), 6.66-6.63 (m, 1H), 5.35 (d,  $J = 12$  Hz, 1H), 3.77 (s, 3H), 2.54 (s, 3H); <sup>13</sup>C NMR (150 MHz, CDCl<sub>3</sub>) ppm 160.6, 160.3, 140.4, 139.1, 135.4, 135.2, 132.4, 131.8, 129.8, 129.0, 128.8, 128.5, 128.3, 127.3, 127.0, 126.7, 126.4, 126.0, 125.8, 121.2, 121.0, 119.7, 119.6, 118.7, 118.7, 114.2, 113.8, 110.6, 110.5, 110.0, 109.5, 93.0, 92.9, 55.3, 55.1, 46.8, 46.1, 12.3, 12.2; HRMS (ESI): Exact mass calcd for C<sub>24</sub>H<sub>23</sub>N<sub>2</sub>O<sub>3</sub> [M+H]<sup>+</sup> 387.1709, found 387.1690.

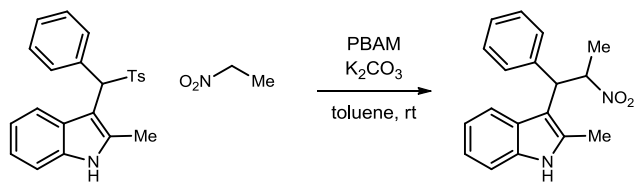


**2-Methyl-3-(2-nitro-2-(4-nitrophenyl)-1-phenylethyl)-1H-indole (138b).** Sulfone (38 mg, 0.10 mmol) and arylnitromethane (18 mg, 0.10 mmol) were combined and stirred for 22 hours according to the general procedure. Flash column chromatography (SiO<sub>2</sub>, 10-20% ethyl acetate in hexanes) yielded the title compound (25 mg, 52%).  $R_f = 0.4$  (25% EtOAc/hexanes); chiral HPLC analysis (Chiralcel IA, 15% IPA/hexanes, 1 mL/min,  $t_r(d_1e_1, \text{major}) = 9.1$  min,  $t_r(d_1e_2, \text{major}) = 9.6$  min,  $t_r(d_2e_1, \text{minor}) = 22.5$  min,  $t_r(d_2e_2, \text{minor}) = 39.5$  min); IR (film) 3409, 1557  $\text{cm}^{-1}$ ; <sup>1</sup>H NMR (600 MHz, CDCl<sub>3</sub>) **d<sub>1</sub>, major**  $\delta$  8.20-7.04 (13H), 7.69 (br s, 1H), 6.79 (d,  $J = 12.1$  Hz, 1H), 5.31 (d,  $J = 12.6$  Hz, 1H), 2.30 (s, 3H); **d<sub>2</sub>, minor**  $\delta$  8.20-7.04 (13H), 7.92 (br s, 1H), 6.79 (d,  $J = 12.1$  Hz, 1H), 5.33 (d,  $J = 12.0$  Hz, 1H), 2.56 (s, 3H); <sup>13</sup>C NMR (150 MHz, CDCl<sub>3</sub>) ppm 148.5, 148.3, 140.2, 140.0, 139.3, 137.9, 135.3, 132.6, 131.9, 129.5, 129.0, 128.7, 128.6, 128.3, 127.4, 127.1, 127.0, 126.3, 126.2, 124.0, 123.5, 121.5, 121.4, 120.0, 119.9, 118.5, 118.3, 110.8, 109.0, 108.3, 92.4, 92.1, 47.3, 47.2, 12.3, 12.1; HRMS (ESI): Exact mass calcd for C<sub>23</sub>H<sub>20</sub>N<sub>3</sub>O<sub>4</sub> [M+H]<sup>+</sup> 402.1454, found 402.1437.

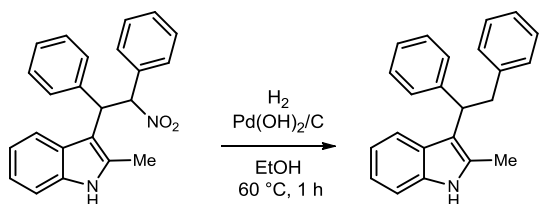


**(S)-2-Methyl-3-(2-nitro-1-phenylethyl)-1H-indole (138c).** To a flame dried vial equipped with a stir bar, was added sulfone **5a** (38 mg, 0.10 mmol), PBAM (5.1 mg, 0.010 mmol) and potassium carbonate (96 mg, 0.70 mmol). The solid was suspended in toluene (1 mL) and stirred, immediately followed by addition of bromonitromethane (21 mg, 0.15 mmol). The reaction was stirred at room temperature for 72 hours, diluted with water and extracted with ethyl acetate. The organic layer was filtered through silica gel and resuspended in THF (1 mL).  $\text{SnCl}_2 \cdot 2\text{H}_2\text{O}$  (36 mg, 0.15 mmol) was added to the solution and the reaction was stirred for 5 min. The crude reaction mixture was diluted with  $\text{H}_2\text{O}$  and extracted with  $\text{Et}_2\text{O}$ . The organic layer was dried over  $\text{MgSO}_4$ , filtered and concentrated. Flash column chromatography of the residue ( $\text{SiO}_2$ , 10-20% ethyl acetate in hexanes) yielded the title compound as a yellow oil (11 mg, 40%) and sulfone **5a** (10 mg, 25%).  $R_f = 0.3$  (20%  $\text{EtOAc}$ /hexanes);  $[\alpha]_D^{20} -13.5$  ( $c$  0.37,  $\text{CHCl}_3$ ). Stereochemistry determined to be (*S*) by correlation to the literature value.<sup>128</sup>

<sup>128</sup> Herrera, R. P.; Sgarzani, V.; Bernardi, L.; Ricci, A. *Angew. Chem. Int. Ed.* **2005**, *44*, 6576-6579.

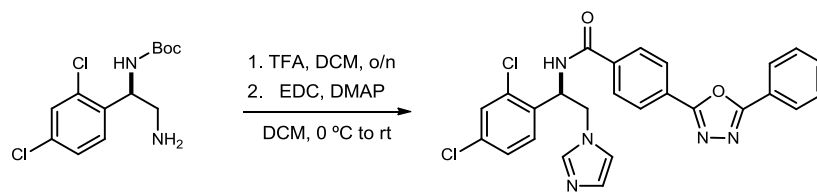


**2-Methyl-3-(2-nitro-1-phenylpropyl)-1H-indole (138d).** Sulfone (38 mg, 0.10 mmol) and nitroethane (11 mg, 0.15 mmol) were combined and stirred for 72 hours according to the general procedure. Flash column chromatography (SiO<sub>2</sub>, 10-20% ethyl acetate in hexanes) yielded the title compound (19 mg, 65%).  $R_f = 0.3$  (20% EtOAc/hexanes); chiral HPLC analysis (Chiralcel IA, 3% IPA/hexanes, 1 mL/min,  $t_r(d_1e_1, \text{major}) = 30.2$ ,  $t_r(d_2e_1, \text{minor}) = 35.2$  min,  $t_r(d_2e_2, \text{minor}) = 45.7$  min,  $t_r(d_1e_2, \text{major}) = 48.8$  min); IR (film) 3408, 2924, 1549 cm<sup>-1</sup>; <sup>1</sup>H NMR (600 MHz, CDCl<sub>3</sub>) ***d*<sub>1</sub>, major**  $\delta$  7.91 (br s, 1H), 7.60 (d,  $J = 7.7$  Hz, 1H), 7.76-7.09 (8H), 5.83-5.76 (m, 1H), 4.75 (d,  $J = 11.4$  Hz, 1H), 2.47 (s, 3H), 1.51 (d,  $J = 6.6$  Hz, 3H); ***d*<sub>2</sub>, minor**  $\delta$  7.76-7.09 (10H), 5.83-5.76 (m, 1H), 4.66 (d,  $J = 12.0$  Hz, 1H), 2.43 (s, 3H), 1.63 (d,  $J = 6.6$  Hz, 3H); <sup>13</sup>C NMR (150 MHz, CDCl<sub>3</sub>) ppm 140.3, 139.7, 135.3, 135.2, 132.5, 132.2, 128.8, 128.6, 128.2, 127.3, 127.0, 127.0, 126.6, 126.6, 121.4, 121.0, 119.9, 119.6, 118.8, 118.7, 110.7, 110.6, 110.0, 109.6, 86.1, 85.6, 48.4, 47.6, 19.7, 19.4, 12.3, 12.2; HRMS (ESI): Exact mass calcd for C<sub>18</sub>H<sub>19</sub>N<sub>2</sub>O<sub>2</sub> [M+H]<sup>+</sup> 295.1447, found 295.1458.



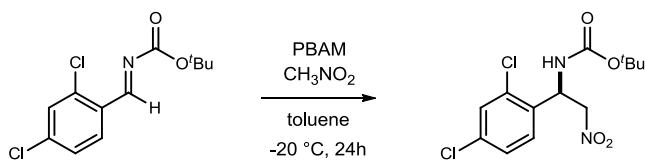
**3-(1,2-Diphenylethyl)-2-methyl-1H-indole (146).** To a flame dried vial equipped with a stir bar was added **6a** (17 mg, 50  $\mu$ mol, 84% ee), Pd(OH)<sub>2</sub>/C (20 wt %, 37 mg) and EtOH (1mL). The reaction was purged twice with hydrogen gas and then placed under 1 bar of hydrogen gas at 60 °C for 1 hour. The reaction was filtered through Celite and concentrated. Flash column chromatography (SiO<sub>2</sub>, 9% ethyl acetate in hexanes) yielded a yellow oil (13 mg, 84%).  $R_f = 0.5$  (20% EtOAc/hexanes);  $[\alpha]_D^{20} -42$  ( $c$  0.80, CHCl<sub>3</sub>); IR (film) 3414, 3059, 2922  $\text{cm}^{-1}$ ; <sup>1</sup>H NMR (400 MHz, CDCl<sub>3</sub>)  $\delta$  7.58 (br s, 1H), 7.46-7.42 (m, 3H), 7.30-7.27 (m, 2H), 7.25-7.18 (m, 2H), 7.16-7.06 (m, 4H), 7.01-6.97 (m, 1H), 6.94-6.91 (m, 2H), 4.42 (dd,  $J = 10.0, 5.6$  Hz, 1H), 3.62 (dd,  $J = 13.0, 5.6$  Hz, 1H), 3.49 (dd,  $J = 12.9, 10.1$  Hz, 1H), 2.00 (s, 3H); <sup>13</sup>C NMR (100 MHz, CDCl<sub>3</sub>) ppm 144.7, 141.3, 135.4, 131.8, 129.0, 128.1, 127.8, 127.6, 125.8, 125.6, 120.6, 119.6, 119.0, 113.3, 110.2, 44.2, 40.2, 11.7; HRMS (CI): Exact mass calcd for C<sub>23</sub>H<sub>22</sub>N [M+H]<sup>+</sup> 312.1705, found 312.1752.



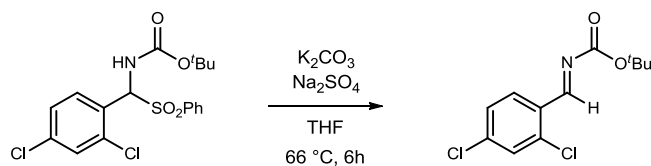


**VNI (161).** *tert*-Butyl (1-(2,4-dichlorophenyl)-2-(1H-imidazol-1-yl)ethyl) (356 mg, 1.00 mmol) was dissolved in CH<sub>2</sub>Cl<sub>2</sub> (10 mL). TFA (1.5 mL, 20 mmol) was added and the mixture was stirred at room temperature for 14 hours. The reaction was poured over sat. aq. NaHCO<sub>3</sub> and extracted with CH<sub>2</sub>Cl<sub>2</sub>. The combined organic layers were dried over MgSO<sub>4</sub>, filtered, and concentrated. The oil was dissolved in CH<sub>2</sub>Cl<sub>2</sub> (10 mL) and 4-(5-phenyl-1,3,4-oxadiazol-2-yl)benzoic acid (234 mg, 0.88 mmol) was added to the flask. The flask was cooled to 0 °C and EDC/HCl (220 mg, 1.2 mmol) and DMAP (20 mg, 0.10 mmol) was added. The reaction was allowed to warm to room temperature and monitored by TLC. Following reaction completion, the reaction was diluted with CH<sub>2</sub>Cl<sub>2</sub>, washed with water, dried over MgSO<sub>4</sub>, and concentrated to an oil. Flash column chromatography (SiO<sub>2</sub>, 1-4% methanol in dichloromethane) yielded a yellow solid (330 mg, 65%). The solid was then washed with DCM to give an analytically pure white solid (220 mg, 44%). Stereochemistry was conserved as the product was determined to be 97% ee by chiral HPLC analysis (Chiralcel OD-H, 20% EtOH/hexanes, 1 mL/min, *t*<sub>r</sub>(*S*-enantiomer) = 21.5 min, *t*<sub>r</sub>(*R*-enantiomer) = 31.4 min; [α]<sub>D</sub><sup>20</sup> +34 (*c* 0.60, CHCl<sub>3</sub>); R<sub>f</sub> = 0.31 (10% MeOH/DCM); IR (film) 3271, 2923, 2851, 1661, 1579 cm<sup>-1</sup>; <sup>1</sup>H NMR (600 MHz, CDCl<sub>3</sub>) δ 8.14-8.11 (m, 4H), 7.89 (d, *J* = 8.2 Hz, 2H), 7.58-7.52 (m, 3H), 7.47 (s, 1H), 7.35 (br s, 1 H), 7.23 (br s, 2H), 7.03 (br s, 1H), 6.91 (br s, 1H), 5.82 (dd, *J* = 13.7, 7.0, 1H), 4.57 (dd, *J* = 14.3, 7.2, 1H), 4.50 (dd, *J* = 14.2, 5.8, 1H), 1.88 (br s, 1H); <sup>13</sup>C NMR

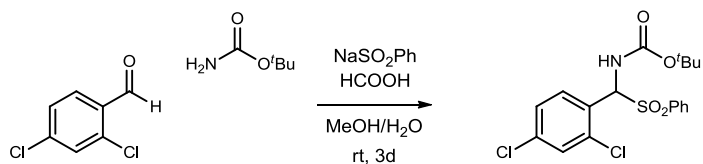
(150 MHz, CDCl<sub>3</sub>) ppm 166.3, 165.1, 163.7, 136.3, 135.2, 133.8, 133.5, 132.1, 130.3, 129.5, 129.5, 129.2, 128.0, 127.1, 127.0, 126.9, 123.5, 52.8, 49.1; HRMS (ESI): Exact mass calcd for C<sub>26</sub>H<sub>20</sub>Cl<sub>2</sub>N<sub>5</sub>O<sub>2</sub> [M+H]<sup>+</sup> 504.0994, found 504.0970.



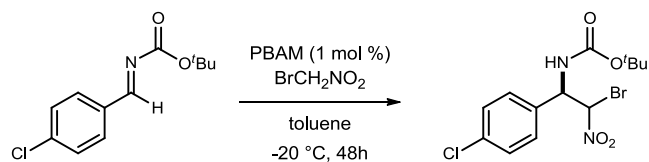
**(R)-tert-Butyl (1-(2,4-dichlorophenyl)-2-nitroethyl)carbamate (166).** A 2-dram vial was charged with imine (27.4 mg, 100  $\mu$ mol), PBAM<sub>4</sub>(HOTf)<sub>5</sub> (6.9 mg, 10  $\mu$ mol) and toluene (0.1 mL) and cooled to -20 °C. Nitromethane (11  $\mu$ L, 200  $\mu$ mol) was added and the reaction was stirred for 24 h. The reaction was filtered through a silica gel plug using ethyl acetate and concentrated to a white solid and determined to be a 74:26 mixture of *single-* to *double-*addition by NMR. The major product (*single* addition) was determined to be 90% ee by chiral HPLC analysis (Chiralcel IA, 5% <sup>t</sup>PrOH/hexanes, 1 mL/min,  $t_r(e_1, \text{major}) = 14.3$  min,  $t_r(e_2, \text{minor}) = 18.5$ ) and was further recrystallized to 99% ee (ethanol/water);  $[\alpha]_D^{20} -7.0$  ( $c$  0.10, CHCl<sub>3</sub>); IR (film) 3344, 2981, 2926, 1690, 1554, 1532 cm<sup>-1</sup>; <sup>1</sup>H NMR (600 MHz, CDCl<sub>3</sub>)  $\delta$  7.43 (d,  $J = 1.5$  Hz, 1H), 7.31-7.27 (m, 2H), 5.67 (br s, 2H), 4.85 (br s, 1H), 4.77 (br d,  $J = 11.8$  Hz, 1H), 1.43 (s, 9H); <sup>13</sup>C NMR (150 MHz, CDCl<sub>3</sub>) ppm 154.4, 135.2, 133.2, 132.9, 130.1, 128.9, 127.8, 81.0, 77.1, 50.0, 28.2; HRMS (ESI): Exact mass calcd for C<sub>13</sub>H<sub>16</sub>Cl<sub>2</sub>N<sub>2</sub>NaO<sub>4</sub> [M+Na]<sup>+</sup> 357.0385, found 357.0400.



***tert*-Butyl 2,4-dichlorobenzylidencarbamate (167).** A 1-L round-bottomed flask was charged with *tert*-butyl ((2,4-dichlorophenyl)(phenylsulfonyl)methyl)carbamate (20.0 g, 48.0 mmol), K<sub>2</sub>CO<sub>3</sub> (53.0 g, 384 mmol), Na<sub>2</sub>SO<sub>4</sub> (61.4 g, 432 mmol) and THF (500 mL). The pot was refluxed for 5 h until completion (checked by NMR). The reaction mixture was filtered through Celite, washed with diethyl ether and concentrated on low heat to yield the title compound as a pure white solid [12.9 g, 98% (<2% aldehyde)]. Mp 48-50 °C; IR (film) 2979, 1717, 1622, 1584 cm<sup>-1</sup>; <sup>1</sup>H NMR (600 MHz, CDCl<sub>3</sub>) δ 9.20 (s, 1H), 8.14 (d, *J* = 8.5 Hz, 1H), 7.46 (d, *J* = 2.0, 1H), 7.33 (ddd, *J* = 8.5, 1.9, 0.5, 1H), 1.59 (s, 9H); <sup>13</sup>C NMR (150 MHz, CDCl<sub>3</sub>) ppm 164.6, 162.1, 140.0, 138.4, 130.0, 130.0, 129.9, 127.8, 82.9, 27.9; HRMS (ESI): Exact mass calcd for C<sub>12</sub>H<sub>14</sub>Cl<sub>2</sub>NO<sub>2</sub> [M+H]<sup>+</sup> 274.0402, found 274.0391.

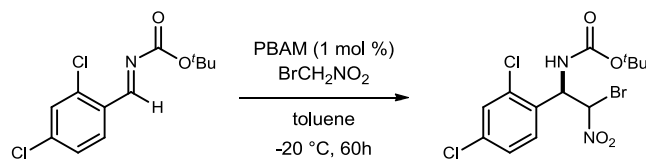


***tert*-Butyl ((2,4-dichlorophenyl)(phenylsulfonyl)methyl)carbamate (171).** A 500-mL Erlenmeyer flask was charged with 2,4-chlorobenzaldehyde (16.8 g, 96.0 mmol), benzenesulfinic acid sodium salt (26.3 g, 160 mmol), *tert*-butyl carbamate (9.38 g, 80.0 mmol), formic acid (6.1 mL, 160 mmol), methanol (70 mL) and water (140 mL) and stirred for 3 days. The solid was filtered and rinsed with water. The washed solid was added to diethyl ether and stirred overnight. Filtration and washing with diethyl ether afforded the pure product as two rotamers (5:1) as a white solid (13.0 grams, 81% based on recovered starting material). Mp 160-162 °C; IR (film) 3387, 3340, 3332, 3301, 3268, 2977, 1722, 1704, 1588  $\text{cm}^{-1}$ ;  $^1\text{H}$  NMR (600 MHz,  $\text{CDCl}_3$ )  $\delta$  7.93 (d,  $J = 7.6$  Hz, 2H), 7.67 (t,  $J = 7.0$  Hz, 1H), 7.57-7.55 (m, 2H), 7.50 (d,  $J = 8.3$  Hz, 1H), 7.45 (d,  $J = 1.2$  Hz, 1H), 7.35 (dd,  $J = 8.4, 2.1$  Hz, 1H), 6.53 (d,  $J = 10.7$  Hz, 1H), 5.82 (d,  $J = 10.7$  Hz, 1H), 1.28 (s, 9H);  $^{13}\text{C}$  NMR (150 MHz,  $\text{CDCl}_3$ ) ppm 153.3, 136.9, 136.5, 136.1, 134.3, 130.1, 129.8, 129.3, 129.2, 127.7, 81.6, 69.6, 28.0; HRMS (ESI): Exact mass calcd for  $\text{C}_{18}\text{H}_{19}\text{Cl}_2\text{NNaO}_4\text{S}$   $[\text{M}+\text{Na}]^+$  438.0310, found 438.0327.

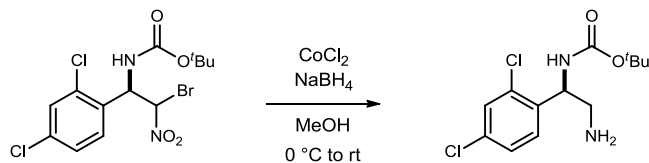


**tert-Butyl ((1R)-2-bromo-1-(4-chlorophenyl)-2-nitroethyl)carbamate (173).** A 250-mL round-bottomed flask was charged with imine (7.19 g, 30.0 mmol), (+)-PBAM (152 mg, 300  $\mu$ mol) and toluene (150 mL) and cooled to -78 °C. Bromonitromethane (6.30 g, 45.0 mmol) was added over 1 minute and the reaction was stirred for 48 h at -20 °C. The reaction was filtered through a silica gel plug using ethyl acetate, concentrated to a white solid (11.0 g, 97%), and determined to be 3:1 dr by <sup>1</sup>H NMR. The white solid was determined to be pure and required no further purification. The major diastereomer was determined to be 97% ee and the minor diastereomer was determined to be 96% ee by chiral HPLC analysis (Chiralcel AD-H, 10% <sup>i</sup>PrOH/hexanes, 1 mL/min,  $t_r(d_1e_1, \text{major}) = 18.9$  min,  $t_r(d_1e_2, \text{minor}) = 14.6$  min,  $t_r(d_2e_1, \text{major}) = 24.8$  min,  $t_r(d_2e_2, \text{minor}) = 15.9$  min). Remainder of analytical data matched previously reported.<sup>129</sup>

<sup>129</sup> Shen, B.; Makley, D. M.; Johnston, J. N. *Nature* **2010**, *465*, 1027-1032.

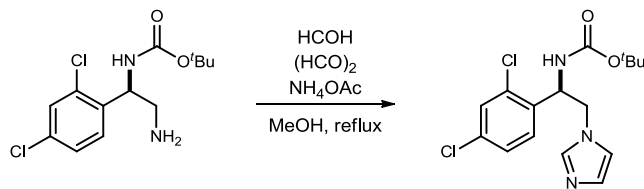


**tert-Butyl ((1R)-2-bromo-1-(2,4-dichlorophenyl)-2-nitroethyl)carbamate (174).** A 500-mL round-bottomed flask was charged with imine (12.9 g, 47.0 mmol), (+)-PBAM (238 mg, 470  $\mu$ mol) and toluene (240 mL) and cooled to  $-78$   $^{\circ}\text{C}$ . Bromonitromethane (9.21 g, 65.8 mmol) was added and the reaction was stirred for 48 h at  $-20$   $^{\circ}\text{C}$  until the reaction was complete. The reaction was filtered through a silica gel plug using ethyl acetate and concentrated to a white solid determined to be 1:1 dr by NMR. The solid recovered (19.2 g, 99%) was used without further purification. Mp  $108$ - $110$   $^{\circ}\text{C}$ ; the major diastereomer was determined to be 98% ee and the minor diastereomer was determined to be 98% ee by chiral HPLC analysis (Chiralcel IA, 3%  $i$ PrOH/hexanes, 1 mL/min,  $t_r(d_1e_1, \text{major}) = 12.9$  min,  $t_r(d_1e_2, \text{minor}) = 24.4$  min,  $t_r(d_2e_1, \text{major}) = 16.3$  min,  $t_r(d_2e_2, \text{minor}) = 20.2$  min);  $R_f = 0.48$  (25% EtOAc/hexanes); IR (film) 3423, 3331, 2980, 1705, 1589  $\text{cm}^{-1}$ ;  **$d_1, \text{major}$ :**  $^1\text{H}$  NMR (600 MHz,  $\text{CDCl}_3$ )  $\delta$  7.44 (s, 1H), 7.31-7.28 (m, 2H), 6.43 (br s, 1H), 6.03-6.02 (m, 1H), 5.71 (d,  $J = 3.0$  Hz, 1H), 1.45 (s, 9H);  $^{13}\text{C}$  NMR (150 MHz,  $\text{CDCl}_3$ ) ppm 154.6, 136.0, 133.4, 131.2, 130.1, 128.1, 81.4, 78.0, 55.6, 28.2.  **$d_2, \text{minor}$ :**  $^1\text{H}$  NMR (600 MHz,  $\text{CDCl}_3$ )  $\delta$  7.45 (s, 1H), 7.31-7.28 (m, 2H), 6.46 (br s, 1H), 6.03-6.02 (m, 1H), 5.50 (d,  $J = 6.0$  Hz, 1H), 1.43 (s, 9H);  $^{13}\text{C}$  NMR (150 MHz,  $\text{CDCl}_3$ ) ppm 154.1, 135.8, 133.2, 131.9, 129.7, 127.8, 83.0, 81.5, 55.0, 28.2. HRMS (ESI): Exact mass calcd for  $\text{C}_{13}\text{H}_{15}\text{BrCl}_2\text{N}_2\text{NaO}_4$   $[\text{M}+\text{Na}]^+$  434.9490, found 434.9486.



**(*R*)-*tert*-Butyl (2-amino-1-(2,4-dichlorophenyl)ethyl)carbamate (175).** A flame dried 1 L round bottom was charged with *tert*-butyl (2-bromo-1-(2,4-dichlorophenyl)-2-nitroethyl)carbamate (19.2 g, 46.4 mmol), CoCl<sub>2</sub> (6.02 g, 46.4 mmol) and MeOH (230 mL). The pot was cooled to 0 °C and NaBH<sub>4</sub> (8.76 g, 231.9 mmol) was added in portions over 5 minutes with the final evolution of H<sub>2</sub> contained in a balloon. The reaction stirred at 0 °C for 20 min and was warmed to rt and the progress was monitored by TLC. Sat. aq. NH<sub>4</sub>Cl (~100 mL) was added to the flask and it was brought to pH 9 with slow addition of 1 M NH<sub>4</sub>OH. The reaction was filtered with MeOH and DCM, concentrated to remove the organics then extracted with DCM (significant amount of emulsions). The combined organic layers were washed with brine, dried over MgSO<sub>4</sub>, filtered, and concentrated to a yellow oil. Flash column chromatography (SiO<sub>2</sub>, 1-3-5-10% methanol in dichloromethane with 0.5% acetic acid) yielded an oil/solid depending on water content (7.42 g, 52%). Mp 86-88 °C; R<sub>f</sub> = 0.11 (10% MeOH/DCM); IR (film) 3316, 3002, 2977, 2932, 1703, 1698, 1694 cm<sup>-1</sup>; <sup>1</sup>H NMR (600 MHz, CDCl<sub>3</sub>) δ 7.36 (d, *J* = 2.0 Hz, 1H), 7.32 (d, *J* = 8.0 Hz, 1H), 7.22 (dd, *J* = 8.3, 2.0, 1H), 5.7 (br s, 1H), 5.02 (br s, 1H), 2.98 (br s, 2H), 1.41 (br s, 9H), 1.12 (br s, 2H); <sup>13</sup>C NMR (150 MHz, CDCl<sub>3</sub>) ppm 155.3, 137.2, 133.3, 129.6, 128.3, 127.2, 127.1, 79.7, 53.1, 44.8, 28.3; HRMS (ESI: Exact mass calcd for C<sub>13</sub>H<sub>19</sub>Cl<sub>2</sub>N<sub>2</sub>O<sub>2</sub> [M+H]<sup>+</sup> 305.0824, found 305.0826.

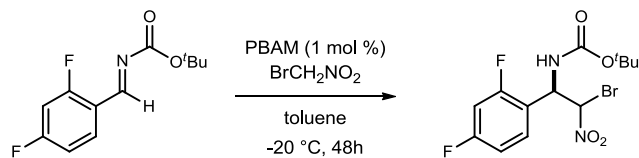




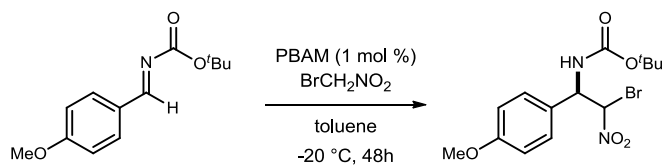
**(R)-tert-Butyl (1-(2,4-dichlorophenyl)-2-(1H-imidazol-1-yl)ethyl)carbamate (179).**<sup>130</sup>

To a 250 mL round bottom containing the amine (7.41 g, 24.2 mmol) was added aqueous glyoxal (40% w/v, 6.88 mL, 48.4 mmol), ammonium acetate (3.74 g, 48.4 mmol), aqueous formaldehyde (37% w/v, 4.00 mL, 48.4 mmol) and methanol (60 mL). The reaction was refluxed with stirring for 20 hrs. The reaction was concentrated and redissolved in 3 M NaOH and was extracted with DCM. The combined organic layers were washed with brine, dried over MgSO<sub>4</sub>, filtered, and concentrated to a brown oil. The oil was dissolved in DCM (~100 mL) and was added to stirring hexanes (~400 mL). The solid that precipitated was filtered and washed with hexanes to give the product as a beige solid (4.21 g, 49%). Flash column chromatography (SiO<sub>2</sub>, 1-5% methanol in dichloromethane) of the remaining organic yielded a beige solid (0.86 g, 10%). Mp 166-168 °C;  $[\alpha]_D^{20}$  -8.5 (c 0.60, CHCl<sub>3</sub>);  $R_f$  = 0.31 (visualized with PIP) (10% MeOH/DCM); IR (film) 3212, 2977, 2934, 1707, 1507 cm<sup>-1</sup>; <sup>1</sup>H NMR (600 MHz, CDCl<sub>3</sub>) δ 7.60 (s, 1H), 7.43 (d, *J* = 2.1 Hz, 1H), 7.28 (br s, 1H), 7.21 (d, *J* = 6.6 Hz, 1H), 7.01 (br s, 2H), 6.75 (br s, 1H), 5.35 (br s, 2H), 4.34-4.27 (m, 2H), 1.40 (s, 9H); <sup>13</sup>C NMR (150 MHz, CDCl<sub>3</sub>) ppm 154.8, 137.5, 134.7, 134.5, 133.3, 130.0, 129.7, 128.8, 127.7, 119.4, 80.7, 52.8, 49.7, 28.2; HRMS (ESI): Exact mass calcd for C<sub>16</sub>H<sub>20</sub>Cl<sub>2</sub>N<sub>3</sub>O<sub>2</sub> [M+H]<sup>+</sup> 356.0933, found 356.0924.

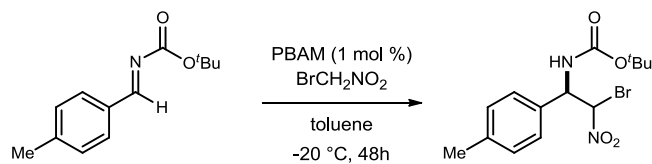
<sup>130</sup> Adapted from: Matsuoka, Y.; Ishida, Y.; Sasaki, D.; Saigo, K. *Tetrahedron* **2006**, 62, 8199-8206



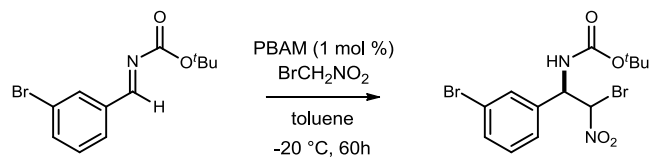
**tert-Butyl ((1R)-2-bromo-1-(2,4-difluorophenyl)-2-nitroethyl)carbamate (185b).** A 250-mL round-bottomed flask was charged with imine (7.00 g, 29.0 mmol), (+)-PBAM (147 mg, 290  $\mu\text{mol}$ ) and toluene (145 mL) and cooled to  $-78\text{ }^{\circ}\text{C}$ . Bromonitromethane (6.02 g, 43.0 mmol) was added over 1 minute and the reaction was stirred for 48 h at  $-20\text{ }^{\circ}\text{C}$ . The reaction was filtered through a silica gel plug using ethyl acetate, concentrated to a white solid (10.8 g, 97%), and determined to be 1:1 dr by  $^1\text{H}$  NMR. The white solid was determined to be pure and required no further purification. The major diastereomer was determined to be 95% ee and the minor diastereomer was determined to be 94% ee by chiral HPLC analysis (Chiralcel AD-H, 4% *i*PrOH/hexanes, 1 mL/min,  $t_{\text{r}}(d_1e_1, \text{major}) = 20.7$  min,  $t_{\text{r}}(d_1e_2, \text{minor}) = 29.6$  min,  $t_{\text{r}}(d_2e_1, \text{major}) = 22.8$  min,  $t_{\text{r}}(d_2e_2, \text{minor}) = 25.5$  min); IR (film) 3355, 2985, 1690, 1607, 1566, 1506  $\text{cm}^{-1}$ ;  $^1\text{H}$  NMR (600 MHz,  $\text{CDCl}_3$ , 1:1 mixture of diastereomers)  $\delta$  7.35-7.28 (m, 2H), 6.91 (dd,  $J = 8.7, 8.7$  Hz, 2H), 6.88 (dd,  $J = 9.7, 9.7$  Hz, 2H), 6.29 (br s, 2H), 5.81 (br s, 1H), 5.73 (br s, 1H), 5.65 (br s, 1H), 5.40 (br d,  $J = 8.7$  Hz, 1H), 1.43 (s, 18 H);  $^{13}\text{C}$  NMR (150 MHz,  $\text{CDCl}_3$ , 1:1 mixture of diastereomers) ppm 163.41 (dd,  $J_{\text{CF}} = 253, 12.1$  Hz), 163.37 (dd,  $J_{\text{CF}} = 252, 12.6$  Hz), 160.4 (dd,  $J_{\text{CF}} = 249, 12.2$  Hz), 154.4, 154.3, 130.5 (m), 118.5, 112.23 (dd,  $J_{\text{CF}} = 21.6, 3.3$  Hz), 112.17 (dd,  $J_{\text{CF}} = 21.5, 3.2$  Hz), 104.7 (dd,  $J_{\text{CF}} = 25.8, 25.8$  Hz), 104.6 (dd,  $J_{\text{CF}} = 25.5, 25.5$  Hz), 82.6, 81.4, 79.1, 53.9, 28.1;  $^{19}\text{F}$  NMR (282 MHz,  $\text{CDCl}_3$ , 1:1 mixture of diastereomers) ppm -106, -110, -111; HRMS (ESI): Exact mass calcd for  $\text{C}_{13}\text{H}_{15}\text{BrF}_2\text{N}_2\text{NaO}_4$   $[\text{M}+\text{Na}]^+$  403.0081, found 403.0065.



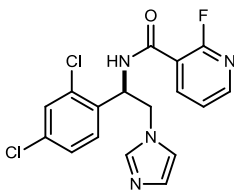
**tert-Butyl ((1*R*)-2-bromo-1-(4-methoxyphenyl)-2-nitroethyl)carbamate (185c).** A 250-mL round-bottomed flask was charged with imine (6.82 g, 29.0 mmol), (+)-PBAM (147 mg, 290  $\mu$ mol) and toluene (145 mL) and cooled to -78 °C. Bromonitromethane (6.02 g, 43.0 mmol) was added over 1 minute and the reaction was stirred for 48 h at -20 °C. The reaction was filtered through a silica gel plug using ethyl acetate, concentrated to a white solid (10.6 g, 97%), and determined to be 5:1 dr by  $^1\text{H}$  NMR. The white solid was determined to be pure and required no further purification. The major diastereomer was determined to be 96% ee and the minor diastereomer was determined to be 96% ee by chiral HPLC analysis (Chiralcel AD-H, 20% *i*PrOH/hexanes, 1 mL/min,  $t_r(d_1e_1, \text{major}) = 13.4$  min,  $t_r(d_1e_2, \text{minor}) = 16.0$  min,  $t_r(d_2e_1, \text{major}) = 21.6$  min,  $t_r(d_2e_2, \text{minor}) = 17.5$  min); IR (film) 3366, 2977, 1681, 1561, 1515  $\text{cm}^{-1}$ ;  $^1\text{H}$  NMR (600 MHz,  $\text{CDCl}_3$ , 1:1 mixture of diastereomers)  $\delta$  7.24 (d,  $J = 8.6$  Hz, 2H), 7.21 (d,  $J = 8.7$  Hz, 2H), 6.90 (d,  $J = 8.8$  Hz, 2H), 6.89 (d,  $J = 8.7$  Hz, 2H), 6.30 (br s, 1H), 6.27 (br s, 1H), 5.64 (br s, 1H), 5.56 (br m, 1H), 5.41 (br s, 1H), 5.31 (br s, 1H), 3.81 (s, 3H), 3.80 (s, 3H), 1.45 (s, 9H), 1.44 (s, 9H);  $^{13}\text{C}$  NMR (150 MHz,  $\text{CDCl}_3$ , 1:1 mixture of diastereomers) ppm 160.1, 160.0, 154.5 (2C), 128.2, 128.1, 126.5 (2C), 114.41, 114.38, 85.1, 82.0, 81.1, 80.9, 57.7 (2C), 55.2 (2C), 28.15, 28.12; HRMS (ESI): Exact mass calcd for  $\text{C}_{14}\text{H}_{20}\text{BrN}_2\text{O}_5$   $[\text{M}+\text{H}]^+$  375.0550, found 375.0551.



***tert*-Butyl ((1*R*)-2-bromo-1-(4-methylphenyl)-2-nitroethyl)carbamate (185d).** A 250-mL round-bottomed flask was charged with imine (6.58 g, 30.0 mmol), (+)-PBAM (152 mg, 300  $\mu$ mol) and toluene (150 mL) and cooled to -78  $^{\circ}$ C. Bromonitromethane (6.30 g, 45.0 mmol) was added over 1 minute and the reaction was stirred for 48 h at -20  $^{\circ}$ C. The reaction was filtered through a silica gel plug using ethyl acetate, concentrated to a white solid (10.6 g, 97%), and determined to be 3:1 dr by  $^1$ H NMR. The white solid was determined to be pure and required no further purification. The major diastereomer was determined to be 91% ee and the minor diastereomer was determined to be 87% ee by chiral HPLC analysis (Chiralcel AD-H, 25%  $i$ PrOH/hexanes, 0.4 mL/min,  $t_r(d_1e_1)$ , major) = 15.8 min,  $t_r(d_1e_2)$ , minor) = 17.5 min,  $t_r(d_2e_1)$ , major) = 23.2 min,  $t_r(d_2e_2)$ , minor) = 19.2 min); IR (film) 3391, 2981, 1690, 1562, 1516  $\text{cm}^{-1}$ ;  $^1$ H NMR (600 MHz,  $\text{CDCl}_3$ , major diastereomer)  $\delta$  7.21-7.15 (m, 4H), 6.28 (br s, 1H), 5.60 (br s, 1H), 5.36 (br d,  $J$  = 8.0 Hz, 1H), 2.35 (s, 3H), 1.44 (s, 9H);  $^1$ H NMR (600 MHz,  $\text{CDCl}_3$ , minor diastereomer)  $\delta$  7.21-7.15 (m, 4H), 6.31 (br s, 1H), 5.68 (br s, 1H), 5.43 (br s, 1H), 2.34 (s, 3H), 1.45 (s, 9H);  $^{13}$ C NMR (150 MHz,  $\text{CDCl}_3$ , 3:1 mixture of diastereomers) ppm 154.7, 154.5, 139.2, 139.1, 132.1, 131.6, 129.80, 129.75, 129.2, 128.8, 126.8, 126.6, 85.2, 81.9, 81.1, 57.9, 28.19, 28.16, 21.1; HRMS (ESI): Exact mass calcd for  $\text{C}_{14}\text{H}_{19}\text{BrN}_2\text{NaO}_4$   $[\text{M}+\text{Na}]^+$  381.0426, found 381.0432.

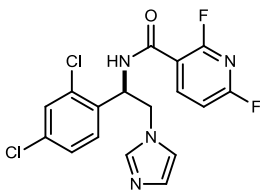


***tert*-Butyl ((1*R*)-2-bromo-1-(3-bromophenyl)-2-nitroethyl)carbamate (185e).** A 250-mL round-bottomed flask was charged with imine (8.53 g, 30.0 mmol), (+)-PBAM (152 mg, 300  $\mu$ mol) and toluene (150 mL) and cooled to -78  $^{\circ}$ C. Bromonitromethane (6.30 g, 45.0 mmol) was added over 1 minute and the reaction was stirred for 60 h at -20  $^{\circ}$ C. The reaction was filtered through a silica gel plug using ethyl acetate, concentrated to a white solid (12.5 g, 98%), and determined to be 1:1 dr by  $^1$ H NMR. The white solid was determined to be pure and required no further purification. The major diastereomer was determined to be 91% ee and the minor diastereomer was determined to be 91% ee by chiral HPLC analysis (Chiralcel AD-H, 7% EtOH/hexanes, 0.6 mL/min,  $t_r(d_1e_1, \text{major}) = 20.9$  min,  $t_r(d_1e_2, \text{minor}) = 16.5$  min,  $t_r(d_2e_1, \text{major}) = 19.2$  min,  $t_r(d_2e_2, \text{minor}) = 17.7$  min); IR (film) 3348, 2980, 1701, 1567, 1504  $\text{cm}^{-1}$ ;  $^1$ H NMR (600 MHz,  $\text{CDCl}_3$ , 1:1 mixture of diastereomers)  $\delta$  7.51-7.46 (m, 4H), 7.27-7.22 (m, 4H), 6.28 (br s, 2H), 5.76 (br d,  $J = 8.9$  Hz, 1H), 5.65 (br s, 1H), 5.43 (br s, 2H), 1.46 (s, 9H), 1.44 (s, 9H);  $^{13}\text{C}$  NMR (150 MHz,  $\text{CDCl}_3$ , 1:1 mixture of diastereomers) ppm 154.6, 154.3, 137.6, 136.9, 132.4, 132.3, 130.64, 130.60, 130.1, 129.9, 125.7, 125.4, 123.17, 123.15, 84.8, 81.3, 81.0, 57.5, 28.2, 28.1; HRMS (ESI): Exact mass calcd for  $\text{C}_{13}\text{H}_{16}\text{Br}_2\text{N}_2\text{NaO}_4$   $[\text{M}+\text{Na}]^+$  444.9374, found 444.9393.



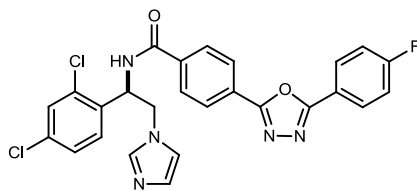
**(R)-N-(1-(2,4-Dichlorophenyl)-2-(1H-imidazol-1-yl)ethyl)-2-fluoronicotinamide**

**(188).** Prepared according to the general procedure.  $[\alpha]_D^{20} +4.0$  ( $c$  0.30,  $\text{CHCl}_3$ );  $R_f = 0.3$  (10% MeOH/ $\text{CH}_2\text{Cl}_2$ ); IR (film) 3287, 2923, 2853, 1650, 1605, 1609, 1572, 1548, 1510, 1432  $\text{cm}^{-1}$ ;  $^1\text{H}$  NMR (600 MHz,  $\text{CDCl}_3$ )  $\delta$  8.50 (ddd,  $J = 9.6, 7.6, 1.8$  Hz, 1H), 8.35 (d,  $J = 4.1$  Hz, 1H), 7.63-7.60 (br m, 1H), 7.48 (d,  $J = 2.1$  Hz, 1H), 7.38-7.36 (br m, 2H), 7.23 (dd,  $J = 8.3, 2.1$  Hz, 1H), 7.05 (d,  $J = 8.5$  Hz, 1H), 7.04 (br s, 1H), 6.82 (br s, 1H), 5.84 (ddd,  $J = 6.3, 6.3, 6.3$  Hz, 1H), 4.50 (dd,  $J = 14.4, 6.0$  Hz, 1H), 4.46 (dd,  $J = 14.3, 6.5$  Hz, 1H);  $^{13}\text{C}$  NMR (150 MHz,  $\text{CDCl}_3$ ) ppm 161.4 (d,  $J_{\text{CF}} = 7.4$  Hz), 160.0 (d,  $J_{\text{CF}} = 235$  Hz), 151.0 (d,  $J_{\text{CF}} = 16.7$  Hz), 143.5, 137.4, 135.3, 133.3 (d,  $J_{\text{CF}} = 14.5$  Hz), 130.4, 129.9, 129.4, 128.0, 122.7 (d,  $J_{\text{CF}} = 3.9$  Hz), 119.2, 115.1 (d,  $J_{\text{CF}} = 27.6$  Hz), 52.7, 49.3; HRMS (ESI): Exact mass calcd for  $\text{C}_{17}\text{H}_{14}\text{Cl}_2\text{FN}_4\text{O}$   $[\text{M}+\text{H}]^+$  379.0529, found 379.0538.



**(R)-N-(1-(2,4-Dichlorophenyl)-2-(1H-imidazol-1-yl)ethyl)-2,6-difluoronicotinamide**

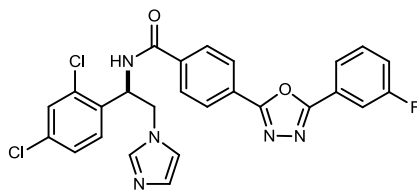
**(189)**. Prepared according to the general procedure.  $[\alpha]_D^{20} +6.6$  (*c* 0.65, CHCl<sub>3</sub>); *R<sub>f</sub>* = 0.3 (10% MeOH/CH<sub>2</sub>Cl<sub>2</sub>); IR (film) 3287, 1658, 1652, 1609, 1590, 1470, 1409 cm<sup>-1</sup>; <sup>1</sup>H NMR (600 MHz, CDCl<sub>3</sub>) δ 8.60 (ddd, *J* = 8.1, 8.1, 8.1 Hz, 1H), 7.48 (d, *J* = 2.1 Hz, 1H), 7.47-7.45 (br m, 1H), 7.30 (br s, 1H), 7.23 (dd, *J* = 8.3, 2.0 Hz, 1H), 7.04 (d, *J* = 8.3 Hz, 1H), 7.02 (br s, 1H), 6.99 (dd, *J* = 8.3, 2.2 Hz, 1H), 6.84 (br s, 1H), 5.81 (ddd, *J* = 7.8, 7.8, 7.8 Hz, 1H), 4.49 (dd, *J* = 14.4, 6.1 Hz, 1H), 4.44 (dd, *J* = 14.3, 6.6 Hz, 1H); <sup>13</sup>C NMR (150 MHz, CDCl<sub>3</sub>) ppm 162.8 (dd, *J<sub>CF</sub>* = 254, 17.8 Hz), 160.5 (d, *J<sub>CF</sub>* = 7.2 Hz), 158.3 (dd, *J<sub>CF</sub>* = 243, 15.4 Hz), 148.3 (d, *J<sub>CF</sub>* = 8.8 Hz), 137.4, 135.4, 133.4, 133.1, 130.5, 130.1, 129.4, 128.0, 119.2, 112.3 (dd, *J<sub>CF</sub>* = 24.9, 5.5 Hz), 108.0 (dd, *J<sub>CF</sub>* = 34.2, 5.4 Hz), 52.8, 49.2; HRMS (ESI): Exact mass calcd for C<sub>17</sub>H<sub>13</sub>Cl<sub>2</sub>F<sub>2</sub>N<sub>4</sub>O [M+H]<sup>+</sup> 397.0434, found 397.0439.



**(R)-N-(1-(2,4-Dichlorophenyl)-2-(1H-imidazol-1-yl)ethyl)-4-(5-(4-fluorophenyl)-**

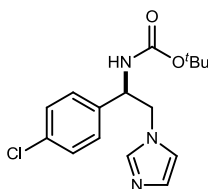
**1,3,4-oxadiazol-2-yl)benzamide (190).**  $[\alpha]_D^{20} +30$  (*c* 0.30, CHCl<sub>3</sub>); IR (film) 3255, 2925, 1661, 1551, 1495 cm<sup>-1</sup>; <sup>1</sup>H NMR (600 MHz, CDCl<sub>3</sub>) δ 8.21 (d, *J* = 8.3 Hz, 2H), 8.16 (dd, *J* = 8.9, 5.2 Hz, 2H), 7.89 (d, *J* = 8.3 Hz, 2H), 7.50 (d, *J* = 2.1 Hz, 1H), 7.34 (br s, 1H), 7.26-7.23 (m, 3H), 7.10 (d, *J* = 8.3 Hz, 1H), 7.05 (br s, 1H), 6.92 (d, *J* = 7.4 Hz, 1H), 6.85 (br s, 1H), 5.79 (ddd, *J* = 6.5, 6.5, 6.5 Hz, 1H), 4.54 (d, *J* = 6.4 Hz, 2H); <sup>13</sup>C NMR (150 MHz, CDCl<sub>3</sub>) ppm 166.0, 165.0 (d, *J*<sub>CF</sub> = 254 Hz), 164.3, 163.6, 137.5, 136.1, 135.4, 133.4 (d, *J*<sub>CF</sub> = 11.9 Hz), 130.5, 129.8, 129.4, 129.3, 128.0, 127.8, 127.3, 127.0, 119.9, 119.3, 116.7, 116.5, 53.0, 49.0; <sup>19</sup>F NMR (282 MHz, CDCl<sub>3</sub>) ppm -104; HRMS (ESI): Exact mass calcd for C<sub>26</sub>H<sub>19</sub>Cl<sub>2</sub>FN<sub>5</sub>O<sub>2</sub> [M+H]<sup>+</sup> 522.0900, found 522.0903.





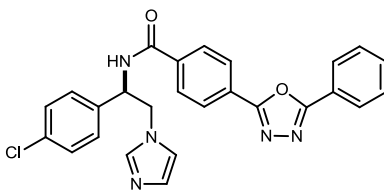
**(R)-N-(1-(2,4-Dichlorophenyl)-2-(1H-imidazol-1-yl)ethyl)-4-(5-(3-fluorophenyl)-**

**1,3,4-oxadiazol-2-yl)benzamide (191).**  $[\alpha]_D^{20} +47$  (*c* 0.27, CHCl<sub>3</sub>); IR (film) 3261, 1657, 1554, 1493 cm<sup>-1</sup>; <sup>1</sup>H NMR (600 MHz, CDCl<sub>3</sub>)  $\delta$  8.19 (d, *J* = 8.4 Hz, 2H), 7.94 (d, *J* = 7.8 Hz, 1H), 7.90 (d, *J* = 8.3 Hz, 2H), 7.84-7.83 (m, 1H), 7.53 (ddd, *J* = 8.1, 8.1, 5.6 Hz, 1H), 7.49 (d, *J* = 2.0 Hz, 1H), 7.33 (br s, 1H), 7.28 (ddd, *J* = 8.3, 8.3, 2.3 Hz, 1H), 7.25 (dd, *J* = 8.4, 2.0 Hz, 1H), 7.14 (d, *J* = 8.3 Hz, 1H), 7.13 (br s, 1H), 7.03 (br s, 1H), 6.87 (br s, 1H), 5.79 (ddd, *J* = 6.4, 6.4, 6.4 Hz, 1H), 4.56 (dd, *J* = 14.2, 6.6 Hz, 1H), 4.52 (dd, *J* = 14.2, 6.4 Hz, 1H); <sup>13</sup>C NMR (150 MHz, CDCl<sub>3</sub>) ppm 166.1, 164.1, 163.9, 162.8 (d, *J*<sub>CF</sub> = 248 Hz), 137.5, 136.3, 135.4, 133.4, 131.1 (d, *J*<sub>CF</sub> = 7.9 Hz), 130.4, 129.9, 129.7, 128.0, 127.9, 127.3, 126.8, 125.4 (d, *J*<sub>CF</sub> = 8.3 Hz), 122.8 (d, *J*<sub>CF</sub> = 3.3 Hz), 119.4, 119.2 (d, *J*<sub>CF</sub> = 21.3 Hz), 114.1 (d, *J*<sub>CF</sub> = 24.5 Hz), 52.9, 49.0; <sup>19</sup>F NMR (282 MHz, CDCl<sub>3</sub>) ppm -109; HRMS (ESI): Exact mass calcd for C<sub>26</sub>H<sub>19</sub>Cl<sub>2</sub>FN<sub>5</sub>O<sub>2</sub> [M+H]<sup>+</sup> 522.0900, found 522.0879.

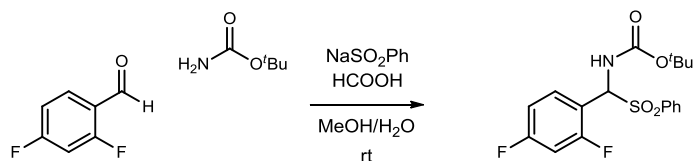


**(R)-tert-Butyl (1-(4-chlorophenyl)-2-(1H-imidazol-1-yl)ethyl)carbamate (192SI).**

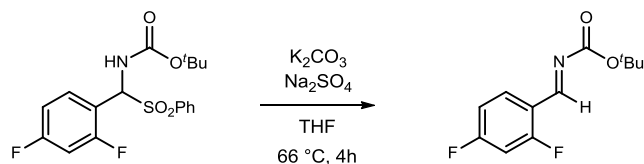
Recovered from large scale reduction of 2,4-dichloro adduct (10:1 mixture) and used in coupling reaction to make VNI analog.  $[\alpha]_D^{20}$  -19 (*c* 0.73, CHCl<sub>3</sub>); IR (film) 3211, 2978, 1703, 1509 cm<sup>-1</sup>; <sup>1</sup>H NMR (400 MHz, CDCl<sub>3</sub>)  $\delta$  7.31 (d, *J* = 8.5 Hz, 2H), 7.20 (s, 1H), 7.04 (d, *J* = 8.8 Hz, 2H), 6.99 (s, 1H), 6.69 (s, 1H), 4.97 (br s, 1H), 4.91 (br s, 1H), 4.30-4.25 (br m, 2H), 1.43 (s, 9H); <sup>13</sup>C NMR (100 MHz, CDCl<sub>3</sub>) ppm 154.9, 137.6, 136.8, 134.3, 129.5, 129.3, 127.8, 119.4, 80.6, 55.1, 51.6, 28.3; HRMS (ESI): Exact mass calcd for C<sub>16</sub>H<sub>21</sub>ClN<sub>3</sub>O<sub>2</sub> [M+H]<sup>+</sup> 322.1322, found 322.1312.



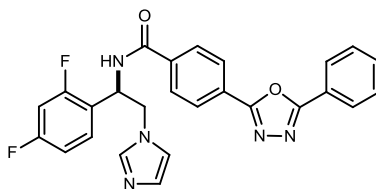
**(R)-N-(1-(4-Chlorophenyl)-2-(1H-imidazol-1-yl)ethyl)-4-(5-phenyl-1,3,4-oxadiazol-2-yl)benzamide (192).** Prepared according to the general procedure.  $[\alpha]_D^{20} +11$  ( $c$  0.19,  $\text{CHCl}_3$ );  $R_f = 0.3$  (10% MeOH/ $\text{CH}_2\text{Cl}_2$ ); mp 124-126 °C; IR (film) 3319, 2923, 1651, 1549, 1491  $\text{cm}^{-1}$ ;  $^1\text{H}$  NMR (400 MHz,  $\text{CDCl}_3$ )  $\delta$  8.15 (d,  $J = 7.8$  Hz, 1H), 8.04 (d,  $J = 7.0$  Hz, 2H), 7.98 (d,  $J = 8.3$  Hz, 2H), 7.84 (d,  $J = 8.4$  Hz, 2H), 7.56-7.47 (m, 3H), 7.32 (br s, 1H), 7.29 (s, 4H), 6.95 (br s, 1H), 6.90 (br s, 1H), 5.50 (ddd,  $J = 7.3, 7.3, 7.3$  Hz, 1H), 4.57 (dd,  $J = 14.1, 7.5$  Hz, 1H), 4.39 (dd,  $J = 14.0, 6.6$  Hz, 1H);  $^{13}\text{C}$  NMR (100 MHz,  $\text{CDCl}_3$ ) ppm 166.7, 165.0, 163.7, 137.6, 136.73, 136.71, 134.4, 132.1, 129.3, 129.1, 128.2, 128.1, 126.92, 126.86, 126.4, 123.3, 119.6, 54.4, 50.8; HRMS (ESI): Exact mass calcd for  $\text{C}_{26}\text{H}_{21}\text{ClN}_5\text{O}_2$   $[\text{M}+\text{H}]^+$  470.1384, found 470.1371.



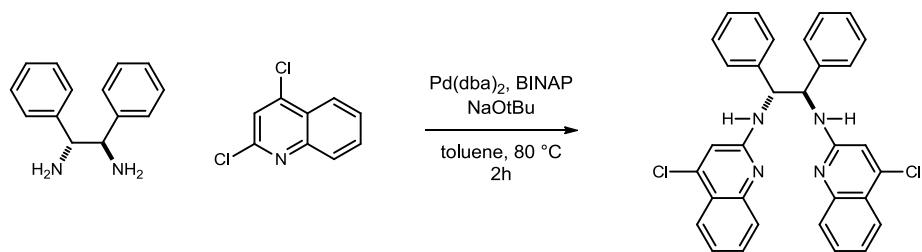
***tert*-Butyl ((2,4-difluorophenyl)(phenylsulfonyl)methyl)carbamate (193SI).** A 1-L round-bottomed flask was charged with 2,4-difluorobenzaldehyde (11.2 mL, 102 mmol), benzenesulfinic acid sodium salt (28.0 g, 170 mmol), *tert*-butyl carbamate (10.0 g, 85.4 mmol), formic acid (6.5 mL, 170 mmol), methanol (70 mL), and water (140 mL) and stirred for 3 days. The solid was filtered and rinsed with water. The washed solid was added to diethyl ether and stirred overnight. Filtration and washing with diethyl ether afforded the pure product as a white solid (28.7 grams, 88% yield). Mp 144-146 °C; IR (film) 3342, 2979, 1705, 1619, 1505 cm<sup>-1</sup>; <sup>1</sup>H NMR (600 MHz, CDCl<sub>3</sub>) δ 7.93 (d, *J* = 7.3 Hz, 2H), 7.66 (t, *J* = 7.3 Hz, 1H), 7.55 (d, *J* = 7.6, 7.6 Hz, 2H), 7.45 (ddd, *J* = 7.9, 7.9, 7.9 Hz, 1H), 6.96 (ddd, *J* = 8.1, 8.1, 1.9 Hz, 1H), 6.87 (ddd, *J* = 10.6, 8.7, 2.5 Hz, 1H), 6.19 (d, *J* = 10.9 Hz, 1H), 5.90 (d, *J* = 10.5 Hz, 1H), 1.27 (s, 9H); <sup>13</sup>C NMR (150 MHz, CDCl<sub>3</sub>) ppm 163.9 (dd, *J*<sub>CF</sub> = 253, 12.3 Hz), 161.4 (dd, *J*<sub>CF</sub> = 252, 11.7 Hz), 153.4, 136.5, 134.2, 131.3 (d, *J*<sub>CF</sub> = 10.3 Hz), 129.4, 129.2, 114.1 (d, *J*<sub>CF</sub> = 14.5 Hz), 112.1 (d, *J*<sub>CF</sub> = 20.0 Hz), 104.6 (dd, *J*<sub>CF</sub> = 25.7, 25.7 Hz), 81.5, 68.7, 28.0; <sup>19</sup>F NMR (282 MHz, CDCl<sub>3</sub>) ppm -104, -109 (d, *J*<sub>HF</sub> = 8.5 Hz); HRMS (ESI): decomposed to imine during analysis (*M* = 242).



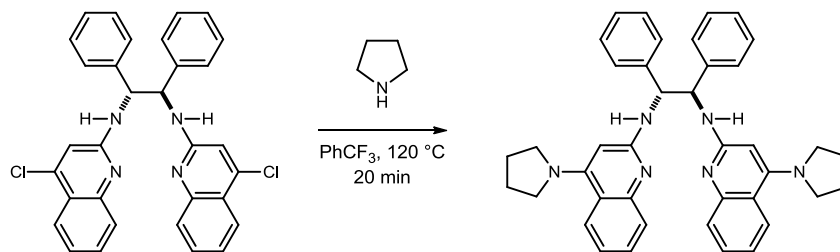
***tert*-Butyl 2,4-difluorobenzylidene carbamate (193SI).** A 500-mL round-bottomed flask was charged with *tert*-butyl ((2,4-difluorophenyl)(phenylsulfonyl)methyl)carbamate (11.9 g, 31.0 mmol), K<sub>2</sub>CO<sub>3</sub> (30.0 g, 217 mmol), Na<sub>2</sub>SO<sub>4</sub> (35.2 g, 248 mmol) and THF (260 mL). The pot was refluxed for 4 h until completion (checked by <sup>1</sup>H NMR). The reaction mixture was filtered through Celite, washed with diethyl ether and concentrated on low heat to yield the title compound as a colorless oil [7.15 g, 96% (<2% aldehyde)]. IR (film) 3079, 2982, 2936, 1718, 1619, 1502 cm<sup>-1</sup>; <sup>1</sup>H NMR (600 MHz, CDCl<sub>3</sub>) δ 9.08 (s, 1H), 8.16 (ddd, *J* = 8.5, 8.5, 6.7 Hz, 1H), 6.96 (ddd, *J* = 8.9, 8.9, 2.3 Hz, 1H), 6.88 (ddd, *J* = 10.7, 8.8, 2.4 Hz, 1H), 1.58 (s, 9H); <sup>13</sup>C NMR (150 MHz, CDCl<sub>3</sub>) ppm 166.5 (dd, *J*<sub>CF</sub> = 258, 12.5 Hz), 164.4 (dd, *J*<sub>CF</sub> = 260, 12.8 Hz), 162.3, 161.7 (d, *J*<sub>CF</sub> = 4.6 Hz), 130.2 (dd, *J*<sub>CF</sub> = 10.5, 3.1 Hz), 118.7 (dd, *J*<sub>CF</sub> = 8.9, 3.5 Hz), 112.6 (dd, *J*<sub>CF</sub> = 22.0, 3.3 Hz), 104.4 (dd, *J*<sub>CF</sub> = 25.0, 25.0 Hz), 82.7, 27.9; <sup>19</sup>F NMR (282 MHz, CDCl<sub>3</sub>) ppm -98, -112; HRMS (ESI): Exact mass calcd for C<sub>12</sub>H<sub>14</sub>F<sub>2</sub>NO<sub>2</sub> [M+H]<sup>+</sup> 242.0987, found 242.0989.



**(R)-N-(1-(2,4-Difluorophenyl)-2-(1*H*-imidazol-1-yl)ethyl)-4-(5-phenyl-1,3,4-oxadiazol-2-yl)benzamide (193, FF-VNI).** Prepared according to the general procedure.  $[\alpha]_D^{20} +18$  (*c* 0.20,  $\text{CHCl}_3$ );  $R_f = 0.28$  (10%  $\text{MeOH}/\text{CH}_2\text{Cl}_2$ ); IR (film) 3261, 3064, 1657, 1617, 1550, 1503  $\text{cm}^{-1}$ ;  $^1\text{H}$  NMR (600 MHz,  $\text{CDCl}_3$ )  $\delta$  8.17 (d,  $J = 8.2$  Hz, 2H), 8.13 (d,  $J = 6.9$  Hz, 2H), 7.90 (d,  $J = 8.2$  Hz, 2H), 7.59-7.52 (m, 3H), 7.32 (br d, 2H), 7.20 (ddd,  $J = 8.3, 8.3, 8.3$  Hz, 1H), 7.00 (br s, 1H), 6.91 (ddd,  $J = 10.9, 8.6, 2.3$  Hz, 1H), 6.87-6.84 (m, 2H), 5.67 (ddd,  $J = 7.2, 7.2, 7.2$  Hz, 1H), 4.54 (dd,  $J = 14.1, 6.8$  Hz, 1H), 4.39 (dd,  $J = 14.1, 7.0$  Hz, 1H);  $^{13}\text{C}$  NMR (150 MHz,  $\text{CDCl}_3$ ) ppm 166.2, 165.1, 163.6, 162.9 (dd,  $J_{\text{CF}} = 252, 12.5$  Hz), 160.8 (dd,  $J_{\text{CF}} = 247, 11.9$  Hz), 137.4, 136.2, 132.1, 130.4, 129.7, 129.2, 127.9, 127.1, 127.0, 126.9, 123.4, 120.6 (d,  $J_{\text{CF}} = 13.8$  Hz), 119.3, 112.2 (dd,  $J_{\text{CF}} = 21.3, 3.5$  Hz), 104.8 (dd,  $J_{\text{CF}} = 25.4, 25.4$  Hz), 51.2, 49.9;  $^{19}\text{F}$  NMR (282 MHz,  $\text{CDCl}_3$ ) ppm -106, -112; HRMS (ESI): Exact mass calcd for  $\text{C}_{26}\text{H}_{20}\text{F}_2\text{N}_5\text{O}_2$   $[\text{M}+\text{H}]^+$  472.1585, found 472.1572.



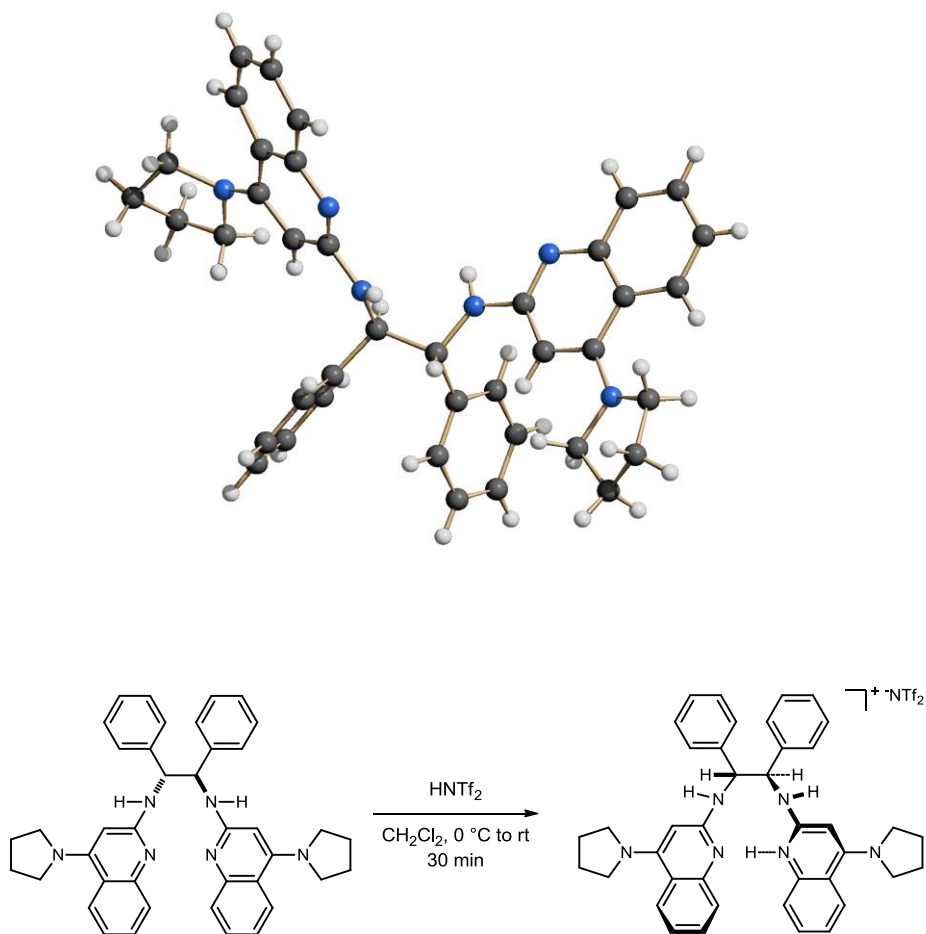
**<sup>4</sup>ClStilbBAM** ((1*R*,2*R*)-*N*1,*N*2-bis(4-Chloroquinolin-2-yl)-1,2-diphenylethane-1,2-diamine) (**115SI**). A 50-mL, round-bottomed flask equipped with a stir bar was charged with (1*R*,2*R*)-(+)-1,2-diphenylethylenediamine (859 mg, 4.00 mmol), Pd(dba)<sub>2</sub> (34 mg, 60 μmol), *rac*-BINAP (74 mg, 120 μmol), sodium *tert*-butoxide (961 mg, 10.0 mmol), and 2,4-dichloroquinoline (1.58 g, 8.00 mmol). The reaction vessel was placed under an argon atmosphere, toluene (23 mL) was dispensed into the flask, and the resulting solution was placed into an oil bath heated to 80 °C with stirring. The reaction was monitored by TLC and after 1 h nearly complete conversion was observed. The reaction was stirred for an additional 1 hour, and cooled to 25 °C, diluted with ethyl acetate, and filtered through plug of Celite. The organic mixture was concentrated and the crude solid was triturated with 40 mL of a benzene/pentane (25/75) mixture. The solid was filtered and dried under vacuum to give a light yellow solid (1.70 g, 79%), which was used in the next step without further purification.  $R_f = 0.45$  (20% EtOAc/hexanes);  $[\alpha]_D^{20} +3.3$  ( $c$  1.0, CHCl<sub>3</sub>); IR (film) 3239, 3060, 1602 cm<sup>-1</sup>; <sup>1</sup>H NMR (45 °C, 600 MHz, CDCl<sub>3</sub>)  $\delta$  7.96 (d,  $J = 8.4$  Hz, 2H), 7.83 (br s, 2H), 7.63 (dd,  $J = 7.8, 7.2$  Hz, 2H), 7.30 (dd,  $J = 7.8, 7.2$  Hz, 2H), 7.23-7.18 (m, 10H), 6.56 (br s, 2H), 6.31 (br s, 2H), 5.62 (br s, 2H); <sup>13</sup>C NMR (45 °C, 150 MHz, CDCl<sub>3</sub>) ppm 156.5, 148.4, 142.9, 140.0, 130.5, 128.4, 127.8, 127.6, 126.4, 124.3, 122.8, 121.9, 111.7, 62.1; HRMS (ESI): Exact mass calcd for C<sub>32</sub>H<sub>25</sub>Cl<sub>2</sub>N<sub>4</sub> [M+H]<sup>+</sup> 535.1456, found 535.1432.



**StilbPBAM (115) [(1*R*,2*R*)-1,2-Diphenyl-*N*1,*N*2-bis(4-(pyrrolidin-1-yl)quinolin-2-yl)ethane-1,2-diamine] (115)** /updated from submitted manuscript. A 2-5 mL microwave vial equipped with a stir bar was charged with <sup>4</sup>ClStilb-BAM (803 mg, 1.50 mmol), pyrrolidine (493  $\mu$ L, 6.00 mmol), and trifluoromethylbenzene (1.5 mL). The vial was sealed, and this suspension was heated with stirring at 120  $^{\circ}$ C in the microwave for 10+10 min. The reaction mixture was diluted with dichloromethane and transferred to a round-bottomed flask for evaporation. Flash column chromatography (SiO<sub>2</sub>, 2-5-10% methanol in dichloromethane) yielded a brown solid that was washed with 3M NaOH to give a yellow solid (707 mg, 78%).  $R_f = 0.66$  (20% MeOH/CH<sub>2</sub>Cl<sub>2</sub>);  $[\alpha]_D^{20} +92$  ( $c$  1.0, CHCl<sub>3</sub>); IR (film) 3238, 3060, 2971, 1584 cm<sup>-1</sup>; <sup>1</sup>H NMR (50  $^{\circ}$ C, 600 MHz, CDCl<sub>3</sub>)  $\delta$  7.90 (d,  $J = 6.6$  Hz, 2H), 7.75 (br s, 2H), 7.43 (dd,  $J = 7.2, 7.2$  Hz, 2H), 7.30 (br s, 4H), 7.26 (s, 2H), 7.19 (br m, 4H), 7.14 (d,  $J = 6.6$  Hz, 2H), 7.02 (br s, 2H), 5.52 (br m, 4H), 3.33 (br s, 4H), 3.22 (br s, 4H), 1.86 (s, 8H); <sup>13</sup>C NMR (150 MHz, CDCl<sub>3</sub>) 157.7, 153.5, 149.7, 141.4, 128.3, 128.0, 127.9, 126.8, 126.6, 124.7, 119.3, 118.6, 92.0, 62.1, 51.5, 25.5 ppm; HRMS (ESI): Exact mass calcd for C<sub>40</sub>H<sub>41</sub>N<sub>6</sub> [M+H]<sup>+</sup> 605.3393, found 605.3372. A crystal structure of the catalyst dimer was obtained. See Appendix.

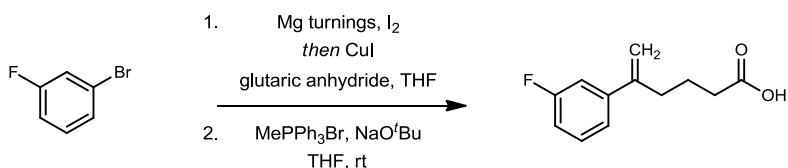


**FIGURE S1.** Crystal Structure of StilbPBAM. See Appendix for complete details.



**StilbPBAM•HNTf<sub>2</sub> (115•HNTf<sub>2</sub>)** A flame dried vial equipped with a stir bar was charged with bistrifluoromethanesulfonimide (141 mg, 500 μmol) and dichloromethane (5 mL), cooled to 0 °C , and Stilb-PBAM (302 mg, 500 μmol) was added. The solution was stirred for 30 minutes before the solvent was removed *in vacuo* to give the catalyst as a beige solid that was used without any purification. *Other acid salts used in reaction optimization were made in a similar fashion using the corresponding acids and equivalents.*

**Preparation of unsaturated acids.** Known compounds were synthesized according to known procedures. A modified procedure (from Ishihara<sup>131</sup> and Rovis<sup>132</sup>) was used to synthesize the keto-acids using an organocuprate addition to minimize double aryllithium addition leading to the alcohol.



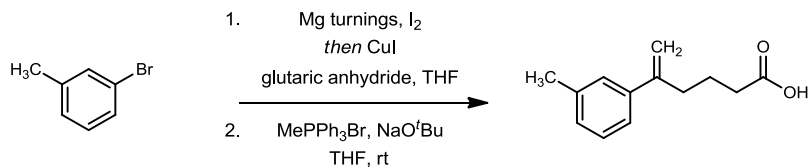
**5-(3-Fluorophenyl)hex-5-enoic acid (270f).** A flame dried, round-bottomed flask, equipped with a stir bar and condenser, was charged with magnesium turnings (0.292 g, 12.0 mmol) and a catalytic amount of iodine. A small amount of heat was applied to produce iodine vapor and tetrahydrofuran (15 mL) was added, followed by dropwise addition of 3-bromofluorobenzene (1.75 g, 10.0 mmol). After a mild reflux, the reaction was allowed to cool to room temperature. The Grignard reagent was then transferred via cannulation to a suspension of copper(I) iodide (952 mg, 5.00 mmol) in tetrahydrofuran (10 mL) at 0 °C. The solution was stirred for 1 hour at room temperature, then cooled to 0 °C before addition of glutaric anhydride (571 mg, 5.00 mmol). The reaction was warmed to room temperature and stirred for 1.5 h, then quenched with 3M HCl and concentrated *in vacuo* to remove tetrahydrofuran. The aqueous layer was diluted with diethyl ether and filtered into a separatory funnel. The aqueous layer was extracted with diethyl ether and the combined organic layers were washed with brine and dried over magnesium sulfate.

<sup>131</sup> Uyanik, M.; Yasui, T.; Ishihara, K. *Bioorg. Med. Chem. Lett.* **2009**, *19*, 3848-3851.

<sup>132</sup> Kütt, A.; Rodima, T.; Saame, J.; Raamat, E.; Mäemets, V.; Kaljurand, I.; Koppel, I. A.; Garlyauskayte, R. Y.; Yagupolskii, Y. L.; Yagupolskii, L. M.; Bernhardt, E.; Willner, H.; Leito, I. *J. Org. Chem.* **2011**, *76*, 391-395.

Flash column chromatography (SiO<sub>2</sub>, 10-30-50% ethyl acetate in hexanes) yielded a colorless oil (0.90 g, 86%) that was determined to be >90% pure (contaminated with double Grignard addition product) and used without further purification. R<sub>f</sub> = 0.10 (50% EtOAc/hexanes).

The title compound was prepared according to the general procedure described by Hartwig<sup>133</sup> using the synthetic keto-acid. Flash column chromatography (SiO<sub>2</sub>, 10-25-40% ethyl acetate in hexanes) yielded a colorless solid (0.24 g, 73%). R<sub>f</sub> = 0.33 (50% EtOAc/hexanes) visualized with CAM; IR (film) 3083, 2931, 1708 cm<sup>-1</sup>; <sup>1</sup>H NMR (400 MHz, CDCl<sub>3</sub>) δ 7.28 (ddd, *J* = 7.9, 7.9, 6.2 Hz, 1H), 7.17 (d, *J* = 7.8 Hz, 1H), 7.09 (ddd, *J* = 10.5, 2.2, 2.2 Hz, 1H), 6.97 (ddd, *J* = 8.2, 8.2, 2.0 Hz, 1H), 5.34 (s, 1H), 5.12 (s, 1H), 2.55 (t, *J* = 7.6 Hz, 2H), 2.39 (t, *J* = 7.4 Hz, 2H), 1.80 (tt, *J* = 7.5, 7.5 Hz, 2H); <sup>13</sup>C NMR (100 MHz, CDCl<sub>3</sub>) ppm 179.6, 162.9 (d, <sup>1</sup>*J*<sub>CF</sub> = 244 Hz), 146.2, 143.1 (d, <sup>3</sup>*J*<sub>CF</sub> = 8.0 Hz), 129.8 (d, <sup>3</sup>*J*<sub>CF</sub> = 8.0 Hz), 121.7 (d, <sup>4</sup>*J*<sub>CF</sub> = 2.0 Hz), 114.2 (d, <sup>2</sup>*J*<sub>CF</sub> = 21 Hz), 114.1, 113.0 (d, <sup>2</sup>*J*<sub>CF</sub> = 22 Hz), 34.3, 33.2, 22.9; <sup>19</sup>F NMR (282 MHz, CDCl<sub>3</sub>) ppm -111.6 (dd, *J*<sub>HF</sub> = 14.1, 8.5 Hz); HRMS (ESI): Exact mass calcd for C<sub>12</sub>H<sub>13</sub>FNaO<sub>2</sub> [M+Na]<sup>+</sup> 208.0894, found 208.0888.

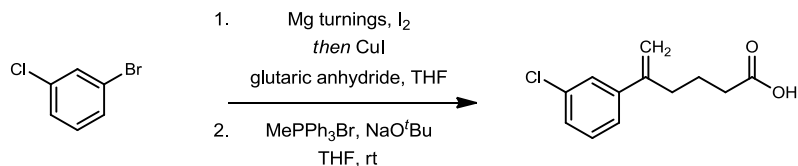


**5-(*m*-Tolyl)hex-5-enoic acid (270k).** A flame dried, round-bottomed flask, equipped with a stir bar and condenser, was charged with magnesium turnings (0.92 g, 38 mmol) and a catalytic amount of iodine. A small amount of heat was applied to produce iodine vapor and tetrahydrofuran (15 mL) was added, followed by dropwise addition of *meta*-bromotoluene (1.21 mL, 10.0 mmol). After a mild reflux, the reaction was allowed to cool to room temperature. The Grignard reagent was then transferred via cannulation to a suspension of copper(I) iodide (950 mg, 5.00 mmol) in tetrahydrofuran (10 mL) at 0 °C. The solution was stirred for 1 hour at room temperature, then cooled to 0 °C before addition of glutaric anhydride (571 mg, 5.00 mmol). The reaction was warmed to room temperature and stirred for 1.5 h, then quenched with 3M HCl and concentrated *in vacuo* to remove tetrahydrofuran. The aqueous layer was diluted with diethyl ether and filtered into a separatory funnel. The aqueous layer was extracted with diethyl ether and the combined organic layers were washed with brine and dried over magnesium sulfate. Flash column chromatography (SiO<sub>2</sub>, 10-30-50% ethyl acetate in hexanes) yielded a colorless oil (158 mg, 15%) that was determined to be >90% pure (contaminated with double Grignard addition product) and used without further purification. R<sub>f</sub> = 0.16 (50% EtOAc/hexanes).

The title compound was prepared according to the general procedure described by Hartwig<sup>133</sup> using the synthetic keto-acid. Flash column chromatography (SiO<sub>2</sub>, 10-25-50% ethyl acetate in hexanes) yielded a colorless oil (88 mg, 72%).  $R_f = 0.40$  (50% EtOAc/hexanes) visualized with CAM; IR (film) 3081, 2928, 1708 cm<sup>-1</sup>; <sup>1</sup>H NMR (400 MHz, CDCl<sub>3</sub>)  $\delta$  7.24-7.18 (m, 3H), 7.09 (d,  $J = 6.7$  Hz, 1H), 5.29 (d,  $J = 1.1$  Hz, 1H), 5.06 (d,  $J = 1.1$  Hz, 1H), 2.57 (t,  $J = 7.6$  Hz, 2H), 2.38 (t,  $J = 7.4$  Hz, 2H), 2.36 (s, 3H), 1.80 (tt,  $J = 7.5, 7.5$  Hz, 2H); <sup>13</sup>C NMR (100 MHz, CDCl<sub>3</sub>) ppm 179.6, 147.4, 140.7, 137.9, 128.23, 128.22, 126.9, 123.2, 112.9, 34.5, 33.2, 23.0, 21.5; HRMS (ESI): Exact mass calcd for C<sub>13</sub>H<sub>16</sub>O<sub>2</sub> [M+H]<sup>+</sup> 204.1145, found 204.1146.

---

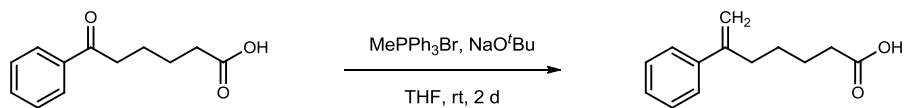
<sup>133</sup> Hatano, M.; Maki, T.; Moriyama, K.; Arinobe, M.; Ishihara, K. *J. Am. Chem. Soc.* **2008**, *130*, 16858-16860.



**5-(3-Chlorophenyl)hex-5-enoic acid (270g).** A flame dried, round-bottomed flask, equipped with a stir bar and condenser, was charged with magnesium turnings (0.466 g, 19.2 mmol) and a catalytic amount of iodine. A small amount of heat was applied to produce iodine vapor and tetrahydrofuran (20 mL) was added, followed by dropwise addition of 3-chlorofluorobenzene (3.06 g, 16.0 mmol). After a mild reflux, the reaction was allowed to cool to room temperature. The Grignard reagent was then transferred via cannulation to a suspension of copper(I) iodide (1.52 g, 8.00 mmol) in tetrahydrofuran (10 mL) at 0 °C. The solution was stirred for 1 hour at room temperature, then cooled to 0 °C before addition of glutaric anhydride (912 mg, 8.00 mmol). The reaction was warmed to room temperature and stirred for 1.5 h, then quenched with 3M HCl and concentrated *in vacuo* to remove tetrahydrofuran. The aqueous layer was diluted with diethyl ether and filtered into a separatory funnel. The aqueous layer was extracted with diethyl ether and the combined organic layers were washed with brine and dried over magnesium sulfate. Flash column chromatography (SiO<sub>2</sub>, 10-30-50% ethyl acetate in hexanes) yielded a colorless oil (0.40 g, 22%) that was determined to be >90% pure (contaminated with double Grignard addition product) and used without further purification. R<sub>f</sub> = 0.20 (60% EtOAc/hexanes).

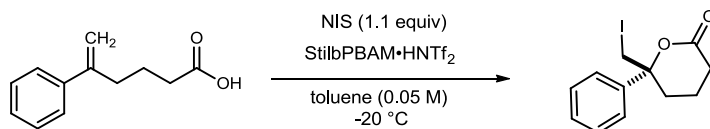
The title compound was prepared according to the general procedure described by Hartwig<sup>133</sup> using the synthetic keto-acid. Flash column chromatography (SiO<sub>2</sub>, 10-20-50% ethyl acetate in hexanes) yielded a white solid (0.25 g, 78%). R<sub>f</sub> = 0.12 (50%

EtOAc/hexanes) visualized with CAM; IR (film) 3414, 2934, 1708  $\text{cm}^{-1}$ ;  $^1\text{H}$  NMR (400 MHz,  $\text{CDCl}_3$ )  $\delta$  7.38 (s, 1H), 7.27-7.24 (m, 3H), 5.33 (s, 1H), 5.12 (s, 1H), 2.54 (t,  $J = 7.4$  Hz, 2H), 2.39 (t,  $J = 7.4$  Hz, 2H), 1.79 (tt,  $J = 7.4, 7.4$  Hz, 2H);  $^{13}\text{C}$  NMR (100 MHz,  $\text{CDCl}_3$ ) ppm 179.9, 146.2, 142.6, 134.3, 129.6, 127.5, 126.3, 124.2, 114.2, 34.3, 33.2, 22.9; HRMS (EI): Exact mass calcd for  $\text{C}_{12}\text{H}_{13}\text{ClO}_2$   $[\text{M}]^+$  224.0599, found 224.0597.



**6-Phenylhept-6-enoic acid (270c).** The title compound was prepared according to the general procedure described by Hartwig using the commercial keto-acid. Flash column chromatography (SiO<sub>2</sub>, 10-40% ethyl acetate in hexanes) yielded a white solid (1.92 g, 94%). Mp 52-53 °C; *R<sub>f</sub>* = 0.46 (50% EtOAc/hexanes); IR (film) 3033, 2933, 1698 cm<sup>-1</sup>; <sup>1</sup>H NMR (400 MHz, CDCl<sub>3</sub>) δ 7.39 (d, *J* = 7.2 Hz, 2H), 7.31 (dd, *J* = 7.7, 7.0 Hz, 2H), 7.25 (t, *J* = 7.3 Hz, 1 H), 5.27 (s, 1H), 5.06 (s, 1H), 2.53 (t, *J* = 7.5 Hz, 2H), 2.34 (t, *J* = 7.6 Hz, 2H), 1.67 (dt, *J* = 15.2, 7.6 Hz, 2H), 1.50 (dt, *J* = 15.2 Hz, 7.6 Hz, 2H); <sup>13</sup>C NMR (100 MHz, CDCl<sub>3</sub>) ppm 180.2, 148.0, 141.1, 128.3, 127.3, 126.1, 112.5, 34.9, 33.8, 27.5, 24.2; HRMS (CI): Exact mass calcd for C<sub>13</sub>H<sub>16</sub>O<sub>2</sub> [M]<sup>+</sup> 204.1145, found 204.1147.

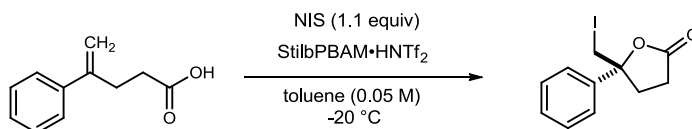




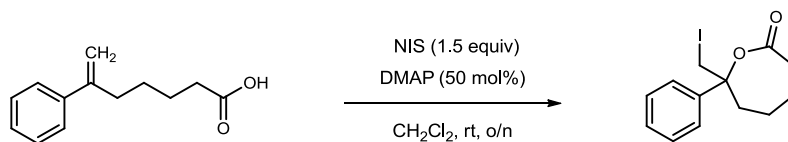
**General procedure for enantioselective esterifications:** To a flame dried vial equipped with a stir bar was added PBAM•HNTf<sub>2</sub> (4.4 mg, 2.0 μmol), 5-phenylhex-5-enoic acid (19.0 mg, 100 μmol) and toluene (2 mL), and the reaction was cooled to -20 °C. NIS (23.3 mg, 104 μmol) was added and the reaction mixture was stirred without light for 12 h. The mixture was treated with 20% aq sodium thiosulfate (2 mL) and then partitioned between dichloromethane (15 mL) and 3 M NaOH (15 mL). The aqueous layer was extracted twice and the organic layers were combined, dried over magnesium sulfate and concentrated. Flash column chromatography (SiO<sub>2</sub>, 10-25-50% ethyl acetate in hexanes) yielded an oil (30 mg, 95%). The product was determined to be 98% ee by chiral HPLC analysis (Chiralcel OD-H, 15% <sup>i</sup>PrOH/hexanes, 1 mL/min, *t<sub>r</sub>*(*e*<sub>1</sub>, minor) = 9.1 min, *t<sub>r</sub>*(*e*<sub>2</sub>, major) = 12.0 min); *R<sub>f</sub>* = 0.30 (25% EtOAc/hexanes) visualized with CAM; [*α*]<sub>D</sub><sup>20</sup> -27 (*c* 1.2, CHCl<sub>3</sub>); Remainder of physical data matched with literature values.<sup>134</sup>

<sup>134</sup> Shackleford, J. P.; Shen, B.; Johnston, J. N. *Proc. Natl. Acad. Sci. U. S. A.* **2012**, *109*, 44-46.

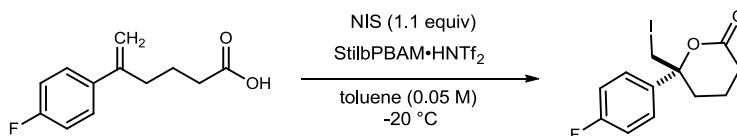
**General procedure for racemic esterification:** To a flame dried vial equipped with a stir bar was added DMAP (2.4 mg, 2.0  $\mu\text{mol}$ ), 5-phenylhex-5-enoic acid (19.0 mg, 100  $\mu\text{mol}$ ) and dichloromethane (1 mL). NIS (31.3 mg, 0.140 mmol) was added and the reaction mixture was stirred without light for 30 min at room temperature. The mixture was treated with 20% aq sodium thiosulfate (2 mL) and then partitioned between dichloromethane (15 mL) and 3 M NaOH (15 mL). The aqueous layer was extracted twice and the organic layers were combined, dried over magnesium sulfate and concentrated. The mixture was dissolved in dichloromethane and passed through a pipet silica plug with 5 mL of mobile phase (50% EtOAc/hexanes). The solvent was removed *in vacuo* to give the product.



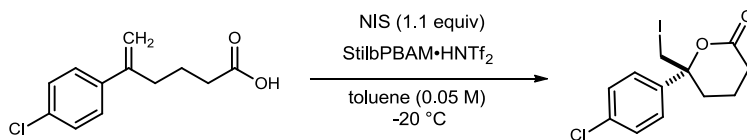
**(R)-5-(Iodomethyl)-5-phenyldihydrofuran-2(3H)-one (271b).** Prepared according to the general procedure using 4-phenylpent-4-enoic acid<sup>132</sup> (17.6 mg, 0.100 mmol), PBAM•HNTf<sub>2</sub> (4.4 mg, 5.0 μmol) and NIS (24.6 mg, 0.110 mmol) over 24 hours. Flash column chromatography (SiO<sub>2</sub>, 10-25-50% ethyl acetate in hexanes) yielded a colorless oil (30 mg, 99%). The product was determined to be 67% ee by chiral HPLC analysis (Chiralcel AD-H, 10% *i*PrOH/hexanes, 1 mL/min, *t*<sub>r</sub>(*e*<sub>1</sub>, major) = 9.0 min, *t*<sub>r</sub>(*e*<sub>2</sub>, minor) = 10.0 min); *R*<sub>f</sub> = 0.31 (50% EtOAc/hexanes) visualized with CAM. Remainder of physical data matched with literature values.<sup>134</sup>



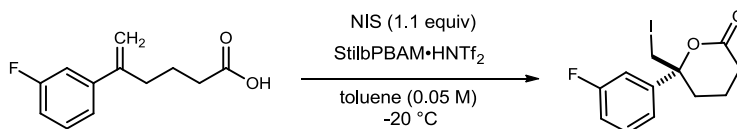
**7-(Iodomethyl)-7-phenyloxepan-2-one (271c).** To a flame dried vial equipped with a stir bar was added DMAP (6 mg, 50  $\mu\text{mol}$ ), 6-phenylhept-6-enoic acid (20 mg, 100  $\mu\text{mol}$ ) and dichloromethane (1 mL). NIS (34 mg, 0.15 mmol) was added and the reaction was stirred without light for 16 h. The reaction was quenched with 2 mL of 20% aq sodium thiosulfate. The mixture was treated with 20% aq sodium thiosulfate (3 mL) and then partitioned between dichloromethane (15 mL) and 3 M NaOH (15 mL). The aqueous layer was extracted twice and the organic layers were combined, dried over magnesium sulfate and concentrated. Flash column chromatography ( $\text{SiO}_2$ , 3-20% ethyl acetate in hexanes) yielded a yellow oil (15 mg, 45%). Chiral HPLC analysis revealed two peaks of equal area (Chiralcel AD-H, 10% *i*PrOH/hexanes, 1 mL/min,  $t_r(e_1) = 8.2$  min,  $t_r(e_2) = 9.3$  min);  $R_f = 0.37$  (20% EtOAc/hexanes) visualized with CAM; IR (film) 3451, 2931, 2860, 1727  $\text{cm}^{-1}$ ;  $^1\text{H NMR}$  (400 MHz,  $\text{CDCl}_3$ )  $\delta$  7.43 (dd,  $J = 7.7, 6.9$  Hz, 2H), 7.36 (t,  $J = 7.2$  Hz, 1H), 7.33 (d,  $J = 7.0$  Hz, 2H), 3.53 (d,  $J = 10.6$  Hz, 1H), 3.42 (d,  $J = 10.6$  Hz, 1H), 2.66 (ddd,  $J = 15.6, 3.1, 3.1$  Hz, 1H), 2.59-2.53 (m, 1H), 2.39 (ddd,  $J = 16.0, 12.9, 3.3$  Hz, 1H), 1.97 (ddd,  $J = 13.4, 13.4, 2.4$  Hz, 1H), 1.92-1.51 (m, 4H);  $^{13}\text{C NMR}$  (100 MHz,  $\text{CDCl}_3$ ) ppm 174.3, 138.9, 129.2, 128.4, 126.0, 82.9, 37.3, 36.6, 24.4, 22.8, 21.2; HRMS (ESI): Exact mass calcd for  $\text{C}_{13}\text{H}_{15}\text{INaO}_2$   $[\text{M}]^+$  353.0015, found 353.0003.



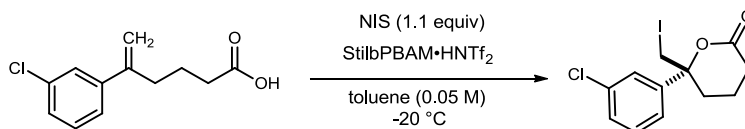
**(R)-6-(4-Fluorophenyl)-6-(iodomethyl)tetrahydro-2H-pyran-2-one (271d).** Prepared according to the general procedure using 4-(4-fluorophenyl)hex-5-enoic acid<sup>134</sup> (20.8 mg, 0.100 mmol), PBAM•HNTf<sub>2</sub> (4.4 mg, 5.0 μmol) and NIS (24.6 mg, 0.110 mmol) over 24 hours. Flash column chromatography (SiO<sub>2</sub>, 10-25-50% ethyl acetate in hexanes) yielded a yellow solid (32 mg, 96%). The product was determined to be 98% ee by chiral HPLC analysis (Chiralcel AD-H, 10% *i*PrOH/hexanes, 1 mL/min, *t*<sub>r</sub>(*e*<sub>1</sub>, minor) = 10.6 min, *t*<sub>r</sub>(*e*<sub>2</sub>, major) = 11.9 min); *R*<sub>f</sub> = 0.50 (50% EtOAc/hexanes) visualized with CAM. Remainder of physical data matched with literature values.<sup>134</sup>



**(R)-6-(4-Chlorophenyl)-6-(iodomethyl)tetrahydro-2H-pyran-2-one (271e).** Prepared according to the general procedure using 5-(4-chlorophenyl)hex-5-enoic acid<sup>134</sup> (22.5 mg, 0.100 mmol), PBAM•HNTf<sub>2</sub> (4.4 mg, 5.0 μmol) and NIS (24.6 mg, 0.110 mmol) over 24 hours. Flash column chromatography (SiO<sub>2</sub>, 10-25-50% ethyl acetate in hexanes) yielded a yellow solid (32 mg, 91%). The product was determined to be 97% ee by chiral HPLC analysis (Chiralcel AD-H, 10% *i*PrOH/hexanes, 1 mL/min, *t*<sub>r</sub>(*e*<sub>1</sub>, minor) = 10.4 min, *t*<sub>r</sub>(*e*<sub>2</sub>, major) = 13.0 min); *R*<sub>f</sub> = 0.27 (25% EtOAc/hexanes) visualized with CAM. Remainder of physical data matched with literature values.<sup>134</sup>

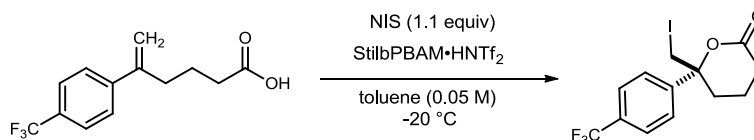


**(R)-6-(3-Fluorophenyl)-6-(iodomethyl)tetrahydro-2H-pyran-2-one (271f).** Prepared according to the general procedure using 5-(3-fluorophenyl)hex-5-enoic acid (20.8 mg, 0.100 mmol), PBAM•HNTf<sub>2</sub> (4.4 mg, 5.0 μmol) and NIS (24.6 mg, 0.110 mmol) over 48 hours. Flash column chromatography (SiO<sub>2</sub>, 10-25-50% ethyl acetate in hexanes) yielded an oil (17 mg, 52%). The product was determined to be 96% ee by chiral HPLC analysis (Chiralcel OD-H, 10% <sup>i</sup>PrOH/hexanes, 1 mL/min, *t<sub>r</sub>*(*e*<sub>1</sub>, minor) = 12.2 min, *t<sub>r</sub>*(*e*<sub>2</sub>, major) = 15.0 min); *R<sub>f</sub>* = 0.47 (50% EtOAc/hexanes) visualized with CAM; [ $\alpha$ ]<sub>D</sub><sup>20</sup> -23 (*c* 0.80, CHCl<sub>3</sub>); IR (film) 2958, 1740 cm<sup>-1</sup>; <sup>1</sup>H NMR (400 MHz, CDCl<sub>3</sub>)  $\delta$  7.37 (ddd, *J* = 8.0, 8.0, 6.0 Hz, 1H), 7.14 (dd, *J* = 7.9 Hz, 0.2 Hz, 1H), 7.09 (ddd, *J* = 10.0, 2.1, 2.1 Hz, 1H), 7.05 (ddd, *J* = 8.7, 8.7, 2.4 Hz, 1H), 3.55 (s, 2H), 2.55-2.30 (m, 4H), 1.85 (dddd, *J* = 13.6, 8.4, 4.4, 4.4 Hz, 1H), 1.64-1.53 (m, 1H); <sup>13</sup>C NMR (100 MHz, CDCl<sub>3</sub>) ppm 169.9, 163.0 (d, <sup>1</sup>*J*<sub>CF</sub> = 247 Hz), 143.0 (d, <sup>3</sup>*J*<sub>CF</sub> = 7.0 Hz), 130.6 (d, <sup>3</sup>*J*<sub>CF</sub> = 8.0 Hz), 120.9 (d, <sup>4</sup>*J*<sub>CF</sub> = 3.0 Hz), 115.4 (d, <sup>2</sup>*J*<sub>CF</sub> = 19 Hz), 112.7 (d, <sup>2</sup>*J*<sub>CF</sub> = 17 Hz), 84.0, 32.1, 29.0, 16.8, 16.5; <sup>19</sup>F NMR (282 MHz, CDCl<sub>3</sub>) ppm -109.1 (dd, *J*<sub>HF</sub> = 14.1, 8.5 Hz); HRMS (ESI): Exact mass calcd for C<sub>12</sub>H<sub>12</sub>FINaO<sub>2</sub> [M+Na]<sup>+</sup> 356.9764, found 356.9781.



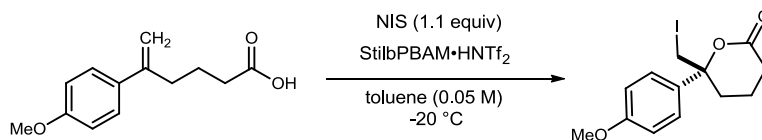
**(R)-6-(3-Chlorophenyl)-6-(iodomethyl)tetrahydro-2H-pyran-2-one (271g).** Prepared according to the general procedure using 5-(3-chlorophenyl)hex-5-enoic acid (22.5 mg, 0.100 mmol), PBAM•HNTf<sub>2</sub> (4.4 mg, 5.0 μmol) and NIS (24.6 mg, 0.110 mmol) over 48 hours. Flash column chromatography (SiO<sub>2</sub>, 10-25-50% ethyl acetate in hexanes) yielded an oil (18 mg, 51%). The product was determined to be 97% ee by chiral HPLC analysis (Chiralcel OD-H, 10% <sup>i</sup>PrOH/hexanes, 1 mL/min, *t<sub>r</sub>*(*e*<sub>1</sub>, minor) = 12.0 min, *t<sub>r</sub>*(*e*<sub>2</sub>, major) = 13.9 min); *R<sub>f</sub>* = 0.62 (50% EtOAc/hexanes) visualized with CAM; [*α*]<sub>D</sub><sup>20</sup> -20 (*c* 0.75, CHCl<sub>3</sub>); IR (film) 2925, 1740 cm<sup>-1</sup>; <sup>1</sup>H NMR (400 MHz, CDCl<sub>3</sub>) δ 7.37-7.31 (m, 3H), 7.29-7.25 (m, 1H), 3.54 (s, 2H), 2.55-2.30 (m, 4H), 1.85 (dddd, *J* = 13.7, 8.5, 4.2, 4.2, 4.2 Hz, 1H), 1.65-1.57 (m, 1H); <sup>13</sup>C NMR (100 MHz, CDCl<sub>3</sub>) ppm 169.8, 142.4, 135.1, 130.3, 128.7, 125.6, 123.5, 83.9, 32.1, 29.0, 16.9, 16.5; HRMS (ESI): Exact mass calcd for C<sub>12</sub>H<sub>12</sub>ClINaO<sub>2</sub> [M+Na]<sup>+</sup> 372.9468, found 372.9482.





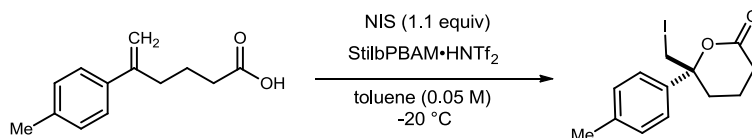
**(R)-6-(Iodomethyl)-6-(4-(trifluoromethyl)phenyl)tetrahydro-2H-pyran-2-one (271h).**

Prepared according to the general procedure using 5-(4-(trifluoromethyl)phenyl)hex-5-enoic acid<sup>135</sup> (25.8 mg, 0.100 mmol), PBAM•HNTf<sub>2</sub> (4.4 mg, 5.0 μmol) and NIS (24.6 mg, 0.110 mmol) over 48 hours. Flash column chromatography (SiO<sub>2</sub>, 10-25-50% ethyl acetate in hexanes) yielded a yellow oil (10 mg, 26%). The product was determined to be 96% ee by chiral HPLC analysis (Chiralcel AD-H, 7% <sup>i</sup>PrOH/hexanes, 1 mL/min, *t<sub>r</sub>*(*e*<sub>1</sub>, minor) = 10.4 min, *t<sub>r</sub>*(*e*<sub>2</sub>, major) = 14.0 min); *R<sub>f</sub>* = 0.53 (50% EtOAc/hexanes) visualized with CAM; [ $\alpha$ ]<sub>D</sub><sup>20</sup> -14 (*c* 0.55, CHCl<sub>3</sub>); IR (film) 2926, 1741 cm<sup>-1</sup>; <sup>1</sup>H NMR (400 MHz, CDCl<sub>3</sub>)  $\delta$  7.67 (d, *J* = 8.4 Hz, 2H), 7.51 (d, *J* = 8.4 Hz, 2H), 3.56 (s, 2H), 2.57-2.33 (m, 4H), 1.86 (dddd, *J* = 13.6, 8.0, 4.0, 4.0, 4.0 Hz, 1H), 1.63-1.55 (m, 1H); <sup>13</sup>C NMR (100 MHz, CDCl<sub>3</sub>) ppm 169.7, 144.4, 130.7 (q, <sup>2</sup>*J*<sub>CF</sub> = 33 Hz), 126.0 (q, <sup>3</sup>*J*<sub>CF</sub> = 4.0 Hz), 125.8, 123.7 (q, <sup>1</sup>*J*<sub>CF</sub> = 272 Hz), 84.1, 32.2, 29.0, 16.6, 16.5; <sup>19</sup>F NMR (282 MHz, CDCl<sub>3</sub>) ppm -60.9; HRMS (ESI): Exact mass calcd for C<sub>13</sub>H<sub>12</sub>F<sub>3</sub>INaO<sub>2</sub> [M+Na]<sup>+</sup> 406.9732, found 406.9745.

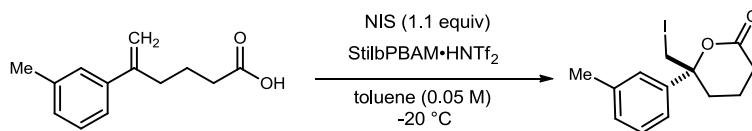


**(R)-6-(Iodomethyl)-6-(4-methoxyphenyl)tetrahydro-2H-pyran-2-one (271i).** Prepared according to the general procedure using 5-(4-methoxyphenyl)hex-5-enoic acid<sup>134</sup> (22.0 mg, 0.100 mmol), PBAM•HNTf<sub>2</sub> (4.4 mg, 5.0 μmol) and 1,3-diiodo-5,5-dimethylhydantoin (22.8 mg, 60.0 μmol) over 2 hours. Flash column chromatography (SiO<sub>2</sub>, 10-30% ethyl acetate in hexanes) yielded a yellow solid (29 mg, 84%) that was quick to decompose. The product was determined to be 85% ee by chiral HPLC analysis (Chiralcel OD-H, 15% *i*PrOH/hexanes, 1 mL/min, *t<sub>r</sub>*(*e*<sub>1</sub>, minor) = 11.7 min, *t<sub>r</sub>*(*e*<sub>2</sub>, major) = 12.9 min); *R<sub>f</sub>* = 0.5 (40% EtOAc/hexanes) visualized with CAM. Remainder of physical data matched with literature values.<sup>134</sup>

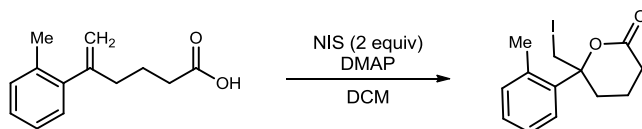
Alternatively, the reaction was prepared according to the general procedure using 5-(4-methoxyphenyl)hex-5-enoic acid (22.0 mg, 0.100 mmol), PBAM•HNTf<sub>2</sub> (4.4 mg, 5.0 μmol) and NIS (24.6 mg, 0.11 mmol) over 16 hours. Flash column chromatography (SiO<sub>2</sub>, 10-30% ethyl acetate in hexanes) yielded a yellow solid (30 mg, 87%) that was quick to decompose. The product was determined to be 74% ee by the chiral HPLC analysis listed above.



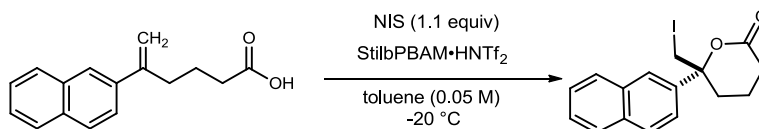
**(R)-6-(Iodomethyl)-6-(p-tolyl)tetrahydro-2H-pyran-2-one (271j).** Prepared according to the general procedure using 4-(*p*-tolyl)hex-5-enoic acid<sup>134</sup> (20.4 mg, 0.100 mmol), PBAM•HNTf<sub>2</sub> (4.4 mg, 5.0 μmol) and NIS (24.6 mg, 0.110 mmol) over 24 hours. Flash column chromatography (SiO<sub>2</sub>, 10-25-50% ethyl acetate in hexanes) yielded a yellow oil (32 mg, 97%). The product was determined to be 96% ee by chiral HPLC analysis (Chiralcel OD-H, 7% *i*PrOH/hexanes, 1 mL/min, *t*<sub>r</sub>(*e*<sub>1</sub>, minor) = 10.8 min, *t*<sub>r</sub>(*e*<sub>2</sub>, major) = 12.9 min); *R*<sub>f</sub> = 0.45 (25% EtOAc/hexanes) visualized with CAM. Remainder of physical data matched with literature values.<sup>134</sup>



**(R)-6-(Iodomethyl)-6-(*m*-tolyl)tetrahydro-2H-pyran-2-one (271k).** Prepared according to the general procedure using 5-(*m*-tolyl)hex-5-enoic acid (20.4 mg, 0.100 mmol), PBAM•HNTf<sub>2</sub> (4.4 mg, 5.0 μmol) and NIS (24.6 mg, 0.110 mmol) over 24 hours. Flash column chromatography (SiO<sub>2</sub>, 10-25-50% ethyl acetate in hexanes) yielded an oil (30 mg, 91%). The product was determined to be 97% ee by chiral HPLC analysis (Chiralcel OD-H, 7% *i*PrOH/hexanes, 1 mL/min, *t<sub>r</sub>*(*e*<sub>1</sub>, minor) = 10.3 min, *t<sub>r</sub>*(*e*<sub>2</sub>, major) = 11.7 min); *R<sub>f</sub>* = 0.28 (25% EtOAc/hexanes) visualized with CAM; [α]<sub>D</sub><sup>20</sup> -30 (*c* 1.3, CHCl<sub>3</sub>); IR (film) 2954, 2921, 1738 cm<sup>-1</sup>; <sup>1</sup>H NMR (400 MHz, CDCl<sub>3</sub>) δ 7.24 (dd, *J* = 7.6, 7.6 Hz, 1H), 7.17 (s, 1H), 7.15 (d, *J* = 7.6 Hz, 1H), 7.14 (d, *J* = 7.6 Hz, 1H), 3.56 (s, 2H), 2.52-2.40 (m, 2H), 2.37 (s, 3H), 2.35-2.29 (m, 2H), 1.81 (dddd, *J* = 13.6, 8.2, 4.1, 4.1, 4.1 Hz, 1H), 1.63-1.56 (m, 1H); <sup>13</sup>C NMR (100 MHz, CDCl<sub>3</sub>) ppm 170.5, 140.1, 138.8, 129.1, 128.8, 125.8, 122.2, 84.4, 32.0, 29.0, 21.6, 17.8, 16.5; HRMS (ESI): Exact mass calcd for C<sub>13</sub>H<sub>15</sub>INaO<sub>2</sub> [M+Na]<sup>+</sup> 353.0015, found 352.9999.

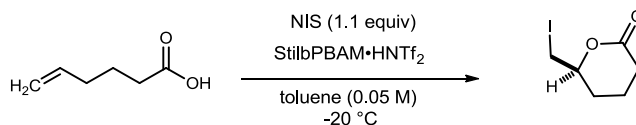


**6-(Iodomethyl)-6-(*o*-tolyl)tetrahydro-2*H*-pyran-2-one (271I).** Prepared according to the general procedure with DMAP (2.4 mg, 20  $\mu\text{mol}$ ), 5-(*o*-tolyl)hex-5-enoic acid (20.4 mg, 0.100 mmol), and dichloromethane (1 mL), and NIS (31.3 mg, 0.140 mmol) without light for 40 min at room temperature. The mixture was treated with 20% aq sodium thiosulfate (2 mL) and then partitioned between dichloromethane (15 mL) and 3 M NaOH (15 mL). The aqueous layer was extracted twice and the organic layers were combined, dried over magnesium sulfate and concentrated. The mixture was dissolved in dichloromethane and passed through a pipet silica plug with 5 mL of mobile phase (50% EtOAc/hexanes). The solvent was removed *in vacuo* to give the product as an oil (29 mg, 88% yield). Chiral HPLC analysis revealed two peaks of equal area (Chiralcel OD-H, 15% *i*PrOH/hexanes, 1 mL/min,  $t_r(e_1) = 8.3$  min,  $t_r(e_2) = 9.4$  min);  $R_f = 0.41$  (25% EtOAc/hexanes) visualized with CAM; IR (film) 2957, 1738  $\text{cm}^{-1}$ ;  $^1\text{H}$  NMR (400 MHz,  $\text{CDCl}_3$ )  $\delta$  7.32 (d,  $J = 7.5$  Hz, 1H), 7.26-7.19 (m, 3H), 3.70 (d,  $J = 11.1$  Hz, 1H), 3.65 (d,  $J = 11.2$  Hz, 1H), 2.62 (ddd,  $J = 14.4, 4.2, 4.2$  Hz, 1H), 2.52-2.44 (m, 1H), 2.48 (s, 3H), 2.32-2.25 (m, 2H), 1.91-1.83 (m, 1H), 1.75-1.64 (m, 1H);  $^{13}\text{C}$  NMR (100 MHz,  $\text{CDCl}_3$ ) ppm 170.8, 137.0, 135.0, 133.6, 128.6, 126.9, 126.4, 85.3, 31.5, 28.4, 22.5, 16.2, 15.6; HRMS (ESI): Exact mass calcd for  $\text{C}_{13}\text{H}_{15}\text{INaO}_2$   $[\text{M}+\text{Na}]^+$  353.0015, found 353.0029.

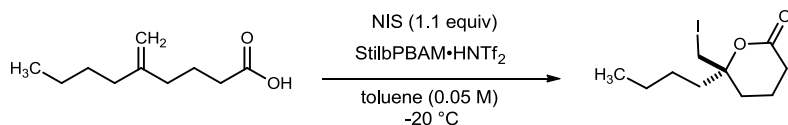


**(R)-6-(Iodomethyl)-6-(naphthalen-2-yl)tetrahydro-2H-pyran-2-one (271m).** Prepared according to the general procedure using 4-(naphthalen-2-yl)hex-5-enoic acid<sup>135</sup> (24.0 mg, 0.100 mmol), PBAM•HNTf<sub>2</sub> (4.4 mg, 5.0 μmol) and NIS (24.6 mg, 0.110 mmol) over 24 hours. Flash column chromatography (SiO<sub>2</sub>, 10-25-50% ethyl acetate in hexanes) yielded an oil (35 mg, 96%). The product was determined to be 96% ee by chiral HPLC analysis (Chiralcel OD-H, 15% *i*PrOH/hexanes, 1 mL/min, *t*<sub>r</sub>(*e*<sub>1</sub>, minor) = 13.1 min, *t*<sub>r</sub>(*e*<sub>2</sub>, major) = 15.4 min); *R*<sub>f</sub> = 0.40 (25% EtOAc/hexanes) visualized with CAM. Remainder of physical data matched with literature values.<sup>134</sup>

<sup>135</sup> Murai, K.; Matsushita, T.; Nakamura, A.; Fukushima, S.; Shimura, M.; Fujioka, H. *Angew. Chem., Int. Ed.* **2010**, *49*, 9174-9177, S9174/1-S9174/129.

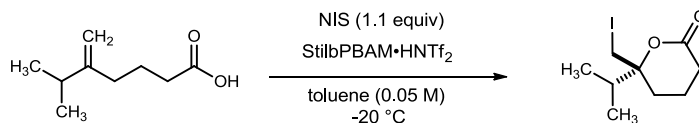


**(S)-6-(Iodomethyl)tetrahydro-2H-pyran-2-one (271q).** Prepared according to the general procedure using hex-5-enoic acid (11.4 mg, 0.100 mmol), PBAM•HNTf<sub>2</sub> (4.4 mg, 5.0 μmol) and NIS (24.6 mg, 0.110 mmol) over 24 hours. Flash column chromatography (SiO<sub>2</sub>, 10-25-50% ethyl acetate in hexanes) yielded an oil (6.0 mg, 25%). The product was determined to be 33% ee by chiral HPLC analysis (Chiralcel AD-H, 10% <sup>i</sup>PrOH/hexanes, 1 mL/min, *t*<sub>r</sub>(*e*<sub>1</sub>, minor) = 11.0 min, *t*<sub>r</sub>(*e*<sub>2</sub>, major) = 12.5 min); *R*<sub>f</sub> = 0.16 (20% EtOAc/hexanes) visualized with CAM; [α]<sub>D</sub><sup>20</sup> -3.5 (*c* 0.60, CHCl<sub>3</sub>); IR (film) 2922, 1730 cm<sup>-1</sup>; <sup>1</sup>H NMR (400 MHz, CDCl<sub>3</sub>) δ 4.28 (dddd, *J* = 10.7, 6.6, 4.4, 4.4 Hz, 1H), 3.36 (dd, *J* = 10.5, 4.6 Hz, 1H), 3.30 (dd, *J* = 10.5, 6.5 Hz, 1H), 2.63-2.56 (m, 1H), 2.45 (ddd, *J* = 16.6, 9.5, 7.0 Hz, 1H), 2.17 (dddd, *J* = 12.7, 8.0, 3.7, 3.7 Hz, 1H), 2.00-1.82 (m, 2H), 1.68-1.61 (m, 1H); <sup>13</sup>C NMR (100 MHz, CDCl<sub>3</sub>) ppm 170.4, 78.7, 29.2, 28.0, 18.1, 7.3; HRMS (ESI): Exact mass calcd for C<sub>6</sub>H<sub>10</sub>IO<sub>2</sub> [M+H]<sup>+</sup> 240.9720, found 240.9712.

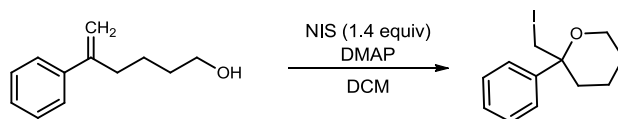


**(S)-6-Butyl-6-(iodomethyl)tetrahydro-2H-pyran-2-one (271o).** Prepared according to the general procedure using 5-methylenenonanoic acid<sup>132</sup> (17.0 mg, 0.100 mmol), PBAM•HNTf<sub>2</sub> (4.4 mg, 5.0 μmol) and NIS (24.6 mg, 0.110 mmol) over 12 hours. Flash column chromatography (SiO<sub>2</sub>, 10-25-50% ethyl acetate in hexanes) yielded a colorless oil (28 mg, 95%). The product was determined to be 89% ee by chiral HPLC analysis (Chiralcel OD-H, 4% <sup>i</sup>PrOH/hexanes, 1 mL/min, *t<sub>r</sub>*(*e*<sub>1</sub>, minor) = 12.3 min, *t<sub>r</sub>*(*e*<sub>2</sub>, major) = 13.3 min); *R<sub>f</sub>* = 0.45 (20% EtOAc/hexanes) visualized with CAM; [ $\alpha$ ]<sub>D</sub><sup>20</sup> -24 (*c* 1.0, CHCl<sub>3</sub>); IR (film) 2955, 2867, 1734 cm<sup>-1</sup>; <sup>1</sup>H NMR (400 MHz, CDCl<sub>3</sub>)  $\delta$  3.38 (d, *J* = 10.9 Hz, 1H), 3.37 (d, *J* = 10.9 Hz, 1H), 2.50-2.48 (m, 2H), 2.08-2.02 (m, 1H), 1.89-1.77 (m, 5H), 1.45-1.24 (m, 4H), 0.92 (dd, *J* = 6.9, 6.9 Hz, 3H); <sup>13</sup>C NMR (100 MHz, CDCl<sub>3</sub>) ppm 170.3, 83.4, 38.7, 29.9, 29.3, 25.0, 22.7, 16.5, 13.9, 12.8; HRMS (ESI): Exact mass calcd for C<sub>10</sub>H<sub>17</sub>INaO<sub>2</sub> [M+Na]<sup>+</sup> 319.0171, found 319.0180.

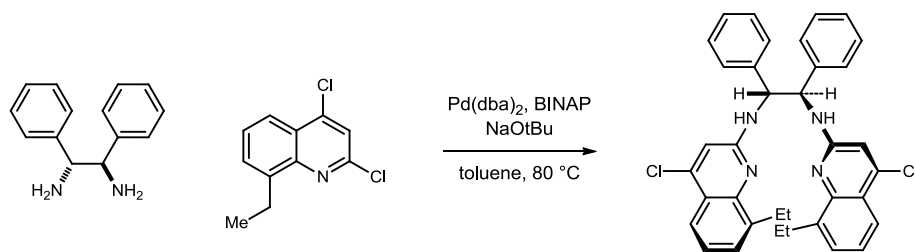




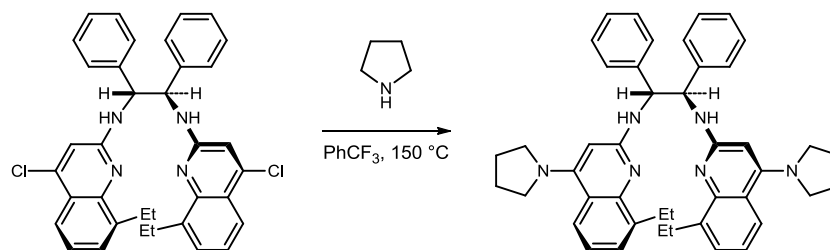
**(R)-6-(Iodomethyl)-6-isopropyltetrahydro-2H-pyran-2-one (271p).** Prepared according to the general procedure using 6-methyl-5-methyleneheptanoic acid<sup>132</sup> (15.6 mg, 0.100 mmol), PBAM•HNTf<sub>2</sub> (4.4 mg, 5.0 μmol) and NIS (24.6 mg, 0.110 mmol) over 48 hours. Flash column chromatography (SiO<sub>2</sub>, 10-25-50% ethyl acetate in hexanes) yielded a colorless oil (24 mg, 86%). The product was determined to be 81% ee by chiral HPLC analysis (Chiralcel IA, 3% EtOH/hexanes, 1 mL/min,  $t_r(e_1, \text{minor}) = 18.2$  min,  $t_r(e_2, \text{major}) = 16.9$  min);  $R_f = 0.24$  (25% EtOAc/hexanes) visualized with CAM. Remainder of physical data matched with literature values.<sup>134</sup>



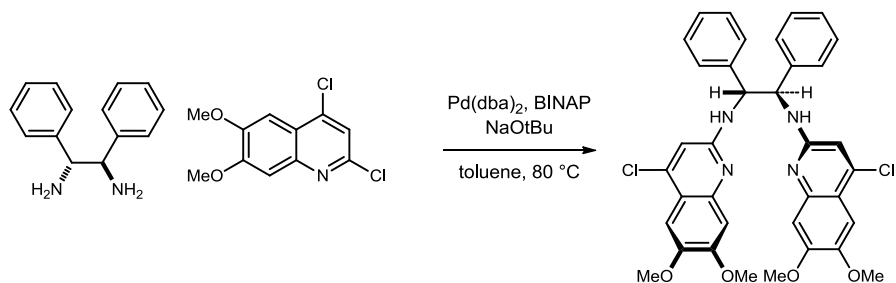
**2-(iodomethyl)-2-phenyltetrahydro-2H-pyran (279).** Prepared according to the general procedure using 5-phenylhex-5-en-1-ol (17.6 mg, 0.100 mmol), DMAP (2.4 mg, 20.0  $\mu\text{mol}$ ) and NIS (31.3 mg, 0.140 mmol) in dichloromethane over 1 hour. Flash column chromatography ( $\text{SiO}_2$ , 10-25-50% ethyl acetate in hexanes) yielded an oil (20 mg, 66%). Chiral HPLC analysis revealed two peaks of equal area (Chiralcel OD-H, 2%  $i\text{PrOH}$ /hexanes, 0.4 mL/min,  $t_r(e_1) = 11.6$  min,  $t_r(e_2) = 12.4$  min);  $R_f = 0.76$  (25% EtOAc/hexanes) visualized with CAM; IR (film) 2939, 2863, 1447  $\text{cm}^{-1}$ ;  $^1\text{H}$  NMR (400 MHz,  $\text{CDCl}_3$ )  $\delta$  7.43-7.37 (m, 4H), 7.32-7.29 (m, 1H), 3.81-3.77 (m, 1H), 3.51 (ddd,  $J = 11.5, 11.5, 2.7$  Hz, 1H), 3.39 (d,  $J = 10.3$  Hz, 1H), 3.35 (d,  $J = 10.4$  Hz, 1H), 2.33 (ddd,  $J = 13.8, 4.1, 4.1$  Hz, 1H), 2.02 (ddd,  $J = 13.8, 12.1, 3.9$ ), 1.75-1.60 (m, 2H), 1.53-1.37 (m, 2H);  $^{13}\text{C}$  NMR (100 MHz,  $\text{CDCl}_3$ ) ppm 140.2, 128.6, 127.5, 126.9, 75.8, 63.4, 32.3, 25.4, 21.4, 19.9; HRMS (ESI): Exact mass calcd for  $\text{C}_{12}\text{H}_{15}\text{IO}$   $[\text{M}+\text{Na}]^+$  302.0162, found 302.0164.



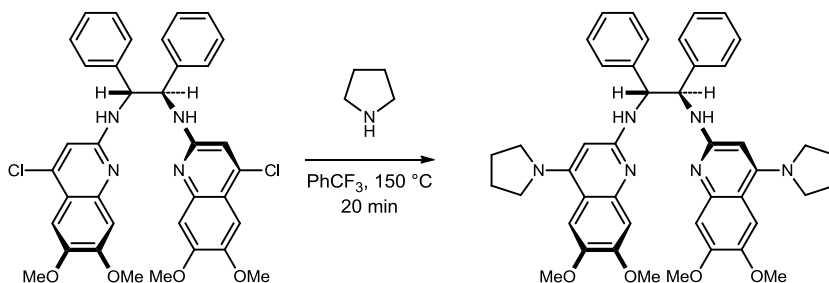
**<sup>4</sup>Cl-<sup>8</sup>EtStilbBAM (<sup>4</sup>Cl-285) [(1*R*,2*R*)-*N*1,*N*2-Bis(4-chloro-8-ethylquinolin-2-yl)-1,2-diphenylethane-1,2-diamine]**. A 25-mL, round-bottomed flask equipped with a stir bar was charged with (1*R*,2*R*)-(+)-1,2-diphenylethylenediamine (318 mg, 1.50 mmol), Pd(dba)<sub>2</sub> (13 mg, 22 μmol), *rac*-BINAP (28 mg, 45 μmol), sodium *tert*-butoxide (360 mg, 3.75 mmol), and 2,4-dichloro-8-ethylquinoline (678 mg, 3.00 mmol). The reaction vessel was placed under an argon atmosphere, toluene (8 mL) was dispensed into the flask, and the resulting solution was placed into an oil bath heated to 80 °C with stirring. The reaction was monitored by TLC and after 1 h nearly complete conversion was observed. The reaction was cooled to 25 °C, diluted with ethyl acetate, and filtered through a plug of Celite. Flash column chromatography (SiO<sub>2</sub>, 1-3% ethyl acetate in hexanes) of the residue yielded a yellow solid (800 mg, 90%). *R*<sub>f</sub> = 0.72 (20% EtOAc/hexanes); [α]<sub>D</sub><sup>20</sup> +37.4 (*c* 1.09, CHCl<sub>3</sub>); IR (film) 3421, 3280, 3030, 2964, 2927, 1605, 1517, 1467 cm<sup>-1</sup>; <sup>1</sup>H NMR (400 MHz, CDCl<sub>3</sub>) δ 7.84 (dd, *J* = 8.2, 0.8 Hz, 2H), 7.47 (d, *J* = 7.0 Hz, 2H), 7.28-7.15 (m, 12H), 6.59 (s, 2H), 6.43 (br s, 2H), 5.62 (br s, 2H), 3.28 (dq, *J* = 14.7, 7.5 Hz, 2H), 3.10 (dq, *J* = 14.8, 7.5 Hz, 2H), 1.34 (dd, *J* = 7.5, 7.5 Hz, 6H); <sup>13</sup>C NMR (100 MHz, CDCl<sub>3</sub>) ppm 155.2, 146.5, 143.0, 140.7, 140.1, 129.3, 128.4, 127.6, 127.4, 122.7, 121.9, 121.7, 111.6, 62.9, 25.1, 14.9; HRMS (ESI): Exact mass calcd for C<sub>36</sub>H<sub>33</sub>Cl<sub>2</sub>N<sub>4</sub> [M+H]<sup>+</sup> 591.2082, found 591.2062.



**<sup>8</sup>EtStilbPBAM (285) [(1R,2R)-N1,N2-Bis(8-ethyl-4-(pyrrolidin-1-yl)quinolin-2-yl)-1,2-diphenylethane-1,2-diamine].** A 0.5-2 mL microwave vial equipped with a stir bar was charged with <sup>4</sup>Cl-<sup>8</sup>EtStilbBAM (660 mg, 1.12 mmol), pyrrolidine (367  $\mu$ L, 4.46 mmol), and trifluoromethylbenzene (1 mL). The vial was sealed, and this suspension was heated with stirring at 150  $^{\circ}$ C in the microwave for 20 m. The reaction mixture was diluted with dichloromethane and transferred to a round-bottomed flask for evaporation. The resulting solid was dissolved in dichloromethane and washed with 3M NaOH (3 x 50 mL), water (3 x 50 mL) and dried over magnesium sulfate. The solvent was removed *in vacuo* to provide a light brown powder. Flash column chromatography (SiO<sub>2</sub>, 1-3-10-20% methanol in dichloromethane) of the residue yielded a yellow solid (622 mg, 84%).  $R_f$  = 0.38 (10% MeOH/CH<sub>2</sub>Cl<sub>2</sub>);  $[\alpha]_D^{20}$  +44.1 (*c* 1.0, CHCl<sub>3</sub>); IR (film) 3417, 3260, 2964, 2869, 1588, 1525, 1485, 1424 cm<sup>-1</sup>; <sup>1</sup>H NMR (400 MHz, CDCl<sub>3</sub>)  $\delta$  7.78 (d, *J* = 8.3 Hz, 2H), 7.35-7.30 (m, 6H), 7.20 (dd, *J* = 7.3 Hz, 4H), 7.15-7.09 (m, 2H), 7.00 (dd, *J* = 7.7, 7.7 Hz, 2H), 6.32 (br s, 2H), 5.65 (s, 2H), 5.57 (s, 2H), 3.37-3.28 (m, 10H), 3.14 (dq, *J* = 14.6, 7.4 Hz, 2H), 1.88 (br s, 8H), 1.37 (dd, *J* = 7.4, 7.4 Hz, 6H); <sup>13</sup>C NMR (100 MHz, CDCl<sub>3</sub>) 156.9, 154.3, 147.7, 142.1, 140.0, 128.1, 127.8, 127.2, 126.8, 122.6, 119.1, 118.6, 92.8, 62.9, 51.9, 25.6, 25.5, 15.0 ppm; HRMS (ESI): Exact mass calcd for C<sub>44</sub>H<sub>49</sub>N<sub>6</sub> [M+H]<sup>+</sup> 661.4019, found 661.4001.



**<sup>4</sup>Cl-<sup>6,7</sup>MeOStilbBAM (<sup>4</sup>Cl-286) [(1*R*,2*R*)-*N*1,*N*2-Bis(4-chloro-6,7-dimethoxyquinolin-2-yl)-1,2-diphenylethane-1,2-diamine]**. A 25-mL, round-bottomed flask equipped with a stir bar was charged with (1*R*,2*R*)-(+)-1,2-diphenylethylenediamine (318 mg, 1.50 mmol), Pd(dba)<sub>2</sub> (13 mg, 22 μmol), *rac*-BINAP (28 mg, 45 μmol), sodium *tert*-butoxide (360 mg, 3.75 mmol), and 2,4-dichloro-6,7-dimethoxyquinoline (774 mg, 3.00 mmol). The reaction vessel was placed under an argon atmosphere, toluene (8 mL) was dispensed into the flask, and the resulting solution was placed into an oil bath heated to 80 °C with stirring. The reaction was monitored by TLC and after 1 h nearly complete conversion was observed. The reaction was cooled to 25 °C, diluted with ethyl acetate, and filtered through a plug of Celite. Flash column chromatography (SiO<sub>2</sub>, 20-40% ethyl acetate in hexanes) of the residue yielded a yellow solid (600 mg, 92%). *R*<sub>f</sub> = 0.10 (20% EtOAc/hexanes); [α]<sub>D</sub><sup>20</sup> +23.7 (*c* 1.12, CHCl<sub>3</sub>); IR (film) 3241, 3027, 1599, 1502, 1380, 1257 cm<sup>-1</sup>; <sup>1</sup>H NMR (600 MHz, DMSO) δ 7.65 (br s, 2H), 7.34 (d, *J* = 7.6 Hz, 4H), 7.17 (dd, *J* = 7.6, 7.6 Hz, 4H), 7.12 (s, 2H), 7.08 (t, *J* = 7.3 Hz, 2H), 6.92 (s, 2H), 6.84 (s, 2H), 5.57 (br s, 2H), 3.85 (s, 6H), 3.82 (s, 6H); <sup>13</sup>C NMR (150 MHz, DMSO) ppm 155.4, 152.6, 146.4, 144.7, 141.8, 139.1, 127.7, 127.6, 126.6, 114.4, 109.2, 106.4, 102.4, 59.2, 55.6, 55.5; HRMS (ESI): Exact mass calcd for C<sub>36</sub>H<sub>33</sub>Cl<sub>2</sub>N<sub>4</sub>O<sub>4</sub> [M+H]<sup>+</sup> 655.1879, found 655.1849.



**<sup>6,7</sup>MeOStilbPBAM (286) [(1R,2R)-N1,N2-Bis(6,7-dimethoxy-4-(pyrrolidin-1-**

**yl)quinolin-2-yl)-1,2-diphenylethane-1,2-diamine].** A 0.5-2 mL microwave vial

equipped with a stir bar was charged with <sup>4</sup>Cl-<sup>6,7</sup>MeOStilbBAM (393 mg, 600 μmol),

pyrrolidine (200 μL, 2.40 mmol), and trifluoromethylbenzene (800 μL). The vial was

sealed, and this suspension was heated with stirring at 110 °C in the microwave for 20 m.

The reaction mixture was diluted with dichloromethane and transferred to a round-

bottomed flask for evaporation. The resulting solid was dissolved in dichloromethane and

washed with 3M NaOH (3 x 50 mL), water (3 x 50 mL) and dried over magnesium

sulfate. The solvent was removed *in vacuo* to provide a light brown powder. Flash

column chromatography (SiO<sub>2</sub>, 1-3-10-20% methanol in dichloromethane) of the residue

yielded a yellow solid (407 mg, 94%). *R<sub>f</sub>* = 0.34 (10% MeOH/CH<sub>2</sub>Cl<sub>2</sub>); [ $\alpha$ ]<sub>D</sub><sup>20</sup> +92.0 (*c*

1.00, CHCl<sub>3</sub>); IR (film) 3241, 2961, 1586, 1515, 1427 cm<sup>-1</sup>; <sup>1</sup>H NMR (600 MHz, DMSO)

δ 7.38 (d, *J* = 7.6 Hz, 4H), 7.22 (s, 2H), 7.18 (dd, *J* = 7.7, 7.7 Hz, 4H), 7.08 (dd, *J* = 7.3,

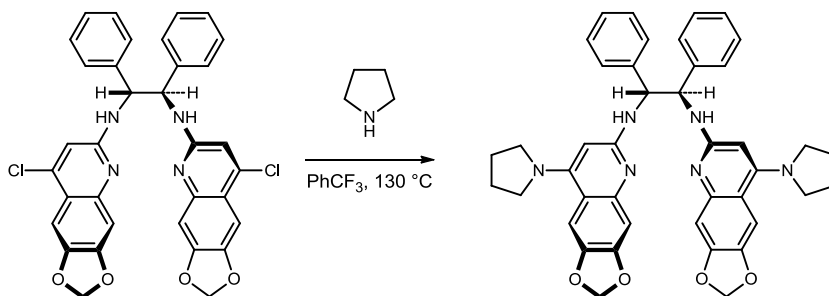
7.3 Hz, 4H), 6.80 (s, 2H), 5.79 (s, 2H), 5.51 (br s, 2H), 3.81 (s, 6H), 3.75 (s, 6H), 3.81-

3.75 (m, 4H), 3.33 (br s, 4H), 1.89 (br s, 8H); <sup>13</sup>C NMR (150 MHz, DMSO) 156.7, 152.4,

150.6, 145.7, 143.4, 142.9, 127.64, 127.57, 126.3, 111.2, 106.7, 105.4, 91.2, 59.9, 55.5,

55.2, 51.2, 25.2 ppm; HRMS (ESI): Exact mass calcd for C<sub>44</sub>H<sub>49</sub>N<sub>6</sub>O<sub>4</sub> [M+H]<sup>+</sup> 725.3815,

found 725.3789.



**<sup>6,7</sup>DioxolStilbPBAM (287) [(1R,2R)-N1,N2-Bis(6,7-dimethoxy-4-(pyrrolidin-1-**

**yl)quinolin-2-yl)-1,2-diphenylethane-1,2-diamine].** A 0.5-2 mL microwave vial

equipped with a stir bar was charged with <sup>4</sup>Cl-<sup>6,7</sup>DioxolStilbBAM (semi-pure, 250 mg,

400 μmol), pyrrolidine (165 μL, 2.00 mmol), and trifluoromethylbenzene (1.4 mL). The

vial was sealed, and this suspension was heated with stirring at 110 °C in the microwave

for 10 m and then 130 °C in the microwave for 10 m. The reaction mixture was diluted

with dichloromethane and transferred to a round-bottomed flask for evaporation. The

resulting solid was dissolved in dichloromethane and washed with 3M NaOH (3 x 50

mL), water (3 x 50 mL) and dried over magnesium sulfate. The solvent was removed *in*

*vacuo* to provide a light brown powder. Flash column chromatography (SiO<sub>2</sub>, 1-3-10-

20% methanol in dichloromethane) of the residue yielded a yellow solid (90 mg, 32%).

$R_f = 0.1$  (10% MeOH/CH<sub>2</sub>Cl<sub>2</sub>);  $[\alpha]_D^{20} +84$  ( $c$  0.71, CHCl<sub>3</sub>); IR (film) 3244, 2967, 2874,

1617, 1574, 1538, 1503 cm<sup>-1</sup>; <sup>1</sup>H NMR (400 MHz, CDCl<sub>3</sub>) δ 7.27 (s, 2H), 7.25-7.23 (m,

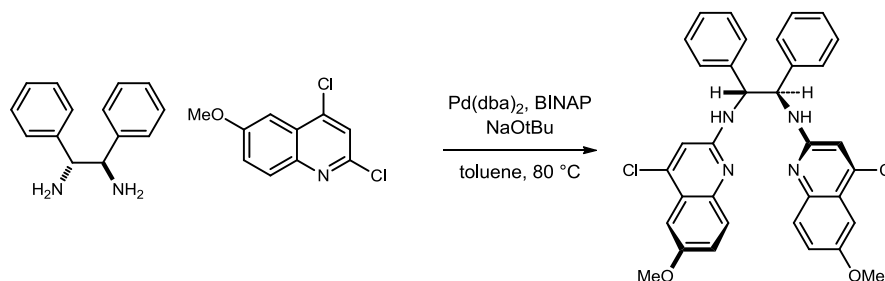
4H), 7.20-7.11 (m, 6H), 7.06 (s, 2H), 5.96 (d,  $J = 1.6$  Hz, 4H), 5.78 (br s, 2H), 5.52 (br s,

2H), 5.38 (br s, 2H), 3.32 (br m, 4H), 3.22 (br m, 4H), 1.89 (br m, 8H); <sup>13</sup>C NMR (150

MHz, CDCl<sub>3</sub>) 156.7, 153.9, 149.1, 147.1, 142.6, 141.1, 128.1, 127.9, 127.0, 112.7, 104.3,

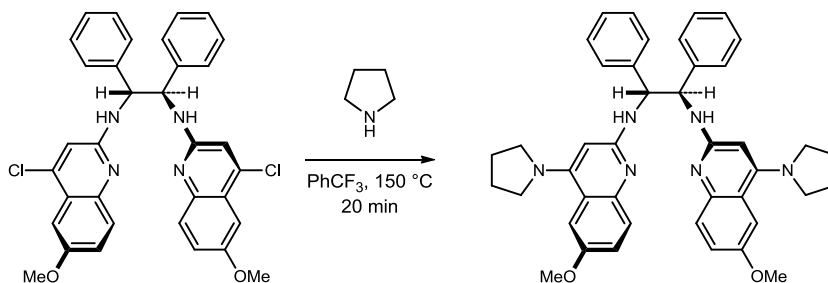
101.8, 100.9, 91.2, 62.1, 51.6, 25.5ppm; HRMS (ESI): Exact mass calcd for C<sub>42</sub>H<sub>41</sub>N<sub>6</sub>O<sub>4</sub>

[M+H]<sup>+</sup> 693.3189, found 693.3172.



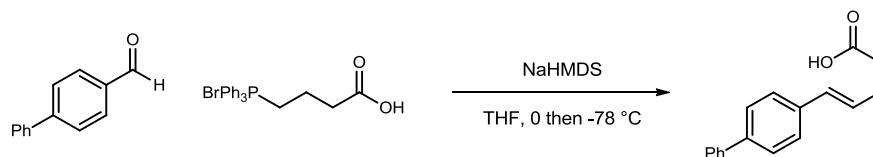
**<sup>4</sup>Cl-<sup>6</sup>MeOSilbBAM (<sup>4</sup>Cl-288) [(1R,2R)-N1,N2-Bis(4-chloro-6-methoxyquinolin-2-yl)-1,2-diphenylethane-1,2-diamine].** A 25-mL, round-bottomed flask equipped with a stir bar was charged with (1R,2R)-(+)-1,2-diphenylethylenediamine (235 mg, 1.11 mmol), Pd(dba)<sub>2</sub> (13 mg, 22 μmol), *rac*-BINAP (28 mg, 45 μmol), sodium *tert*-butoxide (265 mg, 2.76 mmol), and 2,4-dichloro-6-dimethoxyquinoline (505 mg, 2.21 mmol). The reaction vessel was placed under an argon atmosphere, toluene (8 mL) was dispensed into the flask, and the resulting solution was placed into an oil bath heated to 80 °C with stirring. The reaction was monitored by TLC and after 45 m nearly complete conversion was observed. The reaction was cooled to 25 °C, diluted with ethyl acetate, and filtered through a plug of Celite. Flash column chromatography (SiO<sub>2</sub>, 5-10-20% ethyl acetate in hexanes) of the residue yielded a yellow solid (570 mg, 87%). *R<sub>f</sub>* = 0.42 (20% EtOAc/hexanes);  $[\alpha]_D^{20} +15.9$  (*c* 1.12, CHCl<sub>3</sub>); IR (film) 3242, 3028, 1600, 1490, 1462, 1404 cm<sup>-1</sup>; <sup>1</sup>H NMR (600 MHz, DMSO) δ 7.80 (br s, 2H), 7.45 (d, *J* = 9.0 Hz, 4H), 7.30 (d, *J* = 7.6 Hz, 4H), 7.21 (dd, *J* = 9.1, 2.8 Hz, 2H), 7.18 (d, *J* = 2.8 Hz, 2H), 7.14 (dd, *J* = 7.6, 7.6 Hz, 4H), 7.05 (t, *J* = 7.3 Hz, 2H), 7.02 (s, 2H), 5.30 (d, *J* = 4.8 Hz, 2H), 3.81 (s, 6H); <sup>13</sup>C NMR (150 MHz, DMSO) ppm 154.9, 154.7, 143.6, 141.7, 139.5, 127.9, 127.7, 127.64, 126.55, 121.6, 120.8, 112.3, 102.6, 59.3, 55.3; HRMS (ESI): Exact mass calcd for C<sub>34</sub>H<sub>29</sub>Cl<sub>2</sub>N<sub>4</sub>O<sub>2</sub> [M+H]<sup>+</sup> 595.1668, found 595.1653.





**<sup>6</sup>MeOStilbPBAM (288) [(1R,2R)-N1,N2-Bis(6-methoxy-4-(pyrrolidin-1-yl)quinolin-2-yl)-1,2-diphenylethane-1,2-diamine].** A 0.5-2 mL microwave vial equipped with a stir bar was charged with <sup>4</sup>Cl-<sup>6</sup>MeOStilbBAM (550 mg, 924 μmol), pyrrolidine (341 μL, 4.16 mmol), and trifluoromethylbenzene (800 μL). The vial was sealed, and this suspension was heated with stirring at 110 °C in the microwave for 20 m. The reaction mixture was diluted with dichloromethane and transferred to a round-bottomed flask for evaporation. The solvent was removed *in vacuo* to provide a light brown powder. Flash column chromatography (SiO<sub>2</sub>, 1-2-5-10% methanol in dichloromethane) of the residue yielded a yellow solid that was washed with 3M NaOH to give a yellow solid (490 mg, 80%). *R<sub>f</sub>* = 0.35 (10% MeOH/CH<sub>2</sub>Cl<sub>2</sub>); [α]<sub>D</sub><sup>20</sup> +54.4 (*c* 1.10, CHCl<sub>3</sub>); IR (film) 3242, 2965, 1586, 1529, 1428 cm<sup>-1</sup>; <sup>1</sup>H NMR (600 MHz, DMSO) δ 7.37 (d, *J* = 7.3 Hz, 4H), 7.33 (d, *J* = 9.0 Hz, 2H), 7.26 (d, *J* = 2.5 Hz, 2H), 7.16 (dd, *J* = 7.6, 7.6 Hz, 4H), 7.07-7.03 (m, 4H), 5.89 (br s, 2H), 5.51 (br s, 2H), 3.76 (s, 6H), 3.41 (br s, 4H), 3.32 (br s, 4H), 1.89 (br s, 8H); <sup>13</sup>C NMR (150 MHz, DMSO) 156.2, 152.6, 152.2, 144.3, 142.7, 127.7, 127.62, 127.60, 126.3, 118.7, 118.2, 105.3, 93.2, 60.0, 55.1, 51.3, 25.2 ppm; HRMS (ESI): Exact mass calcd for C<sub>42</sub>H<sub>45</sub>N<sub>6</sub>O<sub>2</sub> [M+H]<sup>+</sup> 665.3604, found 665.3610.

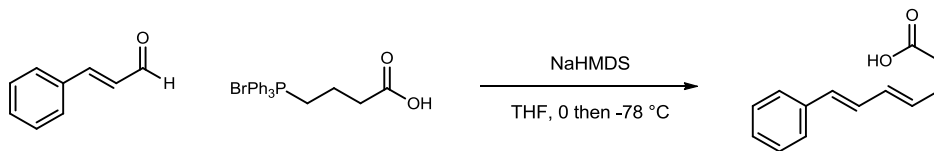
## Preparation of unsaturated acids<sup>136</sup>



**(E)-5-([1,1'-Biphenyl]-4-yl)pent-4-enoic acid (283e).** Prepared according to the known procedure.<sup>137</sup> The resulting solid was washed with DCM and recrystallized from ethyl acetate to give a white solid (500 mg, 43% yield). Mp 194-195 °C;  $R_f = 0.17$  (40% EtOAc/hexanes) visualized with  $\text{KMnO}_4$ ; IR (film) 3057, 2907, 1693  $\text{cm}^{-1}$ ;  $^1\text{H}$  NMR (400 MHz, DMSO)  $\delta$  7.66 (d,  $J = 7.3$  Hz, 2H), 7.62 (d,  $J = 8.2$  Hz, 2H), 7.46 (d,  $J = 7.9$  Hz, 2H), 7.44 (d,  $J = 7.5$  Hz, 2H), 7.35 (t,  $J = 7.3$  Hz, 1H), 6.48 (d,  $J = 15.9$  Hz, 1H), 6.37-6.30 (m, 1H), 2.47-2.38 (m, 4H);  $^{13}\text{C}$  NMR (100 MHz, DMSO) ppm 174.3, 140.1, 139.0, 136.7, 130.0, 129.9, 129.3, 127.8, 127.2, 126.84, 126.79, 33.8, 28.3; HRMS (EI): Exact mass calcd for  $\text{C}_{17}\text{H}_{16}\text{O}_2$   $[\text{M}]^+$  252.1145, found 252.1137.

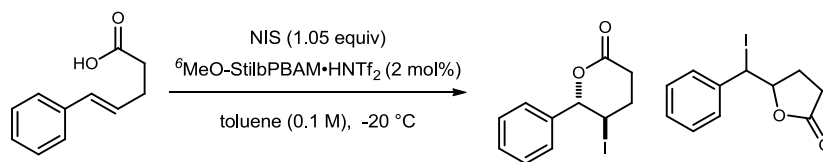
<sup>136</sup> Prepared by analogy to: Davis, T. A.; Wilt, J. C.; Johnston, J. N. *J. Am. Chem. Soc.* **2010**, *132*, 2880-2882. Davis, T. A.; Dobish, M. C.; Schwieter, K. E.; Chun, A. C.; Johnston, J. N. *Org. Synth.* **2012**, *89*, 380.

<sup>137</sup> Tan, C. K.; Zhou, L.; Yeung, Y.-Y. *Org. Lett.* **2011**, *13*, 2738-2741.



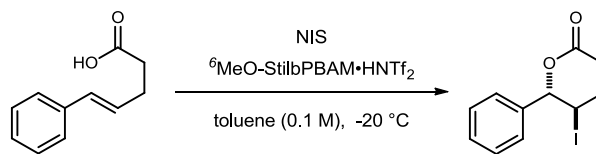
**(4E,6E)-7-Phenylhepta-4,6-dienoic acid (283n).** Prepared according to the known procedure.<sup>137</sup> Flash column chromatography (SiO<sub>2</sub>, 10-30% ethyl acetate in hexanes) of the residue yielded a white solid (490 mg, 53%) further recrystallized from hexanes and ethyl acetate. Mp 128-130 °C;  $R_f = 0.23$  (40% EtOAc/hexanes) visualized with KMnO<sub>4</sub>; IR (film) 3025, 2917, 1699 cm<sup>-1</sup>; <sup>1</sup>H NMR (400 MHz, CDCl<sub>3</sub>)  $\delta$  7.39 (d,  $J = 7.5$  Hz, 2H), 7.19 (dd,  $J = 7.4, 7.4$  Hz, 2H), 7.22 (t,  $J = 7.3$  Hz, 1H), 6.75 (dd,  $J = 15.6, 10.4$  Hz, 1H), 6.49 (d,  $J = 15.7$  Hz, 1H), 6.49 (d,  $J = 15.7$  Hz, 1H), 6.27 (dd,  $J = 15.0, 10.4$  Hz, 1H), 5.85-5.59 (m, 1H), 2.53-2.47 (m, 4H); <sup>13</sup>C NMR (150 MHz, CDCl<sub>3</sub>) ppm 179.3, 137.3, 132.3, 131.8, 131.2, 128.7, 128.6, 127.3, 126.2, 33.7, 27.7; HRMS (EI): Exact mass calcd for C<sub>13</sub>H<sub>14</sub>O<sub>2</sub> [M]<sup>+</sup> 202.0988, found 202.0984.

## Enantioselective iodolactonization

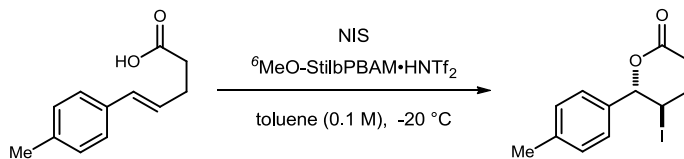


**General procedure for enantioselective iodolactonizations:** To a flame dried vial equipped with a stir bar was added <sup>6</sup>MeOStilbPBAM•HNTf<sub>2</sub> (1.9 mg, 2.0 μmol), (*E*)-5-phenylpent-4-enoic acid (17.6 mg, 100 μmol) and toluene (1 mL), and the reaction was cooled to -20 °C. NIS (23.5 mg, 105 μmol) was added and the reaction mixture was stirred without light until complete by TLC. The mixture was treated with 20% aq sodium thiosulfate (2 mL) and then partitioned between dichloromethane (15 mL) and 3 M NaOH (15 mL). The aqueous layer was extracted twice and the organic layers were combined, dried over magnesium sulfate and concentrated. Flash column chromatography (SiO<sub>2</sub>, 10-30% ethyl acetate in hexanes) of the residue yielded the product. *All compounds were treated as temperature and light sensitive, never being left on high vacuum for more than 10 minutes. (Decomposition was seen as a solid [white solid to black tar] and in solvent [from colorless to pink solution])* The ratio of δ-lactone to γ-lactone of the isolated material was determined using <sup>1</sup>H NMR. The enantiomeric excess of the product was determined by chiral HPLC analysis.

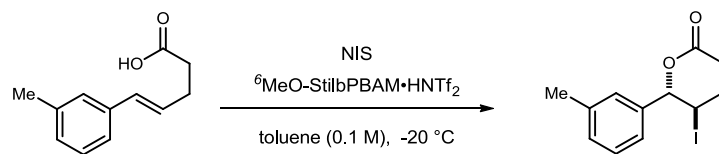
**General procedure for racemic iodolactonization:** To a flame dried vial equipped with a stir bar was added DMAP (2.4 mg, 2.0  $\mu\text{mol}$ ), (*E*)-5-phenylpent-4-enoic acid (17.6 mg, 100  $\mu\text{mol}$ ) and dichloromethane (1 mL). NIS (31.3 mg, 0.140 mmol) was added and the reaction mixture was stirred without light for 30 min at room temperature. The mixture was treated with 20% aq sodium thiosulfate (2 mL) and then partitioned between dichloromethane (15 mL) and 3 M NaOH (15 mL). The aqueous layer was extracted twice and the organic layers were combined, dried over magnesium sulfate and concentrated. Flash column chromatography ( $\text{SiO}_2$ , 10-30% ethyl acetate in hexanes) yielded the product.



**(5R,6S)-5-Iodo-6-phenyltetrahydro-2H-pyran-2-one (284).** Prepared according to the general procedure using the parent acid (17.6 mg, 100  $\mu$ mol), <sup>6</sup>MeOStilbPBAM•HNTf<sub>2</sub> (1.9 mg, 2.0  $\mu$ mol) and NIS (23.5 mg, 105  $\mu$ mol) over 24 hours. Flash column chromatography (SiO<sub>2</sub>, 10-30% ethyl acetate in hexanes) of the residue yielded a white solid (23.0 mg, 76%). The ratio of  $\delta$ -lactone to  $\gamma$ -lactone of the isolated material was determined to be 91:9 (<sup>1</sup>H NMR). The major product was determined to be 94% ee by chiral HPLC analysis (Chiralcel IA, 6% <sup>i</sup>PrOH/hexanes, 1 mL/min,  $t_r$ (*exo*-major/minor) = 14.9 min,  $t_r$ (*e*<sub>1</sub>, *endo*-minor) = 19.7 min,  $t_r$ (*e*<sub>2</sub>, *endo*-major) = 24.5 min);  $R_f$  = 0.66 (40% EtOAc/hexanes) visualized with KMnO<sub>4</sub>; IR (film) 2921, 1721 cm<sup>-1</sup>; <sup>1</sup>H NMR (600 MHz, CDCl<sub>3</sub>)  $\delta$  7.42-7.38 (m, 3H), 7.33 (dd,  $J$  = 7.9, 2.0 Hz, 2H), 5.56 (d,  $J$  = 7.9 Hz, 1H), 4.43 (ddd,  $J$  = 8.0, 8.0, 4.6 Hz, 1H), 2.87 (ddd,  $J$  = 18.1, 6.9, 6.9 Hz, 1H), 2.72 (ddd,  $J$  = 18.2, 7.0, 7.0 Hz, 1H), 2.46 (dddd,  $J$  = 14.4, 6.7, 6.7, 4.6 Hz, 1H), 2.39 (dddd,  $J$  = 14.9, 7.1, 7.1, 7.1 Hz, 1H); <sup>13</sup>C NMR (150 MHz, CDCl<sub>3</sub>) ppm 169.1, 137.7, 129.2, 128.7, 126.8, 87.1, 30.6, 30.5, 24.3; HRMS (ESI): Exact mass calcd for C<sub>11</sub>H<sub>11</sub>INaO<sub>2</sub> [M+Na]<sup>+</sup> 324.9702, found 324.9703.

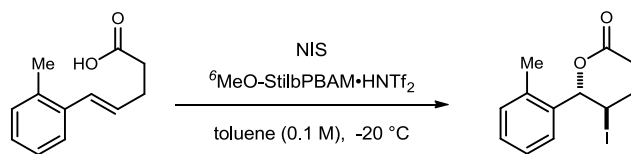


**(5R,6S)-5-Iodo-6-(p-tolyl)tetrahydro-2H-pyran-2-one (284b).** Prepared according to the general procedure using the parent acid (19.0 mg, 100  $\mu\text{mol}$ ), <sup>6</sup>MeOStilbPBAM•HNTf<sub>2</sub> (1.9 mg, 2.0  $\mu\text{mol}$ ) and NIS (23.5 mg, 105  $\mu\text{mol}$ ) over 48 hours. Flash column chromatography (SiO<sub>2</sub>, 10-30% ethyl acetate in hexanes) of the residue yielded a white solid (27.2 mg, 86%). The ratio of  $\delta$ -lactone to  $\gamma$ -lactone of the isolated material was determined to be 95:5 (<sup>1</sup>H NMR). The major product was determined to be 91% ee by chiral HPLC analysis (Chiralcel IA, 4% <sup>i</sup>PrOH/hexanes, 1 mL/min,  $t_r(e_1, \text{minor}) = 25.7$  min,  $t_r(e_2, \text{major}) = 29.6$  min);  $R_f = 0.54$  (40% EtOAc/hexanes) visualized with KMnO<sub>4</sub>; IR (film) 2920, 1740  $\text{cm}^{-1}$ ; <sup>1</sup>H NMR (600 MHz, CDCl<sub>3</sub>)  $\delta$  7.21 (d,  $J = 9.0$  Hz, 2H), 7.19 (d,  $J = 8.9$  Hz, 2H), 5.52 (d,  $J = 7.9$  Hz, 1H), 4.41 (ddd,  $J = 8.0, 8.0, 4.6$  Hz, 1H), 2.84 (ddd,  $J = 18.1, 6.9, 6.9$  Hz, 1H), 2.70 (ddd,  $J = 18.1, 7.0, 7.0$  Hz, 1H), 2.46 (dddd,  $J = 14.2, 6.7, 6.7, 4.6$  Hz, 1H), 2.37 (dddd,  $J = 14.9, 7.3, 7.3, 7.3$  Hz, 1H), 2.36 (s, 3H); <sup>13</sup>C NMR (150 MHz, CDCl<sub>3</sub>) ppm 169.2, 139.1, 134.7, 129.4, 126.7, 87.0, 30.6, 30.5, 24.6, 21.2; HRMS: sample decomposed.

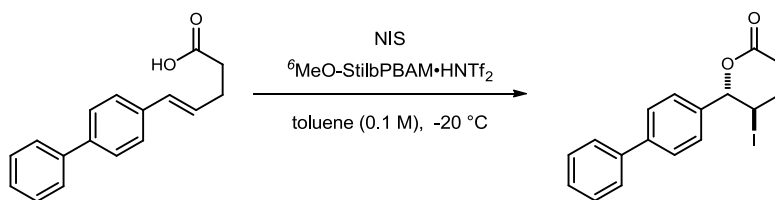


**(5R,6S)-5-Iodo-6-(*m*-tolyl)tetrahydro-2H-pyran-2-one (284c).** Prepared according to the general procedure using the parent acid (19.0 mg, 100  $\mu\text{mol}$ ),  $^6\text{MeO-StilbPBAM}\cdot\text{HNTf}_2$  (1.9 mg, 2.0  $\mu\text{mol}$ ) and NIS (23.5 mg, 105  $\mu\text{mol}$ ) over 72 hours. Flash column chromatography ( $\text{SiO}_2$ , 10-30% ethyl acetate in hexanes) of the residue yielded a white solid (26.7 mg, 84%). The ratio of  $\delta$ -lactone to  $\gamma$ -lactone of the isolated material was determined to be 93:7 ( $^1\text{H NMR}$ ). The product was determined to be 92% ee by chiral HPLC analysis (Chiralcel OD-H, 5% EtOH/hexanes, 1 mL/min,  $t_r(e_1, \text{major}) = 23.2$  min,  $t_r(e_2, \text{minor}) = 26.0$  min);  $R_f = 0.48$  (40% EtOAc/hexanes) visualized with  $\text{KMnO}_4$ ; IR (film) 3029, 2920, 1740  $\text{cm}^{-1}$ ;  $^1\text{H NMR}$  (600 MHz,  $\text{CDCl}_3$ )  $\delta$  7.28 (dd,  $J = 7.6, 7.6$  Hz, 1H), 7.18 (d,  $J = 7.6$  Hz, 1H), 7.11 (d,  $J = 9.0$  Hz, 2H), 5.53 (d,  $J = 7.9$  Hz, 1H), 4.44 (ddd,  $J = 7.8, 7.8, 4.6$  Hz, 1H), 2.85 (ddd,  $J = 18.2, 7.0, 7.0$  Hz, 1H), 2.71 (ddd,  $J = 18.2, 6.8, 6.8$  Hz, 1H), 2.43 (dddd,  $J = 14.3, 6.8, 6.8, 4.6$  Hz, 1H), 2.37 (s, 3H), 2.35 (dddd,  $J = 14.8, 7.3, 7.3, 7.3$  Hz, 1H);  $^{13}\text{C NMR}$  (150 MHz,  $\text{CDCl}_3$ ) ppm 169.1, 138.6, 137.6, 129.9, 128.6, 127.2, 123.9, 87.2, 30.5, 30.4, 24.5, 21.4; HRMS (ESI): Exact mass calcd for  $\text{C}_{12}\text{H}_{13}\text{INaO}_2$   $[\text{M}+\text{Na}]^+$  338.9858, found 338.9874.

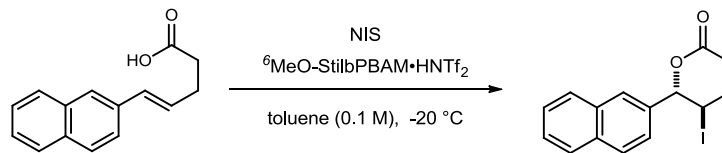




**(5R,6S)-5-Iodo-6-(*o*-tolyl)tetrahydro-2H-pyran-2-one (284d).** Prepared according to the general procedure using the parent acid (19.0 mg, 100  $\mu\text{mol}$ ),  $^6\text{MeO-StilbPBAM}\cdot\text{HNTf}_2$  (1.9 mg, 2.0  $\mu\text{mol}$ ) and NIS (23.5 mg, 105  $\mu\text{mol}$ ) over 48 hours. Flash column chromatography ( $\text{SiO}_2$ , 10-30% ethyl acetate in hexanes) of the residue yielded a white solid (30.1 mg, 95%). The ratio of  $\delta$ -lactone to  $\gamma$ -lactone of the isolated material was determined to be 85:15 ( $^1\text{H NMR}$ ). The product was determined to be 84% ee by chiral HPLC analysis (Chiralcel IA, 5%  $^i\text{PrOH}$ /hexanes, 1 mL/min,  $t_r(e_1, \text{major}) = 15.9$  min,  $t_r(e_2, \text{minor}) = 17.7$  min);  $R_f = 0.66$  (40% EtOAc/hexanes) visualized with  $\text{KMnO}_4$ ; IR (film) 2928, 1739  $\text{cm}^{-1}$ ;  $^1\text{H NMR}$  (600 MHz,  $\text{CDCl}_3$ )  $\delta$  7.28-7.20 (m, 5H), 5.81 (d,  $J = 7.6$  Hz, 1H), 4.46 (ddd,  $J = 7.8, 7.8, 4.4$  Hz, 1H), 2.88 (ddd,  $J = 18.3, 7.0, 7.0$  Hz, 1H), 2.76 (ddd,  $J = 18.2, 7.1, 7.1$  Hz, 1H), 2.46 (dddd,  $J = 14.3, 6.7, 6.7, 4.4$  Hz, 1H), 2.43 (s, 3H), 2.38 (dddd,  $J = 14.9, 7.1, 7.1, 7.1$  Hz, 1H);  $^{13}\text{C NMR}$  (150 MHz,  $\text{CDCl}_3$ ) ppm 169.2, 135.9, 135.6, 130.9, 129.1, 126.5, 126.0, 84.1, 30.6, 30.4, 23.2, 19.5; HRMS (ESI): Exact mass calcd for  $\text{C}_{12}\text{H}_{13}\text{INaO}_2$   $[\text{M}+\text{Na}]^+$  338.9858, found 338.9847.

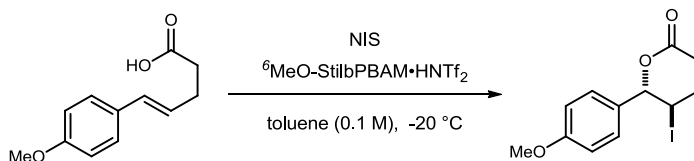


**(5*R*,6*S*)-6-([1,1'-Biphenyl]-4-yl)-5-iodotetrahydro-2*H*-pyran-2-one (284e).** Prepared according to the general procedure using the parent acid (25.2 mg, 100  $\mu\text{mol}$ ),  $^6\text{MeOStilbPBAM}\cdot\text{HNTf}_2$  (4.7 mg, 5.0  $\mu\text{mol}$ ) and NIS (24.6 mg, 110  $\mu\text{mol}$ ) in a toluene:trifluorotoluene (4:1, 1 mL) mixture over 72 hours. Flash column chromatography ( $\text{SiO}_2$ , 10-30% ethyl acetate in hexanes) of the residue yielded a white solid (34.0 mg, 89%). The ratio of  $\delta$ -lactone to  $\gamma$ -lactone of the isolated material was determined to be 87:13 ( $^1\text{H}$  NMR). The product was determined to be 75% ee by chiral HPLC analysis (Chiralcel IA, 25% EtOH/hexanes, 1 mL/min,  $t_r(e_1, \text{minor}) = 28.5$  min,  $t_r(e_2, \text{major}) = 39.1$  min);  $R_f = 0.43$  (40% EtOAc/hexanes) visualized with  $\text{KMnO}_4$ ; IR (film) 3030, 2924, 1738  $\text{cm}^{-1}$ ;  $^1\text{H}$  NMR (600 MHz,  $\text{CDCl}_3$ )  $\delta$  7.63 (d,  $J = 8.3$  Hz, 2H), 7.60 (d,  $J = 7.3$  Hz, 2H), 7.45 (dd,  $J = 7.5, 7.5$  Hz, 2H), 7.41 (d,  $J = 8.2$  Hz, 2H), 7.37 (t,  $J = 7.4$  Hz, 1H), 5.61 (d,  $J = 7.9$  Hz, 1H), 4.47 (ddd,  $J = 8.0, 8.0, 4.6$  Hz, 1H), 2.88 (ddd,  $J = 18.2, 6.9, 6.9$  Hz, 1H), 2.74 (ddd,  $J = 18.2, 7.0, 7.0$  Hz, 1H), 2.50 (dddd,  $J = 14.3, 6.7, 6.7, 4.6$  Hz, 1H), 2.41 (dddd,  $J = 14.9, 7.3, 7.3, 7.3$  Hz, 1H);  $^{13}\text{C}$  NMR (150 MHz,  $\text{CDCl}_3$ ) ppm 169.1, 142.1, 140.2, 136.7, 128.9, 127.7, 127.4, 127.2, 127.1, 86.9, 30.62, 30.57, 24.3; HRMS (ESI): Exact mass calcd for  $\text{C}_{17}\text{H}_{15}\text{INaO}_2$   $[\text{M}+\text{Na}]^+$  401.0015, found 401.0034.

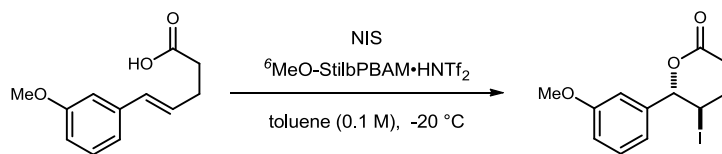


**(5R,6S)-5-Iodo-6-(naphthalen-2-yl)tetrahydro-2H-pyran-2-one (284f).** Prepared according to the general procedure using the parent acid (22.6 mg, 100  $\mu\text{mol}$ ),  $^6\text{MeOStilbPBAM}\cdot\text{HNTf}_2$  (4.7 mg, 5.0  $\mu\text{mol}$ ) and NIS (24.6 mg, 110  $\mu\text{mol}$ ) in a toluene:trifluorotoluene (4:1, 1 mL) mixture over 72 hours. Flash column chromatography ( $\text{SiO}_2$ , 10-30% ethyl acetate in hexanes) of the residue yielded a white solid (33.1 mg, 94%). The ratio of  $\delta$ -lactone to  $\gamma$ -lactone of the isolated material was determined to be 85:15 ( $^1\text{H}$  NMR). The product was determined to be 76% ee by chiral HPLC analysis (Chiralcel IA, 15% EtOH/hexanes, 1 mL/min,  $t_r(e_1, \text{minor}) = 18.7$  min,  $t_r(e_2, \text{major}) = 24.1$  min);  $R_f = 0.39$  (40% EtOAc/hexanes) visualized with  $\text{KMnO}_4$ ; IR (film) 2922, 1740  $\text{cm}^{-1}$ ;  $\delta$ -lactone  $^1\text{H}$  NMR (600 MHz,  $\text{CDCl}_3$ )  $\delta$  7.89-7.81 (m, 4H), 7.54 (d,  $J = 6.2$  Hz, 1H), 7.53 (d,  $J = 6.2$  Hz, 1H), 7.42 (dd,  $J = 8.5, 1.8$  Hz, 1H), 5.74 (d,  $J = 7.8$  Hz, 1H), 4.55 (ddd,  $J = 7.9, 7.9, 4.6$  Hz, 1H), 2.90 (ddd,  $J = 18.2, 7.0, 7.0$  Hz, 1H), 2.77 (ddd,  $J = 18.2, 6.8, 6.8$  Hz, 1H), 2.48 (dddd,  $J = 14.4, 6.8, 6.8, 4.6$  Hz, 1H), 2.41 (dddd,  $J = 14.8, 7.2, 7.2, 7.2$  Hz, 1H);  $^{13}\text{C}$  NMR (150 MHz,  $\text{CDCl}_3$ ) ppm 169.1, 134.9, 133.5, 132.9, 128.8, 128.2, 127.8, 126.8, 126.73, 126.70, 123.5, 87.3, 30.6, 30.5, 24.2;  $\gamma$ -lactone  $^1\text{H}$  NMR (600 MHz,  $\text{CDCl}_3$ )  $\delta$  7.89-7.81 (m, 4H), 7.55-7.49 (m, 3H), 5.31 (d,  $J = 8.2$  Hz, 1H), 5.03 (ddd,  $J = 7.9, 7.9, 6.7$  Hz, 1H), 2.71-2.66 (m, 1H), 2.61-2.56 (m, 2H), 2.21 (dddd,  $J = 13.0, 9.7, 9.7, 8.0$  Hz, 1H);  $^{13}\text{C}$  NMR (150 MHz,  $\text{CDCl}_3$ ) ppm 176.0, 136.4, 133.2, 133.0, 128.9, 128.0, 127.7, 126.9, 126.78, 126.76, 125.8, 82.4, 34.9, 29.3,

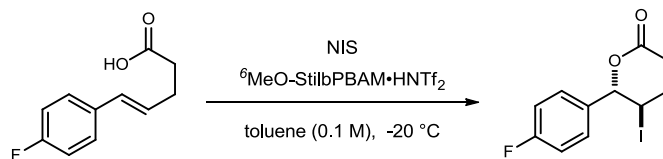
29.0; HRMS (ESI): Exact mass calcd for  $C_{15}H_{13}INaO_2$   $[M+Na]^+$  374.9858, found 374.9863.



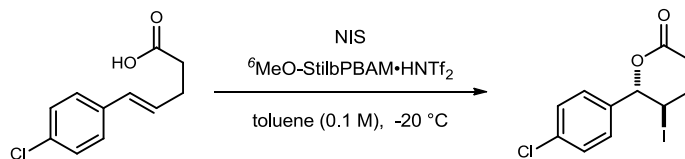
**(5R,6S)-5-Iodo-6-(4-methoxyphenyl)tetrahydro-2H-pyran-2-one (284g).** Prepared according to the general procedure using the parent acid (20.6 mg, 100  $\mu$ mol), <sup>6</sup>MeOStilbPBAM•HNTf<sub>2</sub> (1.9 mg, 2.0  $\mu$ mol) and NIS (23.5 mg, 105  $\mu$ mol) over 24 hours. Flash column chromatography (SiO<sub>2</sub>, 10-30% ethyl acetate in hexanes) of the residue yielded a white solid (24.0 mg, 72%). The ratio of  $\delta$ -lactone to  $\gamma$ -lactone of the isolated material was determined to be >95:5 (<sup>1</sup>H NMR). The product was determined to be 78% ee by chiral HPLC analysis (Chiralcel IA, 6% <sup>i</sup>PrOH/hexanes, 1 mL/min,  $t_r(e_1, \text{minor}) = 30.6$  min,  $t_r(e_2, \text{major}) = 36.1$  min);  $R_f = 0.59$  (40% EtOAc/hexanes) visualized with KMnO<sub>4</sub>; IR (film) 2930, 1738, 1612, 1515 cm<sup>-1</sup>; <sup>1</sup>H NMR (600 MHz, CDCl<sub>3</sub>)  $\delta$  7.25 (d,  $J = 8.7$  Hz, 2H), 6.91 (d,  $J = 8.7$  Hz, 2H), 5.49 (d,  $J = 8.4$  Hz, 1H), 4.38 (ddd,  $J = 8.5, 8.5, 4.7$  Hz, 1H), 3.82 (s, 3H), 2.82 (ddd,  $J = 18.1, 6.7, 6.7$  Hz, 1H), 2.70 (ddd,  $J = 18.1, 7.6, 7.6$  Hz, 1H), 2.50 (ddd,  $J = 14.3, 6.5, 6.5, 4.7$  Hz, 1H), 2.41 (dddd, 14.7, 7.9, 7.9, 7.9 Hz, 1H); <sup>13</sup>C NMR (150 MHz, CDCl<sub>3</sub>) ppm 169.4, 160.1, 129.8, 128.2, 114.0, 86.9, 55.3, 31.0, 30.7, 24.8; HRMS: sample decomposed.



**(5R,6S)-5-Iodo-6-(3-methoxyphenyl)tetrahydro-2H-pyran-2-one (284h).** Prepared according to the general procedure using the parent acid (20.6 mg, 100  $\mu\text{mol}$ ),  $^6\text{MeOStilbPBAM}\cdot\text{HNTf}_2$  (1.9 mg, 2.0  $\mu\text{mol}$ ) and NIS (23.5 mg, 105  $\mu\text{mol}$ ) over 72 hours. Flash column chromatography ( $\text{SiO}_2$ , 10-30% ethyl acetate in hexanes) of the residue yielded a white solid (31.5 mg, 95%). The ratio of  $\delta$ -lactone to  $\gamma$ -lactone of the isolated material was determined to be 85:15 ( $^1\text{H}$  NMR). The product was determined to be 90% ee by chiral HPLC analysis (Chiralcel IA, 9%  $^i\text{PrOH}$ /hexanes, 1 mL/min,  $t_r(e_1, \text{major}) = 22.6$  min,  $t_r(e_2, \text{minor}) = 25.8$  min);  $R_f = 0.46$  (40% EtOAc/hexanes) visualized with  $\text{KMnO}_4$ ; IR (film) 2935, 2837, 1740, 1602  $\text{cm}^{-1}$ ;  $\delta$ -lactone  $^1\text{H}$  NMR (600 MHz,  $\text{CDCl}_3$ )  $\delta$  7.31 (dd,  $J = 8.0, 8.0$  Hz, 1H), 6.91 (dd,  $J = 8.1, 2.2$  Hz, 2H), 6.84 (dd,  $J = 2.0, 2.0$  Hz, 1H), 5.53 (d,  $J = 7.6$  Hz, 1H), 4.43 (ddd,  $J = 7.7, 7.7, 4.5$  Hz, 1H), 3.80 (s, 3H), 2.85 (ddd,  $J = 18.2, 7.1, 7.1$  Hz, 1H), 2.71 (ddd,  $J = 18.2, 6.8, 6.8$  Hz, 1H), 2.43 (dddd,  $J = 14.3, 6.8, 6.8, 4.6$  Hz, 1H), 2.35 (dddd,  $J = 14.6, 7.1, 7.1, 7.1$  Hz, 1H);  $^{13}\text{C}$  NMR (150 MHz,  $\text{CDCl}_3$ ) ppm 169.0, 159.8, 139.1, 129.8, 119.0, 114.4, 112.5, 86.9, 55.3, 30.43, 30.36, 24.2;  $\gamma$ -lactone  $^1\text{H}$  NMR (600 MHz,  $\text{CDCl}_3$ )  $\delta$  7.23 (dd,  $J = 7.8, 7.8$  Hz, 1H), 6.99 (d,  $J = 7.2$  Hz, 1H), 6.95 (dd,  $J = 1.8, 1.8$  Hz, 1H), 6.81 (dd,  $J = 7.8, 1.2$  Hz, 1H), 5.09 (d,  $J = 7.8$  Hz, 1H), 4.87 (ddd,  $J = 7.8, 7.8, 7.8$  Hz, 1H), 3.79 (s, 3H), 2.63-2.49 (m, 3H), 2.16-2.11 (m, 1H);  $^{13}\text{C}$  NMR (150 MHz,  $\text{CDCl}_3$ ) ppm 176.0, 159.6, 140.5, 129.9, 120.4, 114.14, 114.11, 82.5, 55.3, 34.0, 29.2, 28.8; HRMS (ESI): Exact mass calcd for  $\text{C}_{12}\text{H}_{13}\text{INaO}_3$   $[\text{M}+\text{Na}]^+$  354.9807, found 354.9805.

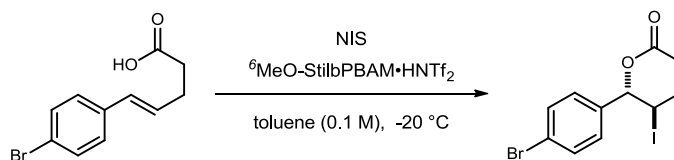


**(5R,6S)-6-(4-Fluorophenyl)-5-iodotetrahydro-2H-pyran-2-one (284i).** Prepared according to the general procedure using the parent acid (19.4 mg, 100  $\mu\text{mol}$ ),  $^6\text{MeO-StilbPBAM}\cdot\text{HNTf}_2$  (1.9 mg, 2.0  $\mu\text{mol}$ ) and NIS (23.5 mg, 105  $\mu\text{mol}$ ) over 72 hours. Flash column chromatography ( $\text{SiO}_2$ , 10-30% ethyl acetate in hexanes) of the residue yielded a white solid (27.7 mg, 87%). The ratio of  $\delta$ -lactone to  $\gamma$ -lactone of the isolated material was determined to be 93:7 ( $^1\text{H NMR}$ ). The product was determined to be 95% ee by chiral HPLC analysis (Chiralcel IA, 9%  $^i\text{PrOH}$ /hexanes, 1 mL/min,  $t_r(e_1, \text{major}) = 28.5$  min,  $t_r(e_2, \text{minor}) = 33.3$  min);  $R_f = 0.53$  (40% EtOAc/hexanes) visualized with  $\text{KMnO}_4$ ; IR (film) 2919, 1740, 1605, 1512  $\text{cm}^{-1}$ ;  $^1\text{H NMR}$  (600 MHz,  $\text{CDCl}_3$ )  $\delta$  7.33 (dd,  $J = 8.7, 5.1$  Hz, 2H), 7.09 (dd,  $J = 8.6, 8.6$  Hz, 2H), 5.49 (d,  $J = 8.9$  Hz, 1H), 4.32 (ddd,  $J = 8.9, 8.9, 4.7$  Hz, 1H), 2.83 (ddd,  $J = 18.1, 6.5, 6.5$  Hz, 1H), 2.72 (ddd,  $J = 18.1, 8.3, 6.7$  Hz, 1H), 2.57-2.51 (m, 1H), 2.48-2.42 (m, 1H);  $^{13}\text{C NMR}$  (150 MHz,  $\text{CDCl}_3$ ) ppm 169.1, 163.5 (d,  $^1J_{\text{CF}} = 249$  Hz), 133.4 (d,  $^4J_{\text{CF}} = 3.2$  Hz), 128.9 (d,  $^3J_{\text{CF}} = 8.6$  Hz), 115.7 (d,  $^2J_{\text{CF}} = 22$  Hz), 86.4, 31.3, 30.8, 24.1;  $^{19}\text{F NMR}$  (376 MHz,  $\text{CDCl}_3$ ) -109.9; HRMS (ESI): Exact mass calcd for  $\text{C}_{11}\text{H}_{10}\text{FINaO}_2$   $[\text{M}+\text{Na}]^+$  342.9607, found 342.9614.

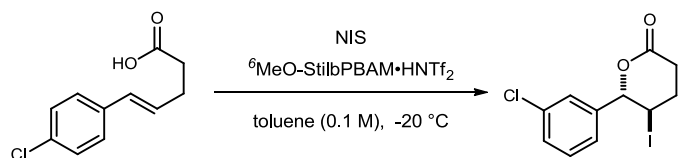


**(5R,6S)-6-(4-Chlorophenyl)-5-iodotetrahydro-2H-pyran-2-one (284j).** Prepared according to the general procedure using the parent acid (21.0 mg, 100  $\mu\text{mol}$ ),  $^6\text{MeOStilbPBAM}\cdot\text{HNTf}_2$  (4.7 mg, 5.0  $\mu\text{mol}$ ) and NIS (24.6 mg, 110  $\mu\text{mol}$ ) over 72 hours. Flash column chromatography ( $\text{SiO}_2$ , 10-30% ethyl acetate in hexanes) of the residue yielded a yellow solid (30.6 mg, 91%). The ratio of  $\delta$ -lactone to  $\gamma$ -lactone of the isolated material was determined to be 81:19 ( $^1\text{H NMR}$ ). The product was determined to be 93% ee by chiral HPLC analysis (Chiralcel IA, 6%  $^i\text{PrOH}$ /hexanes, 1 mL/min,  $t_r(e_1, \text{minor}) = 23.1$  min,  $t_r(e_2, \text{major}) = 26.3$  min);  $R_f = 0.53$  (40% EtOAc/hexanes) visualized with  $\text{KMnO}_4$ ; IR (film) 2923, 1742  $\text{cm}^{-1}$ ;  $\delta$ -lactone  $^1\text{H NMR}$  (600 MHz,  $\text{CDCl}_3$ )  $\delta$  7.38 (d,  $J = 8.5$  Hz, 2H), 7.29 (d,  $J = 8.5$  Hz, 2H), 5.49 (d,  $J = 8.6$  Hz, 1H), 4.32 (ddd,  $J = 8.8, 8.8, 4.7$  Hz, 1H), 2.84 (ddd,  $J = 18.2, 6.6, 6.6$  Hz, 1H), 2.73 (ddd,  $J = 18.2, 8.1, 6.7$  Hz, 1H), 2.54-2.49 (m, 1H), 2.44 (dddd,  $J = 16.9, 8.4, 8.4, 6.8$  Hz, 1H);  $^{13}\text{C NMR}$  (150 MHz,  $\text{CDCl}_3$ ) ppm 169.1, 136.0, 135.1, 128.9, 128.4, 86.4, 31.1, 30.8, 23.8;  $\gamma$ -lactone  $^1\text{H NMR}$  (600 MHz,  $\text{CDCl}_3$ )  $\delta$  7.35 (d,  $J = 9.0$  Hz, 2H), 7.29 (d,  $J = 8.4$  Hz, 2H), 5.04 (d,  $J = 8.4$  Hz, 1H), 4.91 (ddd,  $J = 8.4, 8.4, 6.6$  Hz, 1H), 2.68-2.63 (m, 1H), 2.62-2.56 (m, 2H), 2.11 (dddd,  $J = 12.9, 9.9, 9.9, 8.3$  Hz, 1H);  $^{13}\text{C NMR}$  (150 MHz,  $\text{CDCl}_3$ ) ppm 176.0, 137.9, 134.4, 129.4, 129.1, 82.3, 32.5, 29.3, 29.0; HRMS (ESI): Exact mass calcd for  $\text{C}_{11}\text{H}_{10}\text{ClINaO}_2$   $[\text{M}+\text{Na}]^+$  358.9312, found 358.9318.

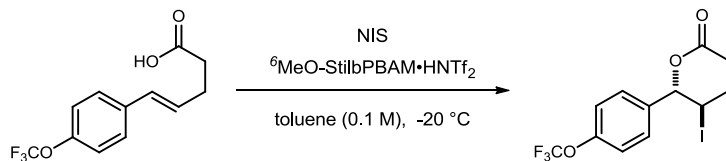




**(5R,6S)-6-(4-Bromophenyl)-5-iodotetrahydro-2H-pyran-2-one (284k).** Prepared according to the general procedure using the parent acid (25.5 mg, 100 μmol), <sup>6</sup>MeOStilbPBAM•HNTf<sub>2</sub> (4.7 mg, 5.0 μmol) and NIS (24.6 mg, 110 μmol) over 72 hours. Flash column chromatography (SiO<sub>2</sub>, 10-30% ethyl acetate in hexanes) of the residue yielded a yellow solid (25.1 mg, 66%). The ratio of δ-lactone to γ-lactone of the isolated material was determined to be 77:23 (<sup>1</sup>H NMR). The product was determined to be 91% ee by chiral HPLC analysis (Chiralcel IA, 9% <sup>i</sup>PrOH/hexanes, 1 mL/min, *t<sub>r</sub>*(*e*<sub>1</sub>, minor) = 18.2 min, *t<sub>r</sub>*(*e*<sub>2</sub>, major) = 20.8 min); *R<sub>f</sub>* = 0.52 (40% EtOAc/hexanes) visualized with KMnO<sub>4</sub>; IR (film) 2921, 1741 cm<sup>-1</sup>; δ-lactone <sup>1</sup>H NMR (600 MHz, CDCl<sub>3</sub>) δ 7.53 (d, *J* = 8.5 Hz, 2H), 7.22 (d, *J* = 8.4 Hz, 2H), 5.48 (d, *J* = 8.6 Hz, 1H), 4.32 (ddd, *J* = 8.6, 8.6, 4.7 Hz, 1H), 2.83 (ddd, *J* = 18.1, 6.6, 6.6 Hz, 1H), 2.71 (ddd, *J* = 18.1, 7.9, 6.6 Hz, 1H), 2.53-2.48 (m, 1H), 2.43 (dddd, *J* = 16.5, 8.2, 8.2, 7.0 Hz, 1H); <sup>13</sup>C NMR (150 MHz, CDCl<sub>3</sub>) ppm 168.8, 136.6, 131.9, 128.6, 123.3, 86.4, 31.1, 30.7, 23.6; γ-lactone <sup>1</sup>H NMR (600 MHz, CDCl<sub>3</sub>) δ 7.45 (d, *J* = 8.4 Hz, 2H), 7.29 (d, *J* = 8.4 Hz, 2H), 5.03 (d, *J* = 8.4 Hz, 1H), 4.88 (ddd, *J* = 7.8, 7.8, 6.6 Hz, 1H), 2.67-2.61 (m, 1H), 2.60-2.56 (m, 2H), 2.10 (dddd, *J* = 12.8, 9.9, 9.9, 8.2 Hz, 1H); <sup>13</sup>C NMR (150 MHz, CDCl<sub>3</sub>) ppm 175.8, 138.4, 132.0, 129.7, 122.5, 82.2, 32.6, 29.3, 28.9; HRMS (EI): Exact mass calcd for C<sub>11</sub>H<sub>10</sub>BrIO<sub>2</sub> [M]<sup>+</sup> 379.8903, found 379.8904.

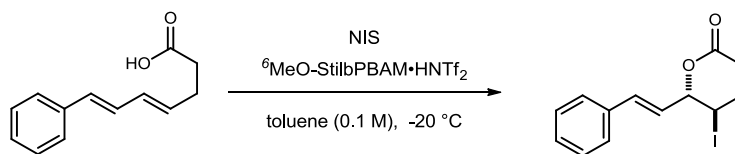


**(5R,6S)-6-(3-Chlorophenyl)-5-iodotetrahydro-2H-pyran-2-one (284I).** Prepared according to the general procedure using the parent acid (21.0 mg, 100  $\mu\text{mol}$ ), <sup>6</sup>MeOStilbPBAM•HNTf<sub>2</sub> (4.7 mg, 5.0  $\mu\text{mol}$ ) and NIS (24.6 mg, 110  $\mu\text{mol}$ ) over 72 hours. Flash column chromatography (SiO<sub>2</sub>, 10-30% ethyl acetate in hexanes) of the residue yielded a yellow solid (17.2 mg, 51%). The ratio of  $\delta$ -lactone to  $\gamma$ -lactone of the isolated material was determined to be 48:52 (<sup>1</sup>H NMR). The product was determined to be 88% ee by chiral HPLC analysis (Chiralcel IA, 8% EtOH/hexanes, 1 mL/min,  $t_r(e_1, \text{minor}) = 24.6$  min,  $t_r(e_2, \text{major}) = 27.6$  min);  $R_f = 0.39$  (40% EtOAc/hexanes) visualized with KMnO<sub>4</sub>; IR (film) 2920, 1775, 1741  $\text{cm}^{-1}$ ;  $\delta$ -lactone <sup>1</sup>H NMR (600 MHz, CDCl<sub>3</sub>)  $\delta$  7.40-7.23 (m, 4H), 5.49 (d,  $J = 8.4$  Hz, 1H), 4.35 (ddd,  $J = 8.5, 8.5, 4.7$  Hz, 1H), 2.84 (ddd,  $J = 18.2, 6.7, 6.7$  Hz, 1H), 2.73 (ddd,  $J = 18.1, 7.7, 6.6$  Hz, 1H), 2.52-2.47 (m, 1H), 2.42 (dddd,  $J = 14.9, 8.0, 8.0, 8.0$  Hz, 1H);  $\gamma$ -lactone <sup>1</sup>H NMR (600 MHz, CDCl<sub>3</sub>)  $\delta$  7.40-7.23 (m, 4H), 5.02 (d,  $J = 8.6$  Hz, 1H), 4.89 (ddd,  $J = 8.0, 8.0, 6.4$  Hz, 1H), 2.67 (dddd,  $J = 13.6, 6.4, 6.4, 6.4$  Hz, 1H), 2.61-2.58 (m, 2H), 2.14 (dddd,  $J = 14.5, 12.9, 12.9, 4.7$  Hz, 1H); mixture of  $\delta$ -lactone &  $\gamma$ -lactone <sup>13</sup>C NMR (150 MHz, CDCl<sub>3</sub>) ppm 175.8, 168.7, 141.3, 139.5, 134.7, 134.6, 130.2, 130.0, 129.5, 128.9, 128.2, 127.1, 126.4, 125.3, 86.3, 82.2, 32.3, 31.0, 30.7, 29.3, 29.1, 23.5; HRMS (ESI): Exact mass calcd for C<sub>11</sub>H<sub>10</sub>ClI<sub>2</sub>NaO<sub>2</sub> [M+Na]<sup>+</sup> 358.9312, found 358.9308.

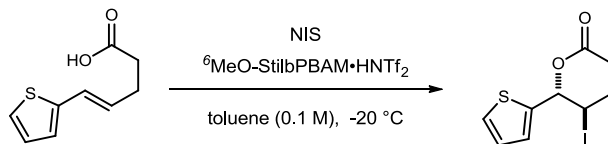


**(5*R*,6*S*)-5-Iodo-6-(4-(trifluoromethoxy)phenyl)tetrahydro-2*H*-pyran-2-one (284*m*).**

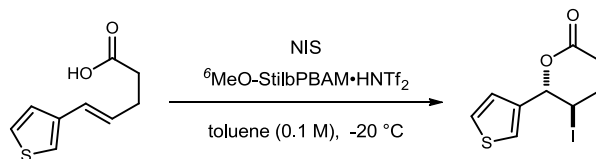
Prepared according to the general procedure using the parent acid (26.0 mg, 100  $\mu$ mol), <sup>6</sup>MeOStilbPBAM•HNTf<sub>2</sub> (4.7 mg, 5.0  $\mu$ mol) and NIS (24.6 mg, 110  $\mu$ mol) over 72 hours. Flash column chromatography (SiO<sub>2</sub>, 10-30% ethyl acetate in hexanes) of the residue yielded an oil (30.6 mg, 79%). The ratio of  $\delta$ -lactone to  $\gamma$ -lactone of the isolated material was determined to be 76:24 (<sup>1</sup>H NMR). The product was determined to be 95% ee by chiral HPLC analysis (Chiralcel IA, 7% EtOH/hexanes, 1 mL/min,  $t_r(e_1, \text{minor}) = 18.5$  min,  $t_r(e_2, \text{major}) = 27.8$  min);  $R_f = 0.53$  (40% EtOAc/hexanes) visualized with KMnO<sub>4</sub>; IR (film) 2921, 1744, 1511 cm<sup>-1</sup>;  $\delta$ -lactone <sup>1</sup>H NMR (600 MHz, CDCl<sub>3</sub>)  $\delta$  7.38 (d,  $J = 8.6$  Hz, 2H), 7.25 (d,  $J = 8.3$  Hz, 2H), 5.53 (d,  $J = 8.8$  Hz, 1H), 4.32 (ddd,  $J = 8.8, 8.8, 4.7$  Hz, 1H), 2.84 (ddd,  $J = 18.1, 6.5, 6.5$  Hz, 1H), 2.73 (ddd,  $J = 18.1, 8.1, 6.6$  Hz, 1H), 2.56-2.50 (m, 1H), 2.45 (dddd,  $J = 16.9, 8.5, 8.5, 7.0$  Hz, 1H); <sup>13</sup>C NMR (150 MHz, CDCl<sub>3</sub>) ppm 168.9, 149.6, 136.1, 128.6, 121.0, 120.3 (q, <sup>1</sup> $J_{CF} = 258$  Hz), 86.2, 31.2, 30.8, 23.6; <sup>19</sup>F NMR (376 MHz, CDCl<sub>3</sub>) -55.98;  $\gamma$ -lactone <sup>1</sup>H NMR (600 MHz, CDCl<sub>3</sub>)  $\delta$  7.45 (d,  $J = 8.6$  Hz, 2H), 7.17 (d,  $J = 8.3$  Hz, 2H), 5.06 (d,  $J = 8.7$  Hz, 1H), 4.92 (ddd,  $J = 8.2, 8.2, 6.4$  Hz, 1H), 2.69-2.65 (m, 1H), 2.61-2.58 (m, 2H), 2.15-2.09 (m, 1H); <sup>13</sup>C NMR (150 MHz, CDCl<sub>3</sub>) ppm 176.0, 148.9, 138.0, 129.6, 121.2, 120.2 (q, <sup>1</sup> $J_{CF} = 258$  Hz), 82.3, 32.1, 29.4, 29.1; <sup>19</sup>F NMR (376 MHz, CDCl<sub>3</sub>) -55.96; HRMS (ESI): Exact mass calcd for C<sub>12</sub>H<sub>10</sub>F<sub>3</sub>INaO<sub>3</sub> [M+Na]<sup>+</sup> 408.9525, found 408.9544.



**(5R,6S)-5-Iodo-6-((E)-styryl)tetrahydro-2H-pyran-2-one (284n).** Prepared according to the general procedure using the parent acid (20.2 mg, 100  $\mu$ mol), <sup>6</sup>MeOStilbPBAM•HNTf<sub>2</sub> (4.7 mg, 5.0  $\mu$ mol) and NIS (24.6 mg, 110  $\mu$ mol) over 24 hours. Flash column chromatography (SiO<sub>2</sub>, 10-30% ethyl acetate in hexanes) of the residue yielded a white solid (29.6 mg, 90%). The ratio of  $\delta$ -lactone to  $\gamma$ -lactone of the isolated material was determined to be >95:5 (<sup>1</sup>H NMR). The product was determined to be 67% ee by chiral HPLC analysis (Chiralcel IA, 9% <sup>i</sup>PrOH/hexanes, 1 mL/min,  $t_r(e_1, \text{minor}) = 15.0$  min,  $t_r(e_2, \text{major}) = 18.2$  min);  $R_f = 0.43$  (40% EtOAc/hexanes) visualized with KMnO<sub>4</sub>; IR (film) 3025, 1738 cm<sup>-1</sup>; <sup>1</sup>H NMR (600 MHz, CDCl<sub>3</sub>)  $\delta$  7.41 (d,  $J = 7.2$  Hz, 2H), 7.35 (dd,  $J = 7.2, 7.2$  Hz, 2H), 7.30 (t,  $J = 7.3$  Hz, 1H), 6.75 (d,  $J = 15.8$  Hz, 1H), 6.19 (dd,  $J = 15.8, 6.5$  Hz, 1H), 5.19 (dd,  $J = 7.6, 7.6$  Hz, 1H), 4.25 (ddd,  $J = 8.2, 8.2, 4.5$  Hz, 1H), 2.80 (ddd,  $J = 18.2, 6.8, 6.8$  Hz, 1H), 2.65 (ddd,  $J = 18.1, 7.2, 7.2$  Hz, 1H), 2.53 (dddd,  $J = 14.3, 6.6, 6.6, 4.5$  Hz, 1H), 2.38 (dddd,  $J = 14.7, 7.4, 7.4, 7.4$  Hz, 1H); <sup>13</sup>C NMR (150 MHz, CDCl<sub>3</sub>) ppm 168.9, 135.38, 135.37, 128.7, 128.6, 126.9, 124.7, 85.5, 30.8, 30.6, 23.1; HRMS: sample decomposed.

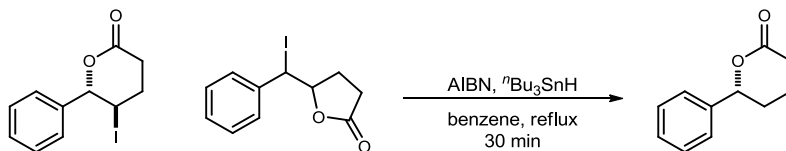


**(5R,6S)-5-Iodo-6-(thiophen-2-yl)tetrahydro-2H-pyran-2-one (284o).** Prepared according to the general procedure using the parent acid (18.2 mg, 100  $\mu$ mol), <sup>6</sup>MeOStilbPBAM•HNTf<sub>2</sub> (4.7 mg, 5.0  $\mu$ mol) and NIS (24.6 mg, 110  $\mu$ mol) over 24 hours. Flash column chromatography (SiO<sub>2</sub>, 10-30% ethyl acetate in hexanes) of the residue yielded a white solid (24.7 mg, 80%). The ratio of  $\delta$ -lactone to  $\gamma$ -lactone of the isolated material was determined to be >95:5 (<sup>1</sup>H NMR). The product was determined to be 29% ee by chiral HPLC analysis (Chiralcel IA, 9% <sup>i</sup>PrOH/hexanes, 1 mL/min,  $t_r(e_1, \text{minor}) = 15.9$  min,  $t_r(e_2, \text{major}) = 17.4$  min);  $R_f = 0.52$  (40% EtOAc/hexanes) visualized with KMnO<sub>4</sub>; IR (film) 2927, 1740 cm<sup>-1</sup>; <sup>1</sup>H NMR (600 MHz, CDCl<sub>3</sub>)  $\delta$  7.37 (dd,  $J = 5.0, 1.1$  Hz, 1H), 7.12 (d,  $J = 3.6$  Hz, 1H), 7.02 (dd,  $J = 5.0, 3.6$  Hz, 1H), 5.80 (d,  $J = 7.7$  Hz, 1H), 4.48 (ddd,  $J = 8.0, 8.0, 4.6$  Hz, 1H), 2.82 (ddd,  $J = 18.2, 6.9, 6.9$  Hz, 1H), 2.68 (ddd,  $J = 18.1, 7.1, 6.7$  Hz, 1H), 2.52 (dddd,  $J = 14.4, 6.7, 6.7, 4.5$  Hz, 1H), 2.40 (dddd,  $J = 14.7, 7.4, 7.4, 7.4$  Hz, 1H); <sup>13</sup>C NMR (150 MHz, CDCl<sub>3</sub>) ppm 168.4, 140.6, 127.2, 126.9, 126.5, 83.1, 30.8, 30.4, 24.1; HRMS: sample decomposed.



**(5R,6S)-5-Iodo-6-(thiophen-3-yl)tetrahydro-2H-pyran-2-one (284p).** Prepared according to the general procedure using the parent acid (18.2 mg, 100  $\mu\text{mol}$ ), <sup>6</sup>MeOStilbPBAM•HNTf<sub>2</sub> (4.7 mg, 5.0  $\mu\text{mol}$ ) and NIS (24.6 mg, 110  $\mu\text{mol}$ ) over 24 hours. Flash column chromatography (SiO<sub>2</sub>, 10-30% ethyl acetate in hexanes) of the residue yielded a white solid (24.2 mg, 79%). The ratio of  $\delta$ -lactone to  $\gamma$ -lactone of the isolated material was determined to be 97:3 (<sup>1</sup>H NMR). The product was determined to be 85% ee by chiral HPLC analysis (Chiralcel IA, 9% <sup>i</sup>PrOH/hexanes, 1 mL/min,  $t_r(e_1, \text{minor}) = 19.9$  min,  $t_r(e_2, \text{major}) = 23.9$  min);  $R_f = 0.66$  (40% EtOAc/hexanes) visualized with KMnO<sub>4</sub>; IR (film) 2926, 1735  $\text{cm}^{-1}$ ; <sup>1</sup>H NMR (600 MHz, CDCl<sub>3</sub>)  $\delta$  7.37 (dd,  $J = 5.0, 2.9$  Hz, 1H), 7.32 (d,  $J = 2.8$  Hz, 1H), 7.06 (dd,  $J = 5.0, 1.2$  Hz, 1H), 5.67 (d,  $J = 7.2$  Hz, 1H), 4.48 (ddd,  $J = 7.4, 7.4, 4.6$  Hz, 1H), 2.84 (ddd,  $J = 18.2, 7.3, 7.3$  Hz, 1H), 2.67 (ddd,  $J = 18.2, 6.6, 6.6$  Hz, 1H), 2.41 (dddd,  $J = 14.4, 6.7, 6.7, 4.6$  Hz, 1H), 2.34 (dddd,  $J = 14.3, 7.0, 7.0, 7.0$  Hz, 1H); <sup>13</sup>C NMR (150 MHz, CDCl<sub>3</sub>) ppm 168.9, 138.9, 127.1, 125.1, 124.1, 83.5, 30.24, 30.21, 23.8; HRMS: sample decomposed.

## Determination of Absolute Stereochemistry

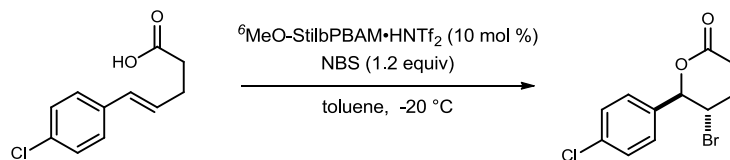


**(R)-6-phenyltetrahydro-2H-pyran-2-one.** Procedure adapted from a previous report.<sup>138</sup>

A 15-mL, round-bottomed flask equipped with a stir bar was charged with (5*R*,6*S*)-5-iodo-6-phenyltetrahydro-2*H*-pyran-2-one [88  $\delta$ -lactone (93% ee)/12  $\gamma$ -lactone, 60.4 mg, 200  $\mu$ mol], benzene (5 mL) and tributyltin hydride (65  $\mu$ L, 240  $\mu$ mol). The reaction was brought to reflux and recrystallized AIBN (6.5 mg, 40  $\mu$ mol) was added. The reaction was monitored by TLC and after 30 m complete conversion was observed. The reaction mixture was concentrated to an oil. Flash column chromatography (SiO<sub>2</sub>, 5-20% ethyl acetate in hexanes) yielded a white solid (23.0 mg, 65%) as only the  $\delta$ -lactone.  $R_f$  = 0.43 (20% EtOAc/hexanes);  $[\alpha]_D^{20}$  +29.0 ( $c$  1.00, CHCl<sub>3</sub>) [reported for 47% ee of (*S*)-material,  $[\alpha]_D^{26}$  -19.1 ( $c$  0.3, CHCl<sub>3</sub>)].<sup>139</sup> Remainder of analytical data matched literature values.

<sup>138</sup> Wang, M.; Gao, L. X.; Mai, W. P.; Xia, A. X.; Wang, F.; Zhang, S. B. *J. Org. Chem.* **2004**, *69*, 2874-2876.

<sup>139</sup> Hsu, J.-L.; Fang, J.-M. *J. Org. Chem.* **2001**, *66*, 8573-8584.



**(5S,6R)-5-bromo-6-(4-chlorophenyl)tetrahydro-2H-pyran-2-one (290).** To a flame dried vial equipped with a stir bar was added StilbPBAM•HNTf<sub>2</sub> (8.8 mg, 10 μmol), (*E*)-5-(4-chlorophenyl)pent-4-enoic acid (21.0 mg, 100 μmol), toluene (1 mL), and the reaction mixture was cooled to -20 °C. NIS (26.9 mg, 120 μmol) was added and the mixture was stirred for 6 hours (protected from light). The mixture was treated with 20% aq sodium thiosulfate (2 mL) and then partitioned between dichloromethane (15 mL) and 3 M NaOH (15 mL). The aqueous layer was extracted twice and the organic layers were combined, dried, and concentrated. Flash column chromatography (SiO<sub>2</sub>, 10-25-50% ethyl acetate in hexanes) yielded the product as a white solid (29 mg, 90%). Remainder of analytical data matched literature values and the ee of the product was determined by chiral HPLC analysis.



Appendix I. Cost of VNI.

| Chemical                 | Y           | Cost        | Amount Supp. (grams) | Cost/gram | equiv | mmol used    | Amount used  | Actual Cost |
|--------------------------|-------------|-------------|----------------------|-----------|-------|--------------|--------------|-------------|
| 2,4-dichlorobenzaldehyde | 175.01      | \$29.00     | 100                  | \$0.29    | 1.20  | 80.74        | 14.130       | \$4.10      |
| benzenesulfonic acid     | 164.16      | \$220.50    | 500                  | \$0.44    | 2.00  | 134.57       | 22.091       | \$9.74      |
| Boc-carbamate            | 117.20      | \$64.50     | 25                   | \$2.58    | 1.00  | 67.28        | 7.886        | \$20.35     |
| HCOOH                    | 46.63       | \$102.00    | 1220                 | \$0.08    | 2.00  | 134.57       | 6.275        | \$0.52      |
| MeOH (mL)                |             |             |                      |           |       |              |              | \$0.01      |
| H2O (mL)                 |             |             |                      |           |       |              |              | \$0.01      |
| <b>sulfone</b>           | <b>81%</b>  | <b>BRSM</b> |                      |           |       |              | <b>54.50</b> |             |
| potassium carbonate      | 138.21      | \$35.35     | 500                  | \$0.07    | 7.00  | 381.50       | 52.727       | \$3.73      |
| sodium sulfate           | 142.04      | \$45.31     | 500                  | \$0.09    | 8.00  | 436.00       | 61.929       | \$5.61      |
| THF (mL)                 |             | \$46.05     | 4                    | \$11.51   |       |              | 0.540        | \$6.22      |
| <b>imine</b>             | <b>98%</b>  |             |                      |           |       | <b>53.41</b> |              |             |
| PBAM                     | 506.70      |             |                      |           | 0.01  | 0.69         | 0.352        | \$0.00      |
| toluene (mL)             |             | \$24.80     | 4                    | \$6.20    |       |              | 0.290        | \$1.80      |
| bromonitromethane        | 139.90      | \$68.70     | 10                   | \$6.87    | 1.50  | 80.12        | 11.208       | \$77.00     |
| <b>aza-Henry adduct</b>  | <b>98%</b>  |             |                      |           |       | <b>52.34</b> |              |             |
| cobalt chloride          | 129.80      | \$41.80     | 50                   | \$0.84    | 1.00  | 52.34        | 6.794        | \$5.68      |
| sodium borohydride       | 37.80       | \$50.30     | 25                   | \$2.01    | 5.00  | 261.71       | 9.893        | \$19.90     |
| MeOH (mL)                |             | \$40.23     | 1                    | \$40.23   |       |              | 0.530        | \$21.32     |
| <b>amine</b>             | <b>52%</b>  |             |                      |           |       | <b>27.22</b> |              |             |
| glyoxal (%)              | 58.00       | \$34.00     | 100                  | \$0.34    | 2.00  | 54.44        | 3.157        | \$1.07      |
| formaldehyde (%)         | 30.00       | \$46.20     | 500                  | \$0.09    | 2.00  | 54.44        | 1.633        | \$0.15      |
| ammonium acetate         | 77.10       | \$37.65     | 500                  | \$0.08    | 2.00  | 54.44        | 4.197        | \$0.32      |
| MeOH (mL)                |             |             |                      |           |       |              |              | \$0.01      |
| <b>imidazole</b>         | <b>59%</b>  |             |                      |           |       | <b>16.06</b> |              |             |
| trifluoroacetic acid     | 114.02      | \$111.80    | 500                  | \$0.22    | 20.00 | 321.17       | 36.620       | \$8.19      |
| dichloromethane          |             | \$12.35     | 4                    | \$3.09    |       |              | 0.153        | \$0.47      |
| <b>amine</b>             | <b>100%</b> |             |                      |           |       | <b>16.06</b> |              |             |
| EDC HCl                  | 191.70      | \$177.00    | 25                   | \$7.08    | 1.50  | 24.09        | 4.618        | \$32.69     |
| DMAP                     | 122.17      | \$396.00    | 500                  | \$0.79    | 0.10  | 1.61         | 0.196        | \$0.16      |
| carboxylic acid          | 266.30      |             | see above            | \$7.06    | 1.00  | 16.06        | 4.276        | \$30.19     |
| dichloromethane          |             | \$12.35     | 4                    | \$3.09    |       |              | 0.149        | \$0.46      |
| <b>(+)-VNI</b>           | <b>65%</b>  |             |                      |           |       | <b>10.44</b> |              |             |
|                          |             | \$1,595.89  |                      |           |       | SUM          |              | \$249.70    |
|                          |             |             |                      |           |       | grams made   |              | 5.26        |
|                          |             |             |                      |           |       | cost/gram    |              | \$47.44     |
|                          |             |             |                      |           |       |              |              | \$0.05      |

## Appendix II. StilbPBAM Crystal Structure

The sample was submitted by Mark Dobish (research group of Jeff Johnston, Department of Chemistry, Vanderbilt University). A colorless needle (approximate dimensions  $0.20 \times 0.12 \times 0.10$  mm<sup>3</sup>) was placed onto the tip of a 0.1 mm diameter glass capillary and mounted on a Bruker APEX II Kappa Duo diffractometer equipped with an APEX II detector at 150(2) K.

### Data collection

The data collection was carried out using Mo K $\alpha$  radiation (graphite monochromator) with a frame time of 10 seconds and a detector distance of 5.00 cm. A collection strategy was calculated and complete data to a resolution of 0.70 Å with a redundancy of 4 were collected. Four major sections of frames were collected with 0.50°  $\omega$  and  $\phi$  scans. Data to a resolution of 0.77 Å were considered in the reduction. Final cell constants were calculated from the xyz centroids of 9863 strong reflections from the actual data collection after integration (SAINT).<sup>140</sup> The intensity data were corrected for absorption (SADABS).<sup>141</sup> Please refer to Table 1 for additional crystal and refinement information.

### Structure solution and refinement

The space group P2<sub>1</sub>2<sub>1</sub>2<sub>1</sub> was determined based on intensity statistics and systematic absences. The structure was solved using SIR-2004<sup>142</sup> and refined with

---

<sup>140</sup> SAINT, Bruker Analytical X-Ray Systems, Madison, WI, current version.

<sup>141</sup> An empirical correction for absorption anisotropy.

<sup>142</sup> Sir2004, A Program for Automatic Solution and Refinement of Crystal Structures. M. C. Burla, R. Caliandro, M. Carnalli, B. Carrozzini, G. L. Cascarano, L. De Caro, C. Giacovazzo, G. Polidori, R. Sagna. Vers. 1.0 (2004).

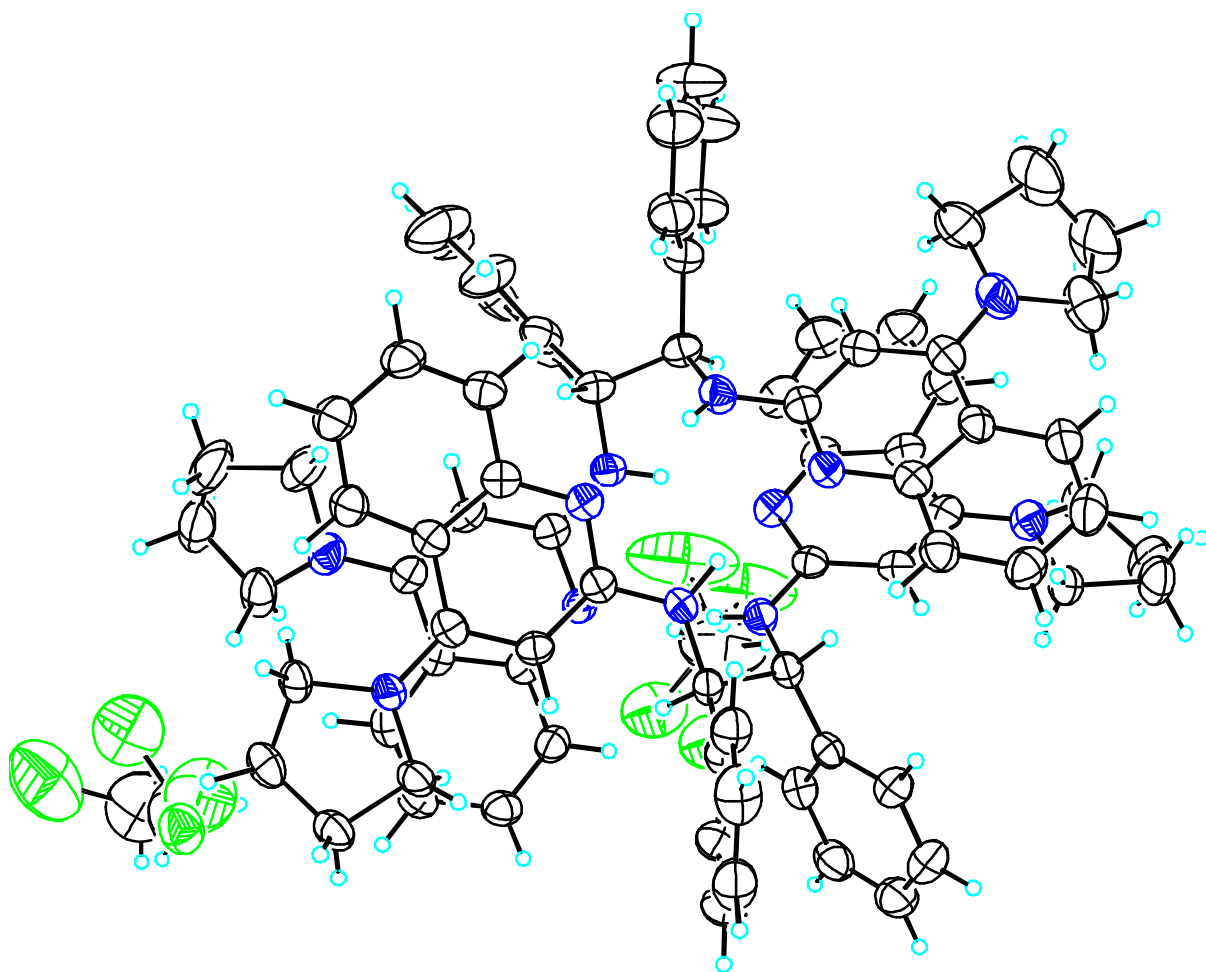
SHELXL-97.<sup>143</sup> A direct-methods solution was calculated, which provided most non-hydrogen atoms from the E-map. Full-matrix least squares / difference Fourier cycles were performed, which located the remaining non-hydrogen atoms. All non-hydrogen atoms were refined with anisotropic displacement parameters. The hydrogen atoms were placed in ideal positions and refined as riding atoms with relative isotropic displacement parameters with the exception of N-bound hydrogen atoms which were refined for all parameters. The final full matrix least squares refinement converged to  $R1 = 0.0668$  and  $wR2 = 0.1959$  ( $F^2$ , all data). The remaining electron density is minuscule and located near the disordered solvent.

### Structure description

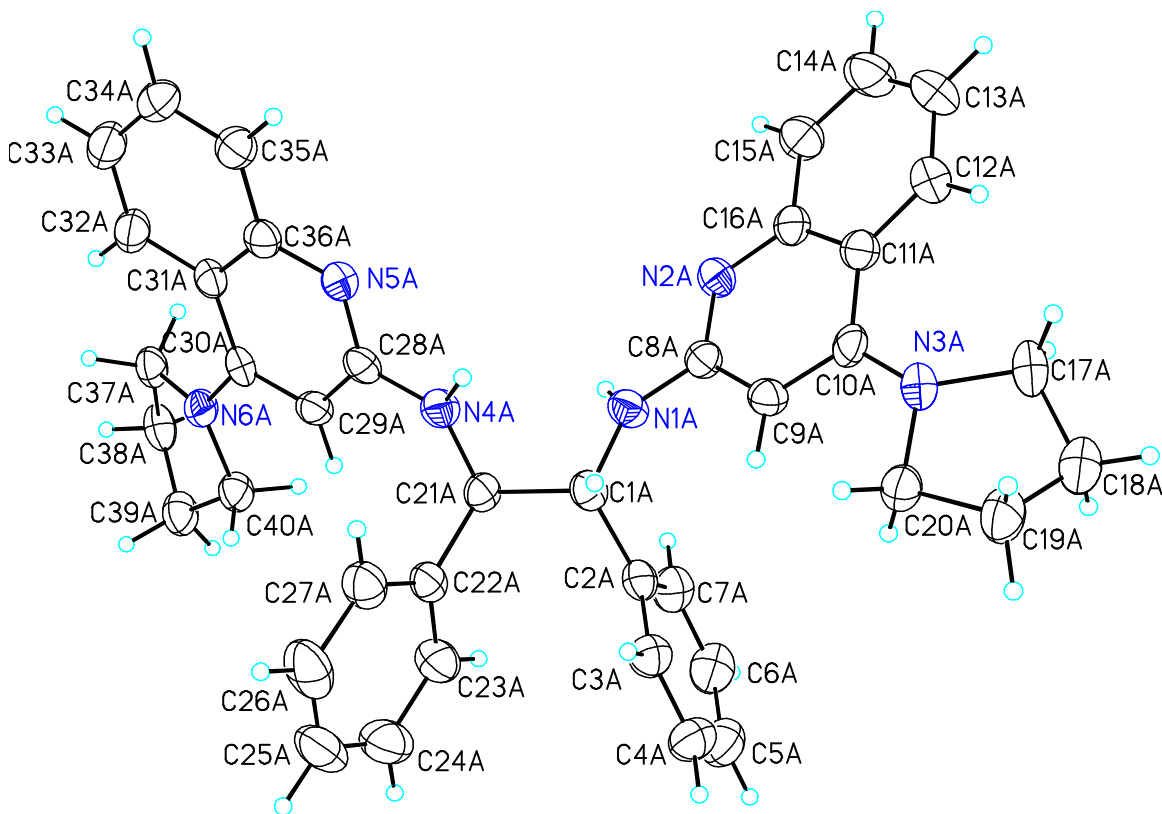
The structure was found as proposed and its absolute configuration was determined by anomalous dispersion. Two crystallographically independent molecules and three solvent molecules are in the asymmetric unit. A least-squares fit of the independent molecules (named A and B) are included in the tables. The solvent molecules (DCM) are disordered over two sites each and were refined with a set of restraints.

---

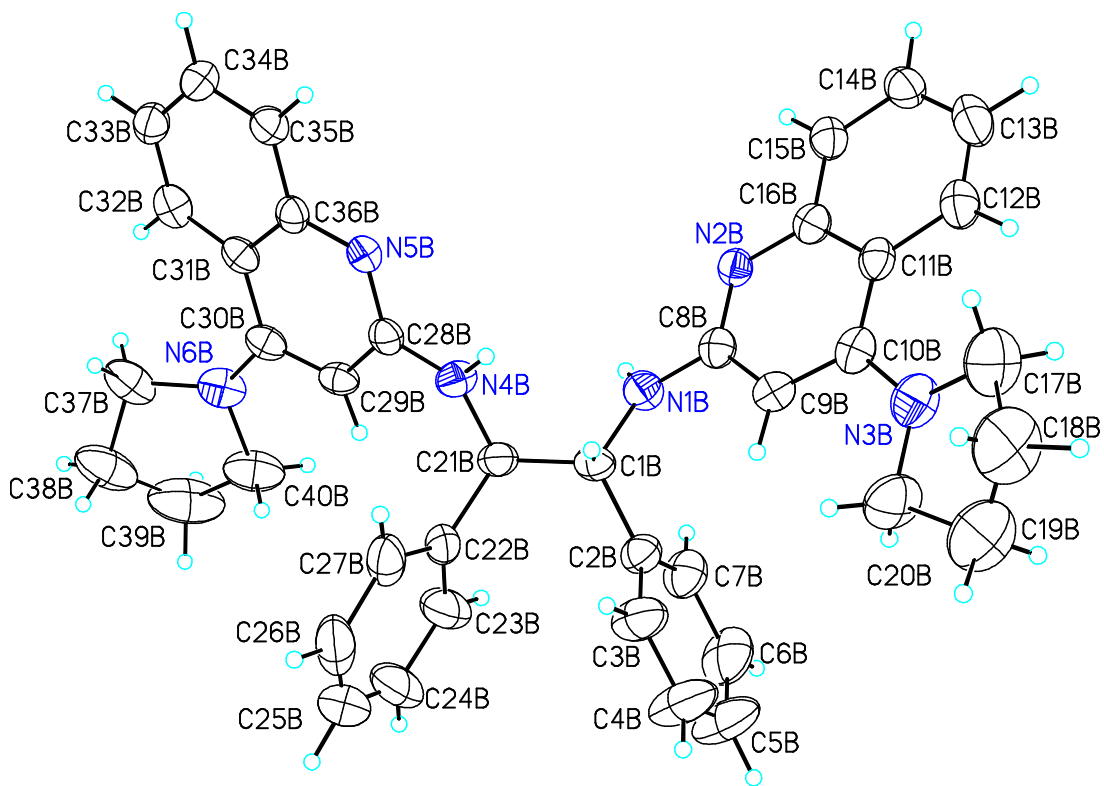
<sup>143</sup> A short history of *SHELX*. G. M. Sheldrick, *Acta Cryst.* A64, 112 - 122 (2008).



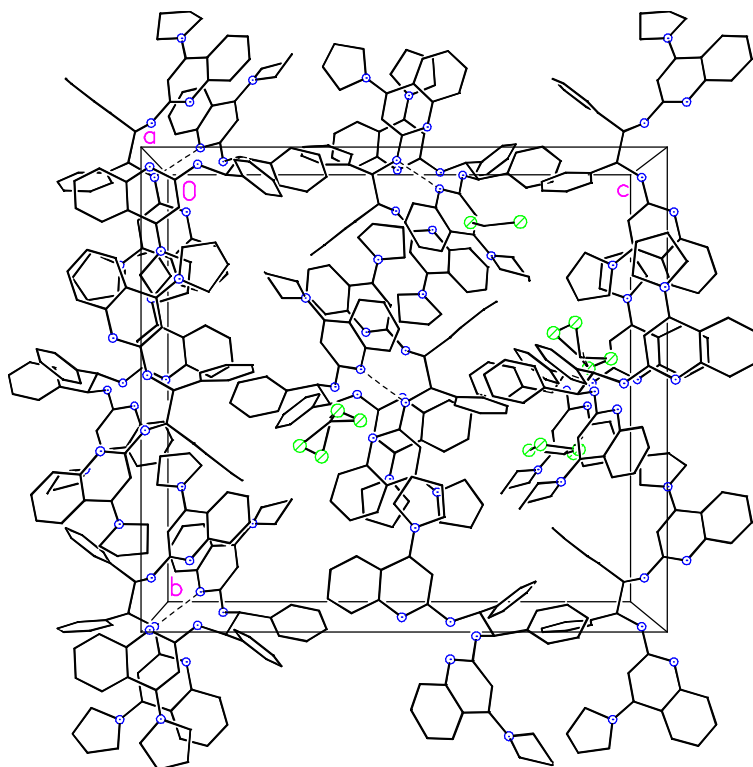
Formula unit.



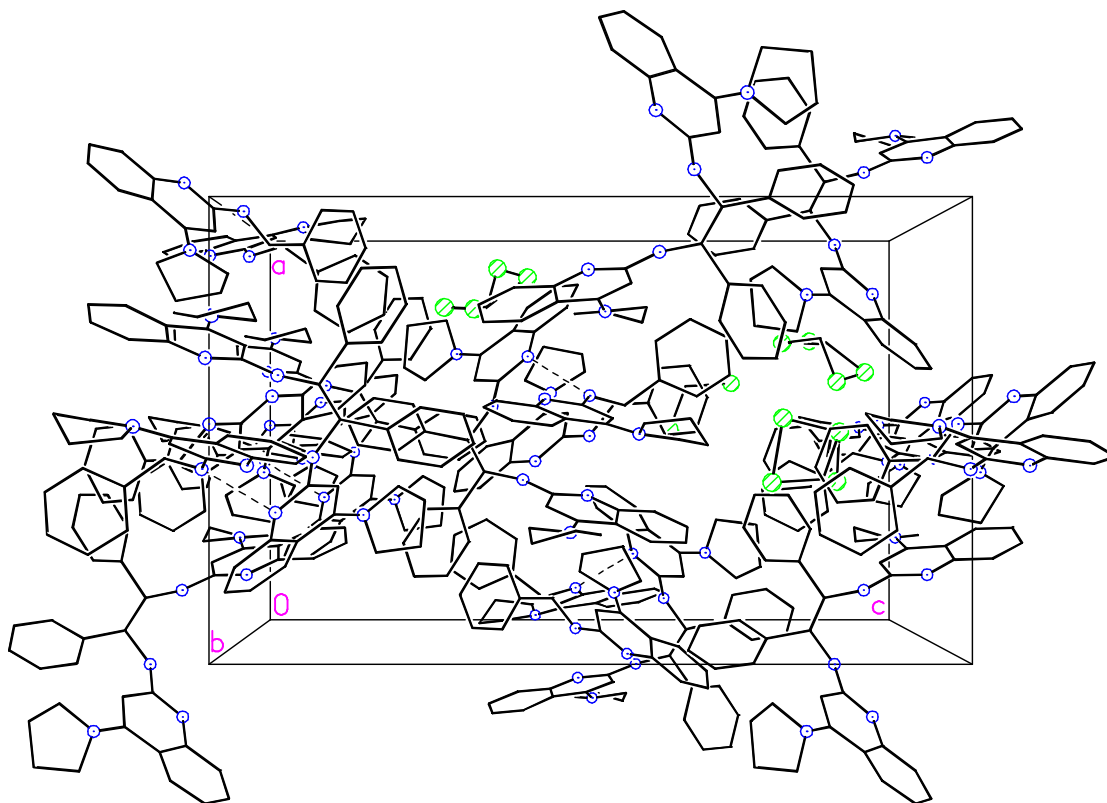
Molecule A.



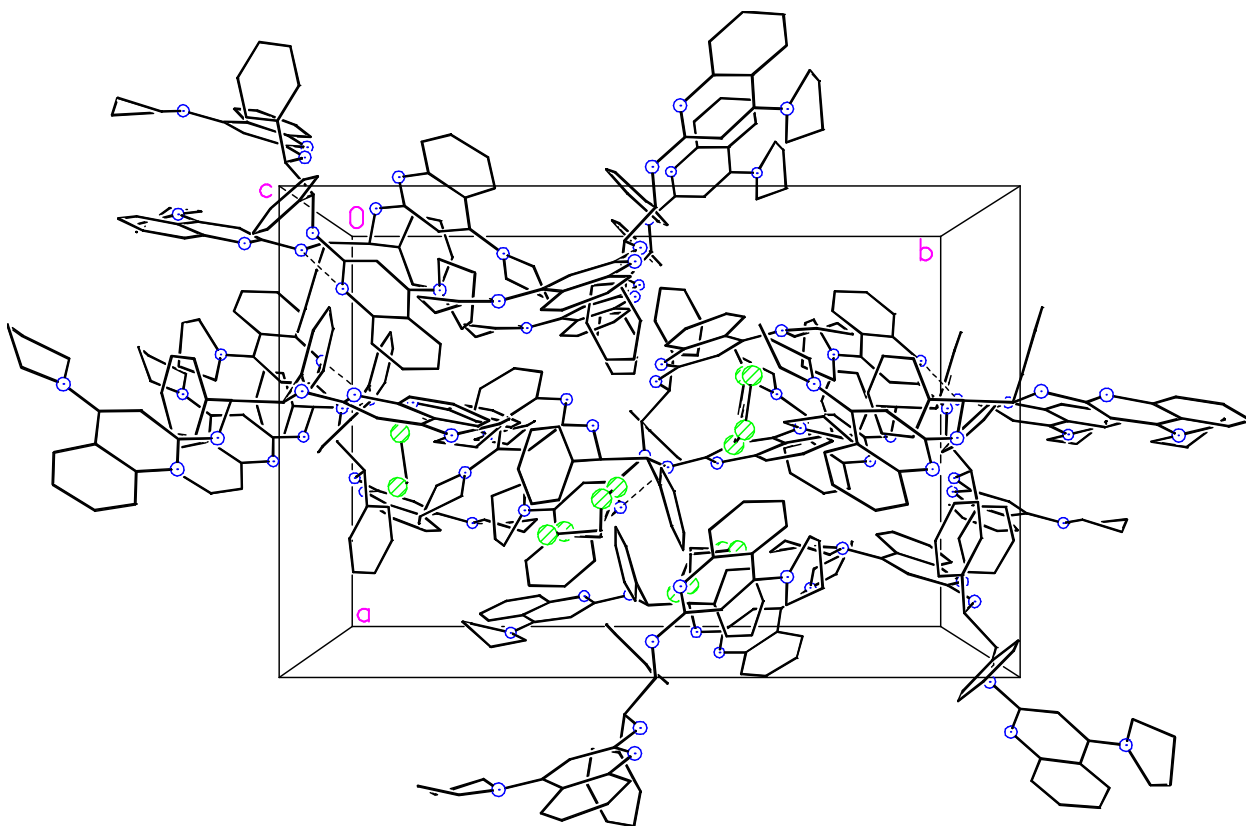
Molecule B



Cell plot, view along *a*.



Cell plot, view along *b*.



Cell plot, view along *c*.

**Table 1. Crystal data and structure refinement for 12021.**

|                                   |  |          |
|-----------------------------------|--|----------|
| Empirical formula                 | C <sub>41.50</sub> H <sub>43</sub> Cl <sub>3</sub> N <sub>6</sub>  |          |
| Formula weight                    | 732.17   |          |
| Crystal color, shape, size        | colorless needle, 0.20 x 0.12 x 0.10 mm <sup>3</sup>   |          |
| Temperature                       | 150(2) K   |          |
| Wavelength                        | 0.71073 Å  |          |
| Crystal system, space group       | Orthorhombic, P2(1)2(1)2(1)  |          |
| Unit cell dimensions              | a = 14.4917(6) Å   | α = 90°. |
|                                   | b = 21.8382(9) Å   | β = 90°. |
|                                   | c = 23.6418(11) Å  | γ = 90°. |
| Volume                            | 7482.0(6) Å <sup>3</sup>   |          |
| Z                                 | 8  |          |
| Density (calculated)              | 1.300 Mg/m <sup>3</sup>  |          |
| Absorption coefficient            | 0.284 mm <sup>-1</sup>   |          |
| F(000)                            | 3080   |          |
| <b>Data collection</b>            |  |          |
| Diffractometer                    | APEX II Kappa Duo, Bruker  |          |
| Theta range for data collection   | 1.27 to 26.40°.  |          |
| Index ranges                      | -18 ≤ h ≤ 18, -27 ≤ k ≤ 26, -29 ≤ l ≤ 29   |          |
| Reflections collected             | 66156  |          |
| Independent reflections           | 15315 [R(int) = 0.0470]  |          |
| Observed Reflections              | 11840  |          |
| Completeness to theta = 26.40°    | 99.8 %   |          |
| <b>Solution and Refinement</b>    |  |          |
| Absorption correction             | Semi-empirical from equivalents  |          |
| Max. and min. transmission        | 0.9722 and 0.9454  |          |
| Solution                          | Direct methods   |          |
| Refinement method                 | Full-matrix least-squares on F <sup>2</sup>  |          |
| Weighting scheme                  | w = [σ <sup>2</sup> F <sub>o</sub> <sup>2</sup> + AP <sup>2</sup> + BP] <sup>-1</sup> , with<br>P = (F <sub>o</sub> <sup>2</sup> + 2 F <sub>c</sub> <sup>2</sup> )/3, A = 0.1127, B = 3.9350 |          |
| Data / restraints / parameters    | 15315 / 155 / 965  |          |
| Goodness-of-fit on F <sup>2</sup> | 1.022  |          |
| Final R indices [I > 2σ(I)]       | R1 = 0.0668, wR2 = 0.1786  |          |
| R indices (all data)              | R1 = 0.0894, wR2 = 0.1959  |          |
| Absolute structure parameter      | 0.04(9)  |          |
| Largest diff. peak and hole       | 0.893 and -0.535 e.Å <sup>-3</sup>   |          |

---

Goodness-of-fit =  $[\sum [w(F_o^2 - F_c^2)^2] / N_{\text{observns}} - N_{\text{params}}]^{1/2}$ , all data.

$R1 = \sum (|F_o| - |F_c|) / \sum |F_o|$ .       $wR2 = [\sum [w(F_o^2 - F_c^2)^2] / \sum [w(F_o^2)^2]]^{1/2}$ .



**Table 2. Atomic coordinates ( $\times 10^4$ ) and equivalent isotropic displacement parameters ( $\text{\AA}^2 \times 10^3$ ) for 12021.  $U(\text{eq})$  is defined as one third of the trace of the orthogonalized  $U^{ij}$  tensor.**

|      | x       | y        | z       | $U(\text{eq})$ |
|------|---------|----------|---------|----------------|
| N1A  | 4423(2) | -41(2)   | 1353(1) | 34(1)          |
| N2A  | 3222(2) | -425(2)  | 835(1)  | 34(1)          |
| N3A  | 3107(2) | -1958(2) | 1920(1) | 39(1)          |
| N4A  | 6174(2) | 127(1)   | 905(1)  | 32(1)          |
| N5A  | 6543(2) | 202(1)   | -33(1)  | 31(1)          |
| N6A  | 7333(2) | 2049(1)  | 233(1)  | 33(1)          |
| C1A  | 5232(2) | -94(2)   | 1714(1) | 31(1)          |
| C2A  | 5024(2) | 39(2)    | 2338(2) | 32(1)          |
| C3A  | 5494(3) | -272(2)  | 2759(2) | 40(1)          |
| C4A  | 5348(3) | -137(2)  | 3326(2) | 48(1)          |
| C5A  | 4715(3) | 310(2)   | 3472(2) | 52(1)          |
| C6A  | 4239(3) | 614(2)   | 3059(2) | 49(1)          |
| C7A  | 4381(3) | 482(2)   | 2495(2) | 41(1)          |
| C8A  | 3809(2) | -502(2)  | 1267(1) | 30(1)          |
| C9A  | 3778(2) | -1013(2) | 1630(1) | 32(1)          |
| C10A | 3142(2) | -1476(2) | 1548(1) | 33(1)          |
| C11A | 2549(2) | -1427(2) | 1053(2) | 35(1)          |
| C12A | 1966(3) | -1896(2) | 852(2)  | 48(1)          |
| C13A | 1428(3) | -1824(2) | 379(2)  | 58(1)          |
| C14A | 1435(3) | -1268(2) | 87(2)   | 54(1)          |
| C15A | 2016(3) | -815(2)  | 258(2)  | 47(1)          |
| C16A | 2607(2) | -882(2)  | 738(2)  | 35(1)          |
| C17A | 2251(3) | -2290(2) | 2079(2) | 55(1)          |
| C18A | 2374(3) | -2461(3) | 2686(2) | 62(1)          |
| C19A | 3418(3) | -2516(2) | 2741(2) | 54(1)          |
| C20A | 3750(3) | -1972(2) | 2399(2) | 38(1)          |
| C21A | 5975(2) | 345(2)   | 1464(1) | 30(1)          |
| C22A | 6842(2) | 419(2)   | 1831(1) | 32(1)          |
| C23A | 6846(3) | 809(2)   | 2298(2) | 46(1)          |
| C24A | 7640(3) | 894(2)   | 2616(2) | 57(1)          |
| C25A | 8443(3) | 603(2)   | 2473(2) | 59(1)          |
| C26A | 8450(3) | 210(2)   | 2006(2) | 59(1)          |
| C27A | 7648(3) | 119(2)   | 1692(2) | 44(1)          |
| C28A | 6506(2) | 478(2)   | 467(1)  | 30(1)          |
| C29A | 6770(2) | 1087(2)  | 564(1)  | 30(1)          |
| C30A | 7095(2) | 1452(2)  | 124(2)  | 31(1)          |
| C31A | 7177(2) | 1166(2)  | -430(1) | 30(1)          |
| C32A | 7579(3) | 1435(2)  | -913(2) | 39(1)          |

|      |         |          |          |        |
|------|---------|----------|----------|--------|
| C33A | 7620(3) | 1145(2)  | -1425(2) | 47(1)  |
| C34A | 7282(3) | 550(2)   | -1478(2) | 42(1)  |
| C35A | 6928(3) | 260(2)   | -1009(2) | 38(1)  |
| C36A | 6880(2) | 547(2)   | -476(2)  | 31(1)  |
| C37A | 7362(2) | 2562(2)  | -176(2)  | 36(1)  |
| C38A | 7244(3) | 3139(2)  | 172(2)   | 43(1)  |
| C39A | 7534(3) | 2947(2)  | 772(2)   | 43(1)  |
| C40A | 7222(3) | 2284(2)  | 809(2)   | 37(1)  |
| N1B  | 5134(2) | -843(2)  | -81(1)   | 37(1)  |
| N2B  | 5752(2) | -1258(1) | 725(1)   | 31(1)  |
| N3B  | 4047(2) | -2815(2) | 481(2)   | 49(1)  |
| N4B  | 4178(2) | 296(2)   | -66(1)   | 35(1)  |
| N5B  | 4266(2) | 1070(1)  | 589(1)   | 32(1)  |
| N6B  | 5080(2) | 2278(2)  | -720(1)  | 44(1)  |
| C1B  | 4363(2) | -712(2)  | -450(1)  | 33(1)  |
| C2B  | 4332(3) | -1126(2) | -965(2)  | 38(1)  |
| C3B  | 3472(3) | -1324(2) | -1160(2) | 57(1)  |
| C4B  | 3397(5) | -1710(3) | -1613(2) | 82(2)  |
| C5B  | 4178(5) | -1899(3) | -1892(2) | 86(2)  |
| C6B  | 5039(4) | -1718(3) | -1707(2) | 71(2)  |
| C7B  | 5113(3) | -1323(2) | -1237(2) | 50(1)  |
| C8B  | 5154(2) | -1311(2) | 301(1)   | 33(1)  |
| C9B  | 4574(2) | -1827(2) | 228(2)   | 34(1)  |
| C10B | 4595(2) | -2316(2) | 596(2)   | 36(1)  |
| C11B | 5244(3) | -2278(2) | 1063(2)  | 34(1)  |
| C12B | 5409(3) | -2738(2) | 1476(2)  | 42(1)  |
| C13B | 6026(3) | -2662(2) | 1906(2)  | 51(1)  |
| C14B | 6522(3) | -2118(2) | 1958(2)  | 43(1)  |
| C15B | 6419(3) | -1668(2) | 1559(2)  | 40(1)  |
| C16B | 5789(2) | -1734(2) | 1102(2)  | 33(1)  |
| C17B | 3723(4) | -3285(2) | 881(2)   | 68(1)  |
| C18B | 2860(4) | -3538(3) | 595(3)   | 87(2)  |
| C19B | 3047(5) | -3470(3) | -10(3)   | 92(2)  |
| C20B | 3519(4) | -2840(2) | -44(2)   | 63(1)  |
| C21B | 4399(2) | -19(2)   | -587(1)  | 35(1)  |
| C22B | 3801(3) | 174(2)   | -1087(2) | 43(1)  |
| C23B | 4193(4) | 190(3)   | -1627(2) | 71(2)  |
| C24B | 3693(6) | 368(3)   | -2095(2) | 100(3) |
| C25B | 2792(5) | 513(3)   | -2040(3) | 88(2)  |
| C26B | 2373(4) | 514(2)   | -1518(3) | 73(2)  |
| C27B | 2886(3) | 346(2)   | -1026(2) | 52(1)  |
| C28B | 4405(2) | 887(2)   | 52(1)    | 30(1)  |
| C29B | 4720(2) | 1284(2)  | -376(1)  | 32(1)  |

|      |          |          |          |        |
|------|----------|----------|----------|--------|
| C30B | 4852(2)  | 1898(2)  | -278(1)  | 33(1)  |
| C31B | 4733(2)  | 2116(2)  | 302(1)   | 32(1)  |
| C32B | 4894(2)  | 2713(2)  | 496(2)   | 37(1)  |
| C33B | 4779(3)  | 2888(2)  | 1042(2)  | 39(1)  |
| C34B | 4471(3)  | 2451(2)  | 1440(2)  | 40(1)  |
| C35B | 4319(3)  | 1861(2)  | 1274(2)  | 37(1)  |
| C36B | 4442(2)  | 1670(2)  | 708(1)   | 30(1)  |
| C37B | 4843(3)  | 2936(2)  | -774(2)  | 55(1)  |
| C38B | 4735(4)  | 3043(3)  | -1399(2) | 73(2)  |
| C39B | 5333(5)  | 2565(3)  | -1662(2) | 90(2)  |
| C40B | 5210(4)  | 2007(3)  | -1288(2) | 61(1)  |
| CI1S | 2139(2)  | 1202(1)  | 2022(1)  | 96(1)  |
| CI2S | 1175(2)  | 448(2)   | 1273(2)  | 188(2) |
| C1S  | 2230(12) | 679(5)   | 1496(8)  | 133(2) |
| CI1D | 2187(6)  | 1428(5)  | 1594(5)  | 96(1)  |
| CI2D | 1404(11) | 656(9)   | 838(9)   | 188(2) |
| C1D  | 2090(60) | 679(12)  | 1420(30) | 133(2) |
| CI3S | 6206(2)  | 1379(1)  | 7362(1)  | 93(1)  |
| CI4S | 5036(4)  | 1337(8)  | 6399(2)  | 182(3) |
| C2S  | 6133(19) | 1460(20) | 6643(7)  | 160(3) |
| CI3D | 6183(8)  | 1446(10) | 6447(4)  | 160(3) |
| CI4D | 4712(8)  | 1216(5)  | 7192(4)  | 233(7) |
| C2D  | 5040(20) | 1250(50) | 6497(10) | 182(3) |
| CI5S | 5477(2)  | 4386(1)  | 246(1)   | 65(1)  |
| CI6S | 4001(2)  | 4627(2)  | -505(2)  | 131(1) |
| C3S  | 4329(8)  | 4575(11) | 189(5)   | 151(2) |
| CI5D | 4651(7)  | 4308(3)  | 156(3)   | 151(2) |
| CI6D | 4474(5)  | 5297(3)  | -561(4)  | 158(3) |
| C3D  | 3957(12) | 4927(8)  | -7(8)    | 131(1) |

---

**Table 3. Bond lengths [Å] and angles [°] for 12021.**

|           |          |           |          |
|-----------|----------|-----------|----------|
| N1A-C8A   | 1.359(5) | N1A-C1A   | 1.454(4) |
| N1A-H1AN  | 0.80(5)  | N2A-C8A   | 1.338(4) |
| N2A-C16A  | 1.358(5) | N3A-C10A  | 1.372(5) |
| N3A-C20A  | 1.466(5) | N3A-C17A  | 1.485(5) |
| N4A-C28A  | 1.375(4) | N4A-C21A  | 1.436(4) |
| N4A-H4AN  | 0.9000   | N5A-C28A  | 1.328(4) |
| N5A-C36A  | 1.379(5) | N6A-C30A  | 1.374(5) |
| N6A-C40A  | 1.464(5) | N6A-C37A  | 1.479(5) |
| C1A-C2A   | 1.535(5) | C1A-C21A  | 1.557(5) |
| C1A-H1A   | 1.0000   | C2A-C3A   | 1.384(5) |
| C2A-C7A   | 1.395(5) | C3A-C4A   | 1.389(5) |
| C3A-H3A   | 0.9500   | C4A-C5A   | 1.384(7) |
| C4A-H4A   | 0.9500   | C5A-C6A   | 1.368(7) |
| C5A-H5A   | 0.9500   | C6A-C7A   | 1.378(6) |
| C6A-H6A   | 0.9500   | C7A-H7A   | 0.9500   |
| C8A-C9A   | 1.410(5) | C9A-C10A  | 1.383(5) |
| C9A-H9A   | 0.9500   | C10A-C11A | 1.455(5) |
| C11A-C16A | 1.408(5) | C11A-C12A | 1.410(6) |
| C12A-C13A | 1.373(6) | C12A-H12A | 0.9500   |
| C13A-C14A | 1.395(7) | C13A-H13A | 0.9500   |
| C14A-C15A | 1.361(6) | C14A-H14A | 0.9500   |
| C15A-C16A | 1.428(5) | C15A-H15A | 0.9500   |
| C17A-C18A | 1.493(6) | C17A-H17A | 0.9900   |
| C17A-H17B | 0.9900   | C18A-C19A | 1.524(7) |
| C18A-H18A | 0.9900   | C18A-H18B | 0.9900   |
| C19A-C20A | 1.515(5) | C19A-H19A | 0.9900   |
| C19A-H19B | 0.9900   | C20A-H20A | 0.9900   |
| C20A-H20B | 0.9900   | C21A-C22A | 1.534(5) |
| C21A-H21A | 1.0000   | C22A-C27A | 1.378(5) |
| C22A-C23A | 1.395(5) | C23A-C24A | 1.387(6) |
| C23A-H23A | 0.9500   | C24A-C25A | 1.369(7) |
| C24A-H24A | 0.9500   | C25A-C26A | 1.399(8) |
| C25A-H25A | 0.9500   | C26A-C27A | 1.394(6) |
| C26A-H26A | 0.9500   | C27A-H27A | 0.9500   |
| C28A-C29A | 1.403(5) | C29A-C30A | 1.391(5) |
| C29A-H29A | 0.9500   | C30A-C31A | 1.456(5) |
| C31A-C32A | 1.412(5) | C31A-C36A | 1.423(5) |
| C32A-C33A | 1.368(6) | C32A-H32A | 0.9500   |
| C33A-C34A | 1.395(6) | C33A-H33A | 0.9500   |
| C34A-C35A | 1.376(6) | C34A-H34A | 0.9500   |
| C35A-C36A | 1.408(5) | C35A-H35A | 0.9500   |

|           |           |           |          |
|-----------|-----------|-----------|----------|
| C37A-C38A | 1.513(6)  | C37A-H37A | 0.9900   |
| C37A-H37B | 0.9900    | C38A-C39A | 1.538(6) |
| C38A-H38A | 0.9900    | C38A-H38B | 0.9900   |
| C39A-C40A | 1.518(5)  | C39A-H39A | 0.9900   |
| C39A-H39B | 0.9900    | C40A-H40A | 0.9900   |
| C40A-H40B | 0.9900    | N1B-C8B   | 1.363(5) |
| N1B-C1B   | 1.446(5)  | N1B-H1BN  | 0.72(4)  |
| N2B-C8B   | 1.331(4)  | N2B-C16B  | 1.369(5) |
| N3B-C10B  | 1.375(5)  | N3B-C20B  | 1.461(6) |
| N3B-C17B  | 1.472(6)  | N4B-C28B  | 1.361(5) |
| N4B-C21B  | 1.445(4)  | N4B-H4BN  | 0.91(4)  |
| N5B-C28B  | 1.346(4)  | N5B-C36B  | 1.364(5) |
| N6B-C30B  | 1.375(5)  | N6B-C40B  | 1.479(6) |
| N6B-C37B  | 1.485(6)  | C1B-C2B   | 1.518(5) |
| C1B-C21B  | 1.549(5)  | C1B-H1BA  | 1.0000   |
| C2B-C7B   | 1.371(6)  | C2B-C3B   | 1.397(6) |
| C3B-C4B   | 1.367(7)  | C3B-H3B   | 0.9500   |
| C4B-C5B   | 1.374(9)  | C4B-H4B   | 0.9500   |
| C5B-C6B   | 1.380(9)  | C5B-H5B   | 0.9500   |
| C6B-C7B   | 1.409(7)  | C6B-H6B   | 0.9500   |
| C7B-H7B   | 0.9500    | C8B-C9B   | 1.416(5) |
| C9B-C10B  | 1.377(5)  | C9B-H9B   | 0.9500   |
| C10B-C11B | 1.454(5)  | C11B-C12B | 1.421(5) |
| C11B-C16B | 1.430(5)  | C12B-C13B | 1.365(6) |
| C12B-H12B | 0.9500    | C13B-C14B | 1.395(6) |
| C13B-H13B | 0.9500    | C14B-C15B | 1.369(5) |
| C14B-H14B | 0.9500    | C15B-C16B | 1.422(5) |
| C15B-H15B | 0.9500    | C17B-C18B | 1.526(8) |
| C17B-H17C | 0.9900    | C17B-H17D | 0.9900   |
| C18B-C19B | 1.464(9)  | C18B-H18C | 0.9900   |
| C18B-H18D | 0.9900    | C19B-C20B | 1.538(7) |
| C19B-H19C | 0.9900    | C19B-H19D | 0.9900   |
| C20B-H20C | 0.9900    | C20B-H20D | 0.9900   |
| C21B-C22B | 1.524(5)  | C21B-H21B | 1.0000   |
| C22B-C27B | 1.386(6)  | C22B-C23B | 1.398(7) |
| C23B-C24B | 1.379(7)  | C23B-H23B | 0.9500   |
| C24B-C25B | 1.350(10) | C24B-H24B | 0.9500   |
| C25B-C26B | 1.375(9)  | C25B-H25B | 0.9500   |
| C26B-C27B | 1.428(7)  | C26B-H26B | 0.9500   |
| C27B-H27B | 0.9500    | C28B-C29B | 1.410(5) |
| C29B-C30B | 1.374(5)  | C29B-H29B | 0.9500   |
| C30B-C31B | 1.462(5)  | C31B-C32B | 1.402(5) |
| C31B-C36B | 1.431(5)  | C32B-C33B | 1.357(5) |

|               |           |               |           |
|---------------|-----------|---------------|-----------|
| C32B-H32B     | 0.9500    | C33B-C34B     | 1.411(6)  |
| C33B-H33B     | 0.9500    | C34B-C35B     | 1.366(6)  |
| C34B-H34B     | 0.9500    | C35B-C36B     | 1.413(5)  |
| C35B-H35B     | 0.9500    | C37B-C38B     | 1.504(6)  |
| C37B-H37C     | 0.9900    | C37B-H37D     | 0.9900    |
| C38B-C39B     | 1.493(10) | C38B-H38C     | 0.9900    |
| C38B-H38D     | 0.9900    | C39B-C40B     | 1.515(8)  |
| C39B-H39C     | 0.9900    | C39B-H39D     | 0.9900    |
| C40B-H40C     | 0.9900    | C40B-H40D     | 0.9900    |
| C11S-C1S      | 1.694(12) | C12S-C1S      | 1.694(12) |
| C1S-H1S1      | 0.9900    | C1S-H1S2      | 0.9900    |
| C11D-C1D      | 1.694(12) | C12D-C1D      | 1.693(12) |
| C1D-H1D1      | 0.9900    | C1D-H1D2      | 0.9900    |
| C13S-C2S      | 1.711(15) | C14S-C2S      | 1.712(15) |
| C2S-H2S1      | 0.9900    | C2S-H2S2      | 0.9900    |
| C13D-C2D      | 1.714(15) | C14D-C2D      | 1.713(15) |
| C2D-H2D1      | 0.9900    | C2D-H2D2      | 0.9900    |
| C15S-C3S      | 1.719(9)  | C16S-C3S      | 1.712(9)  |
| C3S-H3S1      | 0.9900    | C3S-H3S2      | 0.9900    |
| C15D-C3D      | 1.728(9)  | C16D-C3D      | 1.711(9)  |
| C3D-H3D1      | 0.9900    | C3D-H3D2      | 0.9900    |
|               |           |               |           |
| C8A-N1A-C1A   | 124.0(3)  | C8A-N1A-H1AN  | 115(4)    |
| C1A-N1A-H1AN  | 121(4)    | C8A-N2A-C16A  | 117.0(3)  |
| C10A-N3A-C20A | 119.2(3)  | C10A-N3A-C17A | 124.6(3)  |
| C20A-N3A-C17A | 109.0(3)  | C28A-N4A-C21A | 125.3(3)  |
| C28A-N4A-H4AN | 112.0     | C21A-N4A-H4AN | 122.7     |
| C28A-N5A-C36A | 116.4(3)  | C30A-N6A-C40A | 118.7(3)  |
| C30A-N6A-C37A | 127.1(3)  | C40A-N6A-C37A | 110.2(3)  |
| N1A-C1A-C2A   | 113.0(3)  | N1A-C1A-C21A  | 106.7(3)  |
| C2A-C1A-C21A  | 112.6(3)  | N1A-C1A-H1A   | 108.1     |
| C2A-C1A-H1A   | 108.1     | C21A-C1A-H1A  | 108.1     |
| C3A-C2A-C7A   | 118.6(3)  | C3A-C2A-C1A   | 120.1(3)  |
| C7A-C2A-C1A   | 121.2(3)  | C2A-C3A-C4A   | 120.9(4)  |
| C2A-C3A-H3A   | 119.5     | C4A-C3A-H3A   | 119.5     |
| C5A-C4A-C3A   | 119.5(4)  | C5A-C4A-H4A   | 120.3     |
| C3A-C4A-H4A   | 120.3     | C6A-C5A-C4A   | 119.9(4)  |
| C6A-C5A-H5A   | 120.1     | C4A-C5A-H5A   | 120.1     |
| C5A-C6A-C7A   | 120.9(4)  | C5A-C6A-H6A   | 119.5     |
| C7A-C6A-H6A   | 119.5     | C6A-C7A-C2A   | 120.1(4)  |
| C6A-C7A-H7A   | 119.9     | C2A-C7A-H7A   | 119.9     |
| N2A-C8A-N1A   | 116.0(3)  | N2A-C8A-C9A   | 123.0(3)  |
| N1A-C8A-C9A   | 121.0(3)  | C10A-C9A-C8A  | 121.0(3)  |

|                |          |                |          |
|----------------|----------|----------------|----------|
| C10A-C9A-H9A   | 119.5    | C8A-C9A-H9A    | 119.5    |
| N3A-C10A-C9A   | 119.7(3) | N3A-C10A-C11A  | 123.3(3) |
| C9A-C10A-C11A  | 116.9(3) | C16A-C11A-C12A | 118.2(3) |
| C16A-C11A-C10A | 116.9(3) | C12A-C11A-C10A | 124.8(4) |
| C13A-C12A-C11A | 122.1(4) | C13A-C12A-H12A | 119.0    |
| C11A-C12A-H12A | 119.0    | C12A-C13A-C14A | 119.9(4) |
| C12A-C13A-H13A | 120.1    | C14A-C13A-H13A | 120.1    |
| C15A-C14A-C13A | 119.4(4) | C15A-C14A-H14A | 120.3    |
| C13A-C14A-H14A | 120.3    | C14A-C15A-C16A | 122.1(4) |
| C14A-C15A-H15A | 119.0    | C16A-C15A-H15A | 119.0    |
| N2A-C16A-C11A  | 124.9(3) | N2A-C16A-C15A  | 116.9(4) |
| C11A-C16A-C15A | 118.1(4) | N3A-C17A-C18A  | 105.4(3) |
| N3A-C17A-H17A  | 110.7    | C18A-C17A-H17A | 110.7    |
| N3A-C17A-H17B  | 110.7    | C18A-C17A-H17B | 110.7    |
| H17A-C17A-H17B | 108.8    | C17A-C18A-C19A | 102.8(4) |
| C17A-C18A-H18A | 111.2    | C19A-C18A-H18A | 111.2    |
| C17A-C18A-H18B | 111.2    | C19A-C18A-H18B | 111.2    |
| H18A-C18A-H18B | 109.1    | C20A-C19A-C18A | 102.0(4) |
| C20A-C19A-H19A | 111.4    | C18A-C19A-H19A | 111.4    |
| C20A-C19A-H19B | 111.4    | C18A-C19A-H19B | 111.4    |
| H19A-C19A-H19B | 109.2    | N3A-C20A-C19A  | 103.1(3) |
| N3A-C20A-H20A  | 111.1    | C19A-C20A-H20A | 111.1    |
| N3A-C20A-H20B  | 111.1    | C19A-C20A-H20B | 111.1    |
| H20A-C20A-H20B | 109.1    | N4A-C21A-C22A  | 113.0(3) |
| N4A-C21A-C1A   | 106.4(3) | C22A-C21A-C1A  | 114.7(3) |
| N4A-C21A-H21A  | 107.5    | C22A-C21A-H21A | 107.5    |
| C1A-C21A-H21A  | 107.5    | C27A-C22A-C23A | 118.3(3) |
| C27A-C22A-C21A | 120.6(3) | C23A-C22A-C21A | 121.0(3) |
| C24A-C23A-C22A | 121.0(4) | C24A-C23A-H23A | 119.5    |
| C22A-C23A-H23A | 119.5    | C25A-C24A-C23A | 120.6(4) |
| C25A-C24A-H24A | 119.7    | C23A-C24A-H24A | 119.7    |
| C24A-C25A-C26A | 119.1(4) | C24A-C25A-H25A | 120.4    |
| C26A-C25A-H25A | 120.4    | C27A-C26A-C25A | 120.1(4) |
| C27A-C26A-H26A | 120.0    | C25A-C26A-H26A | 120.0    |
| C22A-C27A-C26A | 120.9(4) | C22A-C27A-H27A | 119.6    |
| C26A-C27A-H27A | 119.6    | N5A-C28A-N4A   | 115.5(3) |
| N5A-C28A-C29A  | 124.3(3) | N4A-C28A-C29A  | 120.2(3) |
| C30A-C29A-C28A | 120.9(3) | C30A-C29A-H29A | 119.6    |
| C28A-C29A-H29A | 119.6    | N6A-C30A-C29A  | 119.2(3) |
| N6A-C30A-C31A  | 123.8(3) | C29A-C30A-C31A | 117.0(3) |
| C32A-C31A-C36A | 117.3(3) | C32A-C31A-C30A | 125.7(3) |
| C36A-C31A-C30A | 116.9(3) | C33A-C32A-C31A | 122.8(4) |
| C33A-C32A-H32A | 118.6    | C31A-C32A-H32A | 118.6    |

|                |           |                |           |
|----------------|-----------|----------------|-----------|
| C32A-C33A-C34A | 119.7(4)  | C32A-C33A-H33A | 120.1     |
| C34A-C33A-H33A | 120.1     | C35A-C34A-C33A | 119.1(4)  |
| C35A-C34A-H34A | 120.4     | C33A-C34A-H34A | 120.4     |
| C34A-C35A-C36A | 122.4(4)  | C34A-C35A-H35A | 118.8     |
| C36A-C35A-H35A | 118.8     | N5A-C36A-C35A  | 117.1(3)  |
| N5A-C36A-C31A  | 124.5(3)  | C35A-C36A-C31A | 118.4(3)  |
| N6A-C37A-C38A  | 105.8(3)  | N6A-C37A-H37A  | 110.6     |
| C38A-C37A-H37A | 110.6     | N6A-C37A-H37B  | 110.6     |
| C38A-C37A-H37B | 110.6     | H37A-C37A-H37B | 108.7     |
| C37A-C38A-C39A | 104.1(3)  | C37A-C38A-H38A | 110.9     |
| C39A-C38A-H38A | 110.9     | C37A-C38A-H38B | 110.9     |
| C39A-C38A-H38B | 110.9     | H38A-C38A-H38B | 109.0     |
| C40A-C39A-C38A | 103.4(3)  | C40A-C39A-H39A | 111.1     |
| C38A-C39A-H39A | 111.1     | C40A-C39A-H39B | 111.1     |
| C38A-C39A-H39B | 111.1     | H39A-C39A-H39B | 109.0     |
| N6A-C40A-C39A  | 104.3(3)  | N6A-C40A-H40A  | 110.9     |
| C39A-C40A-H40A | 110.9     | N6A-C40A-H40B  | 110.9     |
| C39A-C40A-H40B | 110.9     | H40A-C40A-H40B | 108.9     |
| C8B-N1B-C1B    | 124.3(3)  | C8B-N1B-H1BN   | 115(3)    |
| C1B-N1B-H1BN   | 120(3)    | C8B-N2B-C16B   | 116.7(3)  |
| C10B-N3B-C20B  | 120.0(4)  | C10B-N3B-C17B  | 127.6(4)  |
| C20B-N3B-C17B  | 110.7(4)  | C28B-N4B-C21B  | 124.9(3)  |
| C28B-N4B-H4BN  | 123.2(13) | C21B-N4B-H4BN  | 111.7(14) |
| C28B-N5B-C36B  | 116.8(3)  | C30B-N6B-C40B  | 118.7(4)  |
| C30B-N6B-C37B  | 126.5(4)  | C40B-N6B-C37B  | 109.8(4)  |
| N1B-C1B-C2B    | 112.9(3)  | N1B-C1B-C21B   | 107.1(3)  |
| C2B-C1B-C21B   | 114.5(3)  | N1B-C1B-H1BA   | 107.3     |
| C2B-C1B-H1BA   | 107.3     | C21B-C1B-H1BA  | 107.3     |
| C7B-C2B-C3B    | 119.0(4)  | C7B-C2B-C1B    | 122.6(4)  |
| C3B-C2B-C1B    | 118.4(3)  | C4B-C3B-C2B    | 121.3(5)  |
| C4B-C3B-H3B    | 119.3     | C2B-C3B-H3B    | 119.3     |
| C3B-C4B-C5B    | 119.8(5)  | C3B-C4B-H4B    | 120.1     |
| C5B-C4B-H4B    | 120.1     | C4B-C5B-C6B    | 120.3(5)  |
| C4B-C5B-H5B    | 119.9     | C6B-C5B-H5B    | 119.9     |
| C5B-C6B-C7B    | 119.7(5)  | C5B-C6B-H6B    | 120.2     |
| C7B-C6B-H6B    | 120.2     | C2B-C7B-C6B    | 119.9(4)  |
| C2B-C7B-H7B    | 120.0     | C6B-C7B-H7B    | 120.0     |
| N2B-C8B-N1B    | 116.6(3)  | N2B-C8B-C9B    | 123.2(3)  |
| N1B-C8B-C9B    | 120.3(3)  | C10B-C9B-C8B   | 121.9(3)  |
| C10B-C9B-H9B   | 119.1     | C8B-C9B-H9B    | 119.1     |
| N3B-C10B-C9B   | 118.5(3)  | N3B-C10B-C11B  | 124.7(3)  |
| C9B-C10B-C11B  | 116.7(3)  | C12B-C11B-C16B | 116.8(3)  |
| C12B-C11B-C10B | 126.2(3)  | C16B-C11B-C10B | 117.0(3)  |



|                |          |                |          |
|----------------|----------|----------------|----------|
| C13B-C12B-C11B | 122.4(4) | C13B-C12B-H12B | 118.8    |
| C11B-C12B-H12B | 118.8    | C12B-C13B-C14B | 120.4(4) |
| C12B-C13B-H13B | 119.8    | C14B-C13B-H13B | 119.8    |
| C15B-C14B-C13B | 119.7(4) | C15B-C14B-H14B | 120.2    |
| C13B-C14B-H14B | 120.2    | C14B-C15B-C16B | 121.4(4) |
| C14B-C15B-H15B | 119.3    | C16B-C15B-H15B | 119.3    |
| N2B-C16B-C15B  | 116.3(3) | N2B-C16B-C11B  | 124.5(3) |
| C15B-C16B-C11B | 119.1(3) | N3B-C17B-C18B  | 103.3(4) |
| N3B-C17B-H17C  | 111.1    | C18B-C17B-H17C | 111.1    |
| N3B-C17B-H17D  | 111.1    | C18B-C17B-H17D | 111.1    |
| H17C-C17B-H17D | 109.1    | C19B-C18B-C17B | 104.1(5) |
| C19B-C18B-H18C | 110.9    | C17B-C18B-H18C | 110.9    |
| C19B-C18B-H18D | 110.9    | C17B-C18B-H18D | 110.9    |
| H18C-C18B-H18D | 109.0    | C18B-C19B-C20B | 103.0(5) |
| C18B-C19B-H19C | 111.2    | C20B-C19B-H19C | 111.2    |
| C18B-C19B-H19D | 111.2    | C20B-C19B-H19D | 111.2    |
| H19C-C19B-H19D | 109.1    | N3B-C20B-C19B  | 102.8(5) |
| N3B-C20B-H20C  | 111.2    | C19B-C20B-H20C | 111.2    |
| N3B-C20B-H20D  | 111.2    | C19B-C20B-H20D | 111.2    |
| H20C-C20B-H20D | 109.1    | N4B-C21B-C22B  | 113.8(3) |
| N4B-C21B-C1B   | 106.2(3) | C22B-C21B-C1B  | 114.5(3) |
| N4B-C21B-H21B  | 107.3    | C22B-C21B-H21B | 107.3    |
| C1B-C21B-H21B  | 107.3    | C27B-C22B-C23B | 118.4(4) |
| C27B-C22B-C21B | 122.6(4) | C23B-C22B-C21B | 119.0(4) |
| C24B-C23B-C22B | 121.9(6) | C24B-C23B-H23B | 119.1    |
| C22B-C23B-H23B | 119.1    | C25B-C24B-C23B | 119.8(7) |
| C25B-C24B-H24B | 120.1    | C23B-C24B-H24B | 120.1    |
| C24B-C25B-C26B | 120.9(5) | C24B-C25B-H25B | 119.5    |
| C26B-C25B-H25B | 119.5    | C25B-C26B-C27B | 120.1(5) |
| C25B-C26B-H26B | 120.0    | C27B-C26B-H26B | 120.0    |
| C22B-C27B-C26B | 118.9(5) | C22B-C27B-H27B | 120.5    |
| C26B-C27B-H27B | 120.5    | N5B-C28B-N4B   | 116.1(3) |
| N5B-C28B-C29B  | 122.9(3) | N4B-C28B-C29B  | 120.9(3) |
| C30B-C29B-C28B | 121.6(3) | C30B-C29B-H29B | 119.2    |
| C28B-C29B-H29B | 119.2    | N6B-C30B-C29B  | 119.6(3) |
| N6B-C30B-C31B  | 123.0(3) | C29B-C30B-C31B | 117.5(3) |
| C32B-C31B-C36B | 117.6(3) | C32B-C31B-C30B | 126.3(3) |
| C36B-C31B-C30B | 116.1(3) | C33B-C32B-C31B | 123.6(3) |
| C33B-C32B-H32B | 118.2    | C31B-C32B-H32B | 118.2    |
| C32B-C33B-C34B | 118.8(4) | C32B-C33B-H33B | 120.6    |
| C34B-C33B-H33B | 120.6    | C35B-C34B-C33B | 119.9(4) |
| C35B-C34B-H34B | 120.1    | C33B-C34B-H34B | 120.1    |
| C34B-C35B-C36B | 122.0(3) | C34B-C35B-H35B | 119.0    |

|                |           |                |          |
|----------------|-----------|----------------|----------|
| C36B-C35B-H35B | 119.0     | N5B-C36B-C35B  | 117.0(3) |
| N5B-C36B-C31B  | 124.9(3)  | C35B-C36B-C31B | 118.1(3) |
| N6B-C37B-C38B  | 105.0(4)  | N6B-C37B-H37C  | 110.8    |
| C38B-C37B-H37C | 110.8     | N6B-C37B-H37D  | 110.8    |
| C38B-C37B-H37D | 110.8     | H37C-C37B-H37D | 108.8    |
| C39B-C38B-C37B | 103.9(5)  | C39B-C38B-H38C | 111.0    |
| C37B-C38B-H38C | 111.0     | C39B-C38B-H38D | 111.0    |
| C37B-C38B-H38D | 111.0     | H38C-C38B-H38D | 109.0    |
| C38B-C39B-C40B | 104.6(4)  | C38B-C39B-H39C | 110.8    |
| C40B-C39B-H39C | 110.8     | C38B-C39B-H39D | 110.8    |
| C40B-C39B-H39D | 110.8     | H39C-C39B-H39D | 108.9    |
| N6B-C40B-C39B  | 102.9(5)  | N6B-C40B-H40C  | 111.2    |
| C39B-C40B-H40C | 111.2     | N6B-C40B-H40D  | 111.2    |
| C39B-C40B-H40D | 111.2     | H40C-C40B-H40D | 109.1    |
| CI2S-C1S-CI1S  | 111.1(11) | CI2S-C1S-H1S1  | 109.4    |
| CI1S-C1S-H1S1  | 109.4     | CI2S-C1S-H1S2  | 109.4    |
| CI1S-C1S-H1S2  | 109.4     | H1S1-C1S-H1S2  | 108.0    |
| CI2D-C1D-CI1D  | 106.1(12) | CI2D-C1D-H1D1  | 110.5    |
| CI1D-C1D-H1D1  | 110.5     | CI2D-C1D-H1D2  | 110.5    |
| CI1D-C1D-H1D2  | 110.5     | H1D1-C1D-H1D2  | 108.7    |
| CI3S-C2S-CI4S  | 112.0(17) | CI3S-C2S-H2S1  | 109.2    |
| CI4S-C2S-H2S1  | 109.2     | CI3S-C2S-H2S2  | 109.2    |
| CI4S-C2S-H2S2  | 109.2     | H2S1-C2S-H2S2  | 107.9    |
| CI4D-C2D-CI3D  | 110.3(18) | CI4D-C2D-H2D1  | 109.6    |
| CI3D-C2D-H2D1  | 109.6     | CI4D-C2D-H2D2  | 109.6    |
| CI3D-C2D-H2D2  | 109.6     | H2D1-C2D-H2D2  | 108.1    |
| CI6S-C3S-CI5S  | 111.1(9)  | CI6S-C3S-H3S1  | 109.4    |
| CI5S-C3S-H3S1  | 109.4     | CI6S-C3S-H3S2  | 109.4    |
| CI5S-C3S-H3S2  | 109.4     | H3S1-C3S-H3S2  | 108.0    |
| CI6D-C3D-CI5D  | 106.6(9)  | CI6D-C3D-H3D1  | 110.4    |
| CI5D-C3D-H3D1  | 110.4     | CI6D-C3D-H3D2  | 110.4    |
| CI5D-C3D-H3D2  | 110.4     | H3D1-C3D-H3D2  | 108.6    |

---

**Table 4. Anisotropic displacement parameters ( $\text{\AA}^2 \times 10^3$ ) for 12021. The anisotropic displacement factor exponent takes the form:  $-2\pi^2 [ h^2 a^{*2} U^{11} + \dots + 2 h k a^* b^* U^{12} ]$**

|      | U <sup>11</sup> | U <sup>22</sup> | U <sup>33</sup> | U <sup>23</sup> | U <sup>13</sup> | U <sup>12</sup> |
|------|-----------------|-----------------|-----------------|-----------------|-----------------|-----------------|
| N1A  | 35(2)           | 32(2)           | 36(2)           | 4(1)            | -8(1)           | -4(1)           |
| N2A  | 23(1)           | 43(2)           | 36(2)           | 1(1)            | -2(1)           | 1(1)            |
| N3A  | 33(2)           | 44(2)           | 41(2)           | 4(1)            | 4(1)            | -11(1)          |
| N4A  | 36(2)           | 26(2)           | 33(2)           | 0(1)            | -1(1)           | -5(1)           |
| N5A  | 26(1)           | 35(2)           | 33(1)           | 0(1)            | 0(1)            | -1(1)           |
| N6A  | 34(1)           | 31(2)           | 34(2)           | 0(1)            | 3(1)            | -9(1)           |
| C1A  | 32(2)           | 26(2)           | 36(2)           | 4(1)            | -3(1)           | -2(1)           |
| C2A  | 33(2)           | 28(2)           | 37(2)           | 1(1)            | 0(1)            | -8(1)           |
| C3A  | 37(2)           | 46(2)           | 37(2)           | 3(2)            | 0(2)            | 0(2)            |
| C4A  | 49(2)           | 58(3)           | 37(2)           | 8(2)            | -1(2)           | 0(2)            |
| C5A  | 62(3)           | 51(3)           | 44(2)           | -6(2)           | 11(2)           | -11(2)          |
| C6A  | 57(2)           | 37(2)           | 53(2)           | -6(2)           | 12(2)           | -2(2)           |
| C7A  | 43(2)           | 34(2)           | 47(2)           | 6(2)            | 2(2)            | 0(2)            |
| C8A  | 28(2)           | 33(2)           | 30(2)           | -4(1)           | 3(1)            | 0(1)            |
| C9A  | 31(2)           | 35(2)           | 30(2)           | -5(1)           | 0(1)            | -1(2)           |
| C10A | 30(2)           | 39(2)           | 31(2)           | -2(1)           | 12(1)           | -3(2)           |
| C11A | 26(2)           | 46(2)           | 33(2)           | -5(2)           | 4(1)            | 0(2)            |
| C12A | 45(2)           | 55(3)           | 45(2)           | 0(2)            | 1(2)            | -18(2)          |
| C13A | 48(2)           | 72(3)           | 54(3)           | -8(2)           | -11(2)          | -22(2)          |
| C14A | 40(2)           | 72(3)           | 52(2)           | -6(2)           | -12(2)          | -4(2)           |
| C15A | 32(2)           | 65(3)           | 45(2)           | 3(2)            | -6(2)           | -1(2)           |
| C16A | 24(2)           | 49(2)           | 33(2)           | -1(2)           | 5(1)            | -1(2)           |
| C17A | 44(2)           | 65(3)           | 56(3)           | 9(2)            | 8(2)            | -25(2)          |
| C18A | 55(3)           | 77(4)           | 55(3)           | 15(2)           | 5(2)            | -24(3)          |
| C19A | 54(3)           | 55(3)           | 52(2)           | 18(2)           | 1(2)            | -14(2)          |
| C20A | 39(2)           | 37(2)           | 37(2)           | 4(2)            | 4(2)            | -4(2)           |
| C21A | 32(2)           | 27(2)           | 32(2)           | 6(1)            | 0(1)            | -2(1)           |
| C22A | 32(2)           | 30(2)           | 36(2)           | 9(2)            | -4(1)           | -5(2)           |
| C23A | 46(2)           | 45(2)           | 47(2)           | -2(2)           | -5(2)           | -9(2)           |
| C24A | 65(3)           | 56(3)           | 50(2)           | -2(2)           | -13(2)          | -15(2)          |
| C25A | 51(3)           | 63(3)           | 65(3)           | 19(2)           | -27(2)          | -19(2)          |
| C26A | 34(2)           | 64(3)           | 80(3)           | 21(3)           | -11(2)          | 1(2)            |
| C27A | 37(2)           | 47(2)           | 48(2)           | 9(2)            | -4(2)           | -1(2)           |
| C28A | 23(2)           | 32(2)           | 34(2)           | 2(1)            | -7(1)           | 1(1)            |
| C29A | 26(2)           | 34(2)           | 29(2)           | -3(1)           | -4(1)           | 0(1)            |
| C30A | 19(1)           | 34(2)           | 39(2)           | 0(1)            | 0(1)            | -5(1)           |
| C31A | 22(2)           | 33(2)           | 36(2)           | -1(1)           | 1(1)            | -2(1)           |
| C32A | 37(2)           | 41(2)           | 40(2)           | 0(2)            | 9(2)            | -6(2)           |

|      |        |        |        |        |        |        |
|------|--------|--------|--------|--------|--------|--------|
| C33A | 46(2)  | 51(3)  | 44(2)  | -1(2)  | 13(2)  | -7(2)  |
| C34A | 44(2)  | 47(2)  | 36(2)  | -8(2)  | 8(2)   | -1(2)  |
| C35A | 34(2)  | 39(2)  | 40(2)  | -5(2)  | 2(2)   | 2(2)   |
| C36A | 23(2)  | 36(2)  | 35(2)  | -2(2)  | -1(1)  | 3(1)   |
| C37A | 30(2)  | 36(2)  | 42(2)  | 8(2)   | 2(2)   | -8(2)  |
| C38A | 33(2)  | 37(2)  | 60(2)  | 1(2)   | 7(2)   | -9(2)  |
| C39A | 41(2)  | 38(2)  | 51(2)  | -6(2)  | 8(2)   | -12(2) |
| C40A | 38(2)  | 33(2)  | 40(2)  | -5(2)  | 5(2)   | -10(2) |
| N1B  | 34(2)  | 35(2)  | 42(2)  | 2(1)   | -8(1)  | -8(2)  |
| N2B  | 31(1)  | 28(2)  | 36(2)  | 0(1)   | -2(1)  | 0(1)   |
| N3B  | 46(2)  | 42(2)  | 60(2)  | 0(2)   | 5(2)   | -12(2) |
| N4B  | 39(2)  | 35(2)  | 30(1)  | -3(1)  | 2(1)   | -4(1)  |
| N5B  | 34(2)  | 31(2)  | 31(1)  | 2(1)   | -4(1)  | 5(1)   |
| N6B  | 38(2)  | 54(2)  | 39(2)  | 6(2)   | 2(1)   | -13(2) |
| C1B  | 27(2)  | 41(2)  | 31(2)  | -3(1)  | -3(1)  | 1(2)   |
| C2B  | 39(2)  | 38(2)  | 37(2)  | -6(2)  | 0(2)   | 2(2)   |
| C3B  | 47(2)  | 69(3)  | 56(3)  | -21(2) | -9(2)  | 3(2)   |
| C4B  | 81(4)  | 92(4)  | 74(4)  | -43(3) | -12(3) | -9(3)  |
| C5B  | 101(5) | 92(4)  | 65(3)  | -47(3) | 1(3)   | -2(4)  |
| C6B  | 85(4)  | 65(3)  | 63(3)  | -14(3) | 27(3)  | 19(3)  |
| C7B  | 51(2)  | 47(2)  | 51(2)  | -5(2)  | 11(2)  | 6(2)   |
| C8B  | 30(2)  | 33(2)  | 36(2)  | -1(2)  | 5(1)   | 3(2)   |
| C9B  | 30(2)  | 37(2)  | 36(2)  | -4(2)  | 3(1)   | -2(2)  |
| C10B | 31(2)  | 33(2)  | 45(2)  | -3(2)  | 9(2)   | -1(2)  |
| C11B | 36(2)  | 29(2)  | 38(2)  | -2(2)  | 6(2)   | 5(2)   |
| C12B | 46(2)  | 35(2)  | 47(2)  | 6(2)   | 6(2)   | 2(2)   |
| C13B | 58(3)  | 44(2)  | 50(2)  | 14(2)  | 8(2)   | 10(2)  |
| C14B | 46(2)  | 45(2)  | 37(2)  | 2(2)   | -1(2)  | 10(2)  |
| C15B | 41(2)  | 35(2)  | 44(2)  | 1(2)   | -1(2)  | 5(2)   |
| C16B | 29(2)  | 33(2)  | 37(2)  | -2(2)  | 4(1)   | 2(1)   |
| C17B | 60(3)  | 56(3)  | 86(4)  | 11(3)  | 11(3)  | -25(2) |
| C18B | 70(4)  | 75(4)  | 116(5) | 13(4)  | 0(3)   | -43(3) |
| C19B | 87(4)  | 71(4)  | 118(5) | 0(4)   | -14(4) | -44(3) |
| C20B | 60(3)  | 58(3)  | 72(3)  | -6(2)  | -6(2)  | -23(2) |
| C21B | 34(2)  | 41(2)  | 31(2)  | -6(2)  | -4(1)  | 3(2)   |
| C22B | 46(2)  | 32(2)  | 50(2)  | -5(2)  | -17(2) | 8(2)   |
| C23B | 91(4)  | 86(4)  | 37(2)  | -6(2)  | -14(2) | 32(3)  |
| C24B | 149(7) | 106(5) | 44(3)  | -5(3)  | -34(3) | 60(5)  |
| C25B | 120(6) | 75(4)  | 70(4)  | -15(3) | -51(4) | 23(4)  |
| C26B | 61(3)  | 35(3)  | 123(5) | -2(3)  | -43(3) | 4(2)   |
| C27B | 44(2)  | 32(2)  | 80(3)  | -3(2)  | -20(2) | 1(2)   |
| C28B | 24(2)  | 35(2)  | 33(2)  | 0(1)   | -4(1)  | 6(1)   |
| C29B | 25(2)  | 44(2)  | 26(2)  | 0(2)   | -1(1)  | 0(2)   |

|      |         |        |        |         |         |        |
|------|---------|--------|--------|---------|---------|--------|
| C30B | 22(2)   | 45(2)  | 33(2)  | 4(2)    | -5(1)   | -4(1)  |
| C31B | 21(1)   | 39(2)  | 34(2)  | 5(2)    | -4(1)   | 0(1)   |
| C32B | 26(2)   | 37(2)  | 48(2)  | 8(2)    | -3(2)   | -4(2)  |
| C33B | 38(2)   | 33(2)  | 47(2)  | -4(2)   | -7(2)   | 2(2)   |
| C34B | 44(2)   | 38(2)  | 39(2)  | -7(2)   | 0(2)    | 6(2)   |
| C35B | 41(2)   | 37(2)  | 33(2)  | 4(2)    | 0(2)    | 4(2)   |
| C36B | 26(2)   | 30(2)  | 34(2)  | 1(1)    | -2(1)   | 4(1)   |
| C37B | 50(2)   | 57(3)  | 58(3)  | 21(2)   | -19(2)  | -20(2) |
| C38B | 80(4)   | 81(4)  | 57(3)  | 31(3)   | -24(3)  | -36(3) |
| C39B | 100(5)  | 127(6) | 42(3)  | 22(3)   | 5(3)    | -57(4) |
| C40B | 56(3)   | 93(4)  | 34(2)  | 7(2)    | 8(2)    | -19(3) |
| CI1S | 83(1)   | 109(2) | 97(2)  | -19(1)  | -4(1)   | 40(1)  |
| CI2S | 116(2)  | 228(4) | 220(4) | -141(4) | -83(3)  | 87(2)  |
| C1S  | 95(5)   | 148(5) | 157(5) | -71(4)  | -16(4)  | 40(4)  |
| CI1D | 83(1)   | 109(2) | 97(2)  | -19(1)  | -4(1)   | 40(1)  |
| CI2D | 116(2)  | 228(4) | 220(4) | -141(4) | -83(3)  | 87(2)  |
| C1D  | 95(5)   | 148(5) | 157(5) | -71(4)  | -16(4)  | 40(4)  |
| CI3S | 146(3)  | 67(2)  | 66(1)  | 2(1)    | -1(2)   | -2(2)  |
| CI4S | 87(2)   | 336(7) | 123(3) | 41(4)   | -33(2)  | 29(3)  |
| C2S  | 120(3)  | 174(5) | 187(6) | 81(8)   | 5(5)    | 25(3)  |
| CI3D | 120(3)  | 174(5) | 187(6) | 81(8)   | 5(5)    | 25(3)  |
| CI4D | 357(16) | 171(8) | 171(7) | 31(6)   | 143(10) | 98(9)  |
| C2D  | 87(2)   | 336(7) | 123(3) | 41(4)   | -33(2)  | 29(3)  |
| CI5S | 67(1)   | 55(1)  | 72(1)  | 9(1)    | -6(1)   | 1(1)   |
| CI6S | 74(2)   | 171(4) | 148(3) | 8(3)    | -19(2)  | -11(2) |
| C3S  | 173(5)  | 131(5) | 148(4) | -4(4)   | 33(4)   | 34(4)  |
| CI5D | 173(5)  | 131(5) | 148(4) | -4(4)   | 33(4)   | 34(4)  |
| CI6D | 143(5)  | 94(4)  | 238(7) | 11(4)   | -39(5)  | 32(4)  |
| C3D  | 74(2)   | 171(4) | 148(3) | 8(3)    | -19(2)  | -11(2) |

---

**Table 5. Hydrogen coordinates ( $\times 10^4$ ) and isotropic displacement parameters ( $\text{\AA}^2 \times 10^{-3}$ ) for 12021.**

|      | x        | y       | z        | U(eq)  |
|------|----------|---------|----------|--------|
| H1AN | 4320(40) | 270(20) | 1180(20) | 58(15) |
| H4AN | 6102     | -268    | 804      | 43(12) |
| H1A  | 5471     | -522    | 1684     | 38     |
| H3A  | 5923     | -583    | 2658     | 48     |
| H4A  | 5681     | -350    | 3611     | 58     |
| H5A  | 4612     | 406     | 3859     | 62     |
| H6A  | 3804     | 920     | 3161     | 58     |
| H7A  | 4041     | 695     | 2213     | 50     |
| H9A  | 4202     | -1040   | 1936     | 38     |
| H12A | 1945     | -2274   | 1051     | 58     |
| H13A | 1051     | -2152   | 250      | 70     |
| H14A | 1039     | -1207   | -228     | 65     |
| H15A | 2028     | -441    | 52       | 57     |
| H17A | 2172     | -2661   | 1842     | 66     |
| H17B | 1704     | -2024   | 2031     | 66     |
| H18A | 2066     | -2854   | 2773     | 75     |
| H18B | 2128     | -2139   | 2939     | 75     |
| H19A | 3616     | -2485   | 3141     | 64     |
| H19B | 3645     | -2906   | 2580     | 64     |
| H20A | 3716     | -1589   | 2622     | 45     |
| H20B | 4393     | -2033   | 2268     | 45     |
| H21A | 5685     | 759     | 1426     | 36     |
| H23A | 6297     | 1019    | 2400     | 55     |
| H24A | 7625     | 1156    | 2937     | 68     |
| H25A | 8989     | 668     | 2687     | 71     |
| H26A | 9003     | 4       | 1903     | 71     |
| H27A | 7656     | -153    | 1378     | 53     |
| H29A | 6727     | 1253    | 935      | 36     |
| H32A | 7832     | 1835    | -882     | 47     |
| H33A | 7877     | 1348    | -1744    | 56     |
| H34A | 7297     | 346     | -1833    | 51     |
| H35A | 6708     | -148    | -1046    | 45     |
| H37A | 6858     | 2523    | -456     | 43     |
| H37B | 7960     | 2568    | -379     | 43     |
| H38A | 6595     | 3279    | 165      | 52     |
| H38B | 7645     | 3471    | 27       | 52     |
| H39A | 8211     | 2981    | 821      | 52     |
| H39B | 7223     | 3202    | 1061     | 52     |

|      |          |          |         |        |
|------|----------|----------|---------|--------|
| H40A | 7611     | 2052     | 1079    | 44     |
| H40B | 6571     | 2258     | 932     | 44     |
| H1BN | 5510(30) | -628(18) | -61(16) | 26(10) |
| H4BN | 3900(20) | 43(11)   | 186(14) | 25(9)  |
| H1BA | 3786     | -787     | -228    | 39     |
| H3B  | 2929     | -1189    | -973    | 69     |
| H4B  | 2807     | -1847    | -1734   | 99     |
| H5B  | 4126     | -2157    | -2215   | 103    |
| H6B  | 5578     | -1858    | -1894   | 85     |
| H7B  | 5703     | -1194    | -1110   | 60     |
| H9B  | 4159     | -1836    | -83     | 41     |
| H12B | 5078     | -3113    | 1451    | 51     |
| H13B | 6118     | -2982    | 2173    | 61     |
| H14B | 6930     | -2059    | 2267    | 51     |
| H15B | 6775     | -1304    | 1589    | 48     |
| H17C | 3574     | -3103    | 1253    | 81     |
| H17D | 4193     | -3609    | 933     | 81     |
| H18C | 2764     | -3973    | 695     | 104    |
| H18D | 2306     | -3301    | 707     | 104    |
| H19C | 2469     | -3476    | -233    | 111    |
| H19D | 3461     | -3798    | -148    | 111    |
| H20C | 3930     | -2814    | -378    | 76     |
| H20D | 3059     | -2506    | -62     | 76     |
| H21B | 5052     | 84       | -684    | 42     |
| H23B | 4820     | 75       | -1673   | 85     |
| H24B | 3981     | 388      | -2456   | 120    |
| H25B | 2442     | 616      | -2366   | 106    |
| H26B | 1742     | 626      | -1484   | 87     |
| H27B | 2605     | 353      | -663    | 63     |
| H29B | 4843     | 1123     | -742    | 38     |
| H32B | 5095     | 3012     | 231     | 45     |
| H33B | 4902     | 3298     | 1155    | 47     |
| H34B | 4371     | 2567     | 1822    | 49     |
| H35B | 4123     | 1570     | 1547    | 45     |
| H37C | 5342     | 3196     | -618    | 66     |
| H37D | 4262     | 3030     | -571    | 66     |
| H38C | 4083     | 2992     | -1516   | 87     |
| H38D | 4944     | 3459     | -1505   | 87     |
| H39C | 5986     | 2697     | -1667   | 108    |
| H39D | 5133     | 2477     | -2054   | 108    |
| H40C | 4663     | 1766     | -1403   | 73     |
| H40D | 5763     | 1741     | -1299   | 73     |
| H1S1 | 2573     | 859      | 1175    | 160    |

|      |      |      |      |     |
|------|------|------|------|-----|
| H1S2 | 2582 | 320  | 1634 | 160 |
| H1D1 | 2700 | 502  | 1335 | 160 |
| H1D2 | 1803 | 446  | 1733 | 160 |
| H2S1 | 6558 | 1165 | 6460 | 192 |
| H2S2 | 6331 | 1878 | 6537 | 192 |
| H2D1 | 4660 | 1560 | 6297 | 218 |
| H2D2 | 4937 | 849  | 6315 | 218 |
| H3S1 | 3951 | 4260 | 381  | 181 |
| H3S2 | 4218 | 4972 | 379  | 181 |
| H3D1 | 3332 | 4788 | -115 | 157 |
| H3D2 | 3903 | 5205 | 323  | 157 |

---



**Table 6. Torsion angles [°] for 12021.**

|                     |           |                     |           |
|---------------------|-----------|---------------------|-----------|
| C8A-N1A-C1A-C2A     | -85.3(4)  | C8A-N1A-C1A-C21A    | 150.5(3)  |
| N1A-C1A-C2A-C3A     | 146.1(3)  | C21A-C1A-C2A-C3A    | -92.9(4)  |
| N1A-C1A-C2A-C7A     | -35.6(5)  | C21A-C1A-C2A-C7A    | 85.3(4)   |
| C7A-C2A-C3A-C4A     | -1.5(6)   | C1A-C2A-C3A-C4A     | 176.8(4)  |
| C2A-C3A-C4A-C5A     | 0.8(6)    | C3A-C4A-C5A-C6A     | 0.1(7)    |
| C4A-C5A-C6A-C7A     | -0.2(7)   | C5A-C6A-C7A-C2A     | -0.6(6)   |
| C3A-C2A-C7A-C6A     | 1.4(6)    | C1A-C2A-C7A-C6A     | -176.8(3) |
| C16A-N2A-C8A-N1A    | 179.4(3)  | C16A-N2A-C8A-C9A    | -3.2(5)   |
| C1A-N1A-C8A-N2A     | -166.2(3) | C1A-N1A-C8A-C9A     | 16.4(5)   |
| N2A-C8A-C9A-C10A    | 1.6(5)    | N1A-C8A-C9A-C10A    | 178.8(3)  |
| C20A-N3A-C10A-C9A   | -0.2(5)   | C17A-N3A-C10A-C9A   | 146.7(4)  |
| C20A-N3A-C10A-C11A  | 178.5(3)  | C17A-N3A-C10A-C11A  | -34.6(6)  |
| C8A-C9A-C10A-N3A    | -177.7(3) | C8A-C9A-C10A-C11A   | 3.6(5)    |
| N3A-C10A-C11A-C16A  | 174.6(3)  | C9A-C10A-C11A-C16A  | -6.7(5)   |
| N3A-C10A-C11A-C12A  | -9.2(6)   | C9A-C10A-C11A-C12A  | 169.6(4)  |
| C16A-C11A-C12A-C13A | -3.1(6)   | C10A-C11A-C12A-C13A | -179.4(4) |
| C11A-C12A-C13A-C14A | -1.2(7)   | C12A-C13A-C14A-C15A | 3.6(7)    |
| C13A-C14A-C15A-C16A | -1.5(7)   | C8A-N2A-C16A-C11A   | -0.5(5)   |
| C8A-N2A-C16A-C15A   | -176.6(3) | C12A-C11A-C16A-N2A  | -171.0(4) |
| C10A-C11A-C16A-N2A  | 5.5(5)    | C12A-C11A-C16A-C15A | 5.0(5)    |
| C10A-C11A-C16A-C15A | -178.4(3) | C14A-C15A-C16A-N2A  | 173.5(4)  |
| C14A-C15A-C16A-C11A | -2.8(6)   | C10A-N3A-C17A-C18A  | -145.3(4) |
| C20A-N3A-C17A-C18A  | 4.4(5)    | N3A-C17A-C18A-C19A  | -28.3(5)  |
| C17A-C18A-C19A-C20A | 41.3(5)   | C10A-N3A-C20A-C19A  | 173.1(3)  |
| C17A-N3A-C20A-C19A  | 21.5(5)   | C18A-C19A-C20A-N3A  | -38.4(4)  |
| C28A-N4A-C21A-C22A  | -78.7(4)  | C28A-N4A-C21A-C1A   | 154.6(3)  |
| N1A-C1A-C21A-N4A    | -61.9(3)  | C2A-C1A-C21A-N4A    | 173.7(3)  |
| N1A-C1A-C21A-C22A   | 172.4(3)  | C2A-C1A-C21A-C22A   | 48.0(4)   |
| N4A-C21A-C22A-C27A  | -19.6(5)  | C1A-C21A-C22A-C27A  | 102.6(4)  |
| N4A-C21A-C22A-C23A  | 157.9(3)  | C1A-C21A-C22A-C23A  | -79.9(4)  |
| C27A-C22A-C23A-C24A | 0.0(6)    | C21A-C22A-C23A-C24A | -177.5(4) |
| C22A-C23A-C24A-C25A | 1.0(7)    | C23A-C24A-C25A-C26A | -1.2(7)   |
| C24A-C25A-C26A-C27A | 0.3(7)    | C23A-C22A-C27A-C26A | -0.9(6)   |
| C21A-C22A-C27A-C26A | 176.6(4)  | C25A-C26A-C27A-C22A | 0.8(7)    |
| C36A-N5A-C28A-N4A   | -179.6(3) | C36A-N5A-C28A-C29A  | 1.0(5)    |
| C21A-N4A-C28A-N5A   | -172.7(3) | C21A-N4A-C28A-C29A  | 6.8(5)    |
| N5A-C28A-C29A-C30A  | 0.3(5)    | N4A-C28A-C29A-C30A  | -179.0(3) |
| C40A-N6A-C30A-C29A  | -0.9(5)   | C37A-N6A-C30A-C29A  | -156.1(3) |
| C40A-N6A-C30A-C31A  | -179.7(3) | C37A-N6A-C30A-C31A  | 25.1(5)   |
| C28A-C29A-C30A-N6A  | 178.9(3)  | C28A-C29A-C30A-C31A | -2.2(5)   |
| N6A-C30A-C31A-C32A  | 5.8(5)    | C29A-C30A-C31A-C32A | -173.0(3) |

|                     |           |                     |           |
|---------------------|-----------|---------------------|-----------|
| N6A-C30A-C31A-C36A  | -178.5(3) | C29A-C30A-C31A-C36A | 2.7(4)    |
| C36A-C31A-C32A-C33A | 5.6(5)    | C30A-C31A-C32A-C33A | -178.7(4) |
| C31A-C32A-C33A-C34A | -2.2(6)   | C32A-C33A-C34A-C35A | -1.1(6)   |
| C33A-C34A-C35A-C36A | 0.9(6)    | C28A-N5A-C36A-C35A  | 179.7(3)  |
| C28A-N5A-C36A-C31A  | -0.3(5)   | C34A-C35A-C36A-N5A  | -177.6(3) |
| C34A-C35A-C36A-C31A | 2.5(5)    | C32A-C31A-C36A-N5A  | 174.6(3)  |
| C30A-C31A-C36A-N5A  | -1.5(5)   | C32A-C31A-C36A-C35A | -5.5(5)   |
| C30A-C31A-C36A-C35A | 178.4(3)  | C30A-N6A-C37A-C38A  | 155.7(3)  |
| C40A-N6A-C37A-C38A  | -1.1(4)   | N6A-C37A-C38A-C39A  | 21.7(3)   |
| C37A-C38A-C39A-C40A | -33.8(4)  | C30A-N6A-C40A-C39A  | -179.3(3) |
| C37A-N6A-C40A-C39A  | -20.2(4)  | C38A-C39A-C40A-N6A  | 33.0(4)   |
| C8B-N1B-C1B-C2B     | -79.9(4)  | C8B-N1B-C1B-C21B    | 153.1(3)  |
| N1B-C1B-C2B-C7B     | -36.1(5)  | C21B-C1B-C2B-C7B    | 86.9(5)   |
| N1B-C1B-C2B-C3B     | 142.2(4)  | C21B-C1B-C2B-C3B    | -94.8(5)  |
| C7B-C2B-C3B-C4B     | 0.1(8)    | C1B-C2B-C3B-C4B     | -178.3(5) |
| C2B-C3B-C4B-C5B     | -1.3(10)  | C3B-C4B-C5B-C6B     | 2.1(11)   |
| C4B-C5B-C6B-C7B     | -1.7(10)  | C3B-C2B-C7B-C6B     | 0.3(7)    |
| C1B-C2B-C7B-C6B     | 178.6(4)  | C5B-C6B-C7B-C2B     | 0.5(8)    |
| C16B-N2B-C8B-N1B    | -178.5(3) | C16B-N2B-C8B-C9B    | -0.1(5)   |
| C1B-N1B-C8B-N2B     | -158.8(3) | C1B-N1B-C8B-C9B     | 22.8(5)   |
| N2B-C8B-C9B-C10B    | -0.3(5)   | N1B-C8B-C9B-C10B    | 178.0(3)  |
| C20B-N3B-C10B-C9B   | 5.2(6)    | C17B-N3B-C10B-C9B   | -158.4(4) |
| C20B-N3B-C10B-C11B  | -171.1(4) | C17B-N3B-C10B-C11B  | 25.2(6)   |
| C8B-C9B-C10B-N3B    | -176.7(3) | C8B-C9B-C10B-C11B   | -0.1(5)   |
| N3B-C10B-C11B-C12B  | -0.7(6)   | C9B-C10B-C11B-C12B  | -177.1(3) |
| N3B-C10B-C11B-C16B  | 177.2(3)  | C9B-C10B-C11B-C16B  | 0.8(5)    |
| C16B-C11B-C12B-C13B | 2.9(5)    | C10B-C11B-C12B-C13B | -179.3(4) |
| C11B-C12B-C13B-C14B | 0.2(6)    | C12B-C13B-C14B-C15B | -2.9(6)   |
| C13B-C14B-C15B-C16B | 2.3(6)    | C8B-N2B-C16B-C15B   | -179.0(3) |
| C8B-N2B-C16B-C11B   | 0.9(5)    | C14B-C15B-C16B-N2B  | -179.2(3) |
| C14B-C15B-C16B-C11B | 0.9(5)    | C12B-C11B-C16B-N2B  | 176.8(3)  |
| C10B-C11B-C16B-N2B  | -1.2(5)   | C12B-C11B-C16B-C15B | -3.4(5)   |
| C10B-C11B-C16B-C15B | 178.6(3)  | C10B-N3B-C17B-C18B  | 156.6(5)  |
| C20B-N3B-C17B-C18B  | -8.3(6)   | N3B-C17B-C18B-C19B  | 30.5(7)   |
| C17B-C18B-C19B-C20B | -40.4(7)  | C10B-N3B-C20B-C19B  | 177.9(4)  |
| C17B-N3B-C20B-C19B  | -15.9(6)  | C18B-C19B-C20B-N3B  | 34.8(6)   |
| C28B-N4B-C21B-C22B  | -74.8(4)  | C28B-N4B-C21B-C1B   | 158.4(3)  |
| N1B-C1B-C21B-N4B    | -68.9(3)  | C2B-C1B-C21B-N4B    | 165.1(3)  |
| N1B-C1B-C21B-C22B   | 164.7(3)  | C2B-C1B-C21B-C22B   | 38.7(4)   |
| N4B-C21B-C22B-C27B  | -33.2(5)  | C1B-C21B-C22B-C27B  | 89.2(5)   |
| N4B-C21B-C22B-C23B  | 145.6(4)  | C1B-C21B-C22B-C23B  | -92.0(5)  |
| C27B-C22B-C23B-C24B | -0.3(8)   | C21B-C22B-C23B-C24B | -179.2(6) |
| C22B-C23B-C24B-C25B | -2.2(11)  | C23B-C24B-C25B-C26B | 3.0(11)   |

|                     |           |                     |           |
|---------------------|-----------|---------------------|-----------|
| C24B-C25B-C26B-C27B | -1.4(9)   | C23B-C22B-C27B-C26B | 1.9(6)    |
| C21B-C22B-C27B-C26B | -179.3(4) | C25B-C26B-C27B-C22B | -1.1(7)   |
| C36B-N5B-C28B-N4B   | -176.6(3) | C36B-N5B-C28B-C29B  | 0.1(5)    |
| C21B-N4B-C28B-N5B   | -170.3(3) | C21B-N4B-C28B-C29B  | 13.0(5)   |
| N5B-C28B-C29B-C30B  | -3.9(5)   | N4B-C28B-C29B-C30B  | 172.6(3)  |
| C40B-N6B-C30B-C29B  | -2.2(5)   | C37B-N6B-C30B-C29B  | 149.9(4)  |
| C40B-N6B-C30B-C31B  | 178.3(3)  | C37B-N6B-C30B-C31B  | -29.5(5)  |
| C28B-C29B-C30B-N6B  | -174.2(3) | C28B-C29B-C30B-C31B | 5.3(5)    |
| N6B-C30B-C31B-C32B  | -4.9(5)   | C29B-C30B-C31B-C32B | 175.6(3)  |
| N6B-C30B-C31B-C36B  | 176.4(3)  | C29B-C30B-C31B-C36B | -3.1(4)   |
| C36B-C31B-C32B-C33B | -0.8(5)   | C30B-C31B-C32B-C33B | -179.4(3) |
| C31B-C32B-C33B-C34B | -0.6(6)   | C32B-C33B-C34B-C35B | 1.6(6)    |
| C33B-C34B-C35B-C36B | -1.2(6)   | C28B-N5B-C36B-C35B  | -178.5(3) |
| C28B-N5B-C36B-C31B  | 2.1(5)    | C34B-C35B-C36B-N5B  | -179.7(3) |
| C34B-C35B-C36B-C31B | -0.2(5)   | C32B-C31B-C36B-N5B  | -179.4(3) |
| C30B-C31B-C36B-N5B  | -0.6(5)   | C32B-C31B-C36B-C35B | 1.2(5)    |
| C30B-C31B-C36B-C35B | 180.0(3)  | C30B-N6B-C37B-C38B  | -148.4(4) |
| C40B-N6B-C37B-C38B  | 5.8(5)    | N6B-C37B-C38B-C39B  | -26.6(5)  |
| C37B-C38B-C39B-C40B | 37.5(5)   | C30B-N6B-C40B-C39B  | 173.4(4)  |
| C37B-N6B-C40B-C39B  | 16.9(5)   | C38B-C39B-C40B-N6B  | -33.5(5)  |

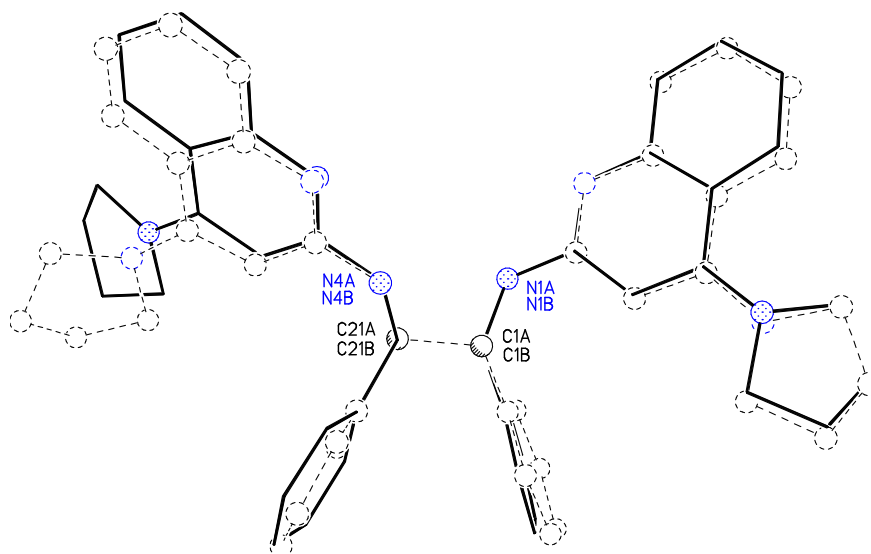
---

**Table 7. Least-squares fit of molecule A and B for 12021.**

ATOM MODEL DEVIATION

N1A N1B 0.044  
 N4A N4B 0.045  
 C1A C1B 0.038  
 C21A C21B 0.036

WEIGHTED R.M.S. DEVIATION = 0.0409 Å



**IDEALIZED CRYSTAL COORDINATES FOR MODEL ATOMS**

| NAME | SFAC | X       | Y        | Z        | NEAREST ATOM | DEVIATION |
|------|------|---------|----------|----------|--------------|-----------|
| N1B  | 3    | 0.44069 | -0.00377 | 0.13685  | N1A          | 0.044     |
| N2B  | 3    | 0.32214 | -0.04358 | 0.08425  | N2A          | 0.030     |
| N3B  | 3    | 0.29979 | -0.18752 | 0.20399  | N3A          | 0.371     |
| N4B  | 3    | 0.62042 | 0.01253  | 0.09069  | N4A          | 0.045     |
| N5B  | 3    | 0.66328 | 0.01999  | -0.00262 | N5A          | 0.131     |
| N6B  | 3    | 0.77931 | 0.19373  | 0.03284  | N6A          | 0.745     |
| C1B  | 1    | 0.52384 | -0.01039 | 0.17008  | C1A          | 0.038     |
| C2B  | 1    | 0.50680 | -0.00433 | 0.23320  | C2A          | 0.191     |
| C3B  | 1    | 0.55641 | -0.04212 | 0.26994  | C3A          | 0.368     |

|      |   |         |          |          |      |       |
|------|---|---------|----------|----------|------|-------|
| C4B  | 1 | 0.54259 | -0.04009 | 0.32709  | C4A  | 0.601 |
| C5B  | 1 | 0.48009 | 0.00062  | 0.34939  | C5A  | 0.677 |
| C6B  | 1 | 0.42912 | 0.03803  | 0.31421  | C6A  | 0.552 |
| C7B  | 1 | 0.44320 | 0.03551  | 0.25528  | C7A  | 0.318 |
| C8B  | 1 | 0.37717 | -0.04904 | 0.12905  | C8A  | 0.082 |
| C9B  | 1 | 0.37041 | -0.09786 | 0.16828  | C9A  | 0.181 |
| C10B | 1 | 0.30527 | -0.14335 | 0.16269  | C10A | 0.246 |
| C11B | 1 | 0.24341 | -0.13887 | 0.11446  | C11A | 0.286 |
| C12B | 1 | 0.16898 | -0.17900 | 0.10193  | C12A | 0.608 |
| C13B | 1 | 0.11463 | -0.17183 | 0.05524  | C13A | 0.623 |
| C14B | 1 | 0.13093 | -0.12403 | 0.01741  | C14A | 0.281 |
| C15B | 1 | 0.19936 | -0.08251 | 0.02853  | C15A | 0.075 |
| C16B | 1 | 0.25676 | -0.08817 | 0.07703  | C16A | 0.096 |
| C17B | 1 | 0.25968 | -0.24921 | 0.19922  | C17A | 0.698 |
| C18B | 1 | 0.30804 | -0.28485 | 0.24615  | C19A | 1.097 |
| C19B | 1 | 0.32673 | -0.23868 | 0.28960  | C19A | 0.511 |
| C20B | 1 | 0.35678 | -0.18266 | 0.25475  | C20A | 0.543 |
| C21B | 1 | 0.59549 | 0.03529  | 0.14599  | C21A | 0.036 |
| C22B | 1 | 0.67789 | 0.04706  | 0.18454  | C22A | 0.149 |
| C23B | 1 | 0.67425 | 0.09590  | 0.22272  | C23A | 0.398 |
| C24B | 1 | 0.74690 | 0.10941  | 0.25824  | C24A | 0.509 |
| C25B | 1 | 0.82296 | 0.07374  | 0.25791  | C25A | 0.495 |
| C26B | 1 | 0.83096 | 0.02559  | 0.22074  | C26A | 0.528 |
| C27B | 1 | 0.75739 | 0.01184  | 0.18262  | C27A | 0.335 |
| C28B | 1 | 0.65770 | 0.04696  | 0.04848  | C28A | 0.113 |
| C29B | 1 | 0.69247 | 0.10609  | 0.05938  | C29A | 0.242 |
| C30B | 1 | 0.73953 | 0.13864  | 0.01886  | C30A | 0.483 |
| C31B | 1 | 0.74533 | 0.11201  | -0.03776 | C31A | 0.430 |
| C32B | 1 | 0.78469 | 0.13951  | -0.08558 | C32A | 0.420 |
| C33B | 1 | 0.78736 | 0.11265  | -0.13730 | C33A | 0.390 |
| C34B | 1 | 0.74944 | 0.05353  | -0.14375 | C34A | 0.324 |
| C35B | 1 | 0.70896 | 0.02514  | -0.09866 | C35A | 0.241 |
| C36B | 1 | 0.70500 | 0.05264  | -0.04463 | C36A | 0.260 |
| C37B | 1 | 0.86345 | 0.22080  | 0.00716  | N6A  | 1.956 |
| C38B | 1 | 0.90784 | 0.25688  | 0.05403  | C39A | 2.447 |
| C39B | 1 | 0.82908 | 0.27332  | 0.09180  | C39A | 1.241 |
| C40B | 1 | 0.76714 | 0.21743  | 0.09096  | C40A | 0.733 |